Biogeochemical impacts of glacial meltwaters across a High Arctic watershed (Lake Hazen, Nunavut, Canada)

by

Kyra St. Pierre

A thesis submitted in partial fulfillment of the requirements for the degree of

Doctor of Philosophy
in
Ecology

Department of Biological Sciences
University of Alberta

Abstract

Climate change across northern latitudes is fundamentally altering the hydrological cycle there, resulting in increased glacial melt, permafrost thaw and precipitation. Whereas enhanced glacial melt has potentially important implications for water quality and productivity in downstream freshwater ecosystems, little is yet known about how glacial meltwaters impact biogeochemical cycles of both nutrients and contaminants across glacierized watersheds, a critical gap in our ability to predict the future quality of freshwater resources in the North. To address this, we integrated principles from glaciology and limnology in a multi-year (2013-2017) study of freshwater quality and productivity across the glacierized High Arctic Lake Hazen watershed on northern Ellesmere Island in Nunavut Canada, from glacier termini through rivers and lakes to the nearshore marine environment. We first examined nutrient (nitrogen, phosphorus, iron, silica) and carbon retention and mobilization across the glacierized land-to-ocean aquatic continuum (Chapter 2). Largely particle-bound nutrients (total phosphorus, iron, nitrogen) from the glacier-fed rivers were deposited to the depths of the lake by turbidity currents generated by the glacial inflows. Lake Hazen was also a sink for dissolved nitrogen species and dissolved organic carbon, likely due to biological processes, but a source of dissolved inorganic carbon (DIC) to the Ruggles River outflow. To understand this source of DIC, we then focused on DIC and by extension, dissolved carbon dioxide (CO_2) concentrations across the watershed (Chapter 3). At the watershed scale, the glacier-fed rivers were a strong, previously overlooked sink of atmospheric CO_2 due to the strength of CO_2-consuming chemical weathering reactions involving the large loads of comminuted sediments entrained by glacial meltwaters as they traveled across the poorly consolidated proglacial zone. As the reactions consumed CO_2, they also generated DIC, resulting in the net export of DIC from Lake Hazen to the Ruggles River. These reactions

intensified with increasing discharge and distance from the glaciers and continued into the lake, resulting in CO_2 undersaturation even at 267 m depth. Finally, we used a mass balance approach to identify sources and sinks of neurotoxic methylmercury (MeHg) and total mercury (THg) across the watershed (Chapter 4). Glacial meltwaters were annually the most important source of THg to Lake Hazen and MeHg. Because much of this mercury was particle-bound and deposited to the bottom of the lake, Lake Hazen was a large sink for both MeHg and THg, resulting in low MeHg and THg exports to the Ruggles River. However, permafrost slumping and erosion along the banks of the Ruggles River significantly increased exports of MeHg and THg to coastal marine waters. This study highlights the importance of climate change-accelerated glacial melt to the biogeochemistry of downstream aquatic ecosystems.

Preface

In an increasingly interdisciplinary environment, scientific research cannot be completed without the collaboration of numerous people. This is especially true for research conducted in the Arctic, where the high costs and the logistical challenges of working in these remote environments make work on one's own exceedingly difficult, if not impossible. Contributions from collaborators on these projects have been acknowledged with co-authorship on the associated publications and are listed below. Chapters are structured according to the journals to which the manuscripts have been submitted.

Chapter 2: St. Pierre, K.A., St. Louis, V.L., Lehnherr, I., Schiff, S.L., Muir, D.C.G., Poulain, A.J., Smol, J.P., Talbot, C., Ma, M., Findlay, D.L., Findlay, W.J., Arnott, S.E. The land-to-ocean aquatic continuum in a glacierized High Arctic watershed: biogeochemical impacts of glacial melt. Submitted to *Limnology and Oceanography*.

Chapter 3: St. Pierre, K.A., St. Louis, V.L., Schiff, S.L., Lehnherr, I., Dainard, P.G., Gardner, A.S., Aukes, P.J.K. Chemical weathering in glacial meltwaters are creating strong downstream freshwater CO_2 sinks. Submitted to *Nature Geoscience*.

Chapter 4: St. Pierre, K.A., St. Louis, V.L., Lehnherr, I., Gardner, A.S., Serbu, J.A., Mortimer, C.A., Szostek, L., Muir, D.C.G., Talbot, C. Climate drives changes in mercury cycling in the watershed of the High Arctic's largest lake by volume (Lake Hazen, Nunavut, Canada). Submitted to *Environmental Science and Technology*.

Acknowledgements

Firstly, thank you to the funding sources which have made this research possible: the NSERC Discovery Grant and Northern Supplement programs, the Northern Contaminants Program (Indigenous and Northern Affairs Canada), the ArcticNet Centre for Excellence, Parks Canada, Environment and Climate Change Canada, the Northern Scientific Training Program, and UAlberta North. Special thanks go to the staff at the Polar Continental Shelf Program (Natural Resources Canada) and Kenn Borek air, without whose expert logistical coordination, this research would not have been possible. Personal funding was provided through Vanier Canada, NSERC CGS-M, and Queen Elizabeth II Graduate Scholarships, Michael Smith Foreign Study Supplements, the Becky Sjare Graduate Award, the John and Patricia Schlosser Environment Scholarship, and the Canadian Institute of Nordic Studies Ph.D. Scholarship.

I would like to thank my Ph.D. supervisor, Vincent St. Louis, for his resolute support throughout my graduate program. I am so incredibly thankful for the opportunities that I have been given during my program and the things that I have gotten to experience. I would also like to thank Dr. Alexandre Poulain and Dr. Emmanuel Yumvihoze at the University of Ottawa, with whom I began my foray into biogeochemistry. The independence and support that they provided during my undergraduate studies showed me how much fun original research could be and gave me the confidence to pursue graduate studies. Also, many thanks to Dr. Bo Elberling and the members of the Center for Permafrost, at the University of Copenhagen, who hosted me for 7 months during my Ph.D. I learned so much during this experience and I look forward to continuing to collaborate with the group in the future.

Thank you to Dr. Martin Sharp and Dr. Suzanne Tank, my supervisory committee members, for their time and invaluable guidance throughout this process. Many thanks also go to

those scientists who have served on my candidacy (Dr. David Hik, Dr. Alberto Reyes) and defense examining committees (Dr. Nigel Roulet, Dr. Rolf Vinebrooke).

Much credit for this work goes to the people who made my 4 field seasons at Lake Hazen some of the best and most memorable months of my life thus far: especially to my two field assistants Jessica Serbu and Lisa Szostek, as well as to Pieter Aukes, Maria Cavaco, Paul Dainard, Igor Lehnherr, Matti Ruuskanen, Charlie Talbot, Victoria Wisniewski, and Cath Wong. I am also hugely grateful for the other members of the St. Louis lab group, Lauren Bortolotti, Maria Cavaco, Craig Emmerton, and Chelsea Willis, who have all become great friends over the years. Also, many thanks to the staff at the Biogeochemical Analytical Service Laboratory, who have had to provide technical support on innumerable occasions.

Lastly and most importantly, thank you to my parents, Rita and Ivan, who have encouraged me to do what I love for longer than I can remember. It would be hard to capture just how much their support, and that of my younger brother, Tristan, have meant to me over the years. I know that at times they are not entirely sure where I am or what I am doing, but it has never mattered one bit and their support has been unwavering.

Table of Contents

Abstract ii
Preface iv
Acknowledgements v
List of Tables ix
List of Figures xi

Chapter 1. General introduction 1
Global climate change 1
Arctic climate change in the 21st century 1
Climate change impacts on the biogeochemistry of freshwater systems 2
Glaciers as a component of the Arctic freshwater system 3
Mercury dynamics in a changing Arctic 4
Global consequences of changes in Arctic freshwater quantity and quality 4
The Lake Hazen watershed as a model system 5
Glacial history of the Lake Hazen watershed 5
Lake Hazen today 5
Objectives 6
References 9

Chapter 2. The land-to-ocean aquatic continuum in a glacierized High Arctic watershed: biogeochemical impacts of glacial melt 14
INTRODUCTION 14
MATERIALS AND METHODS 15
RESULTS AND DISCUSSION 22
Watershed hydrology 22
Nutrient concentrations in major hydrological inputs to Lake Hazen 23
In-lake physical structure and nutrient concentrations 24
Nutrient concentrations in the Ruggles River outflow 26
Nutrient input-output budgets 27
In-lake biological processes. 29
Land-to-ocean aquatic continuum in a glacierized watershed 32
REFERENCES 33
FIGURES AND TABLES 40

Chapter 3. Chemical weathering in glacial meltwaters are creating strong downstream freshwater CO_2 sink 50
$CO_{2(aq)}$ consumption in glacial inflows to Lake Hazen 51
Impact of glacial inputs on net CO_2 consumption in receiving freshwater systems. 53
Projected global glacial melt and downstream freshwater CO_2 cycling 56
METHODS 57
REFERENCES 65
FIGURES AND TABLES 69

Chapter 4. Climate drives catchment-wide changes in mercury cycling in the High Arctic's largest lake by volume (Lake Hazen, Nunavut, Canada) **75**
INTRODUCTION 75
METHODS 76
RESULTS AND DISCUSSION 82
Lake Hazen watershed hydrology 82
Hg concentrations in major inputs to Lake Hazen 82
Hg concentrations in the Lake Hazen water column. 85
Hg concentrations in outputs from Lake Hazen. 86
Lake Hazen MeHg and THg mass balance. 87
Arctic freshwater Hg cycle sensitivity to climate change. 88
REFERENCES 89
FIGURES AND TABLES 95

Chapter 5. General conclusions **100**
References 103

Bibliography **104**

Appendix 1. Supporting information for "Chapter 2. The land-to-ocean aquatic continuum in a glacierized High Arctic watershed: biogeochemical impacts of accelerated glacial melt" **124**
Supporting Figures and Tables 124

Appendix 2. Supporting information for "Chapter 3. Chemical weathering in glacial meltwaters are creating strong downstream freshwater CO_2 sink" **137**
Supporting Figures and Tables 137
References 144

Appendix 3. Supporting information for "Chapter 4. Climate drives catchment-wide changes in mercury cycling in the High Arctic's largest lake by volume (Lake Hazen, Nunavut, Canada)" **145**
Inputs to Lake Hazen. 145
References 164

List of Tables

Table 2-1. Hydrological nutrient mass balances (annual loads in metric tons yr^{-1} ± SE) for Lake Hazen in 2015 and 2016. 49

Table 3-1. Mean annual Lake Hazen watershed CO_2 budgets. 74

Table 4-1. Loadings (± SE) and mass balance budgets for total mercury (THg) and methylmercury (MeHg) in the Lake Hazen watershed in 2015 and 2016. 99

Table A1-1. Sampling and analytical information for the Lake Hazen water column and glacial inflows. 109

Table A1-2. LOADEST log-linear models for glacial inflow chemical fluxes, where [C] is in mg L^{-1} and Q is discharge in m^3 s^{-1}. 110

Table A1-3. Sediment core sampling site information. 111

Table A1-4. Summary of parameters measured on sediment cores collected from Lake Hazen. 111

Table A1-5. Spring physical and chemical limnology of hydrological compartments of the Lake Hazen watershed (mean of *n* ± SE). 112

Table A1-6. Summer physical and chemical limnology of hydrological compartments of the Lake Hazen watershed (mean of *n* ± SE) averaged between summers 2015 and 2016. 113

Table A1-7. Physical and chemical limnology of the glacial river deltas in the Lake Hazen watershed (mean of *n* ± 1 SD) during summers 2015 and 2016. 114

Table A1-8. Seasonal phytoplankton genus and species diversity in Lake Hazen by taxonomic group. 115

Table A1-9. Overlying dissolved O_2 concentrations (1 cm overlying core ± SE), and maximum and depth-integrated oxygen consumption rates (in nmol cm^{-2} s^{-1}) for sediment cores collected throughout the Lake Hazen basin. 116

Table A2-1. Temperature, pH and components of the carbon system in the Lake Hazen watershed, glacial river deltas, Lake Hazen moat and water column and Ruggles River outflow. 120

Table A2-2. Weathering indices in glacial rivers of the Lake Hazen watershed in 2015 and 2016. 121

Table A2-3. Literature documented $CO_{2(aq)}$ undersaturation in glacier-fed freshwater ecosystems. 122

Table A2-4. Best-fit log-linear models of major cation and anion loads in glacial rivers from rLOADEST, where Q is discharge in $m^3\ s^{-1}$ and [x] is the analyte load in kg d^{-1}. 123

Table A3-1. Sampling sites and parameters samples in the Lake Hazen watershed. 138

Table A3-2. Concentrations of total mercury (THg) and methylmercury (MeHg) by hydrologic pool in the Lake Hazen watershed (unfiltered, unless otherwise stated). 139

Table A3-3. Concentrations and loadings of unfiltered total mercury (THg) in snow from the Lake Hazen watershed in 2014 and 2015. 140

Table A3-4. Concentrations and loadings of unfiltered methylmercury (MeHg) in snow from the Lake Hazen watershed in 2014 and 2015. 140

Table A3-5. Log-linear models from LOADEST for prediction of daily THg/MeHg (UF, unfiltered; F, filtered) fluxes in glacial rivers. 141

Table A3-6. Physical features (mean±1SD) of, and total mercury (THg) and methylmercury (MeHg) exports (± SE) from, the glacier-fed river deltas draining into Lake Hazen. 141

Table A3-7. Glacial sub-catchment area-normalized annual fluxes (±SE) of runoff, THg and MeHg in the Lake Hazen watershed. 142

Table A3-8. Concentrations of THg and MeHg (ng g^{-1}) in freeze-dried solid samples collected from throughout the Lake Hazen watershed in 2015, 2016. 143

List of Figures

Figure 1-1. Original conceptual model of terrestrial-aquatic linkages, adapted from Likens and Bormann (1974). 2

Figure 1-2. General map of the Lake Hazen watershed (grey outline), on northern Ellesmere Island (location shown in inset map). 6

Figure 1-3. Conceptual framework of biogeochemical cycles across a glacierized Arctic watershed showing inputs, outputs, and simplified in-river and lake processes. 8

Figure 2-1. Map of the Lake Hazen watershed exemplifying the glacierized land-to-ocean aquatic continuum. 40

Figure 2-2. Time series of glacial river (Snowgoose and Blister) chemistry measured at the inflow to Lake Hazen throughout summer 2016 (2-July to 4-August). 41

Figure 2-3. Seasonal physical and chemical water column profiles of Lake Hazen. 42

Figure 2-4. Sediment core porewater profiles of NH_4^+, NO_2^--NO_3^- and total dissolved phosphorus (TDP) from 5 sites throughout Lake Hazen. 43

Figure 2-5. Sediment core microprofiles for 5 sites in Lake Hazen, representing variable proximity to glacial inflows. 44

Figure 2-6. Seasonal water column profiles of phytoplankton taxonomic group cell densities (top panels) and biomass (bottom panels) in Lake Hazen. 45

Figure 2-7. A: Principal component bi-plot of phytoplankton community composition (as Hellinger-transformed cell densities) and B: the first principal component (PC1) scores as a function of the DIN:TP mass ratio. 46

Figure 2-8. Nutrient concentrations along the land to ocean aquatic continuum (LOAC) in the Lake Hazen watershed. 47

Figure 2-9. Molar ratios of key nutrients along the land to ocean aquatic continuum (LOAC) in the Lake Hazen watershed. 48

Figure 3-1. Theoretical model of glacial meltwater impacts on downstream freshwater $CO_{2(aq)}$ cycling. 69

Figure 3-2. Transects of dissolved gas ($CO_{2(aq)}$, $O_{2(aq)}$), anion (sum of HCO_3^-, SO_4^{2-}, Cl^-), dissolved inorganic carbon (DIC), and silica (SiO_2) concentrations with increasing distance from the glaciers along the Gilman (mean of 2 transects, 11 July and 01 August 70

2016, ± 1 SD), Snowgoose (01 August 2016) and Blister (19 July 2016) rivers.

Figure 3-3. Temporal variability in $CO_{2(aq)}$ concentrations (A), δ^{13}C-DIC (B) and modeled daily mean instantaneous glacial runoff (C) in the Snowgoose and Blister rivers between 2-July and 9-August 2016. 71

Figure 3-4. Mean daily measured CO_2 flux in the moat of Lake Hazen with modeled glacial run-off during the ablation season in (A) 2015 and (B) 2016. 72

Figure 3-5. Spring and summer Lake Hazen water column profiles of (A) $CO_{2(aq)}$ saturation, (B) oxygen ($O_{2(aq)}$) saturation, (C) dissolved inorganic carbon (DIC), (D) particulate carbon (PC), and (E) dissolved calcium ($Ca^{2+}_{(aq)}$) from the deepest station within Lake Hazen (267 m). 73

Figure 4-1. Schematic of MeHg and THg cycles in a glacierized High Arctic watershed. 95

Figure 4-2. Concentrations (ng L^{-1}) of total mercury (THg) and methylmercury (MeHg) by Lake Hazen watershed pool. 96

Figure 4-3. Total mercury (THg), methylmercury (MeHg) and total suspended solids (TSS) concentrations along 3-site transects in the Gilman, Blister, and Ruggles rivers. 97

Figure 4-4. Lake Hazen spring before and after snowmelt (2014) and summer (2015-2016) water column profiles. 98

Figure A1-1. Nitrogen, phosphorus and carbon transects along the Gilman (left panels) and Snowgoose (right panels) rivers in summer 2016 (means of 2 transects ± SE). 104

Figure A1-2. Transects of nitrogen, phosphorus and carbon concentrations along the Ruggles River from Lake Hazen to Chandler Fjord in summer 2016 (means of 2 transects ± SE). 105

Figure A1-3. Seasonal light profiles of the upper water column of Lake Hazen, measured using a Li-COR 1400 light meter. 106

Figure A1-4. Redundancy analysis of phytoplankton community composition by biomass. 107

Figure A1-5. Biogeochemical sediment core profiles from the glacially influenced main deep site (S1) and Abbé shallow (S2, ~44 m) in August and the following May. 108

Figure A2-1. Map of Lake Hazen watershed on northern Ellesmere Island, Quttinirpaaq National Park, Nunavut, Canada. 117

Figure A2-2. Carbon dioxide (CO_2) and oxygen (O_2) saturation in (A) glacial river deltas in 2016 and (B) Lake Hazen in 2015 and 2016. 118

Figure A2-3. Examples of daily instantaneous surface CO_2 fluxes in μmol m^{-2} h^{-1} along the shoreline of Lake Hazen. 119

Figure A3-1. Sampling sites within the Lake Hazen watershed, northern Ellesmere Island, Nunavut, Canada. 131

Figure A3-2. Snow conditions on the Lake Hazen watershed in 2014 (left column) and 2015 (right column). 132

Figure A3-3. Isotopic signatures ($\delta^{18}O$-H_2O and ($\delta^{2}H$-H_2O) of glacial river samples relative to global meteoric water line. 133

Figure A3-4. THg and MeHg concentrations in glacial rivers. Blister and Snowgoose rivers sampled every 5-7 days (n=11); other rivers sampled 1-2 times per summer (n=3, but n=2 for Gilman). 134

Figure A3-5. Concentrations of unfiltered (bulk) and filtered (dissolved) total mercury (THg) and methylmercury (MeHg) throughout the melt season in the Snowgoose and Blister river deltas and along the Lake Hazen shoreline. 135

Figure A3-6. Foam material collected along shoreline of Lake Hazen near the Gilman River. 136

Figure A3-7. Modeled bulk (unfiltered) total mercury (THg) and methylmercury (MeHg) inputs from the glacial rivers to Lake Hazen from 2001 to 2016. 137

Chapter 1. General introduction

Global climate change

Climate change is occurring worldwide at unprecedented rates. Between 1880 and 2012, the mean global surface temperature increased by 0.85°C, concomitant with increasing frequency and intensity of extreme weather events, and a global sea level rise of 1.7 mm yr^{-1}.[1] More than half of these realized changes are directly attributed to the intensification of human activities following the Industrial Revolution, namely via the combustion of fossil fuels, and widespread changes in land use. These activities have cumulatively led to an increase in atmospheric concentrations of infrared radiation-absorbing greenhouse gases (GHG), such as carbon dioxide (CO_2), methane (CH_4), and nitrous oxide (N_2O).

By 2100, global surface temperatures are predicted to increase by between 1.0°C (RCP2.6) and 3.7°C (RCP8.5), depending on the scale of actions taken to reduce GHG emissions.[1] Even if dramatic steps are taken, much of the predicted warming will occur, a commitment to a warmer future insured through past and present GHG emissions and the heat absorbing capacity of the global hydrosphere (oceans, lakes, rivers, ice).[1, 2] Due to both local and global climate forcings, however, these realized and predicted changes are not occurring homogeneously across the planet, such that some regions are experiencing greater warming than others.

Arctic climate change in the 21st century

Nowhere on the planet is climate change occurring more rapidly than in the Arctic.[3] By 2100, temperatures and precipitation in the Arctic could increase by up to 8.3°C and 40% (RCP8.5 in CMIP5), respectively.[1] Arctic amplification, the phenomenon whereby changes in Arctic (global areas north of 66°N) climate occur more dramatically than elsewhere on Earth, is a well-known feature of the global climate system, a result of much of the region being covered by highly reflective ice and snow.[4-6] In its simplest form, small increases in global GHG concentrations instigate the initial melting of snow and ice, which then exposes dark surfaces (both land and water) better able to absorb and store heat. The complexity of the resulting positive feedbacks, which invoke atmospheric and oceanic heat fluxes, then perpetuate the changes in surface temperature.[7]

Warming is already fundamentally altering ecosystem structure and function across the Arctic, from inland tundra to the central Arctic Ocean.[8, 9] Many of these changes result from changes in hydrology, including increased precipitation and a shift from a snow to rain-dominated systems,[10] permafrost thaw,[11] and glacial melt,[12-15] cumulatively increasing overland runoff to downstream freshwater and marine systems.[16, 17]

Climate change impacts on the biogeochemistry of freshwater systems

Limnologists have long recognized the biological, geological, and chemical (hereafter biogeochemical) linkages between terrestrial and aquatic ecosystems (Figure 1-1).[18] Despite this, natural ecosystems are rarely examined holistically as watershed units, especially in the Arctic.[19-21] Watershed-scale studies are hampered by the sheer spatial scale of the required effort, and a still burgeoning culture of interdisciplinary collaboration. This does not, however, diminish the fact that what happens upstream has important consequences on downstream ecosystems.

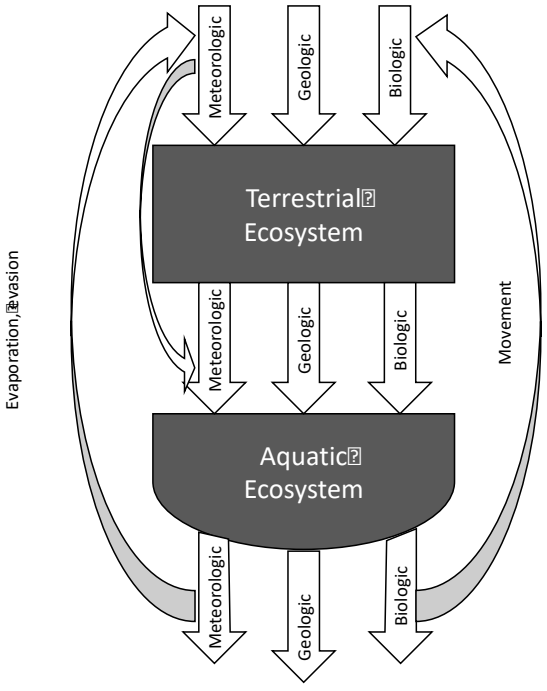

Figure 1-1. Original conceptual model of terrestrial-aquatic linkages, adapted from Likens and Bormann (1974).

Across watersheds, rivers and lakes serve as hydrological conduits between terrestrial and marine ecosystems. Whereas rivers were once considered passive pipes, they are now regarded as active components of global carbon and nutrient cycles.[22-26] Lakes likewise play an important

role within watersheds, serving as intermediate repositories and biogeochemical reactors between headwaters and downstream marine environments.[27-30] Since lakes typically form at low points on the landscape, they integrate changes throughout their watershed area and thus serve as indicators of both natural and anthropogenic ecosystem shifts over a much wider area than they alone cover.[30] Although larger freshwater bodies are generally considered to be more resilient to change than small ponds and streams,[31] large northern lakes and rivers are already exhibiting wide-scale declines in ice cover,[32, 33] as well as shifts in water quality[34] and primary producer community composition.[35]

Glaciers as a component of the Arctic freshwater system

Despite being hydrologically connected to downstream ecosystems, glaciers have rarely been recognized as integral components of the watersheds in which they are located. Whereas the biogeochemistry of subglacial and supraglacial environments is comparatively well studied,[36, 37] our understanding of the biogeochemical impacts of glacial melt on downstream ecosystems (hereafter the proglacial freshwater network) remains poor,[38] a critical gap in our ability to predict the future quality of northern freshwater resources.

Glaciers archive nutrients and contaminants, deposited to high latitude and alpine regions over centuries or millennia (e.g., [39, 40]), which upon melting, may be released to downstream ecosystems. In the High Arctic, the proglacial areas over which meltwaters travel have little vegetation, and large quantities of finely ground, comminuted sediments, created by successive cycles of glacier advance and retreat. With little to impede their movement across the landscape, the rivers formed by meltwaters are characterized by frequent channel reorganization and unpredictable water flows in response to fluctuating glacier dynamics.[41] Chemically reactive, comminuted sediments, already implicated in the biogeochemical cycles of methane, silica, phosphorus, can then be easily mobilized to downstream ecosystems.[42-46] Regardless of whether actions are taken to reduce atmospheric GHG concentrations, glacier mass loss will continue through the next century, a consequence of past GHG emissions.[2] It is therefore imperative that we understand how glacial meltwaters influence water quality and productivity in downstream ecosystems.

Mercury dynamics in a changing Arctic

Mercury (Hg) is a contaminant of global concern, due to its tendency to bioaccumulate and biomagnify through food webs (as methylmercury, MeHg).[47] The global Hg cycle is highly complex, with Hg naturally present in its elemental (Hg^0) and reduced (Hg(II)) forms, as gaseous, aqueous and solid species. While biogeochemical transformations between these species occur by both abiotic and biologically-mediated processes, the global Hg cycle has been highly influenced by anthropogenic activities.[48] Global anthropogenic Hg emissions increased significantly following the Industrial Revolution largely in consequence of fossil fuel combustion, and other commercial activities, such as mining.[49] Gaseous Hg^0, can be transported over long distances before being deposited to landscapes via either wet (rain and snow) or dry deposition. Due to global atmospheric circulation, Hg is preferentially transported and deposited to the Arctic region, although little Hg is released there.[50, 51]

Arctic Indigenous peoples have long relied upon higher trophic level animals, such as beluga, ringed seal, polar bear and arctic char, as part of a traditional diet.[52, 53] As such, the sources and sinks of neurotoxic MeHg and total mercury (all forms of mercury; THg) in Arctic ecosystems are of special interest. Both glacier melt and permafrost thaw have the potential to release large quantities of MeHg and THg hitherto locked in ice, to downstream ecosystems.[40, 54, 55] Whereas it is unknown how much Hg is stored globally in glaciers and ice sheets, northern latitude (still) frozen permafrost stores are estimated to contain 793±461 Gg THg, more than the atmosphere, oceans, and non-frozen soils combined.[54]

Although global anthropogenic emissions of Hg have declined following the implementation of industrial control technologies in advance of the ratification of the Minamata Convention,[56] atmospheric Hg concentrations have continued to increase or remained stable in the Arctic.[57] Exactly why the Arctic bucks the global trend is yet unknown. However, rivers are the primary source of Hg to the Arctic Ocean, accounting for ~68% of total inputs to surface waters.[58] These rivers drain rapidly changing terrain, impacted by increased precipitation, glacial melt and permafrost thaw, leading to enhanced discharge[17], and potentially, Hg mobilization.[59]

Global consequences of changes in Arctic freshwater quantity and quality

For its size, the Arctic Ocean drains a greater land area than any other ocean.[19] Thus, even though the Arctic Ocean contains only 1% of global ocean volume, it collects more than 11% of

global river discharge.[60] This, combined with the fact that the ocean basin is perennially covered by ice, a portion of which melts every year, make the Arctic Ocean seasonally and spatially dynamic with respect to freshwater distribution, a key feature of the global climate system's thermohaline circulation.[61] Any changes to the quality and quantity of Arctic freshwater inputs to the Arctic Ocean, therefore, could have important consequences that extend far beyond the Arctic itself.[62] Naturally then, being able to predict changes in global climate and marine biogeochemical processes requires a thorough understanding of what is happening across Arctic watersheds, a still novel approach in Arctic ecosystem science.[19]

The Lake Hazen watershed as a model system

Within this context, I used the Lake Hazen watershed, on northern Ellesmere Island, in Quttinirpaaq National Park (81.8°N, 71.4°W) (Figure 1-2) as a model system to explore the impacts of climate change on freshwater quality and productivity across a proglacial freshwater network. The Lake Hazen watershed has been a protected area since 1988, and is thus ideally suited to study the impacts of climate change on freshwaters in the absence of significant direct human influence.

Glacial history of the Lake Hazen watershed

During the last glacial maximum, the Lake Hazen watershed was entirely covered by the cold-based ice of the Innuitian Ice Sheet, originating from the Grant Land Mountains.[63] Cycles of glacier advance and retreat across the area were highly dynamic, involving the coalescence of ice centres from the Grant Land Mountains, the (now) Agassiz Ice Cap and the Greenland Ice Sheet. Retreat of the ice covering Lake Hazen itself began around 6000 years before present, with complete ice retreat from the surface of the lake by 4980±70 years ago.[64]

Lake Hazen today

While the Thule people long used the summertime bounty in the Lake Hazen watershed, American Lt. Adolphus Greely and the ill-fated Lady Franklin Bay Expedition first recorded the resources in the region during the First International Polar Year in 1882. Established in 1957-58 under the auspices of the Canada Defence Research Board, the Lake Hazen camp is now one of three stations in Quttinirpaaq National Park, the second largest national park in Canada, founded in 2000. Recent research in the watershed has largely focused on the productive small lakes and ponds adjacent to Lake Hazen (e.g., [65-68]) and on the terrestrial polar semi-desert ecosystems

(e.g., [69-72]), leaving Lake Hazen itself and the glacier-fed rivers that drain into it largely unexplored, despite arguably being the defining hydrological features of the watershed.

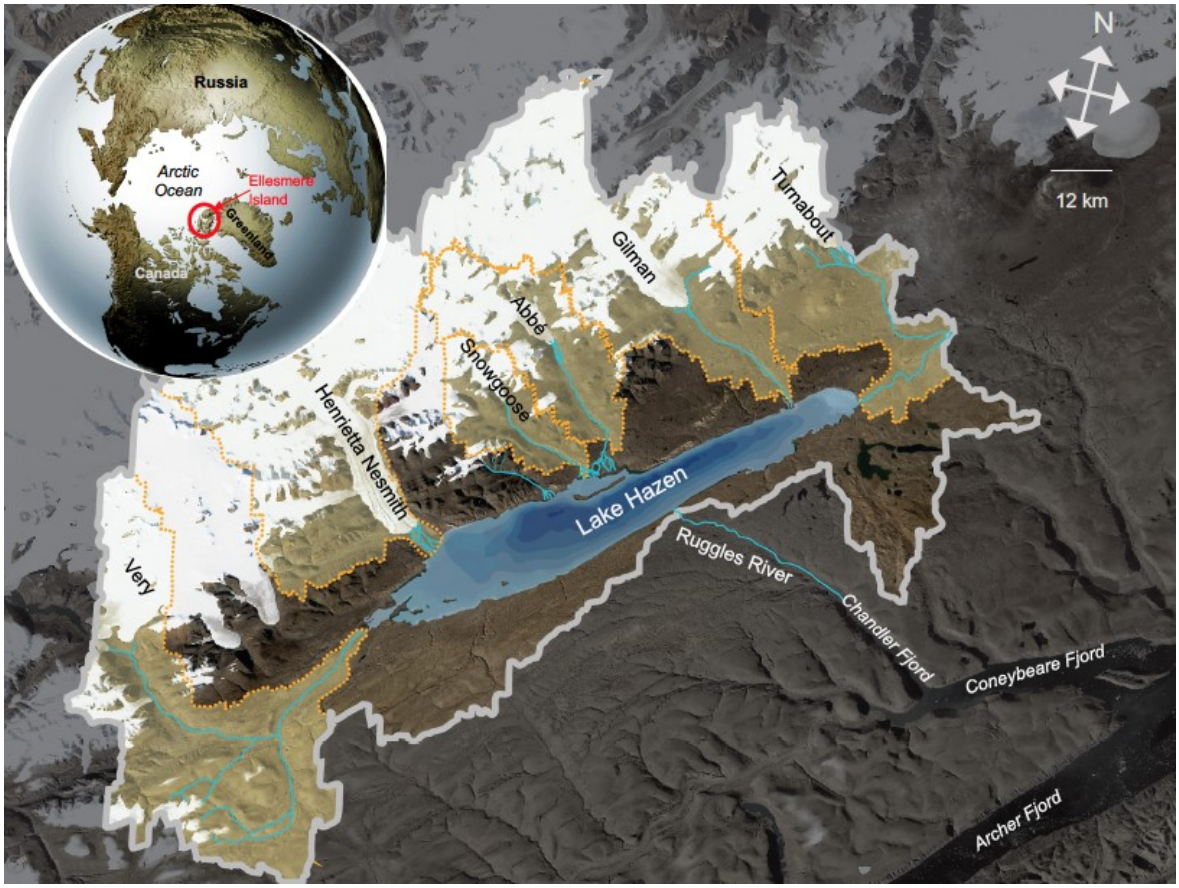

Figure 1-2. General map of the Lake Hazen watershed (grey outline), on northern Ellesmere Island (location shown in inset map). Major hydrologic features are identified in the watershed, as well as the glaciers (sub-watersheds delineated in orange) whose outflows were sampled as part of these studies.

Objectives

To address these knowledge gaps in our understanding of northern freshwater systems, the overarching aim of my doctoral thesis is to quantify the impacts of glacial melt and permafrost thaw on downstream aquatic ecosystems. My research focused on watershed inputs to the lake primarily from snow and glacial meltwater, and to a lesser extent, permafrost thaw waters, as well as in-lake (water column and sedimentary) biogeochemical processes. Lake waters are linked to adjacent terrestrial ecosystems, the sediments and the atmosphere by overland water flow, exchange across the sediment-water interface and exchange with the atmosphere, respectively (Figure 1-3). Thus, no compartment within the watershed is ever truly isolated from

the others and together the processes that link these compartments determine not only water quality, but also whole watershed productivity.

Despite recognizing the magnitude of the changes occurring on High Arctic landscapes, little work has been done to understand freshwater quality across the entire proglacial freshwater network. Moreover, we know little about the impacts of glacial meltwater inputs on freshwater quality and productivity in the High Arctic. Using the Lake Hazen watershed as a model system to address these shortcomings, my research program had three specific objectives:

1. To describe the physical, chemical and biological limnology of major freshwater systems (glacier-fed inflow rivers, Lake Hazen itself, Ruggles River outflow) across the Lake Hazen watershed, and identify major sources and sinks of carbon and nutrients across the proglacial freshwater network, from glacier termini to nearshore environments (Chapter 2);
2. To assess whether freshwater systems in the Lake Hazen watershed are net sources or sinks of carbon dioxide (CO_2) to the atmosphere (Chapter 3); and,
3. To quantify the mass balance budget of Hg for the Lake Hazen watershed and in doing so, identify climatically-sensitive High Arctic sources and sinks of Hg (Chapter 4).

Finally, chapter 5 (*General Conclusions*) summarizes the research presented throughout, provides new avenues for research in the field, as well as discussing the implications for global climate change.

Figure 1-3. Conceptual framework of biogeochemical cycles across a glacierized Arctic watershed showing inputs, outputs, and simplified in-river and lake processes. Carbon, C; nitrogen, N; phosphorus, P; iron, Fe; mercury, Hg. Biogeochemical cycles of C, N, P, Fe are described in chapter 2; C dynamics are further detailed in chapter 3; finally, the Hg cycle is quantified in chapter 4.

References

1. Stocker, T. F.; Qin, D.; Plattner, G.-K.; Tignor, M.; Allen, S. K.; Boschung, J.; Nauels, A.; Xia, Y.; Bex, V.; Midgley, P. M., *IPCC 2013: Climate Change 2013: The Physical Science Basis. Contribution of Working Group I to the Fifth Assessment Report of the Intergovernmental Panel on Climate Change*. Cambridge University Press: Cambridge, UK and New York, NY, USA, 2013; p 1535 pp.
2. Marzeion, B.; Kaser, G.; Maussion, F.; Champollion, N., Limited influence of climate change mitigation on short-term glacier mass loss. *Nature Climate Change* **2018,** *8*, 305-308.
3. Duarte, C. M.; Lenton, T. M.; Wadhams, P.; Wassmann, P., Abrupt climate change in the Arctic. *Nature Climate Change* **2012,** *2*, 60.
4. Arrhenius, S. On the influence of carbonic acid in the air upon the temperature of the ground. *The London, Edinburgh, and Dublin Philosophical Magazine and Journal of Science* **1896,** *41*, (251), 237-276.
5. Serreze, M. C.; Barrett, A. P.; Stroeve, J. C.; Kindig, D. M.; Holland, M. M., The emergency of surface-based Arctic amplification. *Cryosphere* **2009,** *3*, 11-19.
6. Screen, J. A.; Simmonds, I., The central role of diminishing sea ice in recent Arctic temperature amplification. *Nature* **2010,** *464*, 1334-1337.
7. Serreze, M. C.; Barry, R. G., Processes and impacts of Arctic amplification: a research synthesis. *Global and Planetary Change* **2011,** *77*, 85-96.
8. Wassmann, P.; Duarte, C. M.; AgustÍ, S.; Sejr, M. K., Footprints of climate change in the Arctic marine ecosystem. *Global Change Biology* **2011,** *17*, (2), 1235-1249.
9. Hill Geoff, B.; Henry Greg H, R., Responses of High Arctic wet sedge tundra to climate warming since 1980. *Global Change Biology* **2010,** *17*, (1), 276-287.
10. Bintanja, R.; Andry, O., Towards a rain-dominated Arctic. *Nature Clim. Change* **2017,** *7*, (4), 263-267.
11. Westermann, S.; Boike, J.; Langer, M.; Schuler, T. V.; Etzelmüller, B., Modeling the impact of wintertime rain events on the thermal regime of permafrost. *The Cryosphere* **2011,** *5*, (4), 945-959.
12. Radić, V.; Bliss, A.; Beedlow, A. C.; Hock, R.; Miles, E.; Cogley, J. G., Regional and global projections of twenty-first century glacier mass changes in response to climate scenarios from global climate models. *Climate Dynamics* **2013,** *42*, (1), 37-58.
13. Huss, M.; Hock, R., Global-scale hydrological response to future glacier mass loss. *Nature Climate Change* **2018**.
14. Dahlke, H. E.; Lyon, S. W.; Stedinger, J. R.; Rosqvist, G.; Jansson, P., Contrasting trends in floods for two sub-arctic catchments in northern Sweden - does glacier presence matter? *Hydrology and Earth System Sciences* **2012,** *16*, 2123-2141.
15. Bliss, A.; Hock, R.; Radić, V., Global response of glacier runoff to twenty-first century climate change. *Journal of Geophysical Research: Earth Surface* **2014,** *119*, (4), 717-730.
16. Lammers, R. B.; Shiklomanov, A. I.; Vörösmarty, C. J.; Fekete, B. M.; Peterson, B. J., Assessment of contemporary Arctic river runoff based on observational discharge records. *J. Geophys. Res. Atmos.* **2001,** *106*, (D4), 3321-3334.
17. Peterson, B. J.; Holmes, R. M.; McClelland, J. W.; Vorosmarty, C. J.; Lammers, R. B.; Shiklomanov, A. I.; Shiklomanov, I. A.; Rahmstorf, S., Increasing river discharge to the Arctic Ocean. *Science* **2002,** *298*, (5601), 2171-2173.

18. Likens, G. E.; Bormann, F. H., Linkages between Terrestrial and Aquatic Ecosystems. *BioScience* **1974,** *24*, (8), 447-456.
19. Prowse, T.; Bring, A.; Mård, J.; Carmack, E. C.; Holland, M.; Instanes, A.; Vihma, T.; Wrona, F. J., Arctic Freshwater Synthesis: Summary of key emerging issues. *Journal of Geophysical Research Biogeosciences* **2015,** *120*, 1887-1893.
20. Bring, A.; Fedorova, I.; Dibike, Y.; Hinzman, L.; Mård, J.; Mernild, S. H.; Prowse, T.; Semenova, O.; Stuefer, S. L.; Woo, M. K., Arctic terrestrial hydrology: A synthesis of processes, regional effects, and research challenges. *J. Geophys. Res. Biogeosci.* **2016,** *121*, (3), 621-649.
21. Wrona, F. J.; Johansson, M.; Culp, J. M.; Jenkins, A.; Mård, J.; Myers-Smith, I. H.; Prowse, T. D.; Vincent, W. F.; Wookey, P. A., Transitions in Arctic ecosystems: Ecological implications of a changing hydrological regime. *J. Geophys. Res. Biogeosci.* **2016,** *121*, (3), 650-674.
22. Cole, J. J.; Prairie, Y. T.; Caraco, N. F.; McDowell, W. H.; Tranvik, L. J.; Striegl, R. G.; Duarte, C. M.; Kortelainen, P.; Downing, J. A.; Middelburg, J. J.; Melack, J., Plumbing the global carbon cycle: Integrating inland waters into the terrestrial carbon budget. *Ecosystems* **2007,** *10*, (1), 171-184.
23. Battin, T. J.; Kaplan, L. A.; Findlay, S.; Hopkinson, C. S.; Marti, E.; Packman, A. I.; Newbold, J. D.; Sabater, F., Biophysical controls on organic carbon fluxes in fluvial networks. *Nature Geoscience* **2008,** *1*, 95.
24. Battin, T. J.; Luyssaert, S.; Kaplan, L. A.; Aufdenkampe, A. K.; Richter, A.; Tranvik, L. J., The boundless carbon cycle. *Nature Geoscience* **2009,** *2*, 598.
25. Hotchkiss, E. R.; Sadro, S.; Hanson, P. C., Toward a more integrative perspective on carbon metabolism across lentic and lotic inland waters. *Limnology and Oceanography Letters* **2018,** *3*, (3), 57-63.
26. Maranger, R.; Jones Stuart, E.; Cotner James, B., Stoichiometry of carbon, nitrogen, and phosphorus through the freshwater pipe. *Limnology and Oceanography Letters* **2018,** *3*, (3), 89-101.
27. Weyhenmeyer, G. A.; Conley, D. J., Large differences between carbon and nutrient loss rates along the land to ocean aquatic continuum—implications for energy:nutrient ratios at downstream sites. *Limnology and Oceanography* **2017**, S183-S193.
28. Tranvik, L. J.; Downing, J. A.; Cotner, J. B.; Loiselle, S. A.; Striegl, R. G.; Ballatore, T. J.; Dillon, P.; Finlay, K.; Fortino, K.; Knoll, L. B.; Kortelainen, P. L.; Kutser, T.; Larsen, S.; Laurion, I.; Leech, D. M.; McCallister, S. L.; McKnight, D. M.; Melack, J. M.; Overholt, E.; Porter, J. A.; Prairie, Y.; Renwick, W. H.; Roland, F.; Sherman, B. S.; Schindler, D. W.; Sobek, S.; Tremblay, A.; Vanni, M. J.; Verschoor, A. M.; von Wachenfeldt, E.; Weyhenmeyer, G. A., Lakes and reservoirs as regulators of carbon cycling and climate. *Limnology and Oceanography* **2009,** *54*, (6), 2298-2314.
29. Harrison, J. A.; Maranger, R. J.; Alexander, R. B.; Giblin, A. E.; Jacinthe, P.-A.; Mayorga, E.; Seitzinger, S. P.; Sobota, D. J.; Wollheim, W. M., The regional and global significance of nitrogen removal in lakes and reservoirs. *Biogeochemistry* **2009,** *93*, (1), 143-157.
30. Adrian, R.; O'Reilly Catherine, M.; Zagarese, H.; Baines Stephen, B.; Hessen Dag, O.; Keller, W.; Livingstone David, M.; Sommaruga, R.; Straile, D.; Van Donk, E.; Weyhenmeyer Gesa, A.; Winder, M., Lakes as sentinels of climate change. *Limnology and Oceanography* **2009,** *54*, (6part2), 2283-2297.

31. Carpenter, S. R.; Cottingham, K. L., Resilience and Restoration of Lakes. *Conservation Ecology* **1997,** *1*, (1), 2.
32. Magnuson, J. J.; Robertson, D. M.; Benson, B. J.; Wynne, R. H.; Livingstone, D. M.; Arai, T.; Assel, R. A.; Barry, R. G.; Card, V.; Kuusisto, E.; Granin, N. G.; Prowse, T. D.; Stewart, K. M.; Vuglinski, V. S., Historical trends in lake and river ice cover in the Northern Hemisphere. *Science* **2000,** *289*, (5485), 1743-1746.
33. Latifovic, R.; Pouliot, D., Analysis of climate change impacts on lake ice phenology in Canada using the historical satellite data record. *Remote Sensing of Environment* **2007,** *106*, (4), 492-507.
34. Roberts, K. E.; Lamoureux, S. F.; Kyser, T. K.; Muir, D. C. G.; Lafrenière, M. J.; Iqaluk, D.; Pieńkowski, A. J.; Normandeau, A., Climate and permafrost effects on the chemistry and ecosystems of High Arctic Lakes. *Scientific Reports* **2017,** *7*, (1), 13292.
35. Lehnherr, I.; St. Louis, V. L.; Muir, D. C. G.; Sharp, M. J.; Gardner, A. S.; Lamoureux, S.; Smol, J. P.; St. Pierre, K. A.; Michelutti, N.; Schiff, S. L.; Emmerton, C. A.; Tarnocai, C.; Talbot, C., The world's largest High Arctic lake responds rapidly to climate warming. *Nature Commun.* **2018,** *9*, 1290.
36. Tranter, M.; Wadham, J. L., 7.5 - Geochemical Weathering in Glacial and Proglacial Environments A2 - Holland, Heinrich D. In *Treatise on Geochemistry (Second Edition)*, Turekian, K. K., Ed. Elsevier: Oxford, 2014; pp 157-173.
37. Hawes, I.; Howard-Williams, C.; Fountain, A. G., Ice-based freshwater ecosystems. In *Polar Lakes and Rivers: Limnology of Arctic and Antarctic Aquatic Ecosystems*, Vincent, W. F.; Laybourn-Parry, J., Eds. Oxford University Press: New York, NY, 2008; pp 103-118.
38. Milner, A. M.; Khamis, K.; Battin, T. J.; Brittain, J. E.; Barrand, N. E.; Füreder, L.; Cauvy-Fraunié, S.; Gíslason, G. M.; Jacobsen, D.; Hannah, D. M.; Hodson, A. J.; Hood, E.; Lencioni, V.; Ólafsson, J. S.; Robinson, C. T.; Tranter, M.; Brown, L. E., Glacier shrinkage driving global changes in downstream systems. *Proceedings of the National Academy of Sciences* **2017,** *114*, (37), 9770-9778.
39. Hood, E.; Battin, T. J.; Fellman, J.; O'Neel, S.; Spencer, R. G. M., Storage and release of organic carbon from glaciers and ice sheets. *Nature Geoscience* **2015,** *8*, (2), 91-96.
40. Zdanowicz, C.; Krummel, E. M.; Lean, D.; Poulain, A. J.; Yumvihoze, E.; Chen, J. B.; Hintelmann, H., Accumulation, storage and release of atmospheric mercury in a glaciated Arctic catchment, Baffin Island, Canada. *Geochim. Cosmochim. Acta* **2013,** *107*, 316-335.
41. Malard, F.; Uehlinger, U.; Zah, R.; Tockner, K., Flood-pulse and riverscape dynamics in a braided glacial river. *Ecology* **2006,** *87*, (3), 704-716.
42. Telling, J.; Boyd, E. S.; Bone, N.; Jones, E. L.; Tranter, M.; MacFarlane, J. W.; Martin, P. G.; Wadham, J. L.; Lamarche-Gagnon, G.; Skidmore, M. L.; Hamilton, T. L.; Hill, E.; Jackson, M.; Hodgson, D. A., Rock comminution as a source of hydrogen for subglacial ecosystems. *Nature Geosci.* **2015,** *8*, (11), 851-+.
43. Wadham, J. L.; Hawkings, J.; Telling, J.; Chandler, D.; Alcock, J.; O'Donnell, E.; Kaur, P.; Bagshaw, E.; Tranter, M.; Tedstone, A.; Nienow, P., Sources, cycling and export of nitrogen on the Greenland Ice Sheet. *Biogeosciences* **2016,** *13*, (22), 6339-6352.
44. Hawkings, J.; Wadham, J.; Tranter, M.; Telling, J.; Bagshaw, E.; Beaton, A.; Simmons, S. L.; Chandler, D.; Tedstone, A.; Nienow, P., The Greenland Ice Sheet as a hot spot of phosphorus weathering and export in the Arctic. *Global Biogeochemical Cycles* **2016,** *30*, (2), 191-210.

45. Hawkings, J. R.; Wadham, J. L.; Benning, L. G.; Hendry, K. R.; Tranter, M.; Tedstone, A.; Nienow, P.; Raiswell, R., Ice sheets as a missing source of silica to the polar oceans. *Nature Commun.* **2017,** *8*.
46. Hawkings, J. R.; Wadham, J. L.; Tranter, M.; Raiswell, R.; Benning, L. G.; Statham, P. J.; Tedstone, A.; Nienow, P.; Lee, K.; Telling, J., Ice sheets as a significant source of highly reactive nanoparticulate iron to the oceans. *Nature Communications* **2014,** *5*.
47. Lehnherr, I., Methylmercury biogeochemistry: a review with special reference to Arctic aquatic ecosystems. *Environmental Reviews* **2014,** *22*, (3), 229-243.
48. Selin, N. E., Global Biogeochemical Cycling of Mercury: A Review. *Annual Review of Environment and Resources* **2009,** *34*, (1), 43-63.
49. Streets, D. G.; Devane, M. K.; Lu, Z.; Bond, T. C.; Sunderland, E. M.; Jacob, D. J., All-Time Releases of Mercury to the Atmosphere from Human Activities. *Environmental Science & Technology* **2011,** *45*, (24), 10485-10491.
50. Durnford, D.; Dastoor, A.; Figuera-Nieto, D.; Ryjkov, A., Long range transport of mercury to the Arctic and across Canada. *Atmos. Chem. Phys.* **2010,** *10*, 6063-6086.
51. Lim, C.-J.; Cheng, M.-D.; Schroeder, W. H., Transport patterns and potential sources of total gaseous mercury measured in Canadian high Arctic in 1995. *Atmospheric Environment* **2001,** *35*, (6), 1141-1154.
52. Chan, H. M.; Kim, C.; Khoday, K.; Receveur, O.; Kuhnlein, H. V., Assessment of dietary exposure to trace-metals in Baffin Inuit food. *Environmental Health Perspectives* **1995,** *103*, (7-8), 740-746.
53. Laird, B. D.; Goncharov, A. B.; Egeland, G. M.; Chan, H. M., Dietary Advice on Inuit Traditional Food Use Needs to Balance Benefits and Risks of Mercury, Selenium, and n3 Fatty Acids. *J. Nutr.* **2013,** *143*, (6), 923-930.
54. Schuster, P. F.; Schaefer, K. M.; Aiken, G. R.; Antweiler, R. C.; Dewild, J. F.; Gryziec, J. D.; Gusmeroli, A.; Hugelius, G.; Jafarov, E.; Krabbenhoft, D. P.; Liu, L.; Herman - Mercer, N.; Mu, C.; Roth David, A.; Schaefer, T.; Striegl, R. G.; Wickland, K. P.; Zhang, T., Permafrost Stores a Globally Significant Amount of Mercury. *Geophysical Research Letters* **2018,** *45*, (3), 1463-1471.
55. Schuster, P. F.; Striegl, R. G.; Aiken, G. R.; Krabbenhoft, D. P.; Dewild, J. F.; Butler, K.; Kamark, B.; Dornblaser, M., Mercury Export from the Yukon River Basin and Potential Response to a Changing Climate. *Environ. Sci. Technol.* **2011,** *45*, (21), 9262-9267.
56. Zhang, Y.; Jacob, D. J.; Horowitz, H. M.; Chen, L.; Amos, H. M.; Krabbenhoft, D. P.; Slemr, F.; St. Louis, V. L.; Sunderland, E. M., Observed decrease in atmospheric mercury explained by global decline in anthropogenic emissions. *PNAS* **2016,** *113*, (3), 526-531.
57. Cole, A. S.; Steffen, A.; Eckley, C. S.; Narayan, J.; Pilote, M.; Tordon, R.; Graydon, J. A.; St. Louis, V. L.; Xu, X.; Branfireun, B., A Survey of Mercury in Air and Precipitation across Canada: Patterns and Trends. *Atmosphere* **2014,** *5*, 635-668.
58. Fisher, D.; Zheng, J.; Burgess, D.; Zdanowicz, C.; Kinnard, C.; Sharp, M.; Bourgeois, J., Recent melt rates of Canadian arctic ice caps are the highest in four millennia. *Global and Planetary Change* **2012,** *84–85*, 3-7.
59. Fisher, J. A.; Jacob, D. J.; Soerensen, A. L.; Amos, H. M.; Steffen, A.; Sunderland, E. M., Riverine source of Arctic Ocean mercury inferred from atmospheric observations. *Nature Geoscience* **2012,** *5*, (7), 499-504.
60. Shiklomanov, I. A.; Shiklomanov, A. I.; Lammers, R. B.; Peterson, B. J.; Vorosmarty, C. J., The Dynamics of River Water Inflow to the Arctic Ocean. In *The Freshwater Budget of the*

Arctic Ocean, Lewis, E. L.; Jones, E. P.; Lemke, P.; Prowse, T. D.; Wadhams, P., Eds. Springer Netherlands: Dordrecht, 2000; pp 281-296.
61. Carmack, E. C.; Yamamoto-Kawai, M.; Haine, T. W. N.; Bacon, S.; Bluhm, B. A.; Lique, C.; Melling, H.; Polyakov, I. V.; Straneo, F.; Timmermans, M. L.; Williams, W. J., Freshwater and its role in the Arctic Marine System: Sources, disposition, storage, export, and physical and biogeochemical consequences in the Arctic and global oceans. *J. Geophys. Res. Biogeosci.* **2016,** *121*, (3), 675-717.
62. Vellinga, M.; Wood, R. A., Global Climatic Impacts of a Collapse of the Atlantic Thermohaline Circulation. *Climatic Change* **2002,** *54*, (3), 251-267.
63. England, J.; Atkinson, N.; Bednarski, J.; Dyke, A. S.; Hodgson, D. A.; Ó Cofaigh, C., The Innuitian Ice Sheet: configuration, dynamics and chronology. *Quaternary Science Reviews* **2006,** *25*, (7), 689-703.
64. Smith, I. R., Late Quaternary glacial history of Lake Hazen Basin and eastern Hazen Plateau, northern Ellesmere Island, Nunavut, Canada. *Canadian Journal of Earth Sciences* **1999,** *36*, (9), 1547-1565.
65. Emmerton, C. A.; St Louis, V. L.; Lehnherr, I.; Graydon, J. A.; Kirk, J. L.; Rondeau, K. J., The importance of freshwater systems to the net atmospheric exchange of carbon dioxide and methane with a rapidly changing high Arctic watershed. *Biogeosciences* **2016,** *13*, (20), 5849-5863.
66. Lehnherr, I.; St Louis, V. L.; Kirk, J. L., Methylmercury Cycling in High Arctic Wetland Ponds: Controls on Sedimentary Production. *Environ. Sci. Technol.* **2012,** *46*, (19), 10523-10531.
67. Lehnherr, I.; St Louis, V. L.; Emmerton, C. A.; Barker, J. D.; Kirk, J. L., Methylmercury Cycling in High Arctic Wetland Ponds: Sources and Sinks. *Environ. Sci. Technol.* **2012,** *46*, (19), 10514-10522.
68. Keatley, B. E.; Douglas, M. S. V.; Smol, J. P., Prolonged ice cover dampens diatom community responses to recent climatic change in High Arctic lakes. *Arctic Antarctic and Alpine Research* **2008,** *40*, (2), 364-372.
69. Emmerton, C. A.; St Louis, V. L.; Humphreys, E. R.; Gamon, J. A.; Barker, J. D.; Pastorello, G. Z., Net ecosystem exchange of CO2 with rapidly changing high Arctic landscapes. *Global Change Biology* **2016,** *22*, (3), 1185-1200.
70. Emmerton, C. A.; St. Louis, V. L.; Lehnherr, I.; Humphreys, E. R.; Rydz, E.; Kosolofski, H. R., The net exchange of methane with high Arctic landscapes during the summer growing season. *Biogeosciences* **2014,** *11*, (12), 3095-3106.
71. Panchen, Z. A., Arctic plants produce vastly different numbers of flowers in three contrasting years at Lake Hazen, Quttinirpaaq National Park, Ellesmere Island, Nunavut, Canada. *The Canadian Field-Naturalist* **2016,** *130*, (1), 56-63.
72. Panchen, Z. A.; Gorelick, R., Canadian Arctic Archipelago Conspecifics Flower Earlier in the High Arctic than the Mid-Arctic. *International Journal of Plant Sciences* **2016,** *177*, (8), 661-670.

Chapter 2. The land-to-ocean aquatic continuum in a glacierized High Arctic watershed: biogeochemical impacts of glacial melt

INTRODUCTION

Global glacier (non-ice sheet) volume is expected to decline by 29-41% by 2100,[1] with coincident changes to downstream runoff.[2, 3] This loss is particularly important at high northern latitudes, where ~58% of the world's glaciers are located[4] and climate change is predicted to be most intense.[5] Glaciers are important archives of nutrients[6] and contaminants[7, 8] transported and deposited to high latitude regions over centuries or millennia. Thus, as glaciers melt, they become important sources of these compounds to downstream ecosystems. Further, as meltwaters travel across poorly consolidated proglacial zones, they can entrain large quantities of fine, chemically reactive sediments.[9, 10] Whereas the direct impacts of glacial melt on the biogeochemistry of nearshore marine environments has been highlighted,[11-13] we understand little of the hydrological-biogeochemical coupling across changing Arctic landscapes, which hinders our ability to predict the consequences of climate change on valuable northern freshwater function, resources and services. In more temperate latitudes, for example, it is well established that freshwater quality changes dramatically in response to biological (e.g., primary production, respiration), physical (e.g., sediment burial) and chemical processes (e.g., oxidation, reduction) as water flows across landscapes on its way to the ocean.[14]

The land to ocean aquatic continuum (LOAC) framework acknowledges these inherent connections between terrestrial, freshwater and marine systems.[15] The LOAC framework has hitherto only been applied in temperate forested and agricultural watersheds (e.g., [14, 16]) and has focused primarily on rivers and streams, even though lakes are integral parts of the continuum, acting to retain and process nutrients before waters flow further downstream.[14, 17, 18] In glacierized watersheds, lakes are becoming increasingly dynamic components of the LOAC as their area and numbers increase globally in response to rapid glacial melt.[19, 20] The documented function of proglacial lakes, though, has been limited to sediment retention,[21] thus potentially underestimating their overall importance in modifying glacial meltwaters. These proglacial lakes are typically located in sparsely vegetated catchments with poorly developed soils, which limits allochthonous carbon inputs but facilitates the entrainment of easily mobilized mineral sediments and nutrients.

Here we use the Lake Hazen watershed (82°N) as a model system to examine a High Arctic LOAC, from glacial headwaters through proglacial river valleys, into a large lake that then drains out to the coast (Figure 2-1). Our objectives were to: (1) describe the physical, chemical and biological limnology of a glacierized LOAC; (2) quantify the impact of in-lake processing of glacial meltwaters using hydrological input-output budgets; (3) describe water column primary productivity and sediment microbial processes in relation to glacial inputs, (4) apply ecosystem stoichiometry to identify locations of nutrient mobilization and retention across the glacierized LOAC. This study focuses primarily on the biogeochemical processing of carbon and macronutrients within the system (nitrogen, phosphorus), but total iron (TFe) and dissolved silica ($dSiO_2$) are also discussed. Sulfate (SO_4^{2-}) is presented as a conservative tracer throughout.

MATERIALS AND METHODS

Site description

The Lake Hazen watershed, located within Quttinirpaaq National Park on northern Ellesmere Island, Nunavut, Canada (81.8°N, 71.4° W) is 7516 km^2 in area, 40.9% of which is covered by outlet glaciers of the Northern Ellesmere Icefield. In summer, glacial meltwaters form braided rivers that flow between 4.6 and 42 km into Lake Hazen along its northwestern shore (Figure 2-1). Lake Hazen itself sits at 157 m.a.s.l., and with a surface area of 544 km^2 and maximum depth of 267 m, is the world's largest High Arctic lake by volume (51.4 km^3).[22] Ice cover on the lake begins to melt in early June, with complete ice loss, if it occurs, persisting from the end of July or early August to at least mid-September.[23] The southeastern shoreline of the lake rapidly ascends to the Hazen Plateau (300-1000 m.a.s.l.), which lacks major ice or water features.[24] The Ruggles River (~29 km) flows year-round from Lake Hazen into Chandler Fjord on the northeastern coast of Ellesmere Island.

The watershed is a polar semi-desert receiving little precipitation throughout the year (~95 mm),[25] ~65% of which falls as snow between September and May with the remainder as rain in the summer.[26] Snowmelt on the lake surface and adjacent landscape occurs over a 1-2-week period in early June. Meltwaters from the outlet glaciers of the Northern Ellesmere Icefield are by far the dominant hydrological input to the lake (Table 2-1), flowing between mid-June and the end of August. Small permafrost and ground-ice fed streams are found across the landscape but are hydrologically inconsequential at the watershed scale.[23] Base flow in the Ruggles River is ~5

m^3 s^{-1}, increasing up to two orders of magnitude at the height of melt in mid-late July (Water Survey Canada station 10VK001, 1996-2012) to approximate glacial river inputs to Lake Hazen.[23] The hydrograph of the outflow lags that of the combined inflows, though, such that Ruggles River discharge does not return to baseline until November or December, long after the glacial rivers cease flowing.

Sampling campaigns for this study were completed in spring (May/June) 2013, 2014, 2015 and 2017, and summers (July/August) 2015 and 2016 (Table A1-1).

Hydrological input-output budgets

To understand the biogeochemical cycling of key nutrients across the Lake Hazen watershed, we constructed annual hydrological input-output budgets as follows:

$$\Delta\text{Storage}_{\text{C, N, P, Si, Fe}} = \sum \text{Outputs}_{\text{C, N, P, Si, Fe}} - \sum \text{Inputs}_{\text{C, N, P, Si, Fe}}$$

∑Inputs into Lake Hazen included snowmelt on the lake surface, snowmelt runoff from the landscape, and glacier melt from the Northern Ellesmere Icefield. Hydrological inputs from small permafrost and ground-ice fed streams were inconsequential at the watershed scale. ∑Outputs from Lake Hazen is the export of nutrients via the Ruggles River. By convention, a negative ΔStorage indicates that Lake Hazen is a net sink (inputs exceed outputs) and a positive ΔStorage indicates that Lake Hazen is a net source (outputs exceed inputs) of the studied compounds. For each compartment within the watershed, we multiplied nutrient concentrations by water fluxes. This approach was applied to dissolved inorganic nitrogen species (DIN = NH_4^+ and NO_3^--NO_2^-), SO_4^{2-}, $dSiO_2$, dissolved organic carbon (DOC) and dissolved inorganic carbon (DIC). We could not estimate the budgets of particulate constituents (total carbon, TC; total phosphorus, TP; total nitrogen, TN; particulate nitrogen/carbon, PN/PC; total iron, TFe) due to challenges associated with quantifying the glacial flux component of these budgets for particulate parameters, described below. TC is calculated here as the sum of DIC, DOC and PC.

Inputs to Lake Hazen

Snowmelt on the lake surface and from the adjacent landscape.

Integrated snowpack samples were collected from the lake surface (20 sites total) and on the adjacent landscape (13 sites total) in May 2013, 2015 and 2017 using an acid-washed 4.3 cm diameter stainless steel corer. Snow samples were placed in large Ziploc freezer bags pretested for analyte contamination and kept frozen until processing in the Canadian Association for Laboratory Accreditation (CALA)-certified Biogeochemical Analytical Service Laboratory (BASL) at the University of Alberta. All samples were melted at room temperature before sub-sampling and processing as water samples.

Site-specific areal water volumes (AWV; L/m^2) were determined from the weight of three snow cores and the diameter of the corer as follows:

$$\text{AWV}\left(\text{L m}^{-2}\right) = \frac{\text{snow weight (kg, assuming 1 kg = 1 L)}}{\pi(\text{corer radius (m)})^2}$$

Snowmelt samples were collected from 3 streams in June 2017 only (n=4 samplings). Temperature, pH, dissolved oxygen, and turbidity were measured continuously during sampling using an YSI EXO2 sonde. Bulk water samples were collected by dipping acid-washed 1-L Nalgene bottles and/or Platypus bags into the stream. Streams were sampled for the full suite of chemical constituents. Snowmelt runoff volumes were estimated by applying the mean ratio of SO_4^{2-} concentrations in snowpacks and snowmelt in 2017, to the landscape AWV, and assuming all SO_4^{2-} was conserved in the snowpack during melt.

Snow conditions were similar across all three years sampled, as well as for 2016, when snow was not collected (A. Ferguson, *personal communication*). For hydrological budget purposes, we applied 2015 AVW and snow chemistry to the 2015 budget and mean 2013, 2015, 2017 AVW and snow chemistry to the 2016 budget. Snow meltwater chemistry from 2017 was applied to snowmelt runoff volumes calculated from landscape AVW and the runoff ratio, as estimated above.

Glacial meltwater rivers.

Water samples from the deltas of seven glacial inflow rivers (Snowgoose, Blister, Abbé, Gilman, Turnabout, Henrietta Nesmith, Very) were collected in summers 2015 and 2016 (Figure 2- 1). The Blister and Snowgoose rivers, which were within hiking distance of the base camp, were

sampled weekly in both summers to assess seasonal variations in glacial river inputs to Lake Hazen (n=5 in 2015 and n=6 in 2016). The remaining glacial inflow rivers and the Ruggles River were accessed by helicopter once in 2015 (15-July) and twice in 2016 (11-13 July; 1-2-August). To assess biogeochemical changes along the length of the rivers, water samples were also collected at three sites between the glacier termini and Lake Hazen along the Blister, Snowgoose and Gilman rivers, and between Lake Hazen and Chandler Fjord along the Ruggles River. River waters were sampled like snowmelt streams, described above.

River hydrology. The Lake Hazen watershed was divided into glacier sub-catchments for all glacial rivers studied, using the 1:50,000 Canadian Digital Elevation Model (CDEM; Natural Resources Canada) in ArcGIS 10.5. Glacial river discharge for each sub-catchment was then modeled using a glacier surface mass balance approach [27]. The Blister River sub-catchment was too small to delineate using the CDEM, so we applied the modeled runoff from the nearby Snowgoose Glacier (in kg m^{-2} d^{-1}) to the Blister Ice Cap area from the Randolph Glacier Inventory (6 km^2)[4] as an estimate of Blister River discharge.

Chemical constituent fluxes. We generated log-linear models relating river discharge to chemical loads using the *rloadest* package in R.[28, 29] Daily modeled water discharge for each of the rivers were combined with measured concentrations of the dissolved chemical species in each river (SO_4^{2-}, NH_4^+, NO_3^--NO_2^-, $dSiO_2$, DOC). LOADEST model 1 or 2 was selected for each parameter, depending on which iteration minimized bias, while maximizing explanatory power (Table A1-2). Bias across all models was less than 16%, and all models were statistically significant ($R^2 > 0.94$, $p < 0.001$).

Only hydrological input-output budgets for dissolved constituents could be reliably calculated, which unfortunately precludes our ability to calculate budgets for bulk or particulate parameters (TP, TN, PN, TC, PC, TFe, TSS). Braided glacial rivers are highly unpredictable, with frequent channel reorganization and episodic bursts of meltwater. As such, although concentrations of particulate parameters were positively correlated with meltwater volumes (e.g., Figure 2- 2), the relationships were highly irregular and resulted in models with high bias and low predictive power. TDP concentrations were below detection in 73% of glacial rivers

samplings, and TDP loads to the lake from glacial inputs could therefore not be reliably calculated.

Hydrological outputs from Lake Hazen – the Ruggles River

The Lake Hazen outflow to the Ruggles River was accessed by helicopter at the same time as the glacial inflows during summers 2015 and 2016. To quantify changes to Lake Hazen outputs along the length of the river, 2 additional sites downstream of Lake Hazen (mid-way down the river and just prior to the waters exiting to Chandler Fjord) were also sampled during the 2016 sampling campaign.

Due to frequent water level sensor failures, Water Survey discontinued continuous gauging of the Ruggles River in 2012. Between 1996-2012, the volume of water exiting Lake Hazen via the gauged Ruggles River was well approximated by the cumulative modeled glacial river inflows.[23] We therefore summed the modelled glacial inflows and the snow meltwater volumes to approximate Ruggles River discharge in the two years presented here. This approach assumes little evaporation along the length of the glacial rivers and from the surface of Lake Hazen, which is ice-covered most of the year.

The Ruggles River is not easily accessible, so we applied mean concentrations of all chemical parameters, combining samplings in springs 2015 and 2017 and summers 2015 and 2016, to the combined discharge to estimate annual Ruggles River exports from Lake Hazen.

Lake sampling

Water column sampling. We sampled the water column of Lake Hazen at its deepest spot (~267 m) from the ice in May/June 2013, 2014, and 2017, and from a boat in August 2015 and 2016 to assess seasonal differences (with and without glacial inputs) in water column chemistry. Two water column profiles were completed in May/June 2014, to assess changes to upper water column chemistry before and after snowmelt. Continuous measurements of temperature, pH, and dissolved oxygen throughout the water column were recorded with a YSI EXO2 sonde. Depth-specific bulk water samples for full chemical analyses and phytoplankton community composition were then collected using an acid-washed 12-L Teflon-lined General Oceanics Niskin bottle. Each time, 15 discrete depths were sampled with a greater focus on upper and bottom waters (0 (or 2 under ice), 5, 10, 15, 25, 50, 75, 100, 150, 200, 225, 235, 240, 245, 250

m), except in 2016 when inclement conditions allowed for only three depths to be safely sampled (0, 15 and 250 m).

Shoreline sampling. Lake waters along the northwestern shoreline of Lake Hazen were sampled weekly during summers 2015 (7-July to 2-August, n=5) and 2016 (2-July to 8-August, n=6) to quantify the nearshore influence of glacial inputs.

Biological community analyses.

Depth-specific phytoplankton samples were collected at the same time as for water column chemistry, using the 12 L General Oceanics Niskin bottle. Samples for phytoplankton analysis were subsequently fixed with ~1mL Lugol's solution (in 50 mL) upon return to base camp and kept cool until analysis. Phytoplankton communities, biomass and cell densities were identified and enumerated following standard protocols by Plankton R Us (Winnipeg MB) (e.g., [30, 31]). Phytoplankton were identified to at least genus, and species when possible for historical record purposes, and then grouped according to major taxonomic group (cyanobacteria, chlorophyte, euglenophyte, chrysophyte, diatom, cryptophyte, dinoflagellate) for analyses here.

Relative influences of physicochemical variables on phytoplankton community composition were quantified using redundancy analysis (RDA),[32] with the package *vegan.* [33] The eigenvalue of the first ordination axis in a preliminary correspondence analysis on the environmental variables was less than 0.6, supporting the use of linear methods and the RDA.[32] Environmental variables were standardized before running the saturated model and taxonomic cell density or biomass, proxies for growth or abundance, respectively, were Hellinger-transformed. The model was then run on the response covariance matrix. Variance inflation factors for environmental variables in the saturated model were greater than 10, indicating serial autocorrelation within the full model, and justifying our use of stepwise forward selection to identify the most parsimonious model using Akaike Information Criterion. Results presented herein are for the reduced models only.

Zooplankton were collected in spring 2014 and summer 2015 using a Dynamic Aqua 80 μm Wisconsin-style plankton net from the upper 75 m of the water column, and subsequently preserved with ethanol. In spring 2014, zooplankton were identified at Queen's University (S. Arnott), while in summer 2015, zooplankton were identified by Plankton R Us.

The state of the arctic char (*Salvelinus alpinus*) population, the only fish species in Lake Hazen, has been described in detail elsewhere (e.g., [34-39]).

Biogeochemical processes in Lake Hazen sediments

To assess the impacts of glacial meltwater inputs on heterotrophic processes in lake sediments, sediment cores with intact sediment-water interfaces were collected in August 2016 and May/June 2017 using a UWITEC gravity corer (UWITEC, Mondsee, Austria) and 8.6 cm diameter polyvinyl chloride core tubes. Coring sites were chosen to encompass a variety of water depths and proximities to glacial river inflows (Table A1-3). Cores were collected at shallow (~50 m) and deep (~250 m) sites adjacent to the deltas of the Snowgoose-Abbé (S1, S2 in Figure 2- 1) and Blister (S3, S4) rivers, to represent high and low sediment inputs, respectively. We also sampled an additional shallow site near the Ruggles River outflow (S5) that received virtually no direct terrestrial runoff. Two cores were collected at each site.

Immediately upon return to base camp, 100-µm resolution microprofiles of O_2, redox and pH were quantified on one of the cores using Unisense glass microelectrodes interfaced with the Unisense Field Multimeter. Cores were maintained at ambient temperatures (~4°C) throughout profiling. Microprofiles were begun either 1 or 2 cm above the sediment-water interface. Following microprofiling, the core was sectioned at 1 cm intervals to estimate porosity (φ) by weighing sections before and after freeze-drying, assuming all voids were water-filled prior to drying:

$$\varphi = \text{Volume}_{\text{voids}}/\text{Volume}_{\text{total}}$$

Porewaters were extracted from the second core also upon return to the base camp. 1 cm core sections were placed in 50 ml centrifuge tubes, the headspace flushed with UHP N_2 and centrifuged for 15 minutes at 4000 rpm. The supernatant was then filtered through 0.45-µm C/N filters into 15 ml centrifuge tubes and immediately frozen for analysis of NO_3^--NO_2^-, NH_4^+, and TDP (Table A1-4). The remaining sediments were freeze-dried and analyzed for organic carbon (OC) by loss-on-ignition.[40]

Sediment oxygen consumption rates were then estimated using the application PROFILE, which implements a numerical solution.[41] Sediment diffusion coefficients (D_s) were calculated using:

$$D_s = D_0/(1+3*(1-\varphi))$$

where D_0 is the temperature-specific (3.76°C at 250 m depth, n = 7 profiles) diffusion coefficient in water, and φ is the depth interval-specific porosity. For sediment cores from sites S1-3, where oxygen was completely consumed over the profile, the bottom concentration (0 µmol L^{-1}) and bottom flux (0 nmol cm^{-2} s^{-1}) were selected as boundary conditions. For the other sites (S4-5), the site-specific top and bottom concentrations were chosen as boundary conditions.

Sample processing and chemical analyses

All samples were initially processed the day of collection in the analytical room of the Lake Hazen/Quttinirpaaq Field Laboratory, located at Parks Canada's Lake Hazen Base Station. Upon return to base camp, water samples for DIN, TDP, SO_4^{2-}, $dSiO_2$, DIC, and DOC were filtered through 0.45-µm cellulose/nitrate (C/N) filters. Known volumes of water were filtered through muffled 0.7-µm GF/F filters for particulate carbon and nitrogen (PC and PN) analyses and pre-weighed 0.45-µm cellulose acetate filters for total suspended solids (TSS), analyses. Bulk water samples were collected for total phosphorus (TP) and total nitrogen (TN) analysis. For lake water samples, known volumes of water were also filtered through ethanol-washed 0.7-µm GF/F filters for chlorophyll *a* (chl *a*) concentrations. Samples were stored either frozen (chlorophyll *a*, NH_4^+, NO_3^--NO_2^-) or in the dark at ~4°C (all other samples) until transported south for analysis.

All chemical analyses were subsequently completed at the Canadian Association of Laboratory Accreditation (CALA)-certified Biogeochemical Analytical Service Laboratory (BASL) at the University of Alberta (Edmonton, Alberta, Canada) following standard operating procedures (Table A1-1). For statistical purposes, analyte concentrations less than the method detection limit (<D.L.) were quantified as half of the D.L. (Table A1-1). Standard errors (SE) are presented throughout, unless otherwise stated.

RESULTS AND DISCUSSION

Watershed hydrology

Total hydrological inputs to the lake were 1.063±0.027 km^3 in 2015 and 0.400±0.097 km^3 in 2016. Mean annual snowmelt inputs were 0.079±0.013 km^3 over the lake area, assuming no sublimation (Table 2-1), while landscape (non-glacierized, non-lake area) snowmelt contributions to Lake Hazen were 0.075±0.025 km^3 (means of 2013, 2015, 2017). The dominant

annual input was thus glacial runoff, accounting for approximately 86.7% and 67.1% of annual hydrological inputs in 2015 and 2016, respectively. Total glacial runoff was 3.37-times greater in 2015 (0.979 km^3) than in 2016 (0.291 km^3). Three glacial rivers (Henrietta Nesmith, Gilman and Very) cumulatively accounted for ~70% of glacial runoff into Lake Hazen. With cold-based margins, most of the meltwaters from the Northern Ellesmere Icefield flow along the top of the glaciers and ice marginal channels before being discharged to the proglacial zone, thus limiting contact with glacier beds. Complete ice-off on Lake Hazen occurred around 4-Aug-2015 and 8-Aug-2016 in the two summer study years.

Nutrient concentrations in major hydrological inputs to Lake Hazen

Snowmelt on the lake and from the landscape. Snow was slightly alkaline (pH = 7.47±0.126) and contained some particles (TSS = 106±14.9 mg L^{-1}; Table A1-5). Particulates in Arctic snowpacks can originate locally from aeolian processes acting on exposed soils on the desert landscape and from distant sources via long-range atmospheric transport.[42] Concentrations of DIN in snowpacks were 50.4±3.12 µg L^{-1}, most of which was NO_3^--NO_2^-. TP and TDP concentrations in snow were 0.045±0.004 mg L^{-1} and 2.52±0.308 µg L^{-1}, respectively, with snow being the only hydrological compartment for which TDP was detectable. Carbon concentrations in the snowpack were generally low and dominated by PC (2.10±0.194 mg-C L^{-1}).

Snowmelt streams were cold (2.76±1.71°C), neutral (pH: 7.20±0.18), and relatively clear (TSS: 54.9±23.8 mg L^{-1}). Analyte concentrations were generally higher than in snowpacks, reflecting a combination of snowpack sublimation and chemical elution.[43] DIN concentrations were highest in snowmelt relative to concentrations in all other hydrological pools (120±16.9 µg L^{-1}). DIN:TP ratios were less than 6, suggesting that snowmelt streams were largely N and P co-limited. DOC concentrations were also relatively high (4.80±3.74 mg-C L^{-1}), and likely associated with the flushing of DOC from soil surfaces during snowmelt runoff [44].

Glacial inflows. At glacier termini, meltwaters were cold (1.04±0.13°C), approximately neutral (pH: 7.33±0.162) and slightly turbid (TSS: 64.6±24.7 mg L^{-1}; Table A1-6). Waters were fully oxygenated, suggesting little influence of anoxic subglacial waters, or at least partial open system conditions under the ice.[45] Downstream of the glaciers at the river deltas, waters were

warmer (8.01±0.42°C), more alkaline (pH: 7.86±0.08) and very turbid (TSS: 562±163 mg L^{-1}) before flowing into Lake Hazen.

Nutrient concentrations, as well as SO_4^{2-}, $dSiO_2$, and TFe, varied spatially within and between glacial rivers, and temporally throughout the melt season (Table A1-7). Concentrations of both dissolved and particulate constituents increased downstream of glaciers (Figure A1-1), largely due to erosion of highly reactive, comminuted sediments and subsequent chemical weathering.[46] With increasing discharge, dissolved constituent concentrations generally decreased with concomitant increases in particulate concentrations (Figure 2-2), suggesting the adsorption of dissolved constituents to particles. Higher meltwater discharge entrains larger quantities of particulates as rivers erode channel edges and shifted positions across proglacial river valleys.[47]

DIN concentrations were relatively high in glacial river delta waters (83.2±15.2 µg-N L^{-1}) and dominated by NO_3^--NO_2^-, except in the Gilman and Turnabout rivers, where NH_4^+ constituted more than half of the DIN pool (Table A1-7). TP concentrations in glacial rivers (661±187 µg-P L^{-1}) were likewise high. Much of the phosphorus in the glacial rivers likely originated from marginal or proglacial zones given that glaciers of the Northern Ellesmere Icefield have cold-based margins.[48] Indeed, TP concentrations increased between 2 and 3 orders of magnitude between the glacier termini and the lake (Figure A1-1). TDP concentrations were below detection (<1.8 µg-P L^{-1}) in most glacial river samplings.

Early and late in the melt season, TC was dominated by DIC, but as glacial melt increased, PC became a proportionally greater fraction of TC (up to 92%; Figure 2-2). In the Snowgoose River, for example, PC concentrations ranged between 0.04 mg-C L^{-1} early/late in the melt season to 79.7 mg-C L^{-1} at peak flow. DOC concentrations in glacial rivers were extremely low (0.3±0.03 mg-C L^{-1}).

In-lake physical structure and nutrient concentrations

Physical limnology. Lake Hazen exhibited reverse temperature stratification under the ice, where temperatures were 0.52±0.35°C, but below 50 m, were constant at 3.72±0.10°C (Figure 2-3). Thermal stratification disappeared following ice melt (3.37±0.25°C). Secchi depths before and after snowmelt were 27 m and 15 m, respectively, corresponding to light extinction coefficients of 0.063 m^{-1} and 0.111 m^{-1} (calculated from Secchi depth). Turbidity in the water column was

generally extremely low, as evidenced by PC and PN concentrations less than 100 µg-C L^{-1} or 10 µg-N L^{-1}, respectively, but increased marginally immediately following snowmelt in the spring.

In the summer, turbidity varied spatially in Lake Hazen due to river inputs of glacial flour generated from erosion. Glacial flour severely impeded light penetration along the northwestern shoreline of the lake.[49] This effect was, however, limited to nearshore waters due to the density of inflowing glacial river waters; waters at the centre of the lake and along the southeastern shore away from glacial inputs were generally clear. With a Secchi depth of ~16 m, the light extinction coefficient at the centre of the lake was 0.106 m^{-1}, indistinguishable from that measured after snowmelt in the spring.

Glacial river discharge formed turbidity currents upon entering the lake, facilitating the transport of particulate-rich waters to depth and oxygenation of bottom waters.[50] Concentrations of PN and PC, proxies for TSS, increased 3-fold and 6-fold (Figure 2-3), respectively, between surface waters and the depths (200-250 m) of Lake Hazen, a subsidy from glacial inflows. Annual oxygenation of the bottom waters of Lake Hazen is a relatively recent phenomenon,[23] likely a consequence of enhanced glacial meltwater inputs to the lake. Indeed, the strength of the turbidity currents was directly dependent on the volume of glacial runoff in a given year. For example, glacial runoff in 2015 was 3.36 times greater than in 2016 (Table 2-1), mirrored by PC and TP concentrations at depth 2.20 and 3.83 times higher, respectively, in 2015 than in 2016.

Chemical limnology and nutrient limitation. 74.0±1.35% and 51.5±2.52% of total nitrogen in the lake was DIN in spring and summer, respectively, mostly as NO_3^--NO_2^-. Depth-integrated NO_3-NO_2^- concentrations in Lake Hazen were 46.5±0.79 µg-N L^{-1} and 34.7±0.98 µg-N L^{-1} in spring and summer, respectively (Figure 2-3). These concentrations were lower than in more temperate lakes,[51] but higher than in other lakes in the Canadian Arctic Archipelago (CAA).[52] The fact that Lake Hazen is glacier fed is unusual among the lakes previously studied in the CAA,[52] likely explaining the comparatively higher NO_3^--NO_2^- concentrations.[9, 53] Although glacial inputs are higher in DIN than the lake waters, DIN in the summertime upper water column decreased, likely reflecting increased biological utilization combined with the efflux of N_2 or N_2O following denitrification in the absence of lake ice cover.

In spring under the ice, TP concentrations were below detection (<3 µg-P L^{-1}) throughout most of the water column, reaching a maximum concentration of only 6 µg-P L^{-1} near the

sediment-water interface (Figure 2-3). Although total dissolved phosphorous (TDP) was generally below detection (<1.8 µg-P L^{-1}) in the water column throughout the year, phosphorus can be mobilized into the water column from sediments via internal loading.[54] Following deposition of TP at depth with the turbidity currents, reducing conditions in sediments likely lead to the release of TDP to overlying waters. Although TDP concentrations in sediment core porewaters were much higher (up to 44 µg-P L^{-1}) than in the overlying water column (Figure 2-4), how much P diffuses to the water column is unknown and likely varies significantly over space.[55]

Mean DIN:TP mass ratios integrated throughout the springtime Lake Hazen water column were 55.7±3.21 (Figure 2-3), indicative of severe P-limitation.[56] In summer, the upper 200 m of the water column still exhibited strong P-limitation (DIN:TP=21.3±3.02); however, DIN:TP declined below 200 m to a minimum of 2.3 (Figure 2-3), indicative of N and P co-limitation, or even possible N-limitation.[56] These DIN:TP ratios at depth mirrored those in the glacial inflows (8.55±4.84, median: 0.207; Table A1-6), evidence for significant allochthonous nutrient subsidy to the lake.

TC concentrations integrated throughout the water column were 9.40±0.160 mg C L^{-1} (summer) and 9.89±0.150 mg C L^{-1} (spring), ~98% of which was DIC (Figure 2-2). DOC concentrations were extremely low throughout the water column, but marginally higher in the summer (0.228±0.024 mg C L^{-1}) than in the spring (0.191±0.016 mg C L^{-1}).

$dSiO_2$ concentrations were low and constant throughout the water column throughout the year (Figure 2-3). In contrast, while TFe was low or below detection (<7 µg L^{-1}) throughout the entire water column in spring, TFe increased 140-fold below 200 m in summer, reaching 495 µg L^{-1} (Figure 2-3). Summertime turbidity currents transport Fe to the depths from the watershed, where Fe is present in various mineral forms (e.g., sjögrenite, ankerite, pyrite, ferrinatrite).

Nutrient concentrations in the Ruggles River outflow

The Ruggles River was cold (4.09±0.291°C), alkaline (pH: 7.96±0.158) and fully oxygenated (105±1.35% saturation) along its length. Waters were clear at the outflow of Lake Hazen (TSS = 1.40±0.495 mg L^{-1}) but increased in turbidity (TSS up to 551 mg L^{-1}) with increasing distance from Lake Hazen due to permafrost slumping and erosion along the river

banks (Figure A1-2). This effect was particularly pronounced in early August when maximum permafrost thaw was occurring.

TN at the Lake Hazen outflow was mostly DIN (56.4±16.7%), though less than in the glacial rivers, and PN concentrations were very low, suggesting some organic nitrogen production within the lake (Table A1-6). TP concentrations at the lake were 2.23±0.959 μg L^{-1}, but increased up to 120-fold before entering Chandler Fjord. The river was P-limited at the lake (DIN:TP=13.2±6.38), but became N and P co-limited (2.88±2.73) downstream due to erosional P inputs.

TC concentrations at the lake were dominated by DIC (95.5±1.04%), mirroring those in Lake Hazen, but PC became a more important component of TC downstream with slumping and erosion (up to 94.0% of TC). DOC was extremely low across the whole transect (0.30±0.00 mg-C L^{-1}).

$dSiO_2$ concentrations remained constant along the river. Mirroring other particulate parameters, TFe concentrations in the Ruggles River increased downstream of Lake Hazen due to slumping and erosion (Table A1-6).

Nutrient input-output budgets

Hydrological budgets for all chemical species, except for NO_3^--NO_2^-, NH_4^+, DIC and DOC were generally net neutral, with annual Ruggles River exports approximately equaling the combined meltwater inputs. Runoff from glaciers accounted for the majority of all dissolved inputs to Lake Hazen (Table 2-1). The relative importance of glacial inputs to Lake Hazen varied inter-annually, though, such that glaciers accounted for more than 90.9±2.53% of inputs in the high melt year (2015), but only 78.0±4.31% in the low melt year (2016).

Lake Hazen was a strong sink for NO_3^--NO_2^-, and NH_4^+ (Table 2-1). Processes that could account for these sinks are biological uptake, sedimentation or the denitrification of NO_3^- and subsequent evasion to N_2O and/or N_2.[57] Given that denitrification would be limited by the low temperatures and largely aerobic conditions in Lake Hazen,[58] the sedimentation of particle adsorbed-inorganic N and organic N is likely more important at the watershed scale. Anoxic conditions in bottom waters may lead to the release of stored N to overlying waters, but most of the water column is oxic, with the exception of the sediment-water interface at sites receiving large amounts of glacial inputs (Figure 2- 5). As oxygen is consumed by decomposition within

the sediments, the adsorptive capacity of the sediments is diminished (see below). For example, while concentrations of NH_4^+ in sediment porewaters were higher in the two cores characterized by high oxygen consumption rates (Figure 2- 4), NH_4^+ release from the sediments to overlying waters was likely limited by the consistent oxygenation of bottom waters.[59]

Lake Hazen was also a sink for DOC, but this was only significant in 2015 (Table 2-1), suggesting that the strength of the sink is strongly dependent on the volume of glacial inputs to the lake. Even though concentrations of DOC within all freshwater compartments of the watershed were low, the glacial rivers represent an important source of DOC to Lake Hazen due to the sheer volume of water entering the lake. Loss of DOC within the lake can occur by mineralization to CO_2, photo-oxidation or adsorption to particles and subsequent deposition.

In contrast, Lake Hazen was a source of DIC to the Ruggles River. Within the lake, DIC can be generated through respiration, which produces CO_2, and/or chemical weathering of mineral glacial flour, which both consumes CO_2 and produces HCO_3^-. While some respiration within Lake Hazen occurs (Figure 2-3), CO_2 produced by respiration is usually lost from freshwater systems to the atmosphere,[60] and would thus result in a decrease in DIC between inputs and outputs. Chemical weathering is therefore the likely source of the DIC increase within the lake. Glacial flour entering Lake Hazen is largely composed of carbonate minerals, a reflection of the dominant geology of the watershed.[61] As these finely comminuted carbonate sediments are mixed within the water column, they can undergo carbonate carbonation, coupled or not to sulphide oxidation.[62]

Given that the strength of the turbidity currents depends on the magnitude of glacial meltwater inputs in a given year, the lake was also likely a strong sink for particulate parameters (PC, PN, TFe, TP), even though we could not reliably calculate the glacial component of these budgets. Although Lake Hazen is atypically large among Arctic lakes,[63] even small, more ephemeral proglacial lakes may be important modifiers of glacial meltwaters on northern landscapes.[48, 64] While proglacial lake discussions in the literature have typically been restricted to sediment storage,[21] we show that proglacial lakes may act to retain and/or process nutrients before delivery and mobilization to ecosystems further downstream.

In-lake biological processes.

Primary productivity in Lake Hazen. We were unable to explicitly quantify rates of primary production in Lake Hazen due to logistical challenges. Using ^{14}C additions during the first International Polar Year (1957-58), MacLaren found primary production in Lake Hazen to be extremely low, ranging from below detection to 59 mg m^{-2} d^{-1}, even at the height of the summer.[65] Although primary production may have increased since in response to reduced ice cover,[23, 66] autochthonous OC is rapidly decomposed in the lake, leaving little record in the sediments.[23]

Immediately below the lake ice, chl *a* concentrations more than doubled from 0.13 µg L^{-1} before snowmelt to 0.29 µg L^{-1} after snowmelt, likely reflecting an influx of nutrients in meltwaters despite the increase in light extinction coefficients discussed above. Chl *a* concentrations in the upper 25 m, though, were generally very low (0.26±0.01 µg L^{-1}; Figure 2-3), as in other lakes found in the Canadian High Arctic.[52] Upper water column chl *a* concentrations in the summer were higher at the center of the lake (0.39±0.048 µg L^{-1}) than under the ice or along the shoreline (below detection to 0.13 µg L^{-1}), likely in response to differential light availability with and without ice cover on the lake (Figure A1-3), as well as nutrient availability with and without glacial inputs. While both factors likely play a role, it is difficult to discern the relative importance of each.

We identified 48 phytoplankton genera and over 60 species of phytoplankton in the Lake Hazen water column under the ice in the spring (Table A1-8), 33 of which were unique to that time of year. Chrysophytes, chlorophytes and diatoms were the most abundant taxa in the upper water column (Figure 2-6). Cyanobacteria were also found at depths within the water column, but exhibited high spatial and inter-annual variability in abundances. Summer phytoplankton communities were less diverse (34 genera and 39 species, 15 of which were unique to the summer), but had higher biomass than those in the springtime (Figure 2-6). Open water communities were dominated by cryptophytes, diatoms and chrysophytes, the latter of which are a hallmark of Arctic systems and successful competitors at low phosphorus concentrations.[67, 68] Whereas chrysophytes were one of the most diverse taxonomic groups in Lake Hazen, the cryptophytes were represented by only three genera: *Rhodomonas* - often the dominant algae, *Cryptomonas*, and *Kateblepharis*. Both cryptophytes and chrysophytes are mixotrophic and only photosynthesize under optimal conditions.[58] Indeed, the dominance of phytoflagellates in Lake

Hazen in the summer is very similar to what is seen in large temperate lakes in winter.[69] Picocyanobacteria may be an important source of productivity within Lake Hazen due to its ultra-oligotrophic state,[70] but were not sampled for here.

The overwhelming importance of DIN:TP in predicting phytoplankton community structure (both abundance and biomass) highlights the combined role of ice cover and glacial inflows on productivity in this ultra-oligotrophic lake (Figures 2-7 and A1-4). In fact, using cell densities as the response, the reduced RDA included only two variables: the DIN:TP mass ratio (RDA1 eigenvalue = 0.976) and CO_2 saturation (0.120). In the spirit of parsimony, we therefore conducted a principal components analysis on the Hellinger-transformed cell densities as a metric of community composition, and regressed that against the DIN:TP ratio (Figure 2-7; R^2=0.701, $p<0.001$). Whereas communities dominated by chrysophytes, cryptophytes and dinoflagellates, all mixotrophs, were found at the lower DIN:TP ratios (or lower DIN and higher TP concentrations) characteristic of open water conditions, higher abundances of diatoms, chlorophytes and cyanobacteria, were found at the higher DIN:TP associated with the ice-covered water column.

Phytoplankton biomass was best predicted by DIN:TP and TP, water temperature and sulfate concentrations (Figure A1-4). As these latter two variables play a comparatively small role on RDA2, they may reflect seasonality within the water column. Sulfate concentrations were higher under the ice in the spring (Figure 2-3) and varied along the shoreline throughout the ablation season in response to glacial meltwater inputs. Similarly, temperatures were higher in the upper water column and along the shoreline during the summer relative to those under ice.

It is counterintuitive that cyanobacteria capable of N-fixation would be more prevalent at higher DIN concentrations. Given the ultra-oligotrophic nature of Lake Hazen, we speculate that this may be due to competition rather than physicochemical constraints.[71] Whether the mixotrophic taxa (chrysophytes, cryptophytes, dinoflagellates) were autotrophic or heterotrophic at the time of sampling is unknown, but these taxa dominated along the shoreline where light penetration was significantly impeded by glacial flour and likely restricted primary production. Feeding strategy flexibility and motility in mixotrophic taxa likely provides a distinct competitive advantage in cold and unproductive Arctic freshwaters like Lake Hazen.[72]

Secondary productivity. Our springtime zooplankton samples consisted entirely of juveniles that could not be identified to species. In the summer, ~98% of total zooplankton biomass was adult *Daphnia cf. galeata mendotae*. The balance consisted of cyclopoid stages of copepods and adult cyclops (1.89% by weight; likely *Cyclops scutifer* as in [73]) and the planktonic rotifer *Keratella hiemallis* (<0.1%). Copepods were, however, the most numerous zooplankton in Lake Hazen. Such low species richness is rare globally, but more common in the High Arctic islands, where dispersal has been limited over millennia.[74] At such low densities, zooplankton within the lake can only partially support the juvenile (<20% of diet) and small (<10% of diet) forms of the non-anadromous arctic char, which otherwise rely on chironomids and other terrestrial insects for the bulk of their diet.[37] Large char in the lake do not even consume zooplankton, rather relying solely on cannibalism and chironomids for energy sources.[37]

Biogeochemical processes in sediments. OC accumulation rates in Lake Hazen sediments increased from ~8 to 14-71 g OC m^{-2} yr^{-1} in the past decade due to climate warming.[23] These accumulation rates are now similar to or greater than those found in temperate lakes.[75] Increased delivery of OC to sediments has important implications for heterotrophic microbial activity there. Indeed, sediment microbial activity varied depending on the proximity to and size of nearby glacial inflows delivering allochthonous OC and nutrients to the lake. At the two sites receiving large inputs from the Snowgoose and Abbé rivers (Main deep, S1 and Abbé shallow, S2), dissolved O_2 was depleted within 2-3 mm of the sediment-water interface, with a corresponding decline in redox potential, suggesting high levels of heterotrophic activity (Figures 2-4, 2-5). At the two sites presumably receiving less OC and nutrients from the comparatively smaller Blister River (Blister deep and shallow, S3-4), dissolved O_2 penetrated much deeper (25 - >60 mm), with little change in redox. At the site receiving no direct glacial inputs (Ruggles, S5), dissolved O_2 concentrations were still 6 mg L^{-1} at 60 mm depth. Depth-integrated O_2 consumption rates were higher at those sites with higher bottom water O_2 concentrations, reflecting the dependence of aerobic respiration on O_2 availability (Table A1-9).

Unsurprisingly, concentrations of NH_4^+ and TDP were highest at the sites receiving more glacial inputs, reflecting higher rates of organic matter mineralization and consequent reductions in redox potential. Ammonification, as evidenced by high NH_4^+ concentrations, dominated in sediments with low O_2 concentrations, whereas nitrification, as evidenced by higher NO_3^--NO_2^-

and which requires O_2, dominated at the other sites. TDP was also highest in sediments with low dissolved O_2, as phosphate (PO_4^{3-}) was likely being released from mineral sources under the prevailing reducing conditions. pH decreased in the sediments of sites receiving less or no glacial inputs, although why this occurred is unknown.

In summer, when dense turbidity currents facilitated the oxygenation of bottom waters, dissolved O_2 penetrated deeper into the sediments, with concomitant declines in NH_4^+ and TDP concentrations, and increases in NO_3^--NO_2^- (Figure A1-5). Depth-integrated O_2 consumption rates were an order of magnitude higher at both sites during the summer than in the spring, reflecting great O_2 availability at depth with lake mixing. For example, at S1, O_2 consumption rates were 1.10×10^{-3} and 1.61×10^{-4} nmol cm^{-2} s^{-1} in summer and spring, respectively, mirrored by rates of 2.56×10^{-3} and 3.63×10^{-4} nmol cm^{-2} s^{-1} in summer and spring at S2. In the absence of stable reducing conditions during the summer months, nitrification prevailed over ammonification (lower NH_4^+, higher NO_3^--NO_2^-), and the reduction and subsequent desorption of phosphorus from particles was diminished [76].

Land-to-ocean aquatic continuum in a glacierized watershed

The glacierized LOAC observed in the Lake Hazen watershed and downstream is in stark contrast to boreal systems where carbon, nitrogen, and phosphorus concentrations decline according to first order decay.[14] In contrast, TC, TP, TN, and TFe concentrations increased along our glacial rivers, with increasing availability of easily eroded fine materials downstream of glaciers and little retention within the proglacial landscape (Figure 2-8). Whereas CO_2 and CH_4 emissions tend to be an important carbon removal mechanism in non-glacierized freshwaters,[60, 77] erosion and chemical weathering reactions in the glacier-fed freshwaters of the Lake Hazen watershed increase TC concentrations between glacial headwaters and the lake. Waters along the lake shoreline receiving glacial inputs appeared to act as a physico-chemical intermediary between the rivers and central lake waters, where nutrient concentrations were much less variable. Due to turbidity currents transporting many of the glacial inputs directly to the bottom of the lake, the Lake Hazen outflow to the Ruggles River resembled that of central Lake Hazen surface waters. However, permafrost slumping and erosion downstream of the lake increased concentrations of all nutrients except TN in the river.

Stoichiometric ratios between carbon and key macronutrients (N, P) are useful tools to assess preferential nutrient loss or retention along the LOAC (Figure 2-9).[78] Non-glacierized freshwaters tend to be more biologically productive than glacierized ones in the High Arctic.[78] Nutrient stoichiometry across the Lake Hazen watershed was, however, dominated by physical (hydrology, erosion, permafrost thaw and slumping) and chemical (weathering) processes, with important implications for downstream ecosystems. The combination of these processes led to the preferential mobilization of C, then P over N, the latter of which lacks any significant mineral source. Variability in glacial river delta stoichiometry reflected temporal fluctuations in meltwater volumes (Figure 2-2) and spatial differences in geology across the watershed.[61] TC:TP, TN:TP and DIN:TP in the Ruggles River declined before flowing into Chandler Fjord, highlighting mobilization of phosphorus by erosion and permafrost slumping to nearshore marine environments.

With the highest freshwater drainage to ocean basin area globally, the Arctic Ocean is especially sensitive to changes in freshwater quantity and quality from anthropogenic activities.[79] Although annual discharge from the Ruggles River (3.40±1.85 km^3 yr^{-1}, SD) is low compared to the 8 largest Arctic rivers (103-620 km^3 yr^{-1}),[80] cumulative annual discharge from the Canadian Arctic Archipelago is 202 km^3 yr^{-1}.[81] Our results suggest that enhanced glacial melt and permafrost thaw in response to climate warming across the High Arctic will have important biogeochemical consequences for nutrient cycling in freshwaters and nearshore marine ecosystems.

REFERENCES

1. Radić, V.; Bliss, A.; Beedlow, A. C.; Hock, R.; Miles, E.; Cogley, J. G., Regional and global projections of twenty-first century glacier mass changes in response to climate scenarios from global climate models. *Climate Dynamics* **2013,** *42*, (1), 37-58.
2. Bliss, A.; Hock, R.; Radić, V., Global response of glacier runoff to twenty-first century climate change. *Journal of Geophysical Research: Earth Surface* **2014,** *119*, (4), 717-730.
3. Huss, M.; Hock, R., Global-scale hydrological response to future glacier mass loss. *Nature Climate Change* **2018**.
4. Pfeffer, W. T.; Arendt, A. A.; Bliss, A.; Bolch, T.; Cogley, J. G.; Gardner, A. S.; Hagen, J.-O.; Hock, R.; Kaser, G.; Kienholz, C.; Miles, E. S.; Moholdt, G.; Mölg, N.; Paul, F.; Radi; Valentina; Rastner, P.; Raup, B. H.; Rich, J.; Sharp, M. J., The Randolph Glacier Inventory: a globally complete inventory of glaciers. *J. Glaciol.* **2014,** *60*, (221), 537-552.

5. Stocker, T. F.; Qin, D.; Plattner, G.-K.; Tignor, M.; Allen, S. K.; Boschung, J.; Nauels, A.; Xia, Y.; Bex, V.; Midgley, P. M., *IPCC 2013: Climate Change 2013: The Physical Science Basis. Contribution of Working Group I to the Fifth Assessment Report of the Intergovernmental Panel on Climate Change*. Cambridge University Press: Cambridge, UK and New York, NY, USA, 2013; p 1535 pp.
6. Hood, E.; Battin, T. J.; Fellman, J.; O'Neel, S.; Spencer, R. G. M., Storage and release of organic carbon from glaciers and ice sheets. *Nature Geoscience* **2015,** *8*, (2), 91-96.
7. Zdanowicz, C.; Krummel, E. M.; Lean, D.; Poulain, A. J.; Yumvihoze, E.; Chen, J. B.; Hintelmann, H., Accumulation, storage and release of atmospheric mercury in a glaciated Arctic catchment, Baffin Island, Canada. *Geochim. Cosmochim. Acta* **2013,** *107*, 316-335.
8. Beal, S. A.; Osterberg, E. C.; Zdanowicz, C. M.; Fisher, D. A., Ice Core Perspective on Mercury Pollution during the Past 600 Years. *Environ. Sci. Technol.* **2015,** *49*, (13), 7641-7647.
9. Warner, K. A.; Saros, J. E.; Simon, K. S., Nitrogen Subsidies in Glacial Meltwater: Implications for High Elevation Aquatic Chains. *Water Resources Research* **2017,** *53*, (11), 9791-9806.
10. Schroth, A., W.; Crusius, J.; Chever, F.; Bostick Benjamin, C.; Rouxel Olivier, J., Glacial influence on the geochemistry of riverine iron fluxes to the Gulf of Alaska and effects of deglaciation. *Geophysical Research Letters* **2011,** *38*, (16).
11. Hodgkins, R.; Cooper, R.; Wadham, J.; Tranter, M., Suspended sediment fluxes in a high-Arctic glacierised catchment: implications for fluvial sediment storage. *Sedimentary Geology* **2003,** *162*, (1-2), 105-117.
12. Hawkings, J. R.; Wadham, J. L.; Tranter, M.; Raiswell, R.; Benning, L. G.; Statham, P. J.; Tedstone, A.; Nienow, P.; Lee, K.; Telling, J., Ice sheets as a significant source of highly reactive nanoparticulate iron to the oceans. *Nature Communications* **2014,** *5*.
13. Wadham, J. L.; Hawkings, J.; Telling, J.; Chandler, D.; Alcock, J.; O'Donnell, E.; Kaur, P.; Bagshaw, E.; Tranter, M.; Tedstone, A.; Nienow, P., Sources, cycling and export of nitrogen on the Greenland Ice Sheet. *Biogeosciences* **2016,** *13*, (22), 6339-6352.
14. Weyhenmeyer, G. A.; Conley, D. J., Large differences between carbon and nutrient loss rates along the land to ocean aquatic continuum—implications for energy:nutrient ratios at downstream sites. *Limnology and Oceanography* **2017**, n/a-n/a.
15. Bouwman, A. F.; Bierkens, M. F. P.; Griffioen, J.; Hefting, M. M.; Middelburg, J. J.; Middelkoop, H.; Slomp, C. P., Nutrient dynamics, transfer and retention along the aquatic continuum from land to ocean: towards integration of ecological and biogeochemical models. *Biogeosciences* **2013,** *10*, (1), 1-22.
16. Frost, P. C.; Kinsman, L. E.; Johnston, C. A.; Larson, J. H., Watershed discharge modulates relationships between landscape components and nutrient ratios in stream seston. *Ecology* **2009,** *90*, (6), 1631-1640.
17. Tranvik, L. J.; Downing, J. A.; Cotner, J. B.; Loiselle, S. A.; Striegl, R. G.; Ballatore, T. J.; Dillon, P.; Finlay, K.; Fortino, K.; Knoll, L. B.; Kortelainen, P. L.; Kutser, T.; Larsen, S.; Laurion, I.; Leech, D. M.; McCallister, S. L.; McKnight, D. M.; Melack, J. M.; Overholt, E.; Porter, J. A.; Prairie, Y.; Renwick, W. H.; Roland, F.; Sherman, B. S.; Schindler, D. W.; Sobek, S.; Tremblay, A.; Vanni, M. J.; Verschoor, A. M.; von Wachenfeldt, E.; Weyhenmeyer, G. A., Lakes and reservoirs as regulators of carbon cycling and climate. *Limnology and Oceanography* **2009,** *54*, (6), 2298-2314.

18. Weyhenmeyer, G. A.; Kosten, S.; Wallin, M. B.; Tranvik, L. J.; Jeppesen, E.; Roland, F., Significant fraction of CO2 emissions from boreal lakes derived from hydrologic inorganic carbon inputs. *Nature Geosci* **2015,** *8*, (12), 933-936.
19. Song, C.; Sheng, Y.; Ke, L.; Nie, Y.; Wang, J., Glacial lake evolution in the southeastern Tibetan Plateau and the cause of rapid expansion of proglacial lakes linked to glacial-hydrogeomorphic processes. *Journal of Hydrology* **2016,** *540*, 504-514.
20. Stokes, C. R.; Popovnin, V.; Aleynikov, A.; Gurney, S. D.; Shahgedanova, M., Recent glacier retreat in the Caucasus Mountains, Russia, and associated increase in supraglacial debris cover and supra-/proglacial lake development. *Annals of Glaciology* **2007,** *46*, 195-203.
21. Carrivick, J. L.; Tweed, F. S., Proglacial lakes: character, behaviour and geological importance. *Quaternary Science Reviews* **2013,** *78*, 34-52.
22. Köck, G.; Muir, D. C. G.; Yang, F.; Wang, X.; Talbot, C.; Gantner, N.; Moser, D., Bathymetry and Sediment Geochemistry of Lake Hazen (Quttinirpaaq National Park, Ellesmere Island, Nunavut). *Arctic* **2012,** *65*, (1), 56-66.
23. Lehnherr, I.; St. Louis, V. L.; Muir, D. C. G.; Sharp, M. J.; Gardner, A. S.; Lamoureux, S.; Smol, J. P.; St. Pierre, K. A.; Michelutti, N.; Schiff, S. L.; Emmerton, C. A.; Tarnocai, C.; Talbot, C., The world's largest High Arctic lake responds rapidly to climate warming. *Nature Commun.* **2018,** *9*, 1290.
24. Serreze, M. C.; Raup, B.; Braun, C.; Hardy, D. R.; Bradley, R. S., Rapid wastage of the Hazen Plateau ice caps, northeastern Ellesmere Island, Nunavut, Canada. *The Cryosphere* **2017,** *11*, (1), 169-177.
25. Thompson, W., Climate. In *Resource description and analysis: Ellesmere Island, National Park Reserve.* , National Resource Conservation Selection, Prairie and Northern Region, Parks Canada, Department of Canadian Heritage: Winnipeg, Manitoba, 1994; p 78.
26. Emmerton, C. A.; St Louis, V. L.; Lehnherr, I.; Graydon, J. A.; Kirk, J. L.; Rondeau, K. J., The importance of freshwater systems to the net atmospheric exchange of carbon dioxide and methane with a rapidly changing high Arctic watershed. *Biogeosciences* **2016,** *13*, (20), 5849-5863.
27. Gardner, A. S.; Moholdt, G.; Wouters, B.; Wolken, G. J.; Burgess, D. O.; Sharp, M. J.; Cogley, J. G.; Braun, C.; Labine, C., Sharply increased mass loss from glaciers and ice caps in the Canadian Arctic Archipelago. *Nature* **2011,** *473*, (7347), 357-360.
28. Runkel, R. L.; Crawford, C. G.; Cohn, T. A., Load estimator (LOADEST): a FORTRAN program for estimating constituent loads in streams and rivers. In *USGS Techniques and Methods Book 4*, U.S. Geological Survey: Reston, Virginia, USA, 2004.
29. Lorenz, D.; Runkel, R.; De Cicco, L. *rloadest: river load estimation*, U.S. Geological Survey: Mounds View, Minnesota, USA., 2015.
30. Findlay, D. L., Response of Phytoplankton Communities to Acidification and Recovery in Killarney Park and the Experimental Lakes Area, Ontario. *AMBIO: A Journal of the Human Environment* **2003,** *32*, (3), 190-195.
31. Findlay, D. L.; Kling, H. J. *Protocols for measuring biodiversity: Phytoplankton in fresh water lakes*; Department of Fisheries and Oceans Canada: Winnipeg, MB, 1998; p 19 pp.
32. Borcard, D.; Gillet, F.; Legendre, P., *Numerical Ecology with R*. Springer: New York USA, 2011.

33. Oksanen, J.; Blanchet, F. G.; Friendly, M.; Kindt, R.; Legendre, P.; McGlinn, D.; Minchin, P. R.; O'Hara, R. B.; Simpson, G. L.; Solymos, P.; Stevens, M. H. H.; Szoecs, E.; Wagner, H. *Package 'vegan'*, 2.4-6; 2018.
34. Reist, J. D.; Gyselman, E.; Babaluk, J. A.; Johnson, J. D.; Wissink, H. R., Evidence for two morphotypes of Arctic char (*Salvelinus alpinus* (L.)) from Lake Hazen, Ellesmere Island, Northwest Territories, Canada. *Nordic J. Freshwater Res.* **1995,** *71*, 396-410.
35. Babaluk, J. A.; Halden, N. M.; Reist, J. D.; Kristofferson, A. H.; Campbell, J. L.; Teesdale, W. J., Evidence for non-anadromous behaviour of arctic charr (Salvelinus alpinus) from Lake Hazen, Ellesmere Island, northwest Territories, Canada, based on scanning proton microprobe analysis of otolith strontium distribution. *Arctic* **1997,** *50*, (3), 224-233.
36. Babaluk, J. A.; Wissink, H. R.; Troke, B. G.; Clark, D. A.; Johnson, J. D., Summer Movements of Radio-Tagged Arctic Charr (Salvelinus Alpinus) in Lake Hazen, Nunavut, Canada. *Arctic* **2001,** *54*, (4), 418-424.
37. Guiguer, K. R. R. A.; Reist, J. D.; Power, M.; Babaluk, J. A., Using stable isotopes to confirm the trophic ecology of Arctic charr morphotypes from Lake Hazen, Nunavut, Canada. *J. Fish Biol.* **2002,** *60*, (2), 348-362.
38. Babaluk, J. A.; Sawatzky, C. D.; Wastle, R. J.; Reist, J. D., Biological data of Arctic char, Salvelinus alpinus, from Lake Hazen, Quttinirpaaq National Park, Nunavut, 1958-2001. In Babaluk, J. A., Ed. Fisheries and Oceans Canada: [Ottawa] :, 2007.
39. Sinnatamby, R. N.; Reist James, D.; Power, M., Identification of the maternal source of young-of-the-year Arctic charr in Lake Hazen, Canada. *Freshwater Biology* **2013,** *58*, (7), 1425-1435.
40. Heiri, O.; Lotter, A. F.; Lemcke, G., Loss on ignition as a method for estimating organic and carbonate content in sediments: reproducibility and comparability of results. *Journal of Paleolimnology* **2001,** *25*, (1), 101-110.
41. Berg, P.; Risgaard-Petersen, N.; Rysgaard, S., Interpretation of measured concentration profiles in sediment pore water. *Limnology and Oceanography* **1998,** *43*, (7), 1500-1510.
42. Zdanowicz, C. M.; Zielinski, G. A.; Wake, C. P., Characteristics of modern atmospheric dust deposition in snow on the Penny Ice Cap, Baffin Island, Arctic Canada. *Tellus* **1998,** *50B*, 506-520.
43. Kępski, D.; Błaś, M.; Sobik, M.; Polkowska, Ż.; Grudzińska, K., Progressing Pollutant Elution from Snowpack and Evolution of its Physicochemical Properties During Melting Period—a Case Study From the Sudetes, Poland. *Water, Air, and Soil Pollution* **2016,** *227*, 112.
44. Boyer, E. W.; Hornberger, G. M.; Bencala, K. E.; McKnight, D. M., Effects of asynchronous snowmelt on flushing of dissolved organic carbon: a mixing model approach. *Hydrological Processes* **2001,** *14*, (18), 3291-3308.
45. Graly, J. A.; Drever, J. I.; Humphrey, N. F., Calculating the balance between atmospheric CO_2 drawdown and organic carbon oxidation in subglacial hydrochemical systems. *Global Biogeochemical Cycles* **2017,** *31*, (4), 709-727.
46. Anderson, S. P.; Drever, J. I.; Frost, C. D.; Holden, P., Chemical weathering in the foreland of a retreating glacier. *Geochimica Et Cosmochimica Acta* **2000,** *64*, (7), 1173-1189.
47. Malard, F.; Uehlinger, U.; Zah, R.; Tockner, K., Flood-pulse and riverscape dynamics in a braided glacial river. *Ecology* **2006,** *87*, (3), 704-716.

48. Hawkings, J.; Wadham, J.; Tranter, M.; Telling, J.; Bagshaw, E.; Beaton, A.; Simmons, S. L.; Chandler, D.; Tedstone, A.; Nienow, P., The Greenland Ice Sheet as a hot spot of phosphorus weathering and export in the Arctic. *Global Biogeochemical Cycles* **2016,** *30*, (2), 191-210.
49. Rose, K. C.; Hamilton, D. P.; Williamson, C. R.; McBride, C. G.; Fischer, J. M.; Olson, M. H.; Saros, J. E.; Allan, M. G.; Cabrol, N., Light attenuation in glacier-fed lakes. *Journal of Geophysical Research-Biogeosciences* **2014,** *119*, 1446-1457.
50. Crookshanks, S.; Gilbert, R., Continuous, diurnally fluctuating turbidity currents in Kluane Lake, Yukon Territory. *Canadian Journal of Earth Sciences* **2008,** *45*, (10), 1123-1138.
51. Weyhenmeyer, G. A., Synchrony in relationships between the North Atlantic Oscillation and water chemistry among Sweden's largest lakes. *Limnology and Oceanography* **2004,** *49*, (4), 1191-1201.
52. Hamilton, P. B.; Gajewski, K.; Atkinson, D. E.; Lean, D. R. S., Physical and chemical limnology of 204 lakes from the Canadian Arctic Archipelago. *Hydrobiologia* **2001,** *457*, 133-148.
53. Saros, J. E.; Rose, K. C.; Clow, D. W.; Stephens, V. C.; Nurse, A. B.; Arnett, H. A.; Stone, J. R.; Williamson, C. E.; Wolfe, A. P., Melting Alpine Glaciers Enrich High-Elevation Lakes with Reactive Nitrogen. *Environmental Science & Technology* **2010,** *44*, (13), 4891-4896.
54. Pettersson, K., Mechanisms for internal loading of phosphorus in lakes. *Hydrobiologia* **1998,** *373*, (0), 21-25.
55. Boström, B.; Andersen, J. M.; Fleischer, S.; Jansson, M., Exchange of phosphorus across the sediment-water interface. *Hydrobiologia* **1988,** *170*, 229-244.
56. Bergström, A.-K., The use of TN:TP and DIN:TP ratios as indicators for phytoplankton nutrient limitation in oligotrophic lakes affected by N deposition. *Aquatic Sciences* **2010,** *72*, (3), 277-281.
57. Burgin, A., J.; Hamilton, S., K., Have we overemphasized the role of denitrification in aquatic ecosystems? A review of nitrate removal pathways. *Frontiers in Ecology and the Environment* **2007,** *5*, (2), 89-96.
58. Wetzel, R. G., *Limnology*. 3rd ed.; Academic Press: San Diego, California, 2001; p 1006.
59. Beutel, M. W., Inhibition of ammonia release from anoxic profundal sediments in lakes using hypolimnetic oxygenation. *Ecological Engineering* **2006,** *28*, (3), 271-279.
60. Cole, J. J.; Caraco, N. F.; Kling, G. W.; Kratz, T. K., Carbon Dioxide Supersaturation in the Surface Waters of Lakes. *Science* **1994,** *265*, (5178), 1568.
61. Christie, R. L. *Bedrock geology*; Defence Research Board Canada: Ottawa, 1958; pp 16-18.
62. Tranter, M.; Sharp, M. J.; Lamb, H. R.; Brown, G. H.; Hubbard, B. P.; Willis, I. C., Geochemical weathering at the bed of Haut Glacier d'Arolla, Switzerland: a new model. *Hydrol. Processes* **2002,** *16*, (5), 959-993.
63. Paltan, H.; Dash, J.; Edwards, M., A refined mapping of Arctic lakes using Landsat imagery. *International Journal of Remote Sensing* **2015,** *36*, (23), 5970-5982.
64. Liermann, S.; Beylich, A. A.; van Welden, A., Contemporary suspended sediment transfer and accumulation processes in the small proglacial Sætrevatnet sub-catchment, Bødalen, western Norway. *Geomorphology* **2012,** *167-168*, 91-101.
65. McLaren, I. A. *Aquatic Biology*; Defence Research Board Ottawa, ON, May 1959, 1959; pp 70-72.

66. Michelutti, N.; Wolfe Alexander, P.; Vinebrooke Rolf, D.; Rivard, B.; Briner Jason, P., Recent primary production increases in arctic lakes. *Geophysical Research Letters* **2005,** *32*, (19).
67. Christoffersen, K. S.; Amsinck, S. L.; Landkildehus, F.; Lauridsen, T. L.; Jeppesen, E., Lake Flora and Fauna in Relation to Ice-Melt, Water Temperature and Chemistry at Zackenberg. In *Advances in Ecological Research*, Academic Press: 2008; Vol. 40, pp 371-389.
68. Rothhaupt, K. O., Laboratorary Experiments with a Mixotrophic Chrysophyte and Obligately Phagotrophic and Photographic Competitors. *Ecology* **1996,** *77*, (3), 716-724.
69. Vollenweider, R. A.; Munawar, M.; Stadelman, P., A Comparative Review of Phytoplankton and Primary Production in the Laurentian Great Lakes. *Journal of Fisheries Research Board of Canada* **1974,** *31*, (5), 739-762.
70. Vörös, L.; Callieri, C.; V.-Balogh, K.; Bertoni, R. In *Freshwater picocyanobacteria along a trophic gradient and light quality range*, Phytoplankton and Trophic Gradients, Dordrecht, 1998//, 1998; Alvarez-Cobelas, M.; Reynolds, C. S.; Sánchez-Castillo, P.; Kristiansen, J., Eds. Springer Netherlands: Dordrecht, 1998; pp 117-125.
71. Huisman, J.; Weissing, F. J., Biological conditions for oscillatons and chaos generated by multispecies competition. *Ecology* **2001,** *82*, (10), 2682-2695.
72. Laybourn-Parry, J.; Marshall, W. A., Photosynthesis, mixotrophy and microbial plankton dynamics in two high Arctic lakes during summer. *Polar Biology* **2003,** *26*, (8), 517-524.
73. McLaren, I. A., Zooplankton of Lake Hazen, Ellesmere Island, and a nearby pond, with special reference to the copepod Cyclops Scutifer Sars. *Canadian Journal of Zoology* **1964,** *42*, (4), 613-629.
74. Rautio, M.; Bayly, I. A. E.; Gibson, J. A. E.; Nyman, M., Zooplankton and zoobenthos in high-latitude water bodies. In *Polar Lakes and Rivers: Limnology of Arctic and Antarctic Aquatic Ecosystems*, Vincent, W. F.; Laybourn-Parry, J., Eds. Oxford University Press: New York, USA, 2008; pp 231-247.
75. Heathcote, A. J.; Anderson, N. J.; Prairie, Y. T.; Engstrom, D. R.; del Giorgio, P. A., Large increases in carbon burial in northern lakes during the Anthropocene. *Nature Communications* **2015,** *6*.
76. Sondergaard, M.; Jensen, J. P.; Jeppesen, E., Role of sediment and internal loading of phosphorus in shallow lakes. *Hydrobiologia* **2003,** *506*, (1-3), 135-145.
77. Wik, M.; Varner, R. K.; Anthony, K. W.; MacIntyre, S.; Bastviken, D., Climate-sensitive northern lakes and ponds are critical components of methane release. *Nature Geoscience* **2016,** *9*, (2), 99-105.
78. Maranger, R.; Jones Stuart, E.; Cotner James, B., Stoichiometry of carbon, nitrogen, and phosphorus through the freshwater pipe. *Limnology and Oceanography Letters* **2018,** *3*, (3), 89-101.
79. Prowse, T.; Bring, A.; Mård, J.; Carmack, E. C.; Holland, M.; Instanes, A.; Vihma, T.; Wrona, F. J., Arctic Freshwater Synthesis: Summary of key emerging issues. *Journal of Geophysical Research Biogeosciences* **2015,** *120*, 1887-1893.
80. Holmes, R. M.; McClelland, J. W.; Peterson, B. J.; Shiklomanov, I. A.; Shiklomanov, A. I.; Zhulidov, A. V.; Gordeev, V. V.; Bobrovitskaya, N. N., A circumpolar perspective on fluvial sediment flux to the Arctic ocean. *Global Biogeochem. Cycles* **2002,** *16*, (4), 45-1-45-14.

81. Lammers, R. B.; Shiklomanov, A. I.; Vörösmarty, C. J.; Fekete, B. M.; Peterson, B. J., Assessment of contemporary Arctic river runoff based on observational discharge records. *J. Geophys. Res. Atmos.* **2001,** *106*, (D4), 3321-3334.

FIGURES AND TABLES

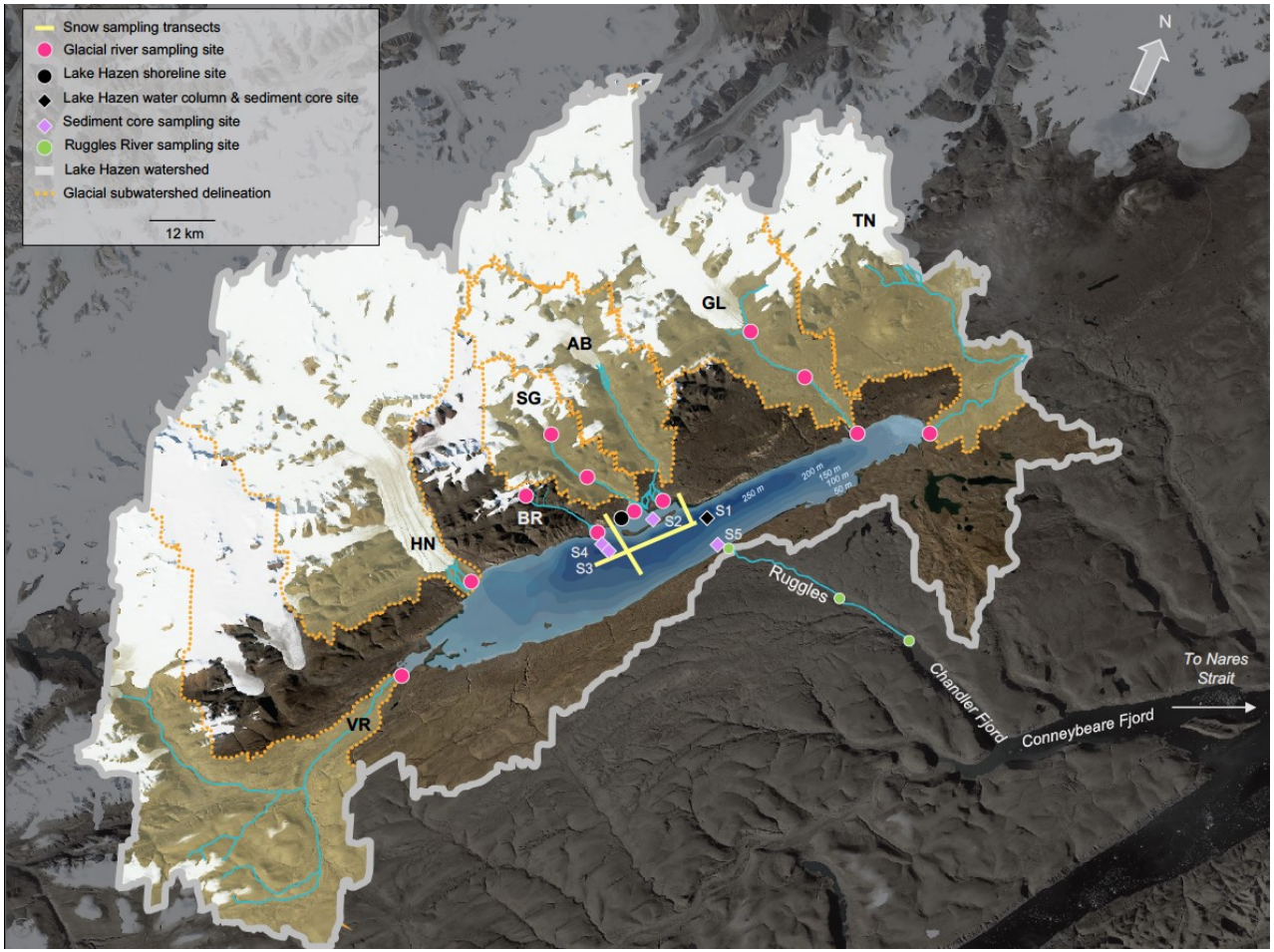

Figure 2-1. Map of the Lake Hazen watershed exemplifying the glacierized land-to-ocean aquatic continuum. The solid grey and orange-dotted lines delineate the entire Lake Hazen watershed and the glacial sub-watersheds, respectively. Sampling sites are highlighted by type. Glacial rivers from south to north: VR, Very; HN, Henrietta Nesmith; BR, Blister; SG, Snowgoose; AB, Abbé; GL, Gilman; TN, Turnabout. The Ruggles River drains Lake Hazen to the coast. Sediment coring sites (S1-5) are described in Table A1-3.

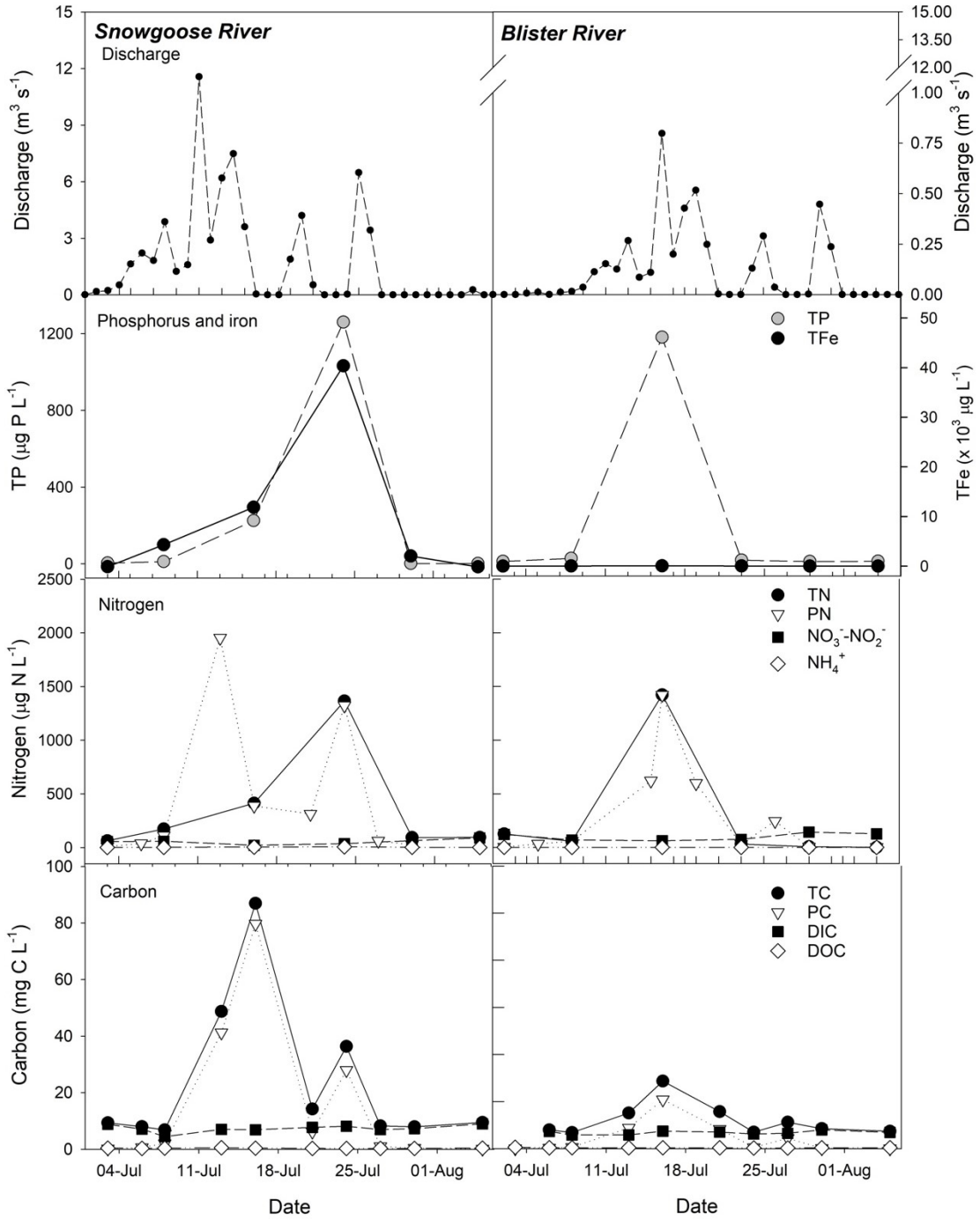

Figure 2-2. Time series of glacial river (Snowgoose and Blister) chemistry measured at the inflow to Lake Hazen throughout summer 2016 (2-July to 4-August).

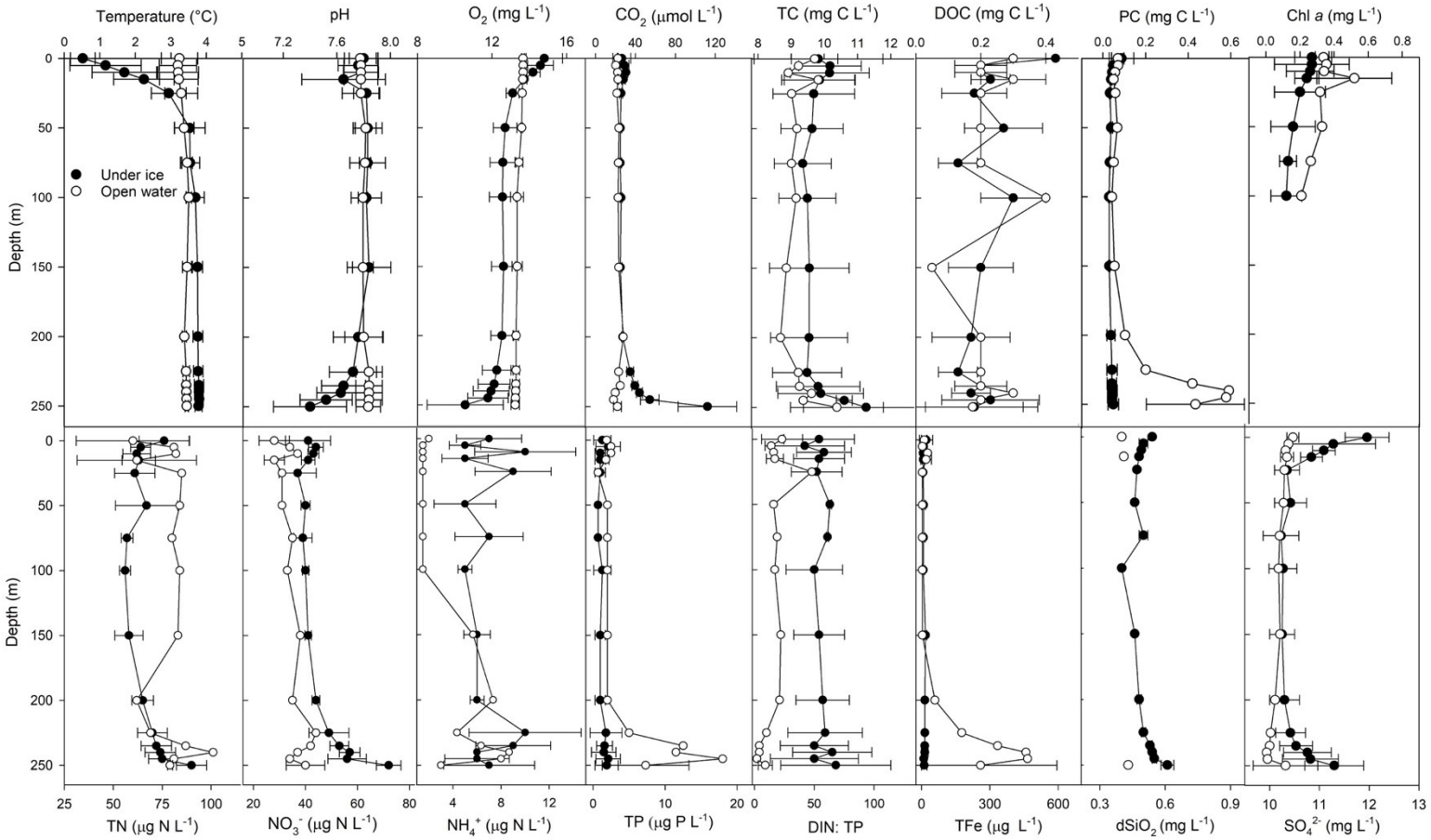

Figure 2-3. Seasonal physical and chemical water column profiles of Lake Hazen. Water column profiles averaged (±1SD) by depth, depending on whether sampling was conducted under ice (May 2012, 2013, 2014 (2 profiles), 2017) or in open water (August 2015, 2016). O_2, dissolved oxygen; DOC, dissolved organic carbon; PC, particulate carbon; Chl *a*, chlorophyll *a*; TN, total nitrogen; TP, total phosphorus; DIN:TP, dissolved inorganic nitrogen to phosphorus mass ratio; TFe, total iron; $dSiO_2$, dissolved silica; SO_4^{2-}, sulfate.

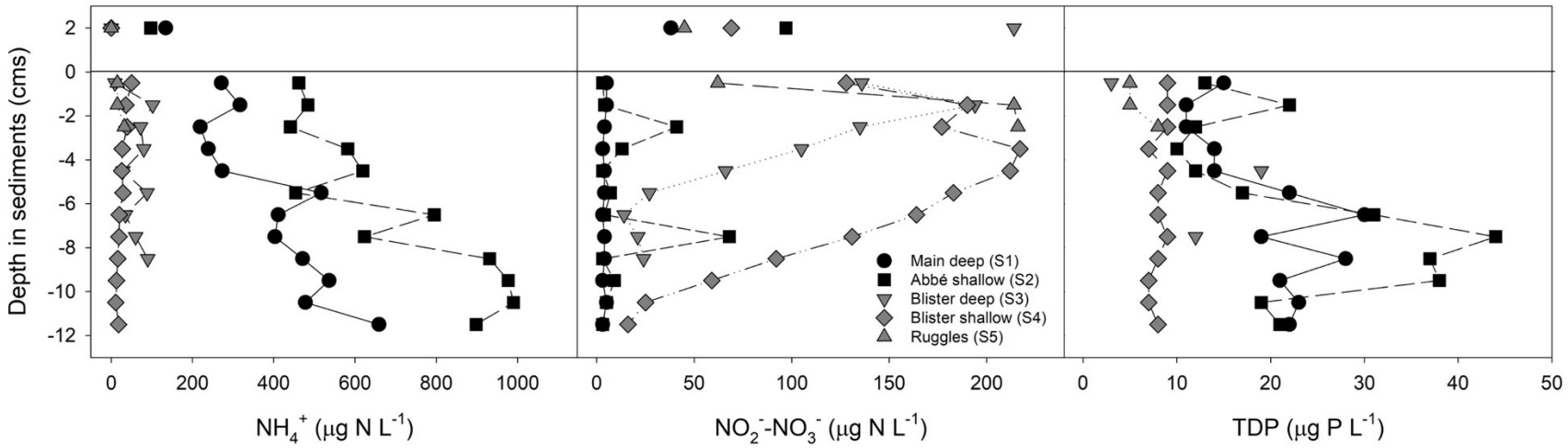

Figure 2-4. Sediment core porewater profiles of NH_4^+, NO_2^--NO_3^- and total dissolved phosphorus (TDP) from 5 sites throughout Lake Hazen. Sites were chosen to represent variable proximity of glacial inflows. Cores nearer large glacial inflows are indicated in black. Concentrations in the overlying water were quantified on water samples collected from the top of the core tube before sectioning.

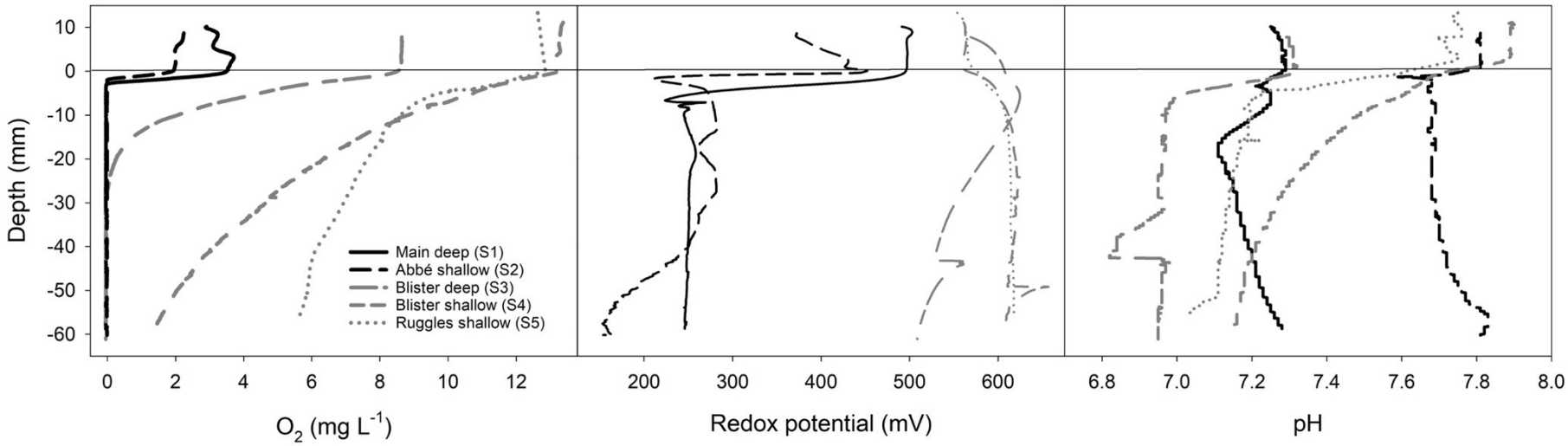

Figure 2-5. Sediment core microprofiles for 5 sites in Lake Hazen, representing variable proximity to glacial inflows. Cores near large glacial inflows are indicated in black.

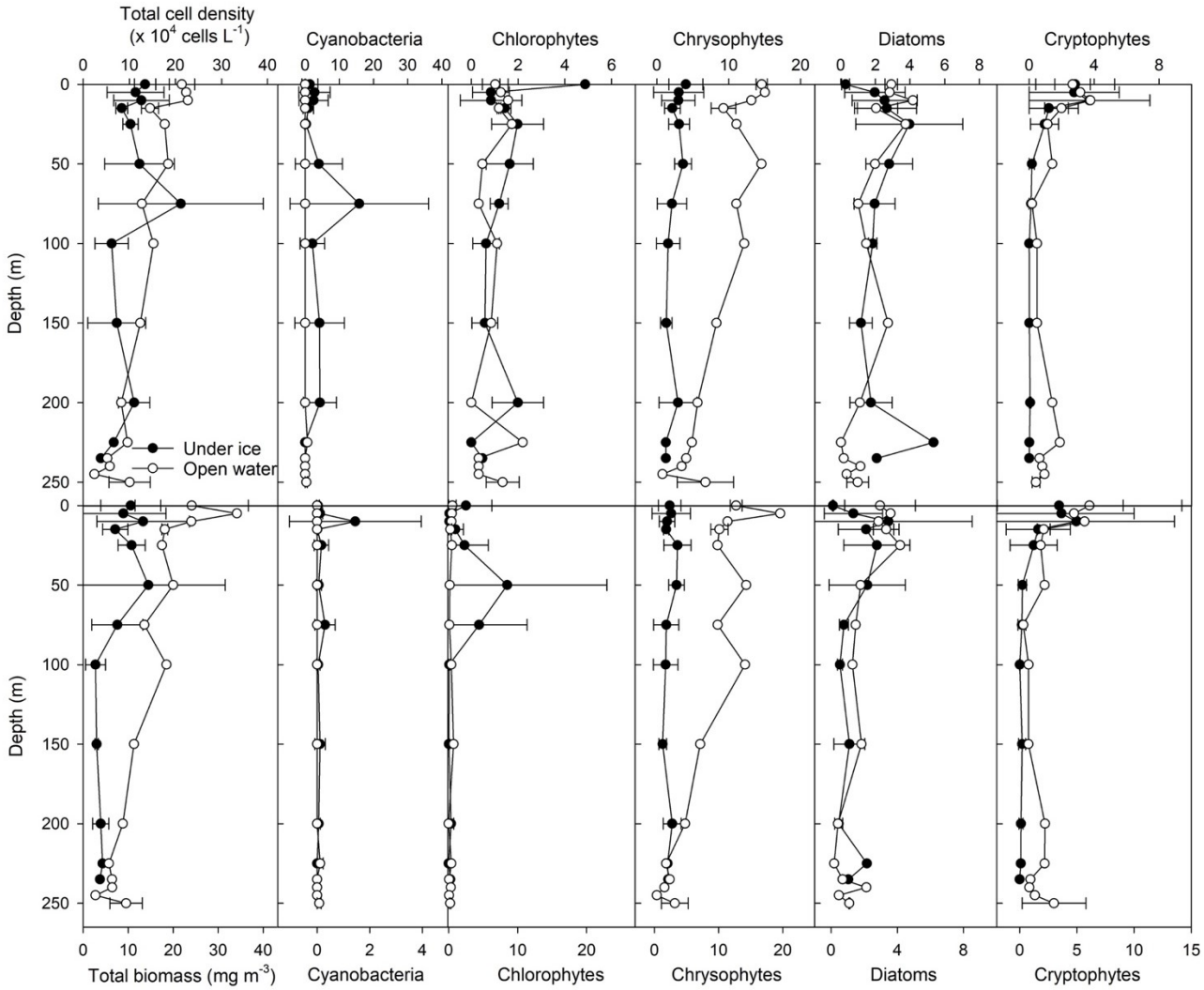

Figure 2-6. Seasonal water column profiles of phytoplankton taxonomic group cell densities (top panels) and biomass (bottom panels) in Lake Hazen. Means (±1SD) by depth shown, over profiles conducted in May (under ice) 2013 (chl *a* only) and 2014 (2 profiles), and in August (open water) 2015 and 2016.

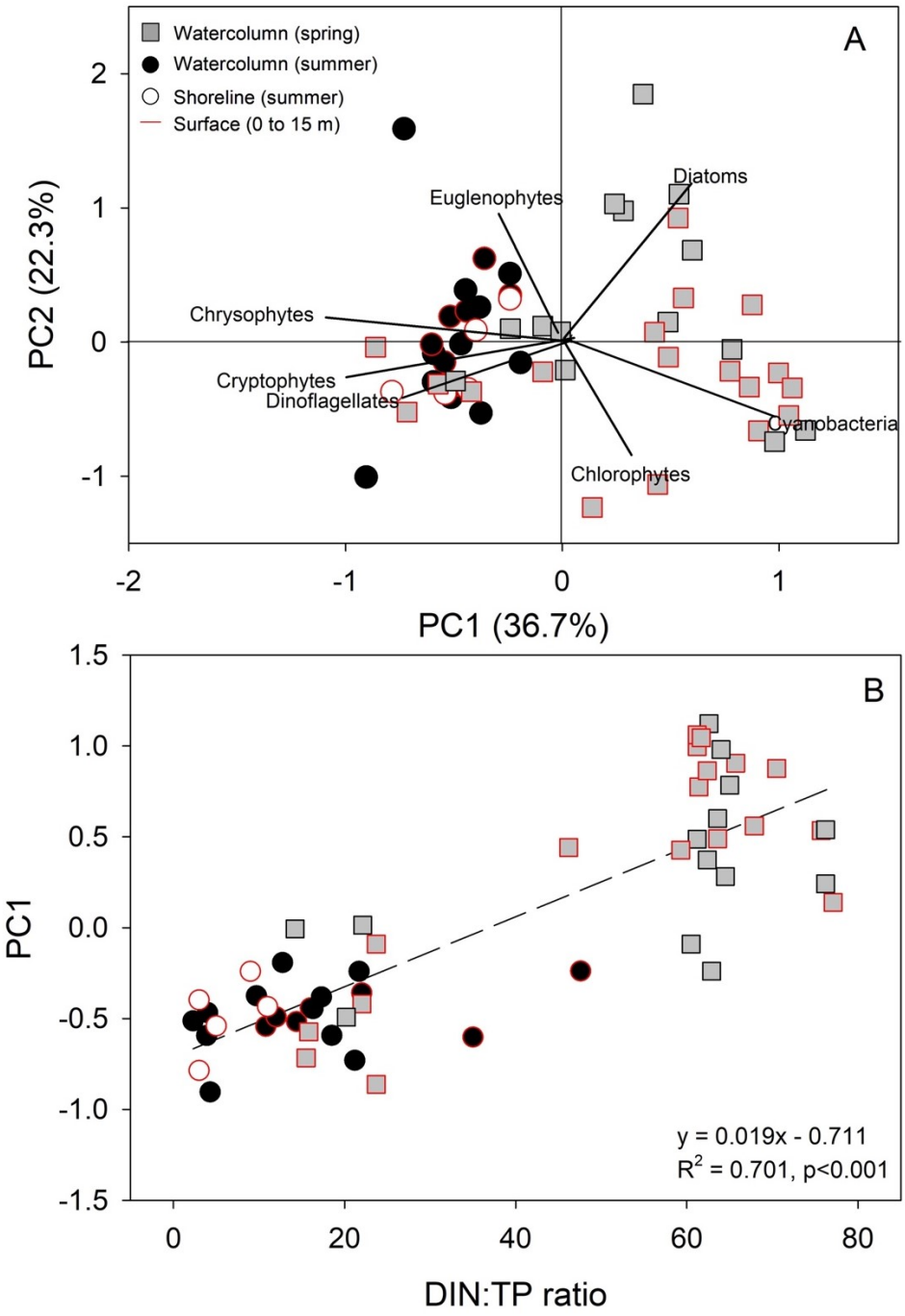

Figure 2-7. A: Principal component bi-plot of phytoplankton community composition (as Hellinger-transformed cell densities) and B: the first principal component (PC1) scores as a function of the DIN:TP mass ratio.

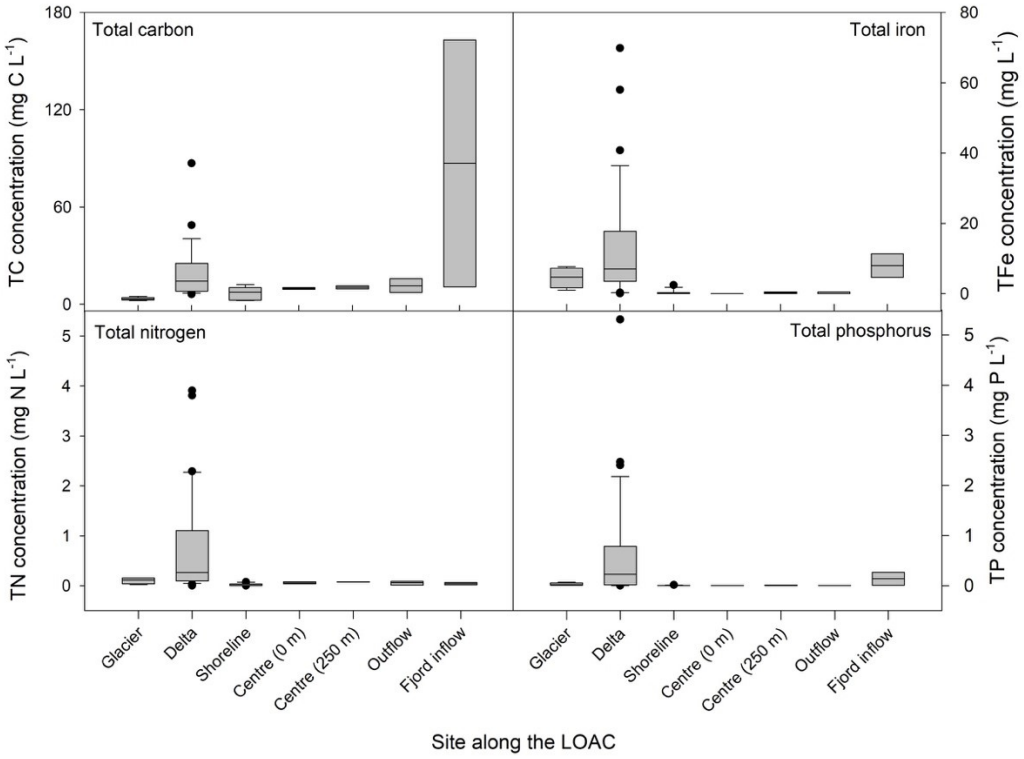

Figure 2-8. Nutrient concentrations along the land to ocean aquatic continuum (LOAC) in the Lake Hazen watershed. Sampling sites extended from immediately in front of the glacier termini to the glacial river deltas, along the shoreline of Lake Hazen, at the surface and bottom of the water column at the deepest (267 m) spot in the lake, along the Ruggles River outflow at Lake Hazen, and the Ruggles River inflow to Chandler Fjord along the northeastern coast of Ellesmere Island.

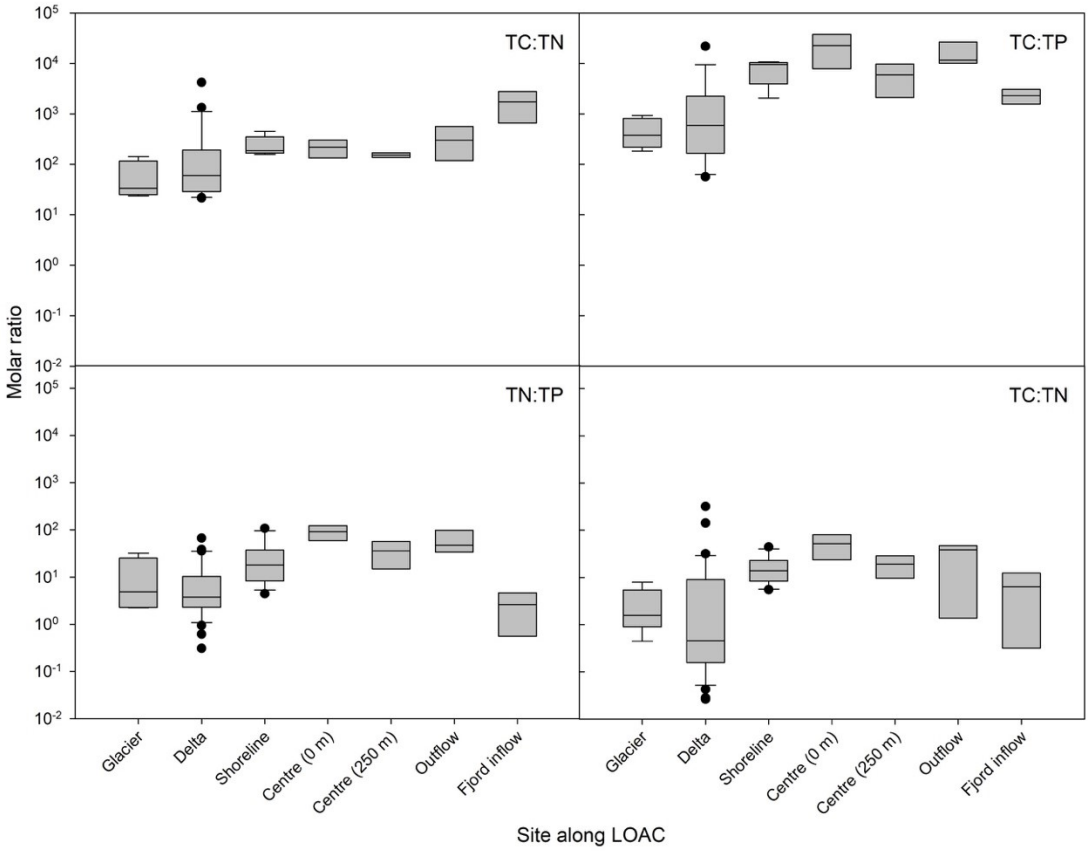

Figure 2-9. Molar ratios of key nutrients along the land to ocean aquatic continuum (LOAC) in the Lake Hazen watershed. Sampling sites extended from immediately in front of the glacier termini to the glacial river deltas, along the shoreline of Lake Hazen, at the surface and bottom of the water column at the deepest (267 m) spot in the lake, along the Ruggles River outflow at Lake Hazen, and the Ruggles River inflow to Chandler Fjord along the northeastern coast of Ellesmere Island. Note that the y-axis is on a log scale.

Table 2-1. Hydrological nutrient mass balances (annual loads in metric tons yr^{-1} ± SE) for Lake Hazen in 2015 and 2016.

		Hydrological inputs				Outputs	
	Year	Snow on lake [1]	Snow from land [2]	Glacial rivers	Total inputs	Ruggles River	% diff.[3]
Water (km^3)	2015	0.069±0.015	0.055±0.012	0.948	1.07±0.027	1.07±0.027	-
	2016	0.060±0.008	0.059±0.089	0.281	0.400±0.097	0.400±0.097	-
NH_4^+	**2015**	**0.584±0.115**	**1.67±0.454**	**22.9±15.9**	**25.2±16.5**	**3.79±1.38**	**-71.1***
	2016	**0.551±0.092**	**1.48±0.371**	**5.42±2.15**	**7.45±2.61**	**1.13±0.411**	**-63.6***
NO_3^--NO_2^-	**2015**	**2.81±0.611**	**5.63±1.89**	**35.1±4.84**	**43.6±7.34**	**12.0±7.59**	**-33.7***
	2016	**2.22±0.361**	**4.98±1.59**	**12.0±1.34**	**19.2±3.29**	**3.57±2.26**	**-40.4***
SO_4^{2-}	2015	73.0±0.016	993±235	13400±2420	14420±2661	9400±1440	-15.5
	2016	77.8±0.016	879±188	3580±411	4540±599	2790±428	-6.66
TDP [4]	2015	0.177±0.037	1.00±0.309	-	-	-	-
	2016	0.134±0.029	1.08±0.282	-	-	-	-
$dSiO_2$	2015	5.88±0.001	16.0±3.21	181±59.2	203±62.4	246±75.8	+15.4
	2016	5.09±0.001	14.2±2.44	56.9±11.0	76.2±13.5	73.2±22.5	+15.5
DIC	**2015**	**139±0.028**	**102±21.0**	**6310±474**	**6550±495**	**9700±2470**	**+24.9***
	2016	**117±0.019**	**88.0±15.4**	**1920±117**	**2120±132**	**2880±735**	**+31.7***
DOC	**2015**	**6.92±0.002**	**0.087±0.023**	**364±59.6**	**371±59.6**	**203±55.9**	**-23.7***
	2016	13.3±0.003	0.077±0.018	109±14.5	123±14.6	60.6±16.6	-17.6

[1] Snow chemistry from 2015 only applied to 2015, and mean snowpack AWV across 2013, 2015, 2017 applied to 2016.
[2] Snowmelt volume calculated assuming 16% runoff of snowpack on landscape (see methods).
[3] % difference between total mean hydrological inputs and outputs by the Ruggles River. Budgets for which output load ranges are outside of the range of inputs (*), suggesting an important annual source (% difference > 0) or sink (% difference < 0) within the lake.
[4] TDP was only above detection in snow, and as such glacial river and Ruggles River compartment fluxes could not be calculated.

Chapter 3. Chemical weathering in glacial meltwaters are creating strong downstream freshwater CO_2 sink

Most inland freshwater systems, such as lakes, rivers, ponds and reservoirs, are net emitters CO_2 to the atmosphere on an annual basis.[1] Biological and abiotic processes leading to CO_2 supersaturation and resultant emissions from surface waters include net heterotrophy,[2] catchment inputs of dissolved inorganic carbon (DIC),[3,4] photochemical mineralization of organic matter,[5,6] and calcite precipitation.[7] Glacier-fed rivers and lakes have hitherto been overlooked in studies of global CO_2 cycling, despite their rapid expansion following enhanced glacier melt.[8-11] CO_2 cycling in glacierized watersheds differs critically from what is observed in other northern, temperate and tropical systems due to 1) little export of organic carbon (OC) from sparsely vegetated landscapes, an important subsidy of heterotrophy;[2,12] and, 2) an abundance of freshly eroded sediments susceptible to rapid chemical weathering. Both of these characteristics have potentially important consequences for carbon budgets in glacierized watersheds.

Sub-glacial chemical weathering has been described extensively (e.g., ref. [13-15]) but comparatively little is known about the extent of such weathering in proglacial freshwaters.[13] Both carbonate and silicate weathering reactions (equations 1, 2 in Figure 3-1) have the potential to consume atmospheric $CO_{2(g)}$ dissolved in water ($CO_{2(aq)}$), but can be limited sub-glacially due to a lack of $CO_{2(g)}$ exchange with the atmosphere,[14] and supra-glacially due to a lack of comminuted sediments.[16]

Although the possibility of atmospheric CO_2 consumption by chemical weathering in proglacial freshwaters has been proposed,[17,18] in-depth studies of proglacial freshwater networks have been limited,[19-22] with very few *in situ* measurements of $CO_{2(aq)}$, despite its importance as an indicator of freshwater ecosystem function and mineral weathering reactions. Moreover, these few studies have focused on small glaciers in isolation rather than as integral parts of watersheds, overlooking the fact that glaciers are hydrologically connected to downstream ecosystems.

Here we extend the study of chemical weathering beyond the glaciers themselves to the proglacial freshwater drainage network, using the Lake Hazen watershed (81.8°N, 71.4°W; 7516 km^2, 40.9% glacierized) in Quttinirpaaq National Park on Ellesmere Island, Nunavut, Canada as

a model system (Figure A2-1). Ultra-oligotrophic Lake Hazen (544 km^2, maximum depth = 267 m) is fed by eleven glacial rivers (4.6 – 42 km long) originating from the southeastern outlet glaciers (6 – 1041 km^2) of the Northern Ellesmere Icefield. The watershed is underlain by sedimentary bedrock, dominated by quartzite, sandstone, and schist to the northwest and sandstone, carbonate, and shale to the southwest along the Hazen Plateau.[23] Using a comprehensive, whole-watershed approach to elucidate the impacts of glacial melt on net freshwater CO_2 fluxes, we first determined $CO_{2(aq)}$ consumption in the rivers between their sources at glacial termini and their deltas along the Lake Hazen shoreline during the ablation season (June, July, August [JJA]), and then quantified annual CO_2 consumption within Lake Hazen itself. To understand the relative importance of glacier-fed freshwater CO_2 cycling in watershed CO_2 budgets, we compared the measured freshwater CO_2 fluxes with CO_2 fluxes from the adjacent terrestrial environment (polar desert and non-glacial wetlands and ponds).[24,25]

$CO_{2(aq)}$ consumption in glacial inflows to Lake Hazen

Seven glacier-fed rivers were sampled between the glacier termini and the deltas (downstream distances 0.1 to 42 km) regularly throughout summer 2016. *In situ* concentrations of $CO_{2(aq)}$ were below atmospheric equilibrium (%CO_2 saturation range: 15.2 to 102%, mean±SD: 70.4±22.7%; Figure A2-2) at all but one of the sites sampled. In contrast, concentrations of dissolved oxygen ($O_{2(aq)}$) were at or above atmospheric equilibrium at all sites (101±4.10%; Figure A2-2), showing that turbulent proglacial river waters were well mixed with the atmosphere, as well as precluding significant anoxic subglacial contributions. $CO_{2(aq)}$ saturation decreased with increasing distance from the glaciers with a concomitant increase in dissolved inorganic carbon (DIC), anions, and silica (Figure 3-2), as a result of weathering reactions (Box 1, Figure 3-1).[26]

δ^{13}C-DIC was highly depleted in the proglacial rivers relative to atmospheric equilibrium (-1.50 to 0.55‰), ranging between -7.32 and 0.40‰ (mean: -2.92‰; Table A2-1). δ^{13}C-DIC depletion in these rivers could result from OC oxidation, or rapid carbonate and silicate weathering (equations 1, 2 in Figure 3-1) and associated kinetic fractionation.[27] However, dissolved organic carbon (DOC) concentrations in all glacial rivers were extremely low (mean: 0.4±0.2 mg L^{-1}; Table A2-1), precluding OC oxidation from significantly influencing δ^{13}C-DIC. As such, rapid mineral weathering within the rivers is the most likely process to account for both

increasing DIC, and declining $CO_{2(aq)}$ concentrations/saturation over the river lengths, and low δ^{13}C-DIC values.

Across the proglacial drainage network, geological formations are poorly consolidated following glacial retreat such that glacial meltwaters can easily erode riverbed sediments and bank deposits. This leads to higher concentrations of suspended mineral sediments (mean TSS±SD: 563±893 mg L^{-1}) capable of weathering in river waters with increasing distance from the glaciers (mean TSS±SD at the deltas: 563±893 mg L^{-1}). Peak glacial river runoff in late July coincided with minimum $CO_{2(aq)}$ and δ^{13}C-DIC, matching a theoretical scenario of rapid calcite weathering following influx of $CO_{2(g)}$ (Figure 3-3).

As weathering reactions consume $CO_{2(aq)}$ in the rivers, $CO_{2(aq)}$ is constantly being replenished from the atmosphere (Figure 3-1), but much more slowly than the weathering reactions can consume it.[27] As such, *in situ* $CO_{2(aq)}$ concentrations in proglacial rivers represent the balance between the rate of consumption by chemical weathering and the resupply from the atmosphere. To quantify the capacity for weathering reactions to consume $CO_{2(aq)}$ in the absence of atmospheric exchange at the time of sampling (termed: weathering endpoint), unfiltered river water samples were collected in pre-evacuated serum bottles containing a KCl preservative to prevent biological activity.[28] The mean weathering endpoint $CO_{2(aq)}$ saturations were 29.5±35.3%, markedly more undersaturated than that measured in situ in the flowing rivers (Table A2-1). Weathering endpoint $CO_{2(aq)}$ concentrations conclusively showed that CO_2 consumption was actively occurring in the rivers, was not due to primary productivity, and that equilibrium with the atmosphere had not been reached at the time of sampling.

High Arctic glaciers with cold-based margins, like those in the Lake Hazen watershed, have traditionally been considered less erosionally intensive than their warm-based or temperate polythermal counterparts.[29,30] Indeed, mean annual sea salt-corrected cation equivalent ($\sum^{+}$) weathering rates for the glacial rivers in the Lake Hazen watershed were 170 meq m^{-2} (2015) and 58.5 meq m^{-2} (2016; Table A2-2), at the low end of, or lower than, those measured in other glacial systems (94 to 4200 meq m^{-2}).[24] Even with annual solute denudation rates (sum of molar fluxes of all dissolved major cations, anions and silicon) and SiO_2 yields only averaging 2.16 to 9.92 t km^{-2} and 0.164 to 29.1 mg m^{-2} (i.e., less than the global average[31]), respectively, receding glaciers and glacial river valleys are still important sources of dissolved cations, anions and

recently comminuted sediments to receiving aquatic systems, for which glaciers are often a major source of water.

DIC accumulation along the length of rivers was therefore used as a measure of realized CO_2 consumption. This approach was adopted in lieu of using $CO_{2(aq)}$ concentrations and calculated gas transfer coefficients (*k*), the latter of which are extremely variable in both channelized systems[32,33] and highly braided glacier-fed rivers such as those in our study. By relating the increases in cations and silica concentrations to weathering stoichiometry (equations 1 and 2, Figure 1), we accounted for all (125±13.6%) of the increase in DIC concentration between the glacier termini and river deltas to weathering (Figure 3-2).

We estimate that the glacial rivers in the Lake Hazen watershed consumed 1020±496 Mg C-CO_2 yr^{-1} (2015-2016 mean) through chemical weathering, making the glacial rivers an important and previously overlooked CO_2 sink at the watershed scale (Table 3-1). Despite covering only 2% of the non-glacierized area in the Lake Hazen watershed, the total melt season CO_2 drawdown by glacial rivers approximately counter-balanced the polar desert efflux (1370 Mg C-CO_2 yr^{-1}; Table 1). On an areal basis, the glacial rivers consumed 0.376±1.20 g C-CO_2 m^{-2} d^{-1}, the second largest watershed flux after wetland consumption of 0.955±0.291 g C-CO_2 m^{-2} d^{-1}. This is in stark contrast to rivers globally, which are almost ubiquitously considered net sources of C to the atmosphere (0.66±0.11 g C-CO_2 m^{-2} d^{-1}, range: -1.60 to 2.06 g C-CO_2 m^{-2} d^{-1}).[34] In fact, during the 2016 melt season (a relatively low melt year), the glacial rivers in the Lake Hazen watershed consumed on a per-m^2 basis about half as much carbon daily (0.085±0.187 g C-CO_2 m^{-2} d^{-1}) as the Amazon rainforest (0.153 g C-CO_2 m^{-2} d^{-1}; calculated from ref 35 and 36). In the 2015 ablation season, when glacial melt was approximately 3-times that in 2016, CO_2 consumption rates in the glacial rivers were, on average, twice that of the Amazon rainforest, with maximum daily rates of up to 40-times higher on a per-m^2 basis (6.14 g C-CO_2 m^{-2} d^{-1}).

Impact of glacial inputs on net CO_2 consumption in receiving freshwater systems.

Like other Arctic and alpine glacier-fed lakes, the chemistry of ultra-oligotrophic Lake Hazen is particularly sensitive to geochemical inputs from its catchment.[12,37] Coincident with the start of watershed inputs to the lake in early June, when the lake is still ice-covered, an open-water moat forms around the periphery of Lake Hazen. As the region warms, lake ice melts, and the surface

area available for exchange with the atmosphere increases gradually until complete ice off, if it occurs, in late July or early August. Whereas the lake rarely went ice-free prior to the early 2000s, a late summer ice-free lake is now common place.[38]

Following lake ice melt (26-July-2015), $CO_{2(aq)}$ concentrations in waters near the shore of Lake Hazen between the inflows of the Blister and Snowgoose rivers ranged between 19.7 and 25.2 µM (mean: 21.8±1.07 µM). The lake surface was a net CO_2 sink over the same period with instantaneous CO_2 consumption from lake surface waters averaging 27.1±18.1 µmol m^{-2} h^{-1} and maximum CO_2 consumption occurring overnight (Figure A2-3). CO_2 fluxes in waters near the shore of Lake Hazen were significantly influenced by glacial runoff (CO_2 flux in µmol m^{-2} d^{-1} = -4.96 log[runoff in m^3 d^{-1}]+60.6; r^2 = 0.21, F = 9.54, $p < 0.001$), such that these waters became a progressively greater CO_2 sink as glacial melt intensified (Figure 3-4). As in the glacial rivers, weathering endpoint $CO_{2(aq)}$ concentrations in near shore waters were significantly lower than *in situ* $CO_{2(aq)}$ concentrations (paired t-test: t=4.73, df = 40, $p < 0.001$), excluding CO_2 consumption by primary productivity as the main cause of CO_2 undersaturation.

By applying daily ice-free areas on the lake delineated using the MODIS snow cover product (MOD10A1) to the mean daily CO_2 fluxes over the continuous measurement period (7-July to 2-August 2015), we estimated a mean daily surface CO_2 consumption rate (sum of hourly fluxes, n=14 days with 24 h records) of 2570±603 kg C-CO_2 d^{-1}, translating to an estimated cumulative surface drawdown of 66.7±11.5 Mg C-CO_2 between 7-July and 2-August 2015. If we extrapolate this to the entire ablation season (JJA), Lake Hazen surface waters are a marginal (<1% of the total budget) CO_2 source, emitting 47.7±19.8 Mg C-CO_2 to the atmosphere (Table 3-1). With the reduction of high turbidity, low $CO_{2(aq)}$ glacial inputs to Lake Hazen in August, turbulent mixing in the nearshore region is reduced, and the respiration of OC, and subsequent production of $CO_{2(aq)}$, become relatively more important contributors to net CO_2 emissions during the shoulder seasons than geochemical weathering processes.

At the centre of the lake, 4.5 kilometers away from the direct influence of the nearest glacial inflows (Figure A2-1), surface waters were likewise under-saturated in $CO_{2(aq)}$ during the summer (84.5±3.34%) (Figure 3-5; $O_{2(aq)}$ saturation = 102±1.98%). Even at 250 m depth, $CO_{2(aq)}$ concentrations were 19.4 µM (August 2015) and 24.8 µM (August 2016), corresponding to $CO_{2(aq)}$ saturations of 72.9% and 93.9% respectively ($O_{2(aq)}$ saturation: 101% and 98.2%). $CO_{2(aq)}$ undersaturation or even equilibrium at depth are highly atypical for large deep lakes, where light

penetration and primary productivity are limited to the upper reaches of the water column.[39] As dense, sediment-laden glacial river waters flow into Lake Hazen, they form turbid underflows, transporting fine particulates, and waters with high $O_{2(aq)}$ and low $CO_{2(aq)}$ from river deltas to the depths of the lake (Figure 3-5). The magnitude of summer melt was thus the primary control on water column $CO_{2(aq)}$ concentrations as the greater glacial melt volume in 2015 was associated with greater $CO_{2(aq)}$ undersaturation at depth. The observation of $CO_{2(aq)}$ undersaturation at depth is particularly striking, given that springtime $CO_{2(aq)}$ concentrations in bottom waters are up to 476% oversaturated (121 μM; Figure 3-5). Indeed, summertime oxygenation and $CO_{2(aq)}$ undersaturation of Lake Hazen bottom waters were historically rare and are believed to be a direct consequence of the intensification of glacial melt in the watershed and the resultant lake mixing.[38]

To quantify CO_2 consumption by chemical weathering in Lake Hazen itself, we calculated annual DIC mass balance budgets for the lake by subtracting DIC inputs from all major water sources (glacial and snow melt waters) from DIC exports out the Ruggles River. We then used water column δ^{13}C-DIC to attribute net DIC exports from Lake Hazen to respiration or chemical weathering (see Methods for details). Lake Hazen was annually a source of DIC (3150±3870 Mg C-CO_2 yr^{-1}, 2015-2016 mean) to the Ruggles River, of which only 12.9% could be attributed to respiration, producing approximately 558±486 and 254±220 Mg C-CO_2 yr^{-1}, in 2015 and 2016, respectively. Given that the remaining DIC must then have originated from chemical weathering, we estimate that 1890±1650 Mg C-CO_2 yr^{-1} and 860±740 Mg C-CO_2 yr^{-1}, or 43.6% of DIC exports in each year, originated from the consumption of CO_2 by carbonate dissolution. This latter chemical weathering estimate was independently confirmed by integrating the difference between weathering endpoint and equilibrium $CO_{2(aq)}$ concentrations throughout the late July 2015 water column, following most of that year's annual delivery of comminuted sediments to the lake, and correcting for water column dilution by CO_2-undersaturated glacial inflows (1581 Mg C-CO_2 yr^{-1}). Because glacial inputs continued for a short time after we sampled the water column, this estimate is conservative, yielding high confidence in our results. Combining our estimates of CO_2 produced by respiration and CO_2 consumed by chemical weathering, we calculate a net CO_2 consumption for the Lake Hazen water column of 1330±1160 (2015) or 606±524 Mg C-CO_2 yr^{-1} (2016), depending on the year.

Internal $CO_{2(aq)}$ consumption within Lake Hazen was thus approximately equal to or greater than $CO_{2(aq)}$ consumption within the glacial rivers in a given year. Together, these estimates show not only that the influence of the glacial rivers extends far beyond the river channels themselves, but also that the magnitude of this net CO_2 uptake due to chemical weathering varies inter-annually, depending on the volume of meltwaters discharging from the glaciers, such that there would be greater uptake during high-melt years, and less uptake during low-melt years. By summing estimates of net CO_2 consumption in glacial rivers and Lake Hazen itself, we calculate a net aquatic CO_2 uptake within the Lake Hazen watershed of 1986±1700 Mg C-CO_2 season^{-1}, or 17% of the total watershed CO_2 budget (Table 3-1).

Projected global glacial melt and downstream freshwater CO_2 cycling

By 2050, global (non-ice sheet) glacier volume could decline by between 28 and 44% (ref 40) with coincident near term changes in glacial river runoff.[41] At high latitudes, glacial runoff is expected to increase at least until the middle of the century[41,42] with yet unknown consequences on the biogeochemistry of receiving aquatic ecosystems.[43] Although Lake Hazen is an unusually large body of water for the High Arctic and theoretically more resilient than smaller systems to short-term (seasonal) phenomena,[44] we show that the lake is annually transformed into a CO_2 sink by glacial river inputs. Meltwaters from projected glacial loss could thus conceivably overwhelm the biogeochemistry of smaller, more common freshwater systems.

While the Lake Hazen watershed is underlain by a diverse, carbonate-rich geology,[23] transient CO_2 consumption by glacial meltwaters has also been inferred in areas dominated by basalt and metamorphic rocks,[17,45] an effect which should extend to the proglacial freshwater network. Indeed, studies directly quantifying the downstream impacts of glacial melt on CO_2 are few, but $CO_{2(aq)}$ undersaturation has been observed at other sites in Greenland, Svalbard, Central Europe and Western Canada (Table A2-3). For example, $CO_{2(aq)}$ concentrations in rivers fed by the Kiattuut Sermiat (61°11.8'N, 45°20.4'W) and Saskatchewan (52°10.2'N, 117°4.6'W) glaciers, measured using the same technique as in the Lake Hazen watershed, were only 22% and 35% saturated with respect to atmospheric CO_2 at locations 2.5 and 5 km downstream of the glaciers, respectively. This strongly suggests that the effects of glacial melt-induced freshwater $CO_{2(aq)}$ consumption observed in the Lake Hazen watershed could be relevant across divergent geologies, glacier thermal regimes and climates.

Understanding the impact of glacial loss on carbon cycling in downstream freshwater ecosystems, however, remains challenging. Due to the dynamic relationship between proglacial systems and fluctuating glacier dynamics,[46] there exists no published estimate of either the number of proglacial rivers and/or area of proglacial lakes globally, hampering our ability to understand the extent of glacial influence on downstream systems. Our results highlight the importance of glacially-fed freshwater systems to the carbon cycle at the watershed scale. We suggest that the effect of glacial melt on CO_2 consumption in downstream ecosystems reported here is not limited to the High Arctic (Table A2-3), but rather, is potentially a globally relevant phenomenon meriting greater in-depth study given future climate change predictions. Based on our results, projected increases to glacial melt imply not only a short-to-medium term increase in water fluxes to downstream ecosystems, but also an increase in the amount and intensity of weathering of highly reactive comminuted sediments being transported downstream, with a concomitant uptake of atmospheric CO_2 that has important implications for regional carbon budgets in certain glacierized catchments.

METHODS

Study area. Lake Hazen, located within Quttinirpaaq National Park on northern Ellesmere Island, Nunavut, Canada, is the world's most voluminous lake entirely above the Arctic Circle (Figure A2-1). Runoff from the outlet glaciers of the Northern Ellesmere Icefield occurs primarily through supraglacial and ice-marginal channels, though subglacial water has been detected for the Henrietta Nesmith Glacier.[49] Ice from the Northern Ellesmere Icefield retreated from Lake Hazen approximately 5000 years ago,[50] exposing diverse geology dominated by the sedimentary bedrock of the Cambrian Grant Land formation (quartzite, sandstone, schist) to the northwest and the Silurian Danish River formation (sandstone, carbonate, shale) to the southwest, along the Hazen Plateau.[23] Faulting and folding along the northwest shore of Lake Hazen have resulted in several unconformities. In parts of the watershed, coal deposits are exposed as well as Permian-age fossil beds.

The glacial rivers surveyed in this study drained 2568 km^2 or 84% of the total glacierized watershed area, and extended between 4 and 42 km along defined river valleys before flowing into Lake Hazen. The annual melt season on northern Ellesmere Island currently extends from early June to late August. Total modelled glacial runoff volumes for the Lake Hazen watershed

were 0.98 km^3 and 0.29 km^3 in 2015 and 2016 respectively (2001-2016 mean = 0.47±0.44 km^3), with the most important contributions coming from the Henrietta Nesmith, Very, and Gilman glaciers. The Ruggles River (28.8 km) flows year-round, connecting Lake Hazen to Chandler and then Coneybeare fjords on the northeastern coast of Ellesmere Island. The Lake Hazen watershed is located within the continuous permafrost zone, and although active layer thaw occurs, it is hydrologically insignificant. Total precipitation for the non-glacierized area of the Lake Hazen watershed is ~95 mm.[51]

Meteorological conditions at the Lake Hazen base camp were recorded hourly throughout the field seasons with a Campbell Scientific CR800 datalogger equipped with a Met One 014A anemometer, 109-L shielded air temperature probe, Young 61302 V barometer, and a Kipp and Zonen PQS1 photosynthetically active radiation sensor. Mean summer (approx. 6 July - 10 August 2015-16) air temperatures were 8.02°C (range: 1.34 – 17.4°C). Snowmelt on the landscape and lake ice surface occurs in late May/early June, followed by a short decrease in runoff before melt from the glacierized area begins in late June. Rainfall during the summer (JJA) ablation season has been previously recorded as only ~34 mm (2008-2012 mean).[24] During summer, snowfall within the watershed outside of the icefield is rare. During the period of this study, the ablation seasons extended from approximately 2 June to 17 August (2015), and 5 June to 28 August (2016). No meltwaters are discharged from the glaciers outside of this period. Mean annual air temperatures for 2015 and 2016 at Alert (82.5°N, 62.3°W) and Eureka (80.0°N, 85.9°W), the closest permanent weather stations, were -14.8±1.3°C and -17.5±0.8°C, respectively (Environment and Climate Change Canada).

Water samples were collected during summers 2015 (6 July to 2 August) and 2016 (2 July to 8 August), focusing on Lake Hazen itself in 2015 and on the glacial rivers in 2016. In so doing, we surveyed the entirety of the arctic freshwater continuum from the glacier termini through to the receiving freshwater ecosystems (river and lake).

Glacial rivers. *Sample collection*. In summer 2016, samples were collected at the Blister and Snowgoose rivers every 3-4 days for analysis of carbon chemistry, anions and total suspended solids (TSS) and weekly for cations. An additional five glacial rivers (Very, Henrietta Nesmith, Abbé, Gilman, Turnabout) were sampled twice during the summer by helicopter (11-13 July and 1-2 August). Transects were completed along the Blister, Snowgoose, and Gilman rivers to

assess the evolution of meltwater chemistry with increasing distance from the glacier. Temperature, pH, dissolved oxygen and turbidity were measured with an EXO2 sonde (YSI Inc., Yellow Springs, OH, USA). $CO_{2(aq)}$ concentrations were measured *in situ* using a Vaisala GM222 0-2000 ppm CO_2 probe (>99% accuracy), waterproofed with a gas-permeable PTFE sleeve (International Polymer Engineering, Tempe, AZ, USA), and connected to a handheld Vaisala GM70 meter set for *in situ* temperature and pressure.[52] Probes were factory calibrated, but calibrations were verified prior to and following each field season using three Praxair-certified CO_2 standards ranging between 48 and 895 ppm.

We collected unfiltered samples for analyses of $CO_{2(aq)}$ concentrations in pre-evacuated 160 ml serum bottles with a 10 ml UHP N_2 headspace and 8.9 g KCl preservative to kill biological activity.[28] Because the samples were unfiltered, weathering reactions were able to proceed to equilibrium inside the bottles without CO_2 exchange with the atmosphere. Hence, CO_2 concentrations measured using this technique should not be considered *in situ*, but rather as a measure of the maximum capacity of the system for chemical weathering (termed weathering endpoint). Triplicate DIC and δ^{13}C-DIC samples were filtered on-site with 0.45 μm cellulose nitrate syringe filters into 12 mL glass exetainers (Labco Ltd., Lampeter, UK) with no headspace, and then preserved with 50 μL of 2.5 mM $ZnCl_2$.

Immediately upon return to the Lake Hazen Field Laboratory, bulk water samples were filtered through pre-weighed 0.45 μm cellulose-acetate filters for other suspended and dissolved parameters. Filters and filtrate were kept in a cool, dark place until analysis of total suspended solids, and dissolved constituents (SO_4^{2-}, Cl^-, Ca^{2+}, Mg^{2+}, Na^+, K^+, DOC, Si) respectively, using accredited protocols at the Biogeochemical Analytical Service Laboratory (BASL, University of Alberta).

Glacial runoff. Watershed areas for each of the glaciers, hereafter termed sub-watersheds, were delineated from the 1:50000 Canadian Digital Elevation Model (CDEM; Natural Resources Canada). Daily glacial runoff (kg m^{-2} d^{-1}) was modeled using a surface mass balance approach within each sub-watershed,[53] where runoff was calculated as the difference between daily melt and refreeze. Due to its size, the Blister River sub-watershed area was not highly resolved in the CDEM, and consequently could not be directly modeled. Areal runoff estimates from the Snowgoose Glacier, the next smallest glacier sampled and closest geographically, were thus

applied to the Blister Ice Cap area (~6 km^2, Randolph Glacier Inventory, Version 5.0) to approximate discharge. Using modelled glacier runoff assumes the proglacial zone makes minimal contributions to either water fluxes or evaporative losses. Water stable isotope signatures (δ^2H-H_2O and $\delta^{18}O$-H_2O) did not change between the glacier and deltas (mean deviation from global meteoric water line=0.39±0.02‰), validating these assumptions. 30-day averaged modelled runoff matched measured discharge from Lake Hazen at the Ruggles River,[38] providing further confidence in our use of modelled runoff volumes. Diurnal variations in meltwater fluxes during the ablation season are muted in High Arctic watersheds, relative to temperate alpine environments, due to 24 h sunlight.[54] Given the logistical constraints imposed by working at the watershed scale on spatially and temporally-dynamic braided river systems in the remote High Arctic, we believe this to be a best available approximation of discharge. Glacial river valley areas were manually delineated in Google Earth Pro 7.3. All areal weathering and flux estimates are thus conservative, given that the valley areas are likely overestimated due to the resolution of Landsat imagery (30 m) and the rivers are unlikely to cover the entire valley floor at any given point in time.

Weathering rates. Log-linear flux models relating solute concentration to glacier runoff were fitted using the rLOADEST package in R.[55,56] Models were generated by pooling samples across all rivers and relating them to their sub-watershed specific discharge. The solute-specific model of best fit (Table A2-4) was used to extend the solute fluxes to the entire melt season. In all cases, we selected the model for which bias was minimized. Variance inflation factors between independent variables for all model 2 iterations were 1, indicating low multicollinearity. r^2 was always > 0.95 ($p << 0.05$), and biases < 20%.

For each sub-watershed, annual cation equivalent weathering rates were calculated as the sum of modeled sea salt-corrected loads of dissolved Ca^{2+}, Mg^{2+}, Na^+ and K^+ at the river deltas.[17,57] Total Lake Hazen watershed weathering rates were calculated based on the sampled watersheds representing 84% of the glacierized watershed area. In 2015, the mean (n=19) sea salt-corrected snowpack SO_4^{2-}:Cl^- ratio was 2.78, an assumed constant contribution to glacial river waters through the summer.[17] Total solute denudation rates were calculated as the sum of all dissolved (< 0.45 μm) crustal-derived cation, anion and Si fluxes.[22] We adapted the solute provenance model of ref [17] and ref [22] because one of the main assumptions, that no SO_4^{2-}

originated from evaporites, could not be made. Gypsum is present throughout watershed at all sites, so we could not calculate the individual contribution of coupled sulphide oxidation-carbonate dissolution (SO-CD) to HCO_3^-. Instead, we calculated a combined SO-CD/carbonate dissolution term. All non-sea salt or aerosol-derived HCO_3^- was therefore crustal, an acknowledged overestimation of the crustal contributions to HCO_3^-. While pyrite exists in the watershed, SO_4^{2-} concentrations are low (mean 17.6±13.3 mg L^{-1}). Further, sulphide oxidation produces CO_2 and thus is likely not significantly contributing to the CO_2 dynamics observed herein.

CO_2 consumption calculations. Proglacial $CO_{2(g)}$ fluxes were calculated for the glacial rivers using the changes in DIC concentrations along the transects of the Blister, Snowgoose and Gilman rivers (n=5) and relating these changes to weathering stoichiometry.[14] Every 1 mol increase in Ca^{2+} and Mg^{2+} between the glacier terminus and the river delta consumes 1 mol $CO_{2(aq)}$ via carbonate dissolution (equation 1, Figure 1), with Ca^{2+} concentrations corrected for the increase in SO_4^{2-} over the same distance. Further, a 1 mol increase in $SiO_{2(aq)}$ consumes 2 mol $CO_{2(aq)}$ via silicate dissolution (equation 2). Although this latter ratio inherently assumes stoichiometric dissolution, which may not always occur in glacierized catchments,[22] silicate weathering conservatively accounted for only 1.50±0.65% of the DIC increase across all transects. Using this approach, we accounted for 125±13.6% of the DIC increase over the length of the glacial rivers, validating our use of the change in DIC concentration along the river lengths as a metric of CO_2 consumption by dissolution. To estimate DIC concentrations at the glacier termini on rivers and days for which transects were not completed, we applied a mean DIC change of 0.045±0.008 mg L^{-1} per 1 m elevation difference between the glacier terminus and the river delta at Lake Hazen, a remarkably consistent factor across all 5 transects, likely reflecting the dependence of lotic gas transfer on slope.[58] Assuming no additional water sources to the rivers downstream of the glaciers, we subtracted the daily modelled DIC load at the glacier from the DIC load at the delta (Table A2-4). We attribute this change in DIC load to dissolution reactions ($CO_{2(aq)}$ consumption and consequent HCO_3^-/DIC production) in the rivers. The difference was then halved to account for the fact that 1 product HCO_3^- results from the $CO_{2(aq)}$ and the other from the mineral ($CaCO_3$ in equation 2).

Lake Hazen (surface). *Sample collection*. In summer 2015, average hourly (15 min intervals) surface pCO_2 concentrations were measured in waters near the shore at Lake Hazen base camp with a Vaisala GM222 0-2000 ppm CO_2 probe interfaced with a Campbell Scientific CR10x data logger and Met One 014A anemometer.[52] We simultaneously logged $O_{2(aq)}$, pH, temperature and turbidity with a YSI EXO2 sonde 1 meter below the water surface. To minimize equipment damage caused by shifting lake ice during the main melt event, there are no continuous in situ CO_2 concentration measurements between 02:00 on July 13th and 19:00 on July 22nd. In 2016, we sampled waters along the northwestern shoreline of Lake Hazen regularly (every 1-2 days) for $CO_{2(aq)}$ (as above with the GM222 probe and handheld GM70 meter) and DIC, and weekly for other chemical parameters to determine the influence of the glacial rivers on water chemistry in nearshore environments. Water samples near the shore of Lake Hazen were collected and processed for dissolved constituents, weathering endpoint and TSS as described above for the glacial rivers.

CO_2 flux calculations. Gas fluxes from the surface of Lake Hazen were calculated,[59] using the wind-speed derived gas exchange coefficient (k_{CO2}),[60] corrected for chemically enhanced CO_2 influx at high pH:[61-63]

$$\text{Flux}\left(\mu\text{mol m}^{-2}\text{ h}^{-1}\right) = k_{CO_2}\alpha\Delta CO_{2\,(aq)}$$

where k_{CO2} is the gas exchange coefficient calculated using mean hourly wind speed (in m s^{-1}), α is the enhancement factor of CO_2 diffusion at high pH, and $\Delta CO_{2(aq)}$ is the difference between the CO_2 concentration measured *in-situ* and the CO_2 concentration that would occur if the waters were at atmospheric equilibrium, calculated using Henry's Law, and *in situ* temperature and barometric pressure. To calculate enhanced fluxes when there was no associated pH measurement, we applied a median enhancement factor of 18% (n= 356) to the uncorrected flux, a conservative estimate based on the mean (25%) and range of enhancement factors observed (2-97%). Net ablation season CO_2 exchange from the Lake Hazen surface in both 2015 and 2016 was estimated from the measured daily flux multiplied by the daily ice-free area, extracted from the MODIS snow cover product (MOD10A1).[38] For days when net daily fluxes were not measured, we used the mean of the previously and subsequently measured daily fluxes. To extrapolate the data outside of the measurement period, either the first (2-July) or last (08-Aug)

measured fluxes from 2016 were applied to the periods before or after measurement, respectively.[64] The 2016 values were also applied to the shoulder seasons in 2015, when a shorter field campaign was undertaken.

Lake Hazen water column (internal). *Sample collection*. Physical and chemical profiles of the Lake Hazen water column at the deepest site in the lake (267 m) were completed in May 2012-2014 and in August 2015. Water samples were collected at 15 specific depths using a Teflon-lined Niskin water sampler (12 L) attached to an electric winch. Water column $CO_{2(aq)}$ concentrations were measured in pre-evacuated serum bottles containing KCl, and as such, represent weathering endpoint concentrations (see above).[24,28] We were unable to repeat sampling of the full summer water column profile in 2016 due to poor weather conditions.

Internal CO_2 consumption within Lake Hazen. CO_2 consumption within the Lake Hazen water column was calculated by conducting a DIC mass balance budget for Lake Hazen in both 2015 and 2016. Briefly, hydrological inputs of DIC to the lake were the sum of glacial river (described above, using the surface mass balance approach and LOADEST log-linear models) and snow meltwater inputs (described in detail in St. Pierre et al. submitted), while the sole hydrological output of DIC from the lake was via the Ruggles River. Ruggles River discharge was estimated as the sum of all hydrological inputs to the lake.[38] The difference between DIC inputs and outputs thus reflects processes occurring within the water column itself, where DIC is produced by chemical weathering and heterotrophic respiration, or consumed by primary productivity which is negligible in ultra-oligotrophic Lake Hazen. We then used δ^{13}C-DIC and DIC concentrations in the Lake Hazen water column to account for respiration contributions to DIC accumulation in the water column: only 12.9% of bottom water DIC (or 210 µM of the 1630 µM of DIC accumulated in the water column in spring 2012, based on δ^{13}C-DIC = -3.8‰ and δ^{13}C-OC of organic matter = -29.0‰) could be attributed to heterotrophic respiration, with the balance of DIC presumably originating from weathering processes. We then applied this respiration constant and weathering stoichiometry (Fig. 1) to the net DIC production in Lake Hazen DIC to constrain the contribution from mineral weathering.

This method for calculating the carbonate dissolution contribution to DIC accumulation was corroborated by calculating the difference between water column weathering endpoint and calculated equilibrium CO_2 concentrations in late July 2015 following most of that year's annual

delivery of comminuted sediments to the lake. This difference was corrected to account for the dilution of lake waters by glacial river waters already undersaturated in CO_2. Molar differences between weathering endpoint and CO_2 at atmospheric equilibrium were then multiplied by the volume of water at each depth interval,[47] and summed to obtain a conservative estimate of internal net CO_2 consumption via carbonate dissolution within Lake Hazen.

Analytical procedures. Serum bottle $CO_{2(aq)}$ concentrations, representing weathering endpoint concentrations, were measured on the headspace of the serum bottles using a Varian Chrompack CP-3800 gas chromatograph, calibrated with Praxair-certified standards.[24] DIC concentrations were also analyzed by gas chromatograph.[65] Briefly, using a gas-tight syringe, a He headspace was injected while exchanging an equal volume (~3 mL) of sample. Acidified (85% H_3PO_4) samples were shaken for 2 hours before injecting 300 µL of the headspace into the GC for quantification of DIC concentrations.

δ^{13}C-DIC analysis was conducted at the Environmental Isotope Laboratory at the University of Waterloo, using a GasBench II gas chromatograph interfaced to a Thermo Fisher Scientific MAT 253 isotope ratio mass spectrometer (IRMS). 1-4 mL water were injected into a He-filled exetainer, containing 1 mL 85% H_3PO_4, and shaken for 90 minutes. The evolved CO_2 was purged from vials through a double-needle sampler into a He-carrier stream (20 mL/min). The headspace was then sampled using a six-port rotary valve with a 100 µL loop, programmed to switch at the maximum CO_2 concentration in the He-carrier. The CO_2 was passed to the IRMS through a Poroplot Q GC column (25m x 0.32mm ID, 45°C, 2.5 mL/min). A reference CO_2 peak was used to calculate provisional delta values of the sample CO_2 peak. Values obtained were the average of three injections. Duplicate samples were run a minimum of every 5 samples. Final δ^{13}C values (relative to international standard Vienna PeeDee Belemnite±0.2‰) were adjusted for changes in linearity and instrumental drift, such that correct δ^{13}C values for reference materials were obtained. At least three reference materials were analyzed with every 10-12 samples.

Molybdate-reactive silicon was determined by flow-injection analysis using a Lachat QuickChem QC8500 FIA Automated Ion Analyzer.[66] Molar dissolved Si (DSi) was calculated using the molar mass of the Si atom.[67] Bicarbonate (HCO_3^-) concentrations were estimated from measured DIC and *in-situ* pH with temperature-dependent K_1 and K_2 for freshwaters.[68] Non-

bicarbonate anions (SO_4^{2-} and Cl^-) were determined by ion chromatography (EPA 300.1), while dissolved organic carbon (DOC) was measured using a Shimadzu TOC5000A Total Organic Carbon Analyzer (EPA Method 415.1). Major dissolved cations (Ca^{2+}, Mg^{2+}, Na^+, K^+) were analyzed by inductively-coupled plasma mass spectrometry at the Canadian Centre for Isotopic Microanalysis (University of Alberta). Total suspended solids (TSS) were measured gravimetrically on pre-weighed 0.45 µm cellulose-nitrate filters.

All analyses conducted at the BASL complied with the standards of the Canadian Association for Laboratory Accreditation (CALA). Relative standard deviations between duplicates for Na, K, Ca, Mg were 1.42±0.022%, 2.13±0.040%, 0.376±0.003%, and 0.361±0.003%, respectively.

Comparison to other geographic locales. To determine if the results obtained in Lake Hazen were isolated, $CO_{2(aq)}$ concentrations were also measured as above in the proglacial rivers downstream of the Kiattuut Sermiat (Greenland, 61°12'N, 45°20'W) and Saskatchewan (52°10'N, 117°4.6'W) glaciers. A systematic search in Web of Science using keywords "carbon dioxide" or "CO_2", and "glacier" was subsequently conducted. To be included in our summary, a study must have been conducted: (a) in freshwater; (b) by either directly measuring or calculating CO_2 concentrations (i.e., studies inferring transient CO_2 drawdown from solute chemistry were excluded); and, (c) at sampling sites 0.5 km or farther downstream of the glacier to minimize the influence of low subglacial $CO_{2(aq)}$ concentrations.

REFERENCES

1. Cole, J. J. *et al.* Plumbing the global carbon cycle: Integrating inland waters into the terrestrial carbon budget. *Ecosystems* **10**, 171-184 (2007).
2. Duarte, C. M. & Prairie, Y. T. Prevalence of heterotrophy and atmospheric CO_2 emissions from aquatic ecosystems. *Ecosystems* **8**, 862-870 (2005).
3. Raymond, P. A. *et al.* Global carbon dioxide emissions from inland waters. *Nature* **503**, 355-359 (2013).
4. Weyhenmeyer, G. A. *et al.* Significant fraction of CO_2 emissions from boreal lakes derived from hydrologic inorganic carbon inputs. *Nat. Geosci.* **8**, 933-936 (2015).
5. Cory, R. M., Ward, C. P., Crump, B. C. & Kling, G. W. Sunlight controls water column processing of carbon in arctic fresh waters. *Science* **345**, 925 (2014).
6. Vachon, D., Lapierre, J.-F. & del Giorgio, P. A. Seasonality of photochemical dissolved organic carbon mineralization and its relative contribution to pelagic CO_2 production in northern lakes. *J. Geophys. Res. Biogeosci.* **121**, 864-878 (2016).

7. Marcé, R. *et al.* Carbonate weathering as a driver of CO_2 supersaturation in lakes. *Nat. Geosci.* **8**, 107-111 (2015).
8. Stokes, C. R., Popovnin, V., Aleynikov, A., Gurney, S. D. & Shahgedanova, M. Recent glacier retreat in the Caucasus Mountains, Russia, and associated increase in supraglacial debris cover and supra-/proglacial lake development. *Ann. Glaciol.* **46**, 195-203 (2007).
9. Song, C., Sheng, Y., Ke, L., Nie, Y. & Wang, J. Glacial lake evolution in the southeastern Tibetan Plateau and the cause of rapid expansion of proglacial lakes linked to glacial-hydrogeomorphic processes. *Journal of Hydrology* **540**, 504-514 (2016).
10. Pelto, M. in *Recent Climate Change Impacts on Mountain Glaciers*, 211-214 (John Wiley & Sons Ltd., 2017).
11. Nie, Y. *et al.* A regional-scale assessment of Himalayan glacial lake changes using satellite observations from 1990 to 2015. *Remote Sens. Enviro.* **189**, 1-13 (2017).
12. Crawford, J. T., Dornblaser, M. M., Stanley, E. H., Clow, D. W. & Striegl, R. G. Source limitation of carbon gas emissions in high-elevation mountain streams and lakes. *J. Geophys. Res. Biogeosci.* **120**, 952-964 (2015).
13. Tranter, M. & Wadham, J. L. in *Treatise on Geochemistry (Second Edition)* (ed Karl K. Turekian) 157-173 (Elsevier, 2014).
14. Tranter, M. *et al.* Geochemical weathering at the bed of Haut Glacier d'Arolla, Switzerland: a new model. *Hydrol. Processes* **16**, 959-993 (2002).
15. Graly, J. A., Drever, J. I. & Humphrey, N. F. Calculating the balance between atmospheric CO_2 drawdown and organic carbon oxidation in subglacial hydrochemical systems. *Global Biogeochem. Cycles* **31**, 709-727 (2017).
16. Raiswell, R. Chemical models of solute acquisition in glacial melt waters. *Journal of Glaciology* **30**, 49-57 (1984).
17. Sharp, M. J., Tranter, M., Brown, G. H. & Skidmore, M. Rates of chemical denudation and CO_2 drawdown in a glacier-covered alpine catchment. *Geology* **23**, 61-64 (1995).
18. Anderson, S. P. Biogeochemistry of Glacial Landscape Systems. *Annu. Rev. Earth Planet. Sci.* **35**, 375-399 (2007).
19. Cooper, R. J., Wadham, J. L., Tranter, M., Hodgkins, R. & Peters, N. E. Groundwater hydrochemistry in the active layer of the proglacial zone, Finsterwalderbreen, Svalbard. *J. Hydrol.* **269**, 208-223 (2002).
20. Wadham, J. L., Cooper, R. J., Tranter, M. & Hodgkins, R. Enhancement of glacial solute fluxes in the proglacial zone of a polythermal glacier. *J. Glaciol.* **47**, 378-386 (2001).
21. Anderson, S. P., Drever, J. I., Frost, C. D. & Holden, P. Chemical weathering in the foreland of a retreating glacier. *Geochim. Cosmochim. Acta* **64**, 1173-1189 (2000).
22. Hodson, A., Tranter, M. & Vatne, G. Contemporary rates of chemical denudation and atmospheric CO_2 sequestration in glacier basins: an Arctic perspective. *Earth Surf. Processes Landforms* **25**, 1447-1471 (2000).
23. Christie, R. L. Bedrock geology. 16-18 (Defence Research Board Canada, Ottawa, 1958).
24. Emmerton, C. A. *et al.* The importance of freshwater systems to the net atmospheric exchange of carbon dioxide and methane with a rapidly changing high Arctic watershed. *Biogeosciences* **13**, 5849-5863 (2016).
25. Emmerton, C. A. *et al.* Net ecosystem exchange of CO_2 with rapidly changing high Arctic landscapes. *Global Change Biol.* **22**, 1185-1200 (2016).

26. Fairchild, I. J., Killawee, J. A., Hubbard, B. & Wolfgang, D. Interactions of calcareous suspended sediment with glacial meltwater: a field test of dissolution behaviour. *Chem. Geol.* **155**, 243-263 (1999).
27. Skidmore, M., Sharp, M. & Tranter, M. Kinetic isotopic fractionation during carbonate dissolution in laboratory experiments: Implications for detection of microbial CO_2 signatures using δ13C-DIC. *Geochimica et Cosmochimica Acta* **68**, 4309-4317 (2004).
28. Hamilton, J. D., Kelly, C. A., Rudd, J. W. M., Hesslein, R. H. & Roulet, N. T. Flux to the atmosphere of CH_4 and CO_2 from wetland ponds on the Hudson Bay lowlands (HBLs). *J. Geophys. Res.* **99**, 1495-1510 (1994).
29. Waller, R. I. The influence of basal processes on the dynamic behaviour of cold-based glaciers. *Quat. Int.* **86**, 117-128 (2001).
30. Hodgkins, R., Tranter, M. & Dowdeswell, J. A. Solute provenance, transport and denudation in a High Arctic glacierized catchment. *Hydrol. Processes* **11**, 1813-1832 (1997).
31. Bluth, G. J. S. & Kump, L. R. Lithologic and climatologic controls of river chemistry. *Geochim. Cosmochim. Acta* **58**, 2341-2359 (1994).
32. Raymond, P. A. & Cole, J. J. Gas Exchange in Rivers and Estuaries: Choosing a Gas Trasnfer Velocity. *Estuaries* **24**, 312-317 (2001).
33. Wallin, M. B. *et al.* Spatiotemporal variability of the gas transfer coefficient (kCO_2) in boreal streams: Implications for large scale estimates of CO_2 evasion. *Global Biogeochemi. Cycles* **25**, GB3025 (2011).
34. Battin, T. J. *et al.* Biophysical controls on organic carbon fluxes in fluvial networks. *Nat. Geosci.* **1**, 95 (2008).
35. Espírito-Santo, F. D. B. *et al.* Size and frequency of natural forest disturbances and the Amazon forest carbon balance. *Nat. Commun.* **5**, 3434 (2014).
36. Brienen, R. J. W. *et al.* Long-term decline of the Amazon carbon sink. *Nature* **519**, 344 (2015).
37. Hamilton, P. B., Gajewski, K., Atkinson, D. E. & Lean, D. R. S. Physical and chemical limnology of 204 lakes from the Canadian Arctic Archipelago. *Hydrobiologia* **457**, 133-148 (2001).
38. Lehnherr, I. *et al.* The world's largest High Arctic lake responds rapidly to climate warming. *Nat. Commun.* **9**, 1290 (2018).
39. Wetzel, R. G. *Limnology*. 3rd edn, 316 (Academic Press, 2001).
40. Marzeion, B., Kaser, G., Maussion, F. & Champollion, N. Limited influence of climate change mitigation on short-term glacier mass loss. *Nat. Clim. Change* **8**, 305-308 (2018).
41. Bliss, A., Hock, R. & Radić, V. Global response of glacier runoff to twenty-first century climate change. *J. Geophysical Res. Earth Surf.* **119**, 717-730 (2014).
42. Huss, M. & Hock, R. Global-scale hydrological response to future glacier mass loss. *Nat. Clim. Change* **8**, 135-140 (2018).
43. Sharp, M. J. *et al.* Mountain Glaciers and Ice Caps. 7.33-7.42 (Arctic Monitoring and Assessment Program, Oslo, Norway, 2011).
44. Carpenter, S. R. & Cottingham, K. L. Resilience and Restoration of Lakes. *Conservation Ecology* **1**, 2 (1997).
45. Gíslason, S. R. *et al.* Direct evidence of the feedback between climate and weathering. *Earth Planet. Sci. Lett.* **277**, 213-222 (2009).
46. Carrivick, J. L. & Tweed, F. S. Proglacial lakes: character, behaviour and geological importance. *Quat. Sci. Rev.* **78**, 34-52 (2013).

47. Köck, G. *et al.* Bathymetry and Sediment Geochemistry of Lake Hazen (Quttinirpaaq National Park, Ellesmere Island, Nunavut). *Arctic* **65**, 56-66 (2012).
48. Wang, J., Han, H. & Zhang, S. Carbon dioxide flux in the ablation area of Koxkar glacier, western Tien Shan, China. *Ann. Glaciol.* **55**, 231-238 (2014).
49. Gray, L. Using multiple RADARSAT InSAR pairs to estimate a full three-dimensional solution for glacial ice movement. *Geophys. Res. Lett.* **38**, L05502 (2011).
50. Smith, I. R. Late Quaternary glacial history of Lake Hazen Basin and eastern Hazen Plateau, northern Ellesmere Island, Nunavut, Canada. *Canadian Journal of Earth Sciences* **36**, 1547-1565 (1999).
51. Thompson, W. in *Resource description and analysis: Ellesmere Island, National Park Reserve.* 78 (National Resource Conservation Selection, Prairie and Northern Region, Parks Canada, Department of Canadian Heritage, 1994).
52. Johnson, M. S. *et al.* Direct and continuous measurement of dissolved carbon dioxide in freshwater aquatic systems-method and applications. *Ecohydrology* **3**, 68-78 (2010).
53. Gardner, A. S. *et al.* Sharply increased mass loss from glaciers and ice caps in the Canadian Arctic Archipelago. *Nature* **473**, 357-360 (2011).
54. Nowak, A. & Hodson, A. J. Changes in meltwater chemistry over a 20-year period following a thermal regime switch from polythermal to cold-based glaciation at Austre Broggerbreen, Svalbard. *Polar Res.* **33**, 22779 (2014).
55. Runkel, R. L., Crawford, C. G. & Cohn, T. A. in *USGS Techniques and Methods Book 4* (U.S. Geological Survey, 2004).
56. rloadest: river load estimation (U.S. Geological Survey, Mounds View, Minnesota, USA., 2015).
57. Holland, H. D. *The Chemistry of the Atmosphere and Oceans*. (John Wiley & Sons, Inc., 1978).
58. Raymond, P. A. *et al.* Scaling the gas transfer velocity and hydraulic geometry in streams and small rivers. *Limnol. Oceanogr. Fluids Environ.* **2**, 41-53 (2012).
59. Liss, P. S. & Slater, P. G. Flux of gases across air-sea interface. *Nature* **247**, 181-184 (1974).
60. Wanninkhof, R., Ledwell, J. R. & Broecker, W. S. Gas exchange-wind speed relation measured with sulfur hexafluoride on a lake. *Science* **227**, 1224-1227 (1985).
61. Jähne, B., Heinz, G. & Dietrich, W. Measurement of the diffusion coefficients of sparingly soluble gases in water. *J. Geophys. Res. Oceans* **92**, 10767-10776 (1987).
62. Wanninkhof, R. & Knox, M. Chemical enhancement of CO_2 exchange in natural waters. *Limnol. Oceanogr.* **41**, 689-697 (1996).
63. Bade, D. L. & Cole, J. J. Impact of chemically enhanced diffusion on dissolved inorganic carbon stable isotopes in a fertilized lake. *J. Geophys. Res. Oceans* **111**, C01014 (2006).
64. Pedersen, E. P., Elberling, B. & Michelsen, A. Seasonal variations in methane fluxes in response to summer warming and leaf litter addition in a subarctic heath ecosystem. *J. Geophys. Res. Biogeosci.* **122**, 2137-2153 (2017).
65 Assayag, N., Rive, K., Ader, M., Jezequel, D. & Agrinier, P. Improved method for isotopic and quantitative analysis of dissolved inorganic carbon in natural water samples. *Rapid Commun. Mass Spectrom.* **20**, 2243-2251 (2006).
66 Rice, E. W., Baird, R. B., Eaton, A. D. & Clesceri, L. S. (ed American Water Works Association) *Standard Methods for the Examination of Water and Wasterwater* (2012).
67 Hawkings, J. R. *et al.* Ice sheets as a missing source of silica to the polar oceans. *Nat. Commun.* **8** (2017).

68 Millero, F. J. Carbonate constants for estuarine waters. *Mar. Freshwater Res.* **61**, 139-142 (2010).

FIGURES AND TABLES

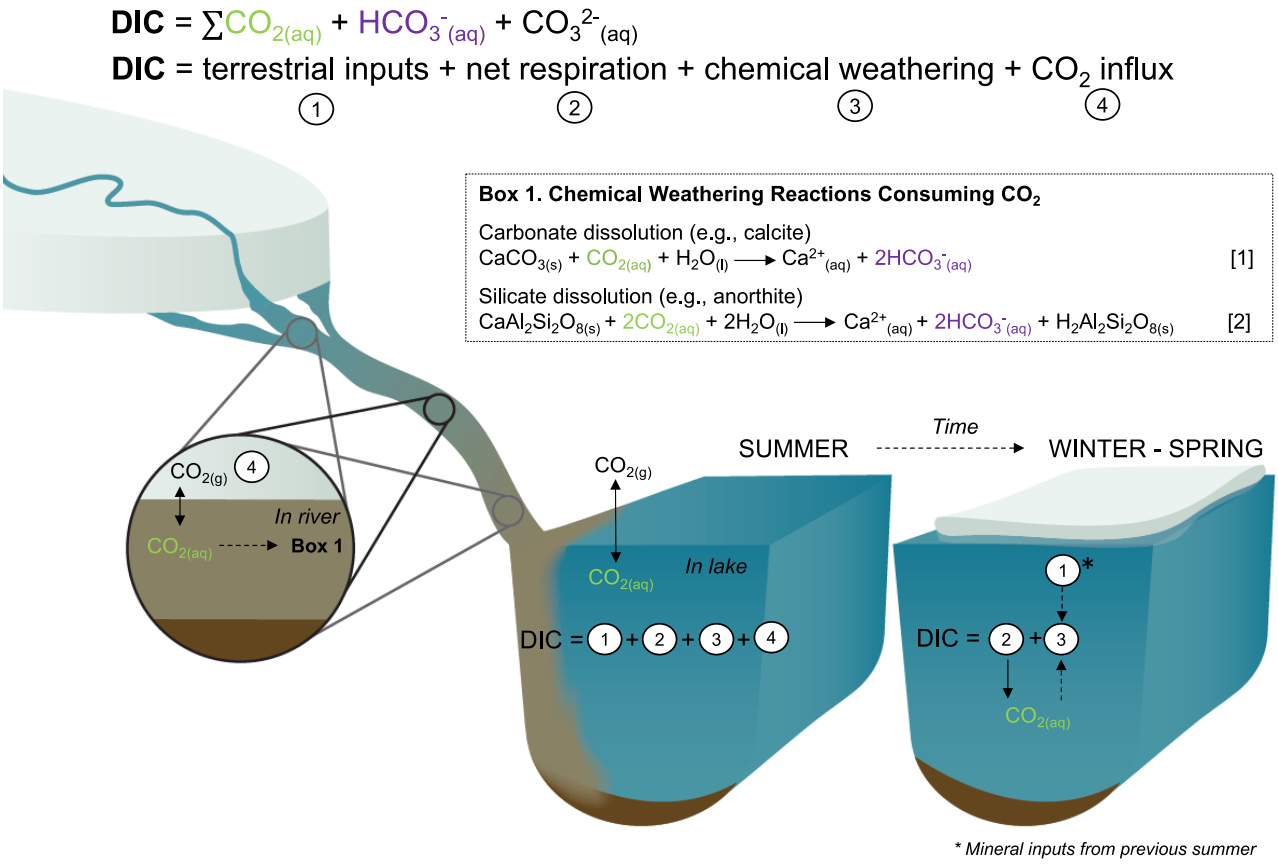

Figure 3-1. Theoretical model of glacial meltwater impacts on downstream freshwater $CO_{2(aq)}$ cycling.

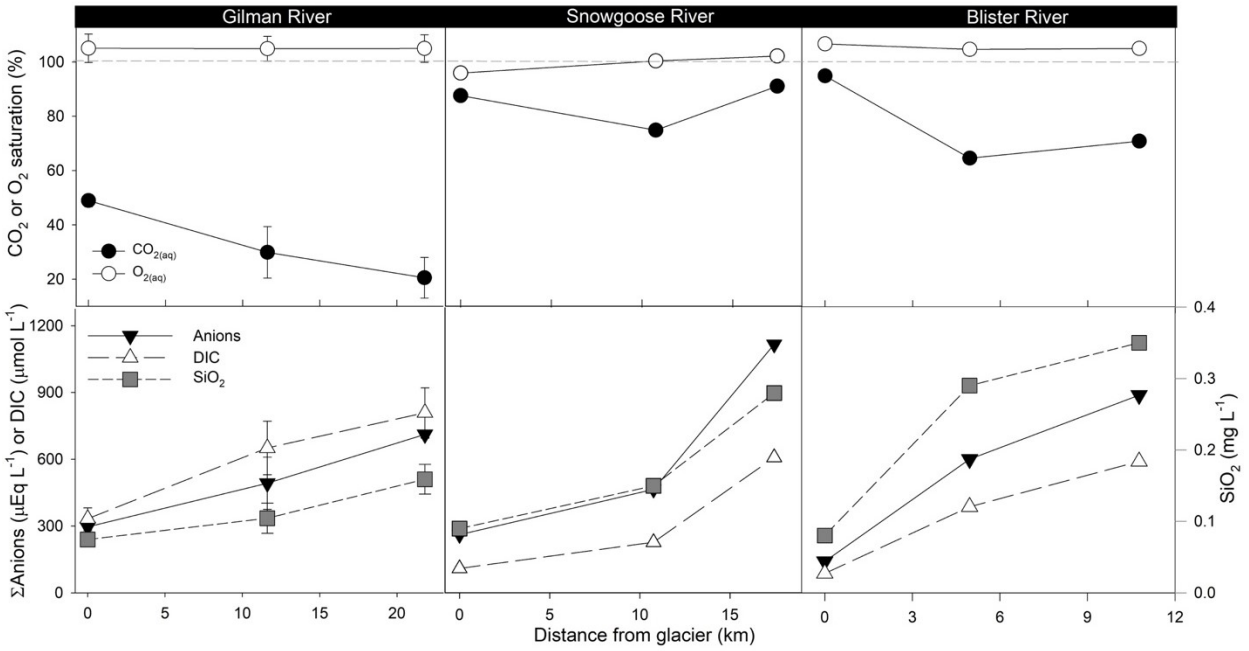

Figure 3-2. Transects of dissolved gas ($CO_{2(aq)}$, $O_{2(aq)}$), anion (sum of HCO_3^-, SO_4^{2-}, Cl^-), dissolved inorganic carbon (DIC), and silica (SiO_2) concentrations with increasing distance from the glaciers along the Gilman (mean of 2 transects, 11 July and 01 August 2016, ± 1 SD), Snowgoose (01 August 2016) and Blister (19 July 2016) rivers. Discharge is assumed to be constant between the glacier and river delta.[35]

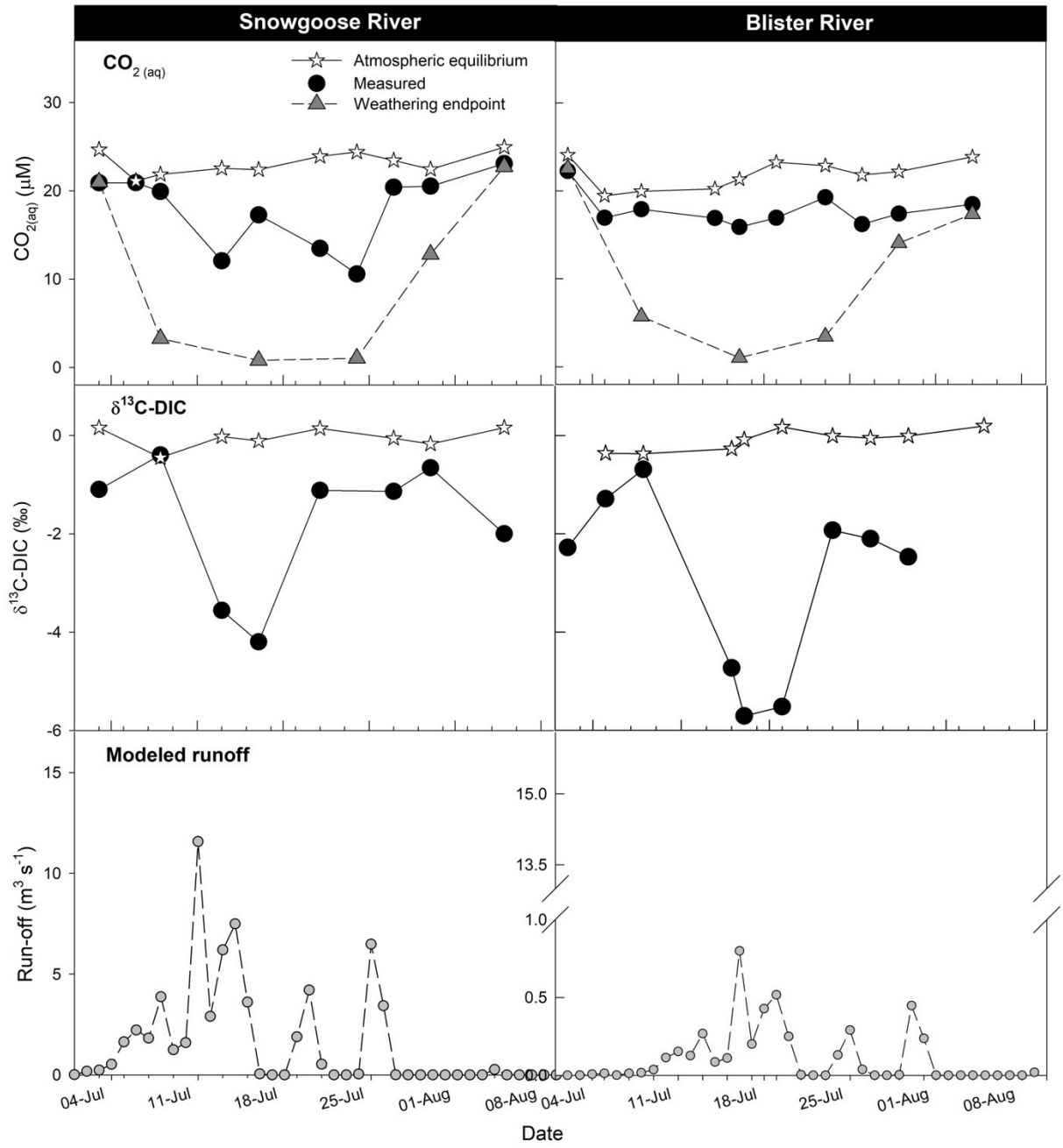

Figure 3-3. Temporal variability in $CO_{2(aq)}$ concentrations, δ^{13}C-DIC and modeled daily mean instantaneous glacial runoff in the Snowgoose and Blister rivers between 2-July and 9-August 2016. Atmospheric equilibrium $CO_{2(aq)}$ and δ^{13}C-DIC calculated from ambient water temperature and barometric pressure. Weathering endpoint $CO_{2(aq)}$ was measured on unfiltered samples preserved with KCl in a closed system. The δ^{13}C-DIC of closed system weathering of $CaCO_3$ with atmospheric CO_2 at the observed pH is in the range of -5 ‰ to -4 ‰.

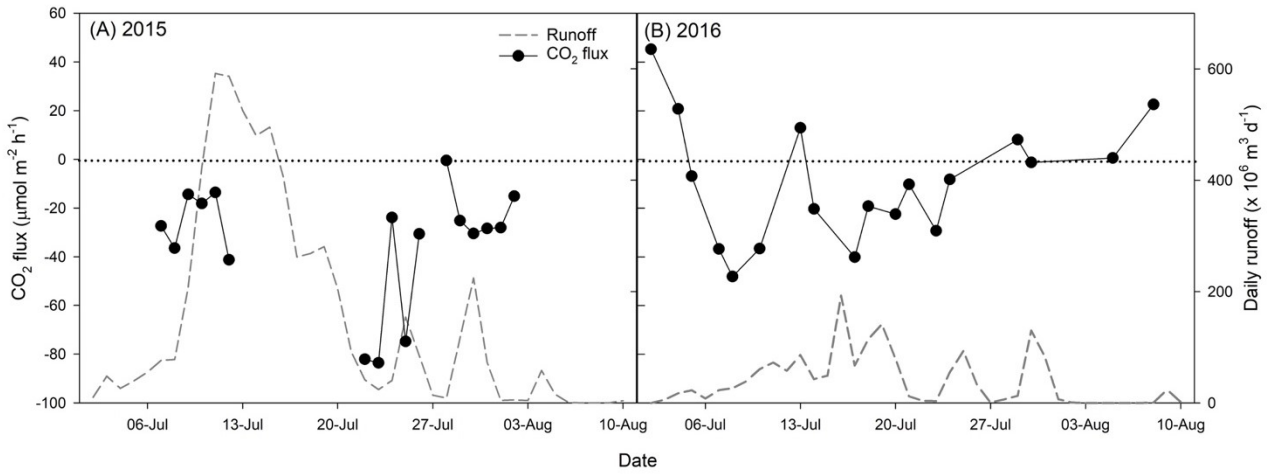

Figure 3-4. Mean daily measured CO_2 flux in the moat of Lake Hazen with modeled glacial run-off during the ablation season in (A) 2015 and (B) 2016. Negative fluxes denote a net CO_2 sink.

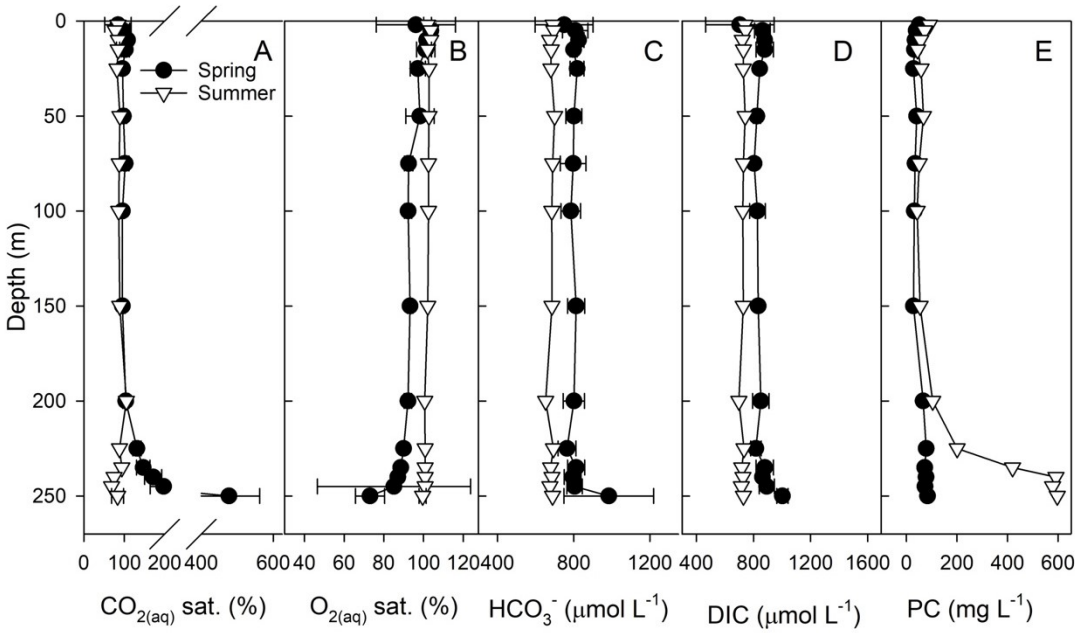

Figure 3-5. Spring and summer Lake Hazen water column profiles of (A) $CO_{2(aq)}$ saturation, (B) oxygen ($O_{2(aq)}$) saturation, (C) bicarbonate (HCO_3^-) anion, (D) dissolved inorganic carbon (DIC), and (E) particulate carbon (PC) from the deepest station within Lake Hazen (267 m). Summer open water samples collected in late July 2015 (all depths) and early August 2016 (0, 15, and 250 m depths only). Spring ice-covered water columns averaged (mean±1 SD) from May 2012-2014 (n=4 profiles). $CO_{2(aq)}$ saturation calculated at surface barometric pressure given that waters were sub-sampled at the lake surface from a Niskin bottle.

Table 3-1. Mean annual Lake Hazen watershed CO_2 budgets. Terrestrial[23] and upland aquatic data[22] are scaled to the watershed area determined herein (7516 km^2). Positive fluxes denote a net source of CO_2 to the atmosphere; negative fluxes denote a net CO_2 sink.

Watershed classification	Relevant season	Area (km^2)	Area (%)	g C-CO_2 m^{-2} d^{-1} (± 1 SD)	Mg C-CO_2 yr^{-1} (±SE)	Total flux (%)
Small lakes and ponds [1]	June to Aug.	145	1.93	+0.045±0.180	598	4
Glacial rivers [This study, 2]	June to Aug.	91	1.21	-0.376±1.20	-1020±496	6
Lake Hazen surface [This study, 3]	July to Aug.	544	7.23	+0.003±0.012	47.7±19.8	0
Lake Hazen internal [This study, 4]	June to May	-	-	-	-1340±516	6
Net aquatic total		*780*	*10*		*-1986*±1700	*17*
Polar semi-desert [1]	June to Aug.	3742	49.8	+0.004±0.223	1370	9
Meadow wetland [1]	June to Aug.	130	1.73	-0.955±0.291	-11370	71
Glacial ice [5]	n/a	3074	40.9	N/A	N/A	
Net terrestrial total		*6946*	*92*		*-10000*	*80*
Watershed totals		7516 [6]	100	-	*-10400±7170*	100

[1] Ref 24, net annual fluxes calculated from mean flux multiplied by scaled area.
[2] The glacial river CO_2 flux calculations presented are means of both 2015 and 2016, across the 7 glacial rivers studied, given that they represent 84% of the watershed glacierized area.
[3] Seasonal flux determined from ice-free area of lake surface, as such these estimates are less than those in ref [24].
[4] Internal Lake Hazen net CO_2 consumption calculated from differences in weathering endpoint and atmospheric equilibrium $CO_{2(aq)}$ concentrations, and correcting for respiratory CO_2 production, using bathymetry from ref [47].
[5] Glacial ice may actively cycle CO_2;[48] but, this is beyond the scope of the present study.
[6] Due to rounding, individual components, as presented here, do not add up to the watershed area (7516 km^2), but the difference between the two is only ~1%

Chapter 4. Climate drives catchment-wide changes in mercury cycling in the High Arctic's largest lake by volume (Lake Hazen, Nunavut, Canada)

INTRODUCTION

Climate models predict that temperatures and precipitation in the High Arctic could increase by up to 8-9ºC and 35%, respectively, by 2100 (CMIP5, RCP8.5).[1] High Arctic watersheds are particularly sensitive to this warming and wetting because they are extensively glaciated and underlain by continuous permafrost. For example, glacial mass loss in the Canadian Arctic Archipelago (CAA) has already tripled from 32 Gt yr^{-1} to 91 Gt yr^{-1} between 2004-2006 and 2007-2009, and is projected to total 12400±8500 Gt by 2100,[2, 3] with a concurrent loss of up to 90% of near-surface permafrost.[4]

Contaminants like mercury (Hg) have been emitted from natural (e.g., lithogenic, volcanic) and anthropogenic (e.g., industrial) sources over centuries or millennia. Due to prevailing atmospheric circulation, Hg is transported to the Arctic [5] where it is has historically been deposited and archived in glaciers and permafrost.[6-8] The melting of glaciers and thawing of permafrost thus potentially contribute to downstream ecosystems not only water, sediment, and nutrients (e.g., [9]), but also Hg (Figure 4-1).[8, 10, 11]

Methylmercury (MeHg) is a potent neurotoxin that bioaccumulates in organisms and biomagnifies through food webs.[12] MeHg is of particular concern in the Arctic because Indigenous peoples consume high trophic level animals such as arctic char (*Salvelinus alpinus*) and marine mammals as part of a traditional diet.[13] How will predicted increases in glacial melt and permafrost thaw affect the biogeochemical cycling of MeHg, and more broadly, total mercury (THg: all forms of Hg) downstream? This question remains unanswered, creating a critical gap in our understanding of the responses of both freshwater[14] and marine[15] ecosystems to climate change-induced transformations of the cryosphere.

Using the Lake Hazen watershed on northern Ellesmere Island, Nunavut, Canada (81.8°N, 71.4°W) as a sentinel system, we quantified MeHg and THg concentrations and fluxes across the Arctic freshwater continuum (snow, snowmelt, glacial rivers, permafrost thaw streams, lake

waters, lake outflow) (Figure 4-1). Located within Quttinirpaaq National Park, the watershed is ideally suited to study the effects of climate changes in the near-absence of human activities. ~41% of the 7156 km^2 watershed is covered by the Northern Ellesmere Icefield and its outlet glaciers, which flow downstream up to 42 km before draining into Lake Hazen (Figure A3-1). Lake Hazen is the world's largest lake by volume (51.4 km^3) entirely above the Arctic Circle, with a surface area of 544 km^2 and maximum depth of 267 m.[16] We integrated in situ field sampling with modelled estimates of glacial runoff to construct annual MeHg and THg mass budgets for Lake Hazen in relatively high- (2015) and low- (2016) melt years. The impact of recent (post-2000)[17] increases in glacial melt on inputs of MeHg and THg to Lake Hazen was then modelled, highlighting the importance of climate change on freshwater fluxes of Hg in the High Arctic.

METHODS

Site description. The Lake Hazen watershed is in the precipitation shadow of the Grant Land Mountains (Figure A3-1), making it a high arctic thermal oasis.[18] The watershed annually receives no sunlight between 15 October and 26 February, and 24 h daylight between 6 April and 4 September.[19] The watershed is classified as polar semi-desert,[20] receiving only ~95 mm of precipitation annually,[21] ~80-85% of which is deposited as snow between September and May.[22] Approximately 11 rivers travel between ~4 to 42 km in defined river valleys from the land-terminating outlet glaciers of the Northern Ellesmere Icefield before reaching Lake Hazen. Small streams fed by snow melt, permafrost thaw and/or ground ice melt also flow into Lake Hazen, though the number of these is difficult to discern and may fluctuate annually, depending on weather. The Ruggles River is the only outflow of Lake Hazen, draining the lake year-round into Chandler and then Coneybeare Fjords, the latter of which opens into Nares Strait on the northeastern coast of Ellesmere Island. Lake Hazen itself is ultra-oligotrophic and only contains morphs of a single fish species, the arctic char (*Salvelinus alpinus*).[23] Recent increases in summer glacial melt have reduced Lake Hazen's water residence time from a historical 89 years[24] to ~25 years in some years.[17]

Mass balance approach. To understand the biogeochemical cycling of MeHg and THg in the Lake Hazen watershed, we constructed annual mass budgets as follows:[25]

$$\Delta Storage_{MeHg,\ THg} = \sum Outputs_{MeHg,\ THg} - \sum Inputs_{MeHg,\ THg} \quad [1]$$

The hydrological year (1 September to 31 August) begins with the onset of freeze-up in September, when glacial rivers cease flowing, Lake Hazen begins to freeze over, and snow begins accumulating (Figure 4-1). In late May/early June, snowmelt begins, a portion of which sublimates to the atmosphere. Snowmelt on the lake ice pools for approximately a week before draining into Lake Hazen through pressure fractures and drain holes. Snowmelt from the landscape drains into Lake Hazen in localized streams. Meltwater flow in glacial river valleys begins in early June with snowmelt and continues until late August with glacial melt. Lake ice begins melting in early June, with complete ice-off, if it occurs, between late July and late August.[17]

$\sum Inputs_{MeHg,THg}$ into Lake Hazen included snowmelt on the lake surface, snowmelt runoff from the landscape, rainfall over the lake surface, glacier melt from the Northern Ellesmere Icefield, and non-glacial streams fed by permafrost thaw and ground ice melt. $\sum Outputs_{MeHg,THg}$ from Lake Hazen included export of Hg via the Ruggles River and loss of gaseous elemental Hg^0 (GEM) to the atmosphere from ice-free regions in summer (Figure 4-1). By convention, a negative ΔStorage indicates that Lake Hazen is a net MeHg or THg sink (inputs exceed outputs) and a positive ΔStorage indicates that Lake Hazen is a net MeHg or THg source (outputs exceed inputs).

Due to the logistical and financial constraints of conducting research in the Canadian High Arctic, we were unable to be on-site for the entire melt season in any given year. Instead, field-sampling campaigns were conducted over a 4-year period from 2014-2017 (Table A3-1). In addition to sampling for Hg, we collected samples at all sites for analyses of basic water chemistry parameters (total suspended solids, TSS; particulate carbon, PC; chlorophyll *a*; sulfate) (sampling techniques described in SI; Table A3-1). Basic physical (temperature, specific conductivity, turbidity) and chemical (dissolved O_2, pH) parameters were measured in situ with an EXO2 sonde (YSI Inc., Yellow Springs, OH, USA), except in snow.

Inputs to Lake Hazen.

Snowmelt on the lake surface. Surface snowmelt inputs to Lake Hazen were quantified by multiplying concentrations of MeHg and THg in integrated snowpack samples by the areal water volume (AWV) of snowpacks (see Supplementary Information), determined just prior to melt in May 2014 and 2015. This protocol provided a maximum input because it did not account for photoreduction of Hg during melt. Snow was collected using an acid-washed stainless steel core tube.

Site-specific AWV was quantified using the average weight of three snowpack cores and a water density of 1g cm^{-3} (equation 2):[26]

$$\mathrm{AWV}\left(\mathrm{L\ m^{-2}}\right) = \frac{\text{snow weight (kg, where 1 kg = 1 L)}}{\pi(\text{corer radius (m)})^2} \qquad [2]$$

Snowmelt runoff from the landscape. Snowmelt MeHg and THg inputs to Lake Hazen were quantified by multiplying concentrations measured in snowmelt runoff with the volume of runoff from the non-glacierized portion of the landscape, estimated from the ratio of sulfate (SO_4^{2-}) concentrations in snow (1.82 mg L^{-1}) and snowmelt (14.9 mg L^{-1}) in 2017, multiplied by the average AWV of the snowpack. Assuming all SO_4^{2-} was conserved in the snow as it melted, and no further SO_4^{2-} was added to runoff as it moved across the landscape, 12.2% of snowfall on the landscape resulted in overland flow, while 87.8% sublimated and/or evaporated.

Rainfall. Hg concentrations in summer rainfall were not directly measured because rain events were infrequent, and the rain that did fall was insufficient for sample analysis. Therefore, we used 2005 summer rainfall MeHg inputs of 0.037±0.013 ng m^{-2} d^{-1} from Lehnherr *et al*.[27]. Due to prioritizing MeHg analyses in the small 2005 rainfall samples, THg concentrations were not quantified, so we applied a THg concentration of 14.2±9.9 ng L^{-1} from Svalbard.[28] Summertime rainfall contributions (~34 mm; ref [29]) were assumed only to be relevant over the lake surface as rainfall onto the landscape did not result in direct overland flow, or was incorporated into glacial melt and permafrost thaw discharges.

Glacial melt. Annual inputs of MeHg and THg from glacial melt were quantified by generating chemical species-specific log-linear flux models relating measured concentrations in the deltas of glacial river waters with daily modeled glacier-specific discharge during the melt season. Glacial river sampling schemes are detailed in the Supplementary Information. Briefly, 7 rivers (names) were sampled throughout summers 2015 and 2016, some by helicopter. Two rivers within walking distance of base camp (Blister and Snowgoose) were sampled weekly to understand temporal variation in MeHg and THg concentrations throughout the ablation season. Three-site transects from the glacier to the river delta were completed on the Blister, Snowgoose and Gilman rivers to quantify changes in Hg over space.

We adopted a glacial surface mass balance approach to estimate runoff from each of the outlet glaciers (hereafter: subwatershed),[2] assuming negligible additional water inputs or evaporative losses over the river lengths. Indeed, glacier melt was the only noteworthy water source to all rivers studied, and similar $\delta^{18}O\text{-}H_2O$ and $\delta^{2}H\text{-}H_2O$ signatures along the glacier river transects suggested little evaporation (Figure A3-3). Subwatershed areas for the 6 largest glacial rivers sampled were delineated from the 1:50,000 Canadian Digital Elevation Model (Natural Resources Canada). The resolution of the CDEM was too low to resolve the smaller Blister River subwatershed, so we estimated its area (6 km^2 or 0.2% of total watershed glacier area) from the Randolph Glacier Inventory[30] and used runoff yields from the nearby Snowgoose Glacier to calculate yields from Blister River.

We used LOADEST log-linear model 2 (eqn. 3) from *rloadest* within the *loadflex* package in R to estimate daily glacial river fluxes of MeHg and THg from modeled glacier runoff (Table A3-5).[31-33]

$$\ln(\text{load}) = \alpha_0 + \alpha_1 \ln(\text{runoff}) + \alpha_2 \ln(\text{runoff})^2 + \epsilon \qquad [3]$$

Statistically significant models ($R^2 > 0.96$, $p < 0.001$, Table A3-5) were generated by relating measured unfiltered or filtered MeHg and THg concentrations across all rivers sampled in both 2015 and 2016 to modeled daily river-specific runoff.

Non-glacial streams. We sampled Skeleton Creek, which drains a network of ponds and wetlands fed by permafrost thaw and ground ice melt, every 7 days for concentrations of Hg during summers 2015 and 2016 to quantify hydrological inputs of MeHg and THg from small streams. Hydrological discharge from Skeleton Creek was quantified with a depth transducer and depth discharge curves. However, extrapolation of this one site to the whole watershed was not feasible as similar streams throughout the watershed are ephemeral and difficult to sample and gauge.

Outputs from Lake Hazen.

Ruggles River: Outputs of MeHg and THg from Lake Hazen via the Ruggles River were quantified by multiplying mean concentrations measured at the mouth of the river by the modeled daily discharge for the entire year. The Ruggles River outflow was accessed by helicopter in summers 2015 (15 July) and 2016 (11, 13 July; 1 – 2 August) at the same time as glacial rivers. In 2016, three sites along the Ruggles River between Lake Hazen and Chandler Fjord were sampled to assess whether Hg concentrations changed with increasing distance downstream.

Water Survey Canada measured Ruggles River discharge volume in situ from 1996 to 2012 (station 10VK001, Environment and Climate Change Canada), but disruptions in the record were extensive due to sensor failure. Modeled glacial runoff from the glacierized area of the watershed matched measured Ruggles River discharge when it was available,[17] so we used the combined modeled glacier runoff from all rivers and the snowmelt volumes to estimate Ruggles River discharge.

Gaseous elemental mercury (GEM) efflux: GEM efflux calculations are detailed in the Supplementary Information. Briefly, GEM efflux was estimated by multiplying the mean GEM flux rate by the daily ice-free areas for Lake Hazen, obtained using the MODIS snow cover product (MOD10A1).[17] However, because GEM concentrations were not measured in either 2015 or 2016, we used mean GEM concentrations (29.1±10.7 pg L^{-1}) previously measured in surface waters of Lake Hazen.[27]

Lake Hazen water column. To understand seasonal variations in Lake Hazen MeHg and THg concentrations, we sampled the water column from the ice surface in May 2014 and 2017, and from a boat in summers 2015 and 2016. 15 discrete depths within the water column were sampled at the deepest point in Lake Hazen (~267 m; 81.8°N, 70.7°W; Figure A3-1) using an acid-washed, Teflon-lined 12 L General Oceanics Niskin water-sampling bottle. However, due to inclement weather following ice-out in 2016, only 3 depths (surface, 15 m at the chlorophyll maximum, and bottom at 250 m) could be sampled.

Annual ΔStorage of Hg in Lake Hazen. THg deposition rates in sediments were quantified on two intact sediment cores collected from the deepest point in Lake Hazen in May 2013. Sediment core dating methods are presented in Lehnherr et al. (2018).[17]

Chemical sampling and analyses. Protocols for field sampling and processing are provided in the SI section. All chemical analyses (Table A3-1) were completed at the CALA-certified Biogeochemical Analytical Service Laboratory (BASL) using standard certified protocols. Standard deviations (SD) are presented throughout, except for in the mass balance budgets, where standard errors (SE) are used.

Analytical protocols for the determination of MeHg and THg concentrations are detailed in the Supplementary Information. Briefly, MeHg concentrations in waters and solids were quantified in duplicate following distillation by isotope dilution using a Tekran 2700 Methylmercury Analyzer coupled to a PerkinElmer Elan DRC-e inductively coupled plasma-mass spectrometer (ICPMS).[34] Water samples were analyzed for THg in duplicate by cold vapour atomic fluorescence spectrometry on a Tekran 2600 Mercury Analyzer (EPA Method 1631) following oxidation by bromine chloride (0.5% BrCl). Solid samples were analyzed for THg in triplicate by thermal decomposition, amalgamation and atomic absorption spectrophotometry on a Milestone Direct Mercury Analyzer (DMA-80; EPA Method 7473).

RESULTS AND DISCUSSION

Lake Hazen watershed hydrology

Total estimated hydrological inputs to the lake were ~1.093 km^3 in 2015 and 0.426 km^3 in 2016. Maximum snowmelt inputs from the surface of Lake Hazen were 0.017±0.012 km^3 and 0.060±0.041 km^3 of water in May 2014 and 2015 (Table 4-1). Non-glacierized landscape snowmelt contributions were negligible in 2014, and 0.067±0.046 km^3 in 2015. Total glacial runoff was 3.37-times greater in 2015 (0.979 km^3) than in 2016 (0.291 km^3), accounting for 86.7% and 65.9% of annual hydrological inputs into Lake Hazen in those years. Three glacial rivers (Henrietta Nesmith, Gilman and Very) cumulatively accounted for ~70% of glacial runoff into Lake Hazen. Skeleton Creek only began flowing into Lake Hazen on 18-July 2015 and 31-July 2016 and continued flowing until after our departure. Maximum discharge from Skeleton Creek was 0.005 $m^3\ s^{-1}$, compared to 377, 254 or 122 $m^3\ s^{-1}$ for the three largest rivers. Because modeled glacier melt closely matched the measured Ruggles River outflow[17], and it would take ~70,000 thaw streams to equal the flow of the Henrietta Nesmith River alone, non-glacial water sources to Lake Hazen were deemed insignificant to annual hydrological budgets. Annually, Ruggles River discharge peaked shortly after the height of glacier melt and declined gradually to its annual baseline flow (~ 5 $m^3\ s^{-1}$) by November/December. Complete ice-off on Lake Hazen occurred around 4-Aug-2015 and 8-Aug-2016 in the two summer study years.

Hg concentrations in major inputs to Lake Hazen

Snow on the lake surface. During winter 2013-14, little snow accumulated on the landscape, resulting in the mobilization of exposed soils during windstorms into what little snow was there. Due to the anomalously small snowpack in 2014, it was not used in our budget calculations, but is discussed in the Supplementary Information.

The May 2015 snowpack was more typical and uniform on the lake surface and landscape. Snow MeHg and THg concentrations were 0.358±0.134 ng L^{-1} and 4.73±1.02 ng L^{-1} (Figure 4-2; Table A3-2). Mean %MeHg in snow was 7.56±2.39%, higher but within the same order of magnitude as in snow at other high arctic sites (0.5-1% MeHg).[35] Only 7-21% of the THg was dissolved, whereas 27-51% of the MeHg was, indicating potentially high bioavailability upon

melt. Snowpack loadings of MeHg and THg were 0.41±0.35 mg ha^{-1} and 5.20±3.31 mg ha^{-1} (Tables 4-1, A3-2, A3-3). There was no difference in MeHg or THg loadings between snow collected from the lake surface and the adjacent landscape ($p > 0.05$).

Possible sources of MeHg in snowpacks include snowpack methylation, aeolian processes and wet/dry atmospheric deposition. While snowpack methylation has been hypothesized,[36] there is little evidence that it occurs in any significant way,[37, 38] suggesting rather that MeHg was deposited to snowpacks via the latter two processes.[26] Concentrations of particle bound MeHg in snowpacks could easily be accounted for by the aeolian deposition of local surface soils with MeHg concentrations of 0.02-2.11 ng g^{-1} (here and other sites in the Canadian Arctic Archipelago[39]). MeHg in snowpacks may also originate from the demethylation of dimethylmercury (DMHg)[39, 40] emitted from nearby open-water coastal regions, or the simple deposition of MeHg in marine aerosols,[41] but that effect weakens as one moves further inland to locations like Lake Hazen.[39]

Possible sources of THg to Arctic snowpacks likewise include aeolian processes and wet/dry atmospheric deposition, but also atmospheric Hg depletion events (AMDEs).[26, 27] However, while AMDEs can be a net source of THg to arctic coastal regions at polar sunrise,[42] the potential contribution of AMDEs to THg deposition at inland regions is diminished by low atmospheric concentrations of the halogens responsible for the heterogeneous reactions.[43] Furthermore, the majority of THg deposited during AMDEs is rapidly photo-reduced and reemitted back to the atmosphere as GEM, with little net accumulation.[26] Like MeHg, concentrations of particle-bound THg in snowpacks could be accounted for by aeolian deposition of local surface soils (THg = 1.64-49.0 ng g^{-1}; here and other sites in the CAA[39]). Recently, dry deposition of GEM to snowpacks and mineral soils like those at Lake Hazen has been recognized as an important source of Hg in arctic terrestrial environments.[44]

Glacial melt. Unfiltered MeHg concentrations in glacial meltwaters were generally low (0.049±0.016 ng L^{-1}), whereas unfiltered THg concentrations were relatively high (9.73±6.11 ng L^{-1}; Figure 4-2, A3-3). 84.3% and 86.8% of the MeHg and THg in glacial meltwaters were particle-bound, as found in other glacier-fed rivers (e.g., [8, 45-47]). Indeed, unfiltered MeHg and

THg concentrations in Snowgoose and Blister rivers, which were sampled frequently, peaked at the height of the melt season when suspended particulate concentrations also peaked (Figure A3-5).

However, unfiltered MeHg and THg concentrations remained constant with increasing distance from the Gilman and Snowgoose outlet glaciers and the Blister Ice Cap (Figure 4-3, $p > 0.05$), suggesting that the glacierized area was the primary Hg source rather than erosional material in proglacial river channels. Because the outlet glaciers of the Northern Ellesmere Icefield have cold-based margins, much of the meltwater being exported downstream is routed through ice-marginal channels, where it can already begin to entrain erosional material before exiting the glacierized area. As these rivers flow across the proglacial landscape, the braided glacial inflow rivers are highly dynamic and unpredictable, such that river channels may access or exhaust different sediment sources as they reorganize across the landscape. TSS concentrations increased up to 20-times downstream of the glaciers, but partitioning between the dissolved and bulk phases of THg did not change (i.e., the % dissolved did not change). In contrast, MeHg in the Gilman River became increasingly particle-bound with increasing distance from the glacier ($F=20.5$, $R^2=0.796$, $p<0.05$).

MeHg in glacial meltwaters may originate from the microbial methylation of inorganic Hg, or atmospheric deposition archived in ice. The subglacial drainage system can become anoxic,[48] creating ideal conditions for microbial Hg-methylators, such as sulfate-reducing bacteria, methanogens and iron-reducing bacteria.[49] However, unlike beneath polythermal and warm-based glaciers, like those in Greenland and on Svalbard with highly developed subglacial drainage systems (e.g.,[50, 51]), the subglacial system is thought to be poorly developed under northern Ellesmere Island glaciers[52] where most runoff flows on the glacier surface and along ice-marginal channels (both oxic environments) prior to reaching the proglacial river channel. As such, the most likely source of MeHg in glacial meltwaters is from atmospheric deposition that was buried in glacial ice and is now being released. Indeed, the range of MeHg and THg concentrations in glacial meltwaters, as well as the % MeHg in the dissolved phase, were indistinguishable from that in snowmelt. As meltwaters moved downstream of the glacier, they

flowed over increasingly comminuted sediments, to which dissolved MeHg from the glacierized area may bind.[53]

Non-glacial streams. MeHg and THg concentrations in Skeleton Creek discharge entering Lake Hazen were 0.025±0.003 ng L^{-1} and 1.05±0.18 ng L^{-1}, of which 90.7±13.7% and 95.2±4.05% were dissolved, indicating potentially very high bioavailability for bioaccumulation and Hg(II) methylation. Although small streams like Skeleton Creek are hydrologically insignificant to Lake Hazen, they may become more important ephemeral features[54] in the High Arctic as warming continues, like they are in Sub- and Low Arctic regions (e.g.,[55, 56]). These small, relatively warm streams are important habitat for juvenile arctic char[57] and may be initial sites of MeHg uptake into food webs, making their biological importance disproportionately greater than their spatial extent on the landscape. Furthermore, highly productive shallow ponds along the shores of Lake Hazen are known hotspots of MeHg production, and hence may act as seasonally important sources of MeHg to Lake Hazen when their gravel shoreline berm breaches in high glacial melt years.[27, 58]

Hg concentrations in the Lake Hazen water column.

Concentrations of both MeHg and THg throughout most of the Lake Hazen water column were low or below our detection limits of 0.008 ng L^{-1} and 0.016 ng L^{-1} for MeHg and THg. However, upper water column concentrations of MeHg and THg tripled following snowmelt, from 0.019 to 0.065 ng L^{-1} and from 0.42 to 1.28 ng L^{-1}, respectively (Figure 4-4). In ultra-oligotrophic freshwaters, snowmelt inputs of atmospherically-derived limiting nutrients (nitrogen, sulphur), combined with greater light penetration through ice following snowmelt, often initiate a spring pulse of primary and secondary productivity. In Lake Hazen, for example, below ice chlorophyll *a* concentrations increased from 0.16 µg L^{-1} to 0.29 µg L^{-1} after snowmelt (Figure 4-4). This springtime pulse of productivity can then initiate MeHg bioaccumulation through uptake by or adsorption to primary producers.[59]

Whereas spring upper water column MeHg and THg concentrations increased following discharge of snowmelt under the ice, in the summer Lake Hazen bottom water THg

concentrations increased due to glacial melt. THg concentrations were uniform throughout the upper water column in summer (0-200 m; 0.161 ±0.067 ng L^{-1}), but began to increase below 200 m in parallel with particulate concentrations, reaching maximum concentrations at 250 m that were 4 and 7-times higher than the upper water column in low (2016) and high (2015) melt years (Figure 4-4). Glacial river waters were highly turbid and dense, resulting in the formation of temperature-independent underflows[60] that rapidly transported glacial river waters and entrained material, including Hg, to the bottom of Lake Hazen.

Hg concentrations in outputs from Lake Hazen.

Ruggles River. Unfiltered MeHg (0.008±0.007 ng L^{-1}) and THg (0.598±0.535 ng L^{-1}) concentrations in the mouth of the Ruggles River were very low and comparable to those measured in surface waters at the nearby water column profiling site. Both MeHg and THg concentrations in the Ruggles River increased exponentially downstream of Lake Hazen as erosion and permafrost slumping along the river's banks added substantial particulate matter to the river (Figure 4-3). Whereas TSS concentrations increased 20-times along the length of the Gilman River, TSS concentrations in the Ruggles River increased 100 to 600-times over a similar distance. Although hydrological contributions to arctic marine waters from individual small rivers like the Ruggles (3.40±1.85 km^3 yr^{-1}) are dwarfed by the 8 largest arctic rivers, cumulative annual discharge from the Canadian Arctic Archipelago is estimated at 202 km^3 yr^{-1},[61] less than the Yenisey, Lena, Ob' and Mackenzie Rivers (307-620 km^3 yr^{-1}), but the same as or more than the Yukon, Pechora, Kolyma and Severnya Dvina Rivers (103-203 km^3 yr^{-1}).[62] Our results suggest that small rivers, like the Ruggles, may also be important sources of Hg to nearshore marine waters, particularly as their watersheds are undergoing rapid climate change-induced glacier melt and permafrost thaw.

GEM surface efflux. Annual GEM efflux from the surface of Lake Hazen was estimated at 0.208 kg in 2015 and 0.189 kg in 2016. While this inter-annual variation is based solely on variation in ice phenology, GEM concentrations also likely vary throughout the summer.[27, 63] This estimated

GEM efflux is equivalent to 37% or 112% of the Ruggles River exports in 2015 and 2016, suggesting an important loss of Hg from Lake Hazen that merits greater in-depth study.

Lake Hazen MeHg and THg mass balance.

Total MeHg and THg inputs to Lake Hazen were 0.10 kg and 17.4 kg in 2015, and 0.06 kg and 9.37 kg in 2016 (Table 4-1). Glacial rivers accounted for 53% (0.05 kg) or 27% (0.02 kg) of MeHg inputs and 94% (16.4 kg) or 89% (8.35 kg) of THg inputs in 2015 and 2016. The 3.1- and 2.0-times higher export of MeHg and THg from glacial rivers in 2015 relative to 2016 was directly related to the greater glacial meltwater volumes. Subwatershed area-normalized specific MeHg yields for the glacial rivers ranged from 2.23 to 11.7 mg km^{-2} yr^{-1}. These are the first ever estimates of MeHg yields from glacierized catchments. THg yields ranged between 0.61 and 3.88 g km^{-2} yr^{-1} (Table A3-6), comparable to the range (1.4-3.1 g km^{-2} yr^{-1}) reported for the Zackenberg River in northeast Greenland,[46] but lower than that measured in a small glacial river in southern Alaska (19.9 g km^{-2} yr^{-1}).[47] Whereas glacial rivers accounted for the vast majority of THg inputs to Lake Hazen, snowmelt on the lake surface was much more important for MeHg, accounting for up to 53.9% of total inputs in 2016. Surface snowmelt MeHg and THg inputs to Lake Hazen were 0.03 and 0.33 kg yr^{-1}, while snowmelt runoff from the ice-free terrestrial landscape contributed another 0.01 and 0.43 kg yr^{-1} of MeHg and THg. Rainfall MeHg and THg contributions to Lake Hazen were estimated to be 0.002 kg yr^{-1} and 0.26 kg yr^{-1}, respectively.

Conversely, the Ruggles River only discharged from Lake Hazen 0.01 kg MeHg and 0.65 kg THg in 2015 and 0.004 kg MeHg and 0.26 kg THg in 2016 (Table 4-1). Thus, Lake Hazen was annually a significant sink of bulk MeHg and THg, sequestering more than 90% of MeHg inputs, and 95% of THg inputs. The magnitude of the sink was a direct reflection of the volume of glacial runoff in each year and consequently, the strength of turbid underflows that facilitated rapid deposition of Hg-laden sediments to the bottom of the lake. Indeed, our mass balance budgets for Lake Hazen match well with an earlier measurement of THg sedimentation rate of 32.6 kg yr^{-1} (based on a median post-2007 rate of 60 μg m^{-2} yr^{-1}).[17]

Arctic freshwater Hg cycle sensitivity to climate change.

We extended annual estimates of glacial MeHg and THg loadings into Lake Hazen back to 2001 using daily modeled glacial melt and the LOADEST log-linear models. From 2001 to 2016, glacial inputs of total MeHg and THg to Lake Hazen increased modestly by 0.001 kg yr^{-1} and 0.41 kg yr^{-1}, while inputs of dissolved MeHg and THg only increased by 0.0004 kg yr^{-1} and 0.01 kg yr^{-1} (Figure A3-7). However, from 2007-2012, during which time the watershed underwent a dramatic warming that shifted the net glacier mass balance from positive to negative,[17] total MeHg and THg inputs increased by 0.004 kg yr^{-1} and 1.45 kg yr^{-1}, respectively, while dissolved inputs of MeHg and THg increased by 0.006 kg yr^{-1} and 0.002 kg yr^{-1}. In high runoff years, higher particulate loads strengthen the underflows and enhance sedimentation,[17] making Lake Hazen a greater net Hg sink in high melt years, as clearly demonstrated by the difference in sequestration of THg between 2015 and 2016 and the THg deposition rates.

While large and deep lakes are uncommon in the Arctic,[64] Lake Hazen bears many similarities to High Arctic fjord systems, and is therefore an interesting analog for glacier-fed arctic marine systems. The turbidity underflows described here also occur in outwash fjords that are fed by, but not in direct contact, with glaciers.[65] Thus, land-terminating glaciers, which account for 68.4% of arctic glacier area,[66] may constitute a potentially important source of Hg to fjord sediments. Interestingly, despite increasing exports of largely particulate-bound Hg to coastal regions, coastal arctic sediments are not an important source of MeHg to the overlying water column.[67, 68] However, meltwaters from marine-terminating glaciers and calved ice may also flow along the surface of or within the water column of receiving fjord systems, with flowpaths ultimately determined by differences in salinity/density between incoming meltwaters and receiving waters.[65] In contrast to the underflows observed in Lake Hazen, meltwaters in fjords with marine-terminating glaciers may flow directly into high productivity zones (e.g.,[69]) within the water column, where the potential for methylation is also high[67] with consequent uptake into coastal food webs.

Even before the legal ratification of the Minimata Convention, global emissions and subsequent deposition of Hg declined following the implementation of pollution-control technologies and the gradual phase-out of Hg in commercial applications.[70] These declines,

however, have been much slower in the Arctic.[71] Based on the recent decadal increase in MeHg and THg exports from glacial rivers observed here, we posit that enhanced glacial melt and permafrost thaw predicted in the Arctic could compensate for a reduction in anthropogenic Hg emissions by remobilizing Hg hitherto locked in the cryosphere. Our results further highlight the need to examine Hg cycling at watershed scales to enable the identification of climatically-sensitive sources and sinks of Hg, and the development of mitigation strategies for the future.

REFERENCES

1. Collins, M. R. K., J; Arblaster, J.-L., 2013: Long-term Climate Change: Projections, Commitments and Irreversibility. In *Climate Change 2013: The Physical Science Basis. Contribution of Working Group I to the Fifth Assessment Report of the Intergovernmental Panel on Climate Change*, T.F. Stocker, D. Q., G.-K. Plattner, M., Tignor, S.K. Allen, J. Boschung, A. Nauels, Y. Xia, V. Bex, P.M. Midgley, Ed. Cambridge University Press: Cambridge, U.K. and New York 2013.
2. Gardner, A. S.; Moholdt, G.; Wouters, B.; Wolken, G. J.; Burgess, D. O.; Sharp, M. J.; Cogley, J. G.; Braun, C.; Labine, C., Sharply increased mass loss from glaciers and ice caps in the Canadian Arctic Archipelago. *Nature* **2011,** *473*, (7347), 357-360.
3. Lenaerts, J. T. M.; van Angelen, J. H.; van den Broeke, M. R.; Gardner, A. S.; Wouters, B.; van Meijgaard, E., Irreversible mass loss of Canadian Arctic Archipelago glaciers. *Geophys. Res. Lett.* **2013,** *40*, (5), 870-874.
4. Lawrence, D. M.; Slater, A. G., A projection of severe near-surface permafrost degradation during the 21st century. *Geophys. Res. Lett.* **2005,** *32*, (24), GL025080.
5. Macdonald, R. W.; Barrie, L. A.; Bidleman, T. F.; Diamond, M. L.; Gregor, D. J.; Semkin, R. G.; Strachan, W. M. J.; Li, Y. F.; Wania, F.; Alaee, M.; Alexeeva, L. B.; Backus, S. M.; Bailey, R.; Bewers, J. M.; Gobeil, C.; Halsall, C. J.; Harner, T.; Hoff, J. T.; Jantunen, L. M. M.; Lockhart, W. L.; Mackay, D.; Muir, D. C. G.; Pudykiewicz, J.; Reimer, K. J.; Smith, J. N.; Stern, G. A.; Schroeder, W. H.; Wagemann, R.; Yunker, M. B., Contaminants in the Canadian Arctic: 5 years of progress in understanding sources, occurrence and pathways. *Sci. Total Environ.* **2000,** *254*, (2), 93-234.
6. Beal, S. A.; Osterberg, E. C.; Zdanowicz, C. M.; Fisher, D. A., Ice Core Perspective on Mercury Pollution during the Past 600 Years. *Environ. Sci. Technol.* **2015,** *49*, (13), 7641-7647.
7. Rydberg, J.; Klaminder, J.; Rosén, P.; Bindler, R., Climate driven release of carbon and mercury from permafrost mires increases mercury loading to sub-arctic lakes. *Sci. Total Environ.* **2010,** *408*, (20), 4778-4783.
8. Zdanowicz, C.; Krummel, E. M.; Lean, D.; Poulain, A. J.; Yumvihoze, E.; Chen, J. B.; Hintelmann, H., Accumulation, storage and release of atmospheric mercury in a glaciated Arctic catchment, Baffin Island, Canada. *Geochim. Cosmochim. Acta* **2013,** *107*, 316-335.

9. Hawkings, J. R.; Wadham, J. L.; Benning, L. G.; Hendry, K. R.; Tranter, M.; Tedstone, A.; Nienow, P.; Raiswell, R., Ice sheets as a missing source of silica to the polar oceans. *Nature Commun.* **2017,** *8*.
10. Schuster, P. F.; Striegl, R. G.; Aiken, G. R.; Krabbenhoft, D. P.; Dewild, J. F.; Butler, K.; Kamark, B.; Dornblaser, M., Mercury Export from the Yukon River Basin and Potential Response to a Changing Climate. *Environ. Sci. Technol.* **2011,** *45*, (21), 9262-9267.
11. Wrona, F. J.; Johansson, M.; Culp, J. M.; Jenkins, A.; Mård, J.; Myers-Smith, I. H.; Prowse, T. D.; Vincent, W. F.; Wookey, P. A., Transitions in Arctic ecosystems: Ecological implications of a changing hydrological regime. *J. Geophys. Res. Biogeosci.* **2016,** *121*, (3), 650-674.
12. Scheuhammer, A. M.; Meyer, M. W.; Sandheinrich, M. B.; Murray, M. W., Effects of Environmental Methylmercury on the Health of Wild Birds, Mammals, and Fish. *Ambio* **2007,** *36*, (1), 7.
13. Laird, B. D.; Goncharov, A. B.; Egeland, G. M.; Chan, H. M., Dietary Advice on Inuit Traditional Food Use Needs to Balance Benefits and Risks of Mercury, Selenium, and n3 Fatty Acids. *J. Nutr.* **2013,** *143*, (6), 923-930.
14. Chételat, J.; Amyot, M.; Arp, P.; Blais, J. M.; Depew, D.; Emmerton, C. A.; Evans, M.; Gamberg, M.; Gantner, N.; Girard, C.; Graydon, J.; Kirk, J.; Lean, D.; Lehnherr, I.; Muir, D.; Nasr, M.; J. Poulain, A.; Power, M.; Roach, P.; Stern, G.; Swanson, H.; van der Velden, S., Mercury in freshwater ecosystems of the Canadian Arctic: Recent advances on its cycling and fate. *Sci. Total Environ.* **2015,** *509*, 41-66.
15. Carmack, E. C.; Yamamoto-Kawai, M.; Haine, T. W. N.; Bacon, S.; Bluhm, B. A.; Lique, C.; Melling, H.; Polyakov, I. V.; Straneo, F.; Timmermans, M. L.; Williams, W. J., Freshwater and its role in the Arctic Marine System: Sources, disposition, storage, export, and physical and biogeochemical consequences in the Arctic and global oceans. *J. Geophys. Res. Biogeosci.* **2016,** *121*, (3), 675-717.
16. Herdendorf, C. E., Large Lakes of the World. *J. Great Lakes Res.* **1982,** *8*, (3), 379-412.
17. Lehnherr, I.; St. Louis, V. L.; Muir, D. C. G.; Sharp, M. J.; Gardner, A. S.; Lamoureux, S.; Smol, J. P.; St. Pierre, K. A.; Michelutti, N.; Schiff, S. L.; Emmerton, C. A.; Tarnocai, C.; Talbot, C., The world's largest High Arctic lake responds rapidly to climate warming. *Nature Commun.* **2018,** *9*, 1290.
18. France, R. L., The Lake Hazen trough - a late winter oasis in a polar desert. *Biol. Conserv.* **1993,** *63*, 149-151.
19. Cornwall, C.; Horiuchi, A.; Lehman, C. *Sunrise/Sunset Calculator*, US Department of Commerce: 2017.
20. Edlund, S. A., Vegetation. In *Resource Description and Analysis - Ellesmere Island National Park Reserve*, Natural Resource Conservation Section Prairie and Northern Region Parks Canada Department of Canadian Heritage: Winnipeg, Canada, 1994; p 55.
21. Thompson, W., Climate. In *Resource description and analysis: Ellesmere Island, National Park Reserve.* , National Resource Conservation Selection, Prairie and Northern Region, Parks Canada, Department of Canadian Heritage: Winnipeg, Manitoba, 1994; p 78.
22. Bintanja, R.; Andry, O., Towards a rain-dominated Arctic. *Nature Clim. Change* **2017,** *7*, (4), 263-267.

23. Guiguer, K. R. R. A.; Reist, J. D.; Power, M.; Babaluk, J. A., Using stable isotopes to confirm the trophic ecology of Arctic charr morphotypes from Lake Hazen, Nunavut, Canada. *J. Fish Biol.* **2002,** *60*, (2), 348-362.
24. Köck, G.; Muir, D. C. G.; Yang, F.; Wang, X.; Talbot, C.; Gantner, N.; Moser, D., Bathymetry and Sediment Geochemistry of Lake Hazen (Quttinirpaaq National Park, Ellesmere Island, Nunavut). *Arctic* **2012,** *65*, (1), 56-66.
25. St. Louis, V. L.; Rudd, J. W. M.; Kelly, C. A.; Bodaly, R. A.; Paterson, M. J.; Beaty, K. G.; Hesslein, R. H.; Heyes, A.; Majewski, A. R., The Rise and Fall of Mercury Methylation in an Experimental Reservoir†. *Environ. Sci. Technol.* **2004,** *38*, (5), 1348-1358.
26. Kirk, J. L.; Louis, V. L. S.; Sharp, M. J., Rapid reduction and reemission of mercury deposited into snowpacks during atmospheric mercury depletion events at Churchill, Manitoba, Canada. *Environ. Sci. Technol.* **2006,** *40*, (24), 7590-7596.
27. Lehnherr, I.; St Louis, V. L.; Emmerton, C. A.; Barker, J. D.; Kirk, J. L., Methylmercury Cycling in High Arctic Wetland Ponds: Sources and Sinks. *Environ. Sci. Technol.* **2012,** *46*, (19), 10514-10522.
28. Berg, T.; Bartnicki, J.; Munthe, J.; Lattila, H.; Hrehoruk, J.; Mazur, A., Atmospheric mercury species in the European Arctic: measurements and modelling. *Atmos. Environ.* **2001,** *35*, 2569-2582.
29. Emmerton, C. A.; St Louis, V. L.; Lehnherr, I.; Graydon, J. A.; Kirk, J. L.; Rondeau, K. J., The importance of freshwater systems to the net atmospheric exchange of carbon dioxide and methane with a rapidly changing high Arctic watershed. *Biogeosciences* **2016,** *13*, (20), 5849-5863.
30. Arendt, A.; Bliss, A.; Bolch, T.; Cogley, J. G.; Gardner, A. S.; Hagen, J. O.; Hock, R.; Huss, M.; Kaser, G.; Kienholz, C.; Pfeffer, W. T.; Moholdt, G.; Paul, F.; Radić, V.; Andreassen, L.; Bajracharya, S.; Barrand, N. E.; Beedle, M.; Berthier, E.; Bhambri, R.; Brown, I.; Burgess, E.; Burgess, D. O.; Cawkwell, F.; Chinn, T.; Copland, L.; Davies, B.; De Angelis, H.; Dolgova, E.; Earl, L.; Filbert, K.; Forester, R.; Fountain, A. G.; Frey, H.; Giffen, B.; Glasser, N.; Guo, W. Q.; Gurney, S.; Hagg, W.; Hall, D. K.; Haritashya, U. K.; Hartmann, G.; Helm, C.; Herreid, S.; Howat, I.; Kapustin, G.; Khromova, T.; König, M.; Kohler, J.; Kriegel, D.; Kutuzov, S.; Lavrentiev, I.; LeBris, R.; Liu, S. Y.; Lund, J.; Manley, W.; Marti, R.; Mayer, C.; Miles, E. S.; Li, X.; Menounos, B.; Mercer, A.; Mölg, N.; Mool, P.; Nosenko, G.; Negrete, A.; Nuimura, T.; Nuth, C.; Pettersson, R.; Racoviteanu, A.; Ranzi, R.; Rastner, P.; Rau, F.; Raup, B.; Rich, J.; Rott, H.; Sakai, A.; Schneider, C.; Seliverstov, Y.; Sharp, M.; Sigurðsson, O.; Stokes, C.; Way, R. G.; Wheate, R.; Winsvold, S.; Wolken, G. J.; Wyatt, F.; Zheltyhina, N., Randolph Glacier Inventory – A Dataset of Global Glacier Outlines: Version 5.0. In 5.0 ed.; Global Land Ice Measurements from Space: Boulder Colorado USA, 2015.
31. Appling, A. P.; Leon, M. C.; McDowell, W. H., Reducing bias and quantifying uncertainty in watershed flux estimates: the R package loadflex. *Ecosphere* **2015,** *6*, (12), 1-25.
32. Runkel, R. L.; Crawford, C. G.; Cohn, T. A., Load estimator (LOADEST): a FORTRAN program for estimating constituent loads in streams and rivers. In *USGS Techniques and Methods Book 4*, U.S. Geological Survey: Reston, Virginia, USA, 2004.
33. Lorenz, D.; Runkel, R.; De Cicco, L. *rloadest: river load estimation*, U.S. Geological Survey: Mounds View, Minnesota, USA., 2015.

34. Hintelmann, H.; Ogrinc, N., Determination of stable mercury isotopes by ICP/MS and their application in environmental studies. *Biogeochemistry of Environmentally Important Trace Elements* **2003,** *835*, 321-338.
35. Dommergue, A.; Ferrari, C. P.; Gauchard, P.-A.; Boutron, C. F.; Poissant, L.; Pilote, M.; Jitaru, P.; Adams, F. C., The fate of mercury species in a sub-arctic snowpack during snowmelt. *Geophys. Res. Lett.* **2003,** *30*, (12), GL017308.
36. Barkay, T.; Kroer, N.; Poulain, A. J., Some like it cold: microbial transformations of mercury in polar regions. *Polar Res.* **2011,** *30*, 15.
37. Willis, C. E.; Kirk, J. L.; St. Louis, V. L.; Lehnherr, I.; Ariya, P. A.; Rangel-Alvarado, R. B., Sources of Methylmercury to Snowpacks of the Alberta Oil Sands Region: A Study of In Situ Methylation and Particulates. *Environ. Sci. Technol.* **2018,** *52*, (2), 531-540.
38. Lahoutifard, N.; Sparling, M.; Lean, D., Total and methyl mercury patterns in Arctic snow during springtime at Resolute, Nunavut, Canada. *Atmos. Environ.* **2005,** *39*, (39), 7597-7606.
39. St. Pierre, K. A.; St. Louis, V. L.; Kirk, J. L.; Lehnherr, I.; Wang, S.; La Farge, C., Importance of Open Marine Waters to the Enrichment of Total Mercury and Monomethylmercury in Lichens in the Canadian High Arctic. *Environ. Sci. Technol.* **2015,** *49*, (10), 5930-5938.
40. Kirk, J. L.; St. Louis, V. L.; Hintelmann, H.; Lehnherr, I.; Else, B.; Poissant, L., Methylated Mercury Species in Marine Waters of the Canadian High and Sub Arctic. *Environ. Sci. Technol.* **2008,** *42*, (22), 8367-8373.
41. St. Louis, V. L.; Sharp, M. J.; Steffen, A.; May, A.; Barker, J.; Kirk, J. L.; Kelly, D. J. A.; Arnott, S. E.; Keatley, B.; Smol, J. P., Some sources and sinks of monomethyl and inorganic mercury on Ellesmere island in the Canadian high arctic. *Environ. Sci. Technol.* **2005,** *39*, (8), 2686-2701.
42. Steffen, A.; Douglas, T.; Amyot, M.; Ariya, P.; Aspmo, K.; Berg, T.; Bottenheim, J.; Brooks, S.; Cobbett, F.; Dastoor, A.; Dommergue, A.; Ebinghaus, R.; Ferrari, C.; Gardfeldt, K.; Goodsite, M. E.; Lean, D.; Poulain, A. J.; Scherz, C.; Skov, H.; Sommar, J.; Temme, C., A synthesis of atmospheric mercury depletion event chemistry in the atmosphere and snow. *Atmos. Chem. Phys.* **2008,** *8*, (6), 1445-1482.
43. Poulain, A. J.; Garcia, E.; Amyot, M.; Campbell, P. G. C.; Ariya, P. A., Mercury distribution, partitioning and speciation in coastal vs. inland High Arctic snow. *Geochim. Cosmochim. Acta* **2007,** *71*, (14), 3419-3431.
44. Obrist, D.; Agnan, Y.; Jiskra, M.; Olson, C. L.; Colegrove, D. P.; Hueber, J.; Moore, C. W.; Sonke, J. E.; Helmig, D., Tundra uptake of atmospheric elemental mercury drives Arctic mercury pollution. *Nature* **2017,** *547*, 201-204.
45. Søndergaard, J.; Riget, F.; Tamstorf, M. P.; Larsen, M. M., Mercury Transport in a Low-Arctic River in Kobbefjord, West Greenland (64A degrees N). *Water Air Soil Pollut.* **2012,** *223*, (7), 4333-4342.
46. Søndergaard, J.; Tamstorf, M.; Elberling, B.; Larsen, M. M.; Mylius, M. R.; Lund, M.; Abermann, J.; Riget, F., Mercury exports from a High-Arctic river basin in Northeast Greenland (74 degrees N) largely controlled by glacial lake outburst floods. *Sci. Total Environ.* **2015,** *514*, 83-91.

47. Vermilyea, A. W.; Nagorski, S. A.; Lamborg, C. H.; Hood, E. W.; Scott, D.; Swarr, G. J., Continuous proxy measurements reveal large mercury fluxes from glacial and forested watersheds in Alaska. *Sci. Total Environ.* **2017,** *599-600*, 145-155.
48. Tranter, M.; Sharp, M. J.; Lamb, H. R.; Brown, G. H.; Hubbard, B. P.; Willis, I. C., Geochemical weathering at the bed of Haut Glacier d'Arolla, Switzerland: a new model. *Hydrol. Processes* **2002,** *16*, (5), 959-993.
49. Parks, J. M.; Johs, A.; Podar, M.; Bridou, R.; Hurt, R. A.; Smith, S. D.; Tomanicek, S. J.; Qian, Y.; Brown, S. D.; Brandt, C. C.; Palumbo, A. V.; Smith, J. C.; Wall, J. D.; Elias, D. A.; Liang, L. Y., The Genetic Basis for Bacterial Mercury Methylation. *Science* **2013,** *339*, (6125), 1332-1335.
50. Wadham, J. L.; Tranter, M.; Hodson, A. J.; Hodgkins, R.; Bottrell, S.; Cooper, R.; Raiswell, R., Hydro-biogeochemical coupling beneath a large polythermal Arctic glacier: Implications for subice sheet biogeochemistry. *J. Geophys. Res. Earth Surf.* **2010,** *115*.
51. Chandler, D. M.; Wadham, J. L.; Lis, G. P.; Cowton, T.; Sole, A.; Bartholomew, I.; Telling, J.; Nienow, P.; Bagshaw, E. B.; Mair, D.; Vinen, S.; Hubbard, A., Evolution of the subglacial drainage system beneath the Greenland Ice Sheet revealed by tracers. *Nature Geosci.* **2013,** *6*, (3), 195-198.
52. Hattersley-Smith, G., Studies of englacial profiles in the Lake Hazen area of northern Ellesmere Island. *J. Glaciol.* **1960,** *3*, (27), 610-625.
53. Hintelmann, H., 11 Organomercurials. Their Formation and Pathways in the Environment. In *Organometallics in Environment and Toxicology: Metal Ions in Life Sciences*, The Royal Society of Chemistry: 2010; Vol. 7, pp 365-401.
54. Smol, J. P.; Douglas, M. S. V., Crossing the final ecological threshold in high Arctic ponds. *PNAS* **2007,** *104*, (30), 12395-12397.
55. Burn, C. R., Tundra lakes and permafrost, Richards Island, western Arctic coast, Canada. *Can. J. Earth Sci.* **2002,** *39*, (8), 1281-1298.
56. Hinkel, K. M.; Sheng, Y.; Lenters, J. D.; Lyons, E. A.; Beck, R. A.; Eisner, W. R.; Wang, J., Thermokarst Lakes on the Arctic Coastal Plain of Alaska: Geomorphic Controls on Bathymetry. *Permafrost Periglacial Processes* **2012,** *23*, (3), 218-230.
57. Sinnatamby, R. N.; Babaluk, J. A.; Power, G.; Reist, J. D.; Power, M., Summer habitat use and feeding of juvenile Arctic charr, Salvelinus alpinus, in the Canadian High Arctic. *Ecol. Freshwater Fish* **2012,** *21*, 309-322.
58. Lehnherr, I.; St Louis, V. L.; Kirk, J. L., Methylmercury Cycling in High Arctic Wetland Ponds: Controls on Sedimentary Production. *Environ. Sci. Technol.* **2012,** *46*, (19), 10523-10531.
59. Mason, R. P.; Reinfelder, J. R.; Morel, F. M. M., Bioaccumulation of mercury and methylmercury. *Water, Air, and Soil Pollution* **1995,** *80*, (1), 915-921.
60. Gilbert, R.; Lamoureux, S., Processes affecting deposition of sediment in a small, morphologically complex lake. *J. Paleolimnol.* **2004,** *31*, (1), 37-48.
61. Lammers, R. B.; Shiklomanov, A. I.; Vörösmarty, C. J.; Fekete, B. M.; Peterson, B. J., Assessment of contemporary Arctic river runoff based on observational discharge records. *J. Geophys. Res. Atmos.* **2001,** *106*, (D4), 3321-3334.
62. Holmes, R. M.; McClelland, J. W.; Peterson, B. J.; Shiklomanov, I. A.; Shiklomanov, A. I.; Zhulidov, A. V.; Gordeev, V. V.; Bobrovitskaya, N. N., A circumpolar perspective on

fluvial sediment flux to the Arctic ocean. *Global Biogeochem. Cycles* **2002,** *16*, (4), 45-1-45-14.
63. Poissant, L.; Amyot, M.; Pilote, M.; Lean, D., Mercury Water−Air Exchange over the Upper St. Lawrence River and Lake Ontario. *Environ. Sci. Technol.* **2000,** *34*, (15), 3069-3078.
64. Paltan, H.; Dash, J.; Edwards, M., A refined mapping of Arctic lakes using Landsat imagery. *International Journal of Remote Sensing* **2015,** *36*, (23), 5970-5982.
65. Zajaczkowski, M., Sediment supply and fluxes in glacial and outwash fjords, Kongsfjorden and Adventfjorden, Svalbard. *Pol. Polar Res.* **2008,** *29*, (1), 59-72.
66. Pfeffer, W. T.; Arendt, A. A.; Bliss, A.; Bolch, T.; Cogley, J. G.; Gardner, A. S.; Hagen, J.-O.; Hock, R.; Kaser, G.; Kienholz, C.; Miles, E. S.; Moholdt, G.; Mölg, N.; Paul, F.; Radi; Valentina; Rastner, P.; Raup, B. H.; Rich, J.; Sharp, M. J., The Randolph Glacier Inventory: a globally complete inventory of glaciers. *J. Glaciol.* **2014,** *60*, (221), 537-552.
67. Lehnherr, I.; St. Louis, V. L.; Hintelmann, H.; Kirk, J. L., Methylation of inorganic mercury in polar marine waters. *Nature Geosci.* **2011,** *4*, (5), 298-302.
68. St. Pierre, K. A.; Chételat, J.; Yumvihoze, E.; Poulain, A. J., Temperature and the Sulfur Cycle Control Monomethylmercury Cycling in High Arctic Coastal Marine Sediments from Allen Bay, Nunavut, Canada. *Environ. Sci. Technol.* **2014,** *48*, (5), 2680-2687.
69. Smith, K. L.; Robison, B. H.; Helly, J. J.; Kaufmann, R. S.; Ruhl, H. A.; Shaw, T. J.; Twining, B. S.; Vernet, M., Free-Drifting Icebergs: Hot Spots of Chemical and Biological Enrichment in the Weddell Sea. *Science* **2007,** *317*, (5837), 478-482.
70. Zhang, Y.; Jacob, D. J.; Horowitz, H. M.; Chen, L.; Amos, H. M.; Krabbenhoft, D. P.; Slemr, F.; St. Louis, V. L.; Sunderland, E. M., Observed decrease in atmospheric mercury explained by global decline in anthropogenic emissions. *PNAS* **2016,** *113*, (3), 526-531.
71. Cole, A. S.; Steffen, A.; Eckley, C. S.; Narayan, J.; Pilote, M.; Tordon, R.; Graydon, J. A.; St. Louis, V. L.; Xu, X.; Branfireun, B., A Survey of Mercury in Air and Precipitation across Canada: Patterns and Trends. *Atmosphere* **2014,** *5*, 635-668.

FIGURES AND TABLES

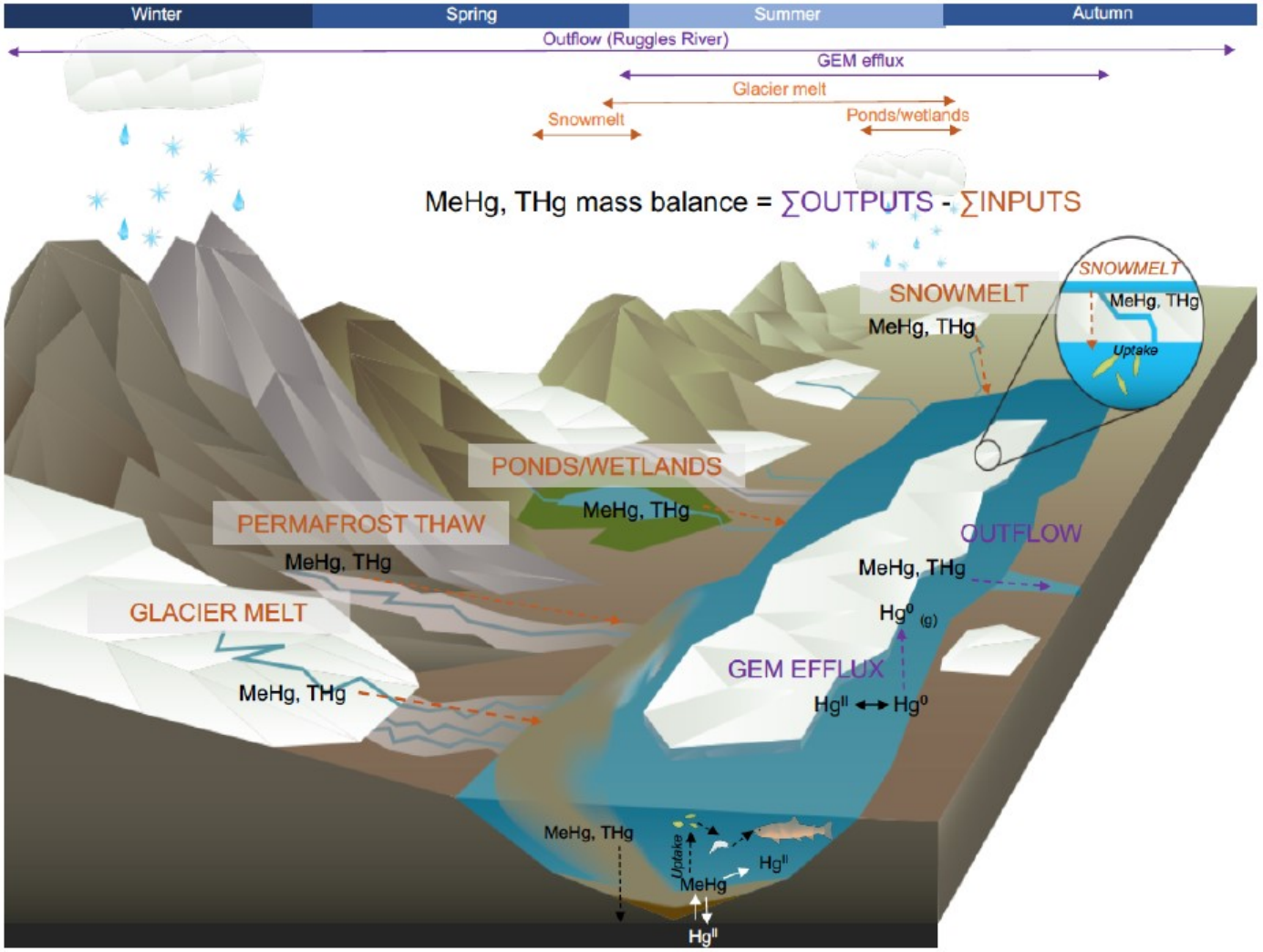

Figure 4-1. Schematic of MeHg and THg cycles in a glacierized High Arctic watershed. Timing of key outputs (purple) and inputs (orange) are shown. Dashed arrows show routes of transport, solid arrows show biogeochemical transformation.

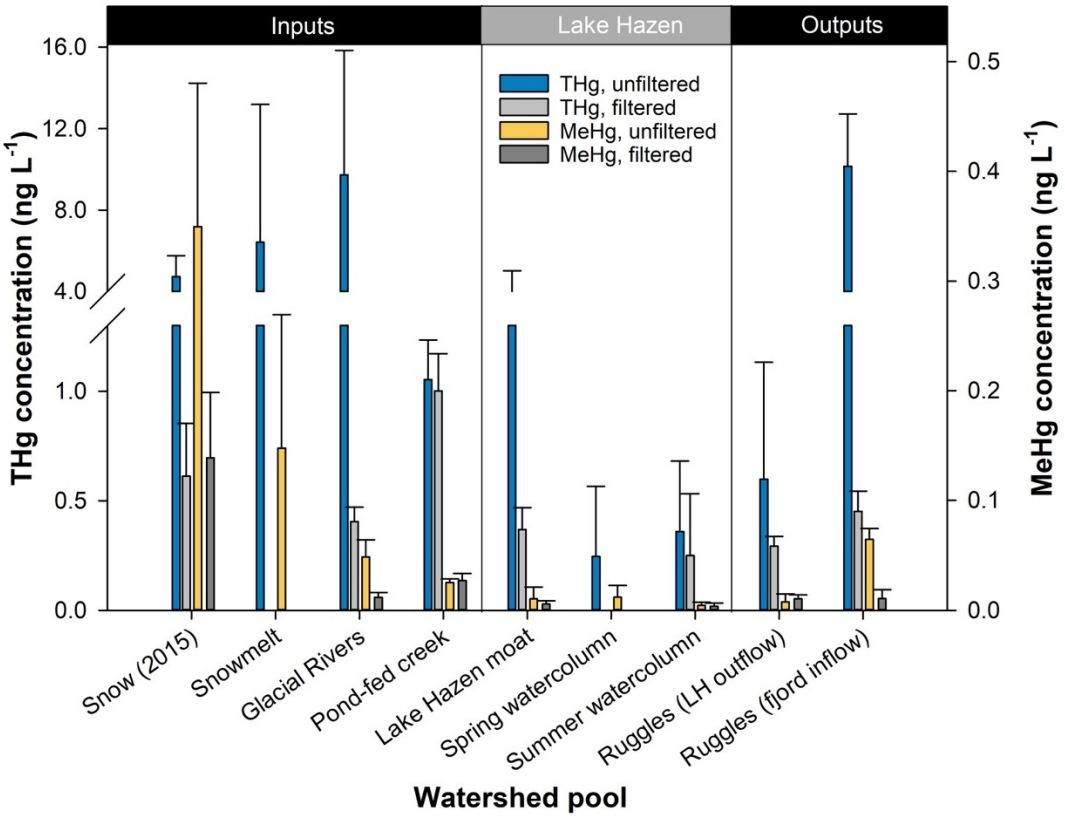

Figure 4-2. Concentrations (ng L^{-1}) of total mercury (THg) and methylmercury (MeHg) by Lake Hazen watershed pool. Means ± 1 SD of unfiltered (bulk) and filtered (dissolved) THg and MeHg concentrations are shown.

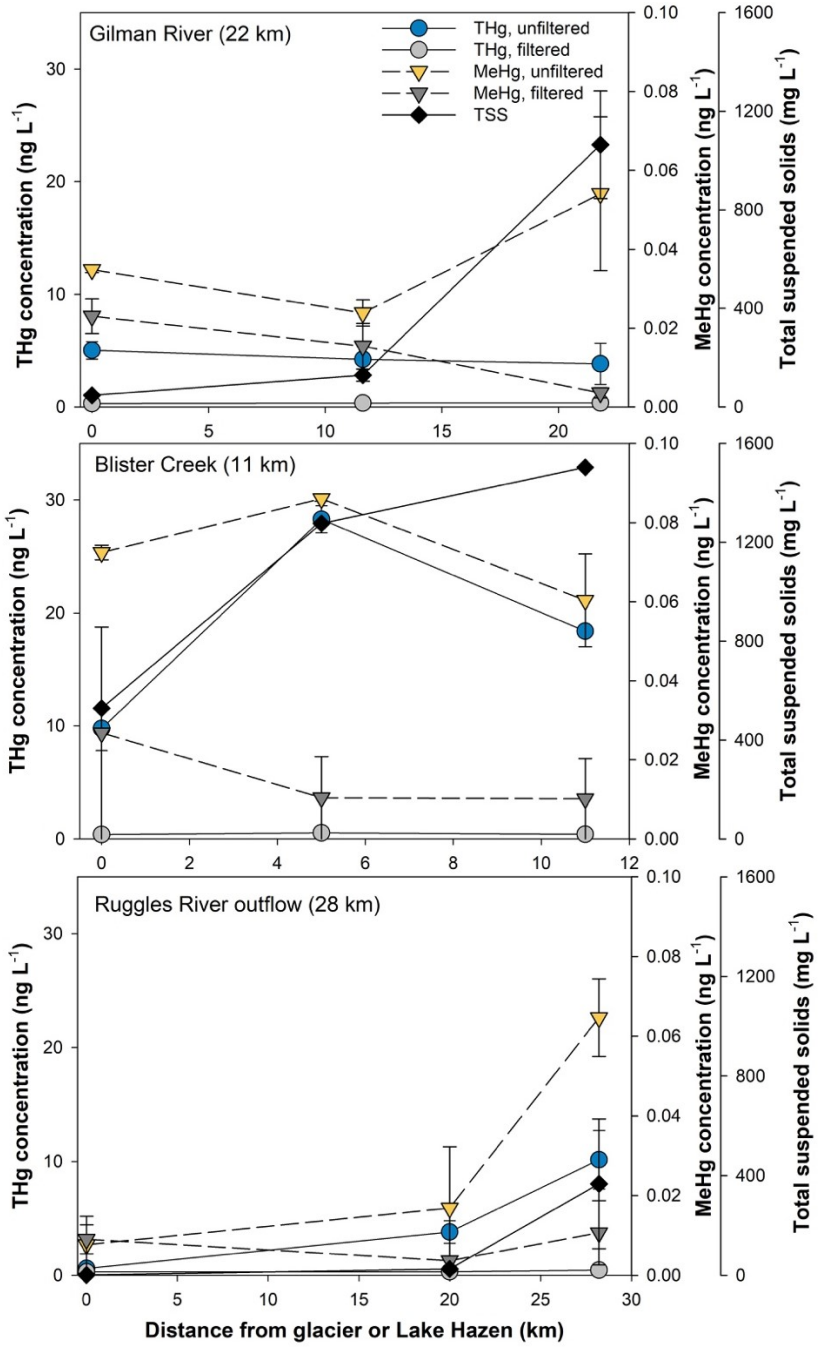

Figure 4-3. Total mercury (THg), methylmercury (MeHg) and total suspended solids (TSS) concentrations along 3-site transects in the Gilman, Blister, and Ruggles rivers. Means (n=2) ± SD shown.

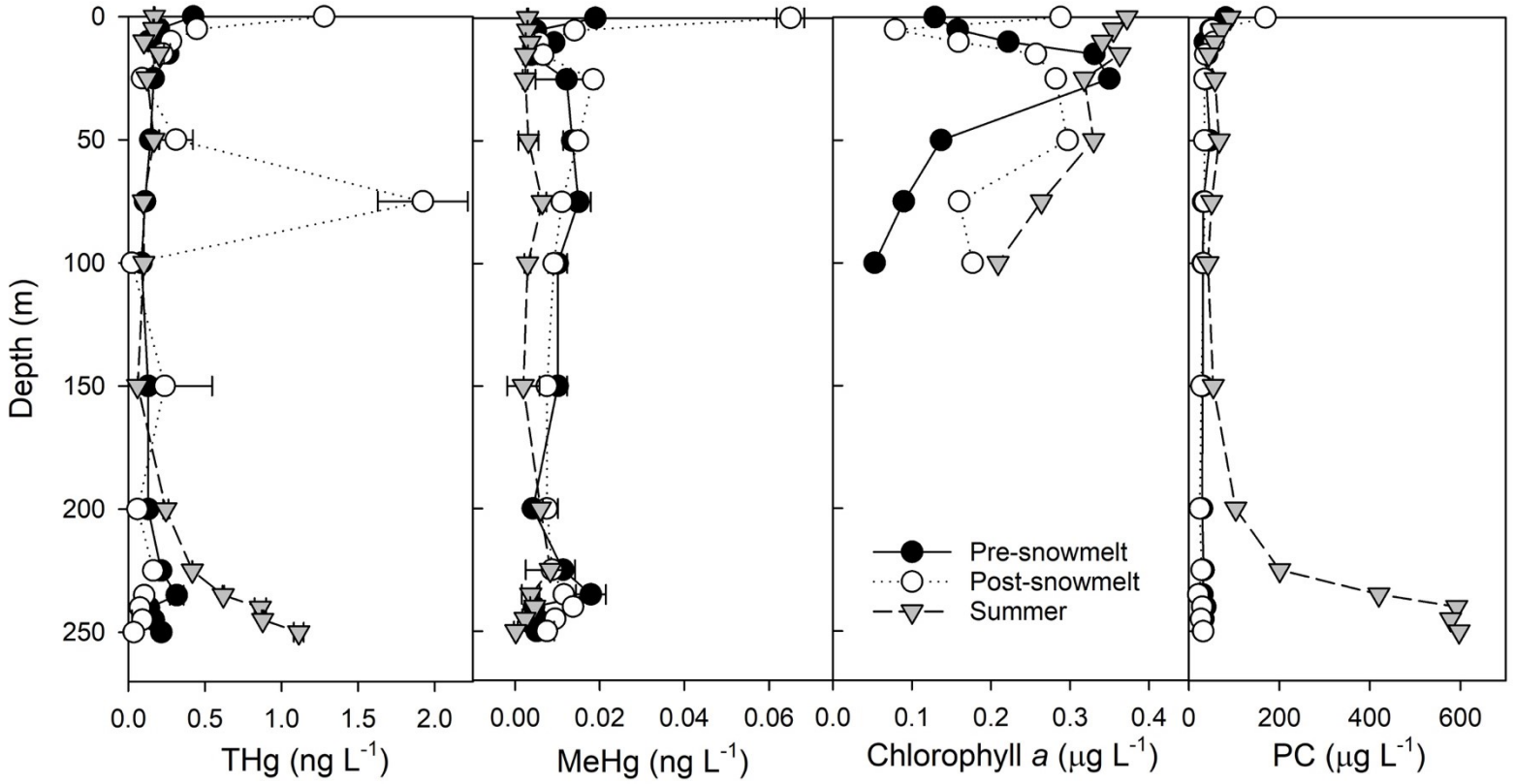

Figure 4-4. Lake Hazen spring before and after snowmelt (2014) and summer (2015-2016) water column profiles. THg: total mercury; MeHg: methylmercury; PC: particulate carbon. Mean (n=2) ± SD for THg/MeHg.

Table 4-1. Loadings (± SE) and mass balance budgets for total mercury (THg) and methylmercury (MeHg) in the Lake Hazen watershed in 2015 and 2016.

Hydrological Pool	Time of year	Water volume (km^3)		Unfiltered THg ($kg\ yr^{-1}$)		Filtered THg ($kg\ yr^{-1}$)		Unfiltered MeHg ($kg\ yr^{-1}$)		Filtered MeHg ($kg\ yr^{-1}$)	
		2015	2016	2015	2016	2015	2016	2015	2016	2015	2016
Inputs											
Snow on lake ice [a]	Sept.-May/early June	0.060±0.041		0.330±0.067		0.036±0.006		0.033±0.007		0.006	
Snowmelt [b]	Early June	0.067±0.046		0.429±0.144		n/a		0.010±0.075		n/a	
Rainfall over lake [c]	July-Aug.	0.018		0.263±0.075		n/a		0.002±0.001		n/a	
Glacial rivers	June-Aug.	0.948	0.281	16.4±8.65	8.35±1.77	0.494±0.056	0.135±0.011	0.050±0.017	0.016±0.004	0.018±0.006	0.006±0.002
Small streams [d]	Mid July-early Aug.	n/a	n/a	n/a	n/a	n/a	n/a	n/a	n/a	n/a	n/a
Outputs											
Ruggles River [e]	All year	1.093±0.02	0.426±0.02	0.653±0.338	0.255±0.132	0.319±0.035	0.124±0.015	0.009±0.004	0.004±0.002	0.009±0.005	0.003±0.002
GEM efflux	June-Aug.	-	-	0.208±0.047	0.189±0.037	-	-	-	-	-	-
Lake Hazen basin [f]		**-**	**-**	**-16.5**	**-8.92**	**-0.211**	**-0.046**	**-0.085**	**-0.057**	**-0.015**	**-0.008**

[a] 2015 and 2016 snowpack loadings calculated from 2015 measured concentrations and areal water volume over the lake surface (544 km^2, n=19).
[b] Snowmelt from glacier-free landscape, assuming 15.6% runoff (see Methods).
[c] Based on mean annual (2008-2012) rainfall estimate of 34 mm[29]; MeHg flux estimates of 0.037 ng m^{-2} d^{-1} [27] over 90 days (June, July, August); THg concentrations from Berg et al.[28].
[d] Small streams fed by permafrost thaw and ground ice melt figure in conceptually to the mass balance. However, given their small size and ephemeral nature, it is impossible to estimate their hydrological contributions to Lake Hazen, although it is likely hydrologically insignificant.
[e] Ruggles River exports were roughly equivalent to glacial inputs, as shown in Lehnherr et al. 2017[17].
[f] Net storage of THg or MeHg in Lake Hazen basin. Positive values indicate Lake Hazen is a source; negative values indicate Lake Hazen is a sink.

Chapter 5. General conclusions

Glaciers, ice caps and ice sheets store ~87% of the world's freshwater,[1] and yet are rarely considered as an integral part of the watersheds in which they are located, despite the fact that they annually contribute meltwaters to downstream ecosystems. With climate change projected to increase glacier mass loss and therefore glacial meltwater fluxes to downstream ecosystems in the coming decades,[2-5] it is imperative that we understand the changes in water quality occurring across glacierized watersheds. To address this knowledge gap, we conducted a multi-year (2013-2017), whole watershed study in the Lake Hazen watershed on northern Ellesmere Island in Quttinirpaaq National Park, assessing freshwater quality throughout the proglacial freshwater network from glacial headwaters, through river valleys, a large deep lake, and out the riverine outflow to the nearshore coastal environment.

The physical, chemical and biological limnology of hydrological compartments in the proglacial freshwater network are presented in Chapter 2. Using hydrological input-output budgets, we found that glacial meltwaters were annually the most important source of nutrients to Lake Hazen, accounting for more than 50% of hydrological inputs of all dissolved constituents in a given year. Budgets for all chemical constituents, except NO_3^--NO_2^-, NH_4^+, dissolved inorganic carbon (DIC) and dissolved organic carbon (DOC), were approximately neutral, with combined snow and glacial melt inputs equal to outputs by the Ruggles River. Glacial inputs and loss of lake ice cover cumulatively shifted the lake water column from being phosphorus-limited under ice before glacial inputs to nitrogen and phosphorus co-limited or nitrogen-limited during the summer months. This occurred in conjunction with a shift in phytoplankton community composition from strictly autotrophic cyanobacteria and chlorophytes under the ice to mixotrophic chrysophytes and cryptophytes in open water. Turbid glacial inputs to the lake significantly impacted light penetration into the upper water column, favouring organisms with flexible metabolic strategies during the ablation season.

By applying the land-to-ocean aquatic continuum framework for the first time in a glacierized watershed, we showed that nutrient (carbon, nitrogen, phosphorus) mobilization and retention processes throughout the proglacial freshwater continuum differ significantly from more temperate systems. Whereas temperate systems are dominated by the biological processes of

primary production and respiration, lower productivity glacierized High Arctic watersheds are largely governed by the physical and chemical processes of erosion, permafrost thaw, adsorption, and oxidation/reduction, preferentially mobilizing carbon and phosphorus, both of which have significant mineral sources, over nitrogen to downstream ecosystems.

Carbon dioxide (CO_2) dynamics across the proglacial freshwater network, with special emphasis on glacier-fed rivers, are presented in Chapter 3. We showed that glacier-fed rivers are a previously-overlooked CO_2 sink at the watershed scale due to chemical weathering across the proglacial zone. Carbonate and silicate dissolution reactions actively consumed atmospheric CO_2 along the length of the rivers, as evidenced by a decline in *in situ* CO_2 concentrations, in concert with an increase in DIC. As glacial meltwaters entered Lake Hazen, they cumulatively transformed the lake into a summertime CO_2 sink. Due to dense turbidity currents generated by the glacial inflow rivers, CO_2 undersaturation during the summer months was observed even at depth in the lake, an unusual observation for such a deep system, where heterotrophic processes typically dominate. Spot measurements of CO_2 concentrations in rivers draining glaciers in the Canadian Rockies and southern Greenland suggest that this may be a globally relevant phenomenon, across diverse underlying geologies and locations.

Continuous monitoring of pCO_2, turbidity, O_2 and discharge in these systems would be a logical next step in improving our understanding of this mechanism, but dynamic glacial river systems present unique hydrological and biogeochemical challenges requiring sometimes unconventional solutions. With meltwaters potentially originating from the top, edges and/or bottom of glaciers and large fluctuations in meltwater volumes over short periods of time across the poorly consolidated proglacial zone, rivers draining glacial meltwaters are extreme forms of braided rivers, that are difficult to both measure and model. Advances in drone and remote sensing technologies may help address some of these issues in the future.

Finally, annual mercury (Hg) mass balance budgets for the Lake Hazen watershed, highlighting the sources and sinks of Hg across the rapidly changing High Arctic proglacial freshwater network, are presented in Chapter 4. We showed that Lake Hazen was a significant annual sink of bulk methylmercury (MeHg) and total mercury (THg) deposited to its depths by glacial inflows. Concentrations of MeHg and THg leaving Lake Hazen via the Ruggles River were low, but increased up to an order of magnitude downstream of the lake due to the erosion of river banks and permafrost slumping.

Although mass balances of the Arctic Ocean have identified rivers to be the primary source of Hg to the basin,[6] these modelled fluxes have never been corroborated by in situ monitoring of the six largest Arctic rivers (Yenisey, Lena, Ob', Mackenzie, Yukon, Kolyma).[7] The much more abundant small Arctic rivers, like the Ruggles River, have, however, rarely been studied, even though their cumulative discharge is equal to or greater than that of these individual larger rivers.[8, 9] Our few measurements from the Ruggles River suggest that small rivers may be important sources of Hg to the Arctic marine system due to the rapid changes (glacier melt, permafrost thaw) occurring across their watersheds in response to warming, a potential source of Hg which merits greater study.

Overall, our results suggest that accelerated glacial melt will have important consequences for the biogeochemical cycles of carbon, nitrogen, phosphorus and mercury, among other compounds, across glacierized watersheds. As warming and wetting continues across the Arctic, permafrost thaw slumps and other active layer detachments are likely to become more prevalent features across these landscapes. Indeed, even over the five years of fieldwork presented in this thesis (2013-2017), permafrost thaw became more noticeable across the Lake Hazen watershed, with the appearance and subsequent enlargement of slumps. Given that glacial melt and permafrost thaw have largely been studied in isolation of one another, whether these processes will act synergistically or antagonistically is anyone's guess, a new frontier in the study of multiple stressors. The results from our transects of the glacial rivers and Ruggles River presented herein suggest that both processes have similar effects on water quality, generally acting to increase particulate loads. We note, however, that the magnitude of particulate concentration increases across the permafrost thaw-influenced Ruggles River were much greater than those in the glacial rivers, suggesting that permafrost thaw may be a more efficient erosional mechanism than glacial melt.

The three studies presented in this thesis were conducted as part of a multi-year, interdisciplinary project, one of the primary goals of which was to establish a water quality baseline for Lake Hazen, the world's largest High Arctic lake by volume, by studying changes within Lake Hazen itself, but also throughout its watershed. Already in the relatively short period of time that we have been working in the watershed, there has been a phenomenal amount of change there. Since 2007, glacial meltwater inputs to the lake have increased 10-fold, reflected in sedimentation rates at the depths of the lake.[10] While there is unfortunately little funding or

support for the development of ecosystem monitoring programs in Arctic, there is an incredible amount of information that can be gleaned from continued research at these remote sites. Particularly as our understanding of future global climate regulation hinges on that of Arctic freshwater systems,[11, 12] interdisciplinary, watershed-scale studies are exactly what is needed.

References

1. Wetzel, R. G., *Limnology*. 3rd ed.; Academic Press: San Diego, California, 2001.
2. Marzeion, B.; Kaser, G.; Maussion, F.; Champollion, N., Limited influence of climate change mitigation on short-term glacier mass loss. *Nature Climate Change* **2018,** *8*, 305-308.
3. Huss, M.; Hock, R., Global-scale hydrological response to future glacier mass loss. *Nature Climate Change* **2018**.
4. Bliss, A.; Hock, R.; Radić, V., Global response of glacier runoff to twenty-first century climate change. *Journal of Geophysical Research: Earth Surface* **2014,** *119*, (4), 717-730.
5. Radić, V.; Bliss, A.; Beedlow, A. C.; Hock, R.; Miles, E.; Cogley, J. G., Regional and global projections of twenty-first century glacier mass changes in response to climate scenarios from global climate models. *Climate Dynamics* **2013,** *42*, (1), 37-58.
6. Fisher, J. A.; Jacob, D. J.; Soerensen, A. L.; Amos, H. M.; Steffen, A.; Sunderland, E. M., Riverine source of Arctic Ocean mercury inferred from atmospheric observations. *Nature Geoscience* **2012,** *5*, (7), 499-504.
7. Amos, H. M.; Jacob, D. J.; Kocman, D.; Horowitz, H. M.; Zhang, Y.; Dutkiewicz, S.; Horvat, M.; Corbitt, E. S.; Krabbenhoft, D. P.; Sunderland, E. M., Global Biogeochemical Implications of Mercury Discharges from Rivers and Sediment Burial. *Environmental Science & Technology* **2014,** *48*, (16), 9514-9522.
8. Lammers, R. B.; Shiklomanov, A. I.; Vörösmarty, C. J.; Fekete, B. M.; Peterson, B. J., Assessment of contemporary Arctic river runoff based on observational discharge records. *J. Geophys. Res. Atmos.* **2001,** *106*, (D4), 3321-3334.
9. Holmes, R. M.; McClelland, J. W.; Peterson, B. J.; Shiklomanov, I. A.; Shiklomanov, A. I.; Zhulidov, A. V.; Gordeev, V. V.; Bobrovitskaya, N. N., A circumpolar perspective on fluvial sediment flux to the Arctic ocean. *Global Biogeochem. Cycles* **2002,** *16*, (4), 45-1-45-14.
10. Lehnherr, I.; St. Louis, V. L.; Muir, D. C. G.; Sharp, M. J.; Gardner, A. S.; Lamoureux, S.; Smol, J. P.; St. Pierre, K. A.; Michelutti, N.; Schiff, S. L.; Emmerton, C. A.; Tarnocai, C.; Talbot, C., The world's largest High Arctic lake responds rapidly to climate warming. *Nature Commun.* **2018,** *9*, 1290.
11. Prowse, T.; Bring, A.; Mård, J.; Carmack, E. C.; Holland, M.; Instanes, A.; Vihma, T.; Wrona, F. J., Arctic Freshwater Synthesis: Summary of key emerging issues. *Journal of Geophysical Research Biogeosciences* **2015,** *120*, 1887-1893.
12. Carmack, E. C.; Yamamoto-Kawai, M.; Haine, T. W. N.; Bacon, S.; Bluhm, B. A.; Lique, C.; Melling, H.; Polyakov, I. V.; Straneo, F.; Timmermans, M. L.; Williams, W. J., Freshwater and its role in the Arctic Marine System: Sources, disposition, storage, export, and physical and biogeochemical consequences in the Arctic and global oceans. *J. Geophys. Res. Biogeosci.* **2016,** *121*, (3), 675-717.

Bibliography

1-1. Stocker, T. F.; Qin, D.; Plattner, G.-K.; Tignor, M.; Allen, S. K.; Boschung, J.; Nauels, A.; Xia, Y.; Bex, V.; Midgley, P. M.; *IPCC 2013: Climate Change 2013: The Physical Science Basis. Contribution of Working Group I to the Fifth Assessment Report of the Intergovernmental Panel on Climate Change*. Cambridge University Press: Cambridge, UK and New York, NY, USA, 2013; p 1535 pp.

1-2. Marzeion, B.; Kaser, G.; Maussion, F.; Champollion, N.; Limited influence of climate change mitigation on short-term glacier mass loss. *Nature Climate Change* **2018,** *8*, 305-308.

1-3. Duarte, C. M.; Lenton, T. M.; Wadhams, P.; Wassmann, P.; Abrupt climate change in the Arctic. *Nature Climate Change* **2012,** *2*, 60.

1-4. Arrhenius, S. On the influence of carbonic acid in the air upon the temperature of the ground. *The London, Edinburgh, and Dublin Philosophical Magazine and Journal of Science* **1896,** *41*, (251), 237-276.

1-5. Serreze, M. C.; Barrett, A. P.; Stroeve, J. C.; Kindig, D. M.; Holland, M. M.; The emergency of surface-based Arctic amplification. *Cryosphere* **2009,** *3*, 11-19.

1-6. Screen, J. A.; Simmonds, I.; The central role of diminishing sea ice in recent Arctic temperature amplification. *Nature* **2010,** *464*, 1334-1337.

1-7. Serreze, M. C.; Barry, R. G.; Processes and impacts of Arctic amplification: a research synthesis. *Global and Planetary Change* **2011,** *77*, 85-96.

1-8. Wassmann, P.; Duarte, C. M.; AgustÍ, S.; Sejr, M. K.; Footprints of climate change in the Arctic marine ecosystem. *Global Change Biology* **2011,** *17*, (2), 1235-1249.

1-9. Hill Geoff, B.; Henry Greg H, R.; Responses of High Arctic wet sedge tundra to climate warming since 1980. *Global Change Biology* **2010,** *17*, (1), 276-287.

1-10. Bintanja, R.; Andry, O.; Towards a rain-dominated Arctic. *Nature Clim. Change* **2017,** *7*, (4), 263-267.

1-11. Westermann, S.; Boike, J.; Langer, M.; Schuler, T. V.; Etzelmüller, B.; Modeling the impact of wintertime rain events on the thermal regime of permafrost. *The Cryosphere* **2011,** *5*, (4), 945-959.

1-12. Radić, V.; Bliss, A.; Beedlow, A. C.; Hock, R.; Miles, E.; Cogley, J. G.; Regional and global projections of twenty-first century glacier mass changes in response to climate scenarios from global climate models. *Climate Dynamics* **2013,** *42*, (1), 37-58.

1-13. Huss, M.; Hock, R.; Global-scale hydrological response to future glacier mass loss. *Nature Climate Change* **2018**.

1-14. Dahlke, H. E.; Lyon, S. W.; Stedinger, J. R.; Rosqvist, G.; Jansson, P.; Contrasting trends in floods for two sub-arctic catchments in northern Sweden - does glacier presence matter? *Hydrology and Earth System Sciences* **2012,** *16*, 2123-2141.

1-15. Bliss, A.; Hock, R.; Radić, V.; Global response of glacier runoff to twenty-first century climate change. *Journal of Geophysical Research: Earth Surface* **2014,** *119*, (4), 717-730.

1-16. Lammers, R. B.; Shiklomanov, A. I.; Vörösmarty, C. J.; Fekete, B. M.; Peterson, B. J.; Assessment of contemporary Arctic river runoff based on observational discharge records. *J. Geophys. Res. Atmos.* **2001,** *106*, (D4), 3321-3334.

1-17. Peterson, B. J.; Holmes, R. M.; McClelland, J. W.; Vorosmarty, C. J.; Lammers, R. B.; Shiklomanov, A. I.; Shiklomanov, I. A.; Rahmstorf, S.; Increasing river discharge to the Arctic Ocean. *Science* **2002,** *298*, (5601), 2171-2173.

1-18. Likens, G. E.; Bormann, F. H.; Linkages between Terrestrial and Aquatic Ecosystems. *BioScience* **1974,** *24*, (8), 447-456.
1-19. Prowse, T.; Bring, A.; Mård, J.; Carmack, E. C.; Holland, M.; Instanes, A.; Vihma, T.; Wrona, F. J.; Arctic Freshwater Synthesis: Summary of key emerging issues. *Journal of Geophysical Research Biogeosciences* **2015,** *120*, 1887-1893.
1-20. Bring, A.; Fedorova, I.; Dibike, Y.; Hinzman, L.; Mård, J.; Mernild, S. H.; Prowse, T.; Semenova, O.; Stuefer, S. L.; Woo, M. K.; Arctic terrestrial hydrology: A synthesis of processes, regional effects, and research challenges. *J. Geophys. Res. Biogeosci.* **2016,** *121*, (3), 621-649.
1-21. Wrona, F. J.; Johansson, M.; Culp, J. M.; Jenkins, A.; Mård, J.; Myers-Smith, I. H.; Prowse, T. D.; Vincent, W. F.; Wookey, P. A.; Transitions in Arctic ecosystems: Ecological implications of a changing hydrological regime. *J. Geophys. Res. Biogeosci.* **2016,** *121*, (3), 650-674.
1-22. Cole, J. J.; Prairie, Y. T.; Caraco, N. F.; McDowell, W. H.; Tranvik, L. J.; Striegl, R. G.; Duarte, C. M.; Kortelainen, P.; Downing, J. A.; Middelburg, J. J.; Melack, J.; Plumbing the global carbon cycle: Integrating inland waters into the terrestrial carbon budget. *Ecosystems* **2007,** *10*, (1), 171-184.
1-23. Battin, T. J.; Kaplan, L. A.; Findlay, S.; Hopkinson, C. S.; Marti, E.; Packman, A. I.; Newbold, J. D.; Sabater, F.; Biophysical controls on organic carbon fluxes in fluvial networks. *Nature Geoscience* **2008,** *1*, 95.
1-24. Battin, T. J.; Luyssaert, S.; Kaplan, L. A.; Aufdenkampe, A. K.; Richter, A.; Tranvik, L. J.; The boundless carbon cycle. *Nature Geoscience* **2009,** *2*, 598.
1-25. Hotchkiss, E. R.; Sadro, S.; Hanson, P. C.; Toward a more integrative perspective on carbon metabolism across lentic and lotic inland waters. *Limnology and Oceanography Letters* **2018,** *3*, (3), 57-63.
1-26. Maranger, R.; Jones Stuart, E.; Cotner James, B.; Stoichiometry of carbon, nitrogen, and phosphorus through the freshwater pipe. *Limnology and Oceanography Letters* **2018,** *3*, (3), 89-101.
1-27. Weyhenmeyer, G. A.; Conley, D. J.; Large differences between carbon and nutrient loss rates along the land to ocean aquatic continuum—implications for energy:nutrient ratios at downstream sites. *Limnology and Oceanography* **2017**, S183-S193.
1-28. Tranvik, L. J.; Downing, J. A.; Cotner, J. B.; Loiselle, S. A.; Striegl, R. G.; Ballatore, T. J.; Dillon, P.; Finlay, K.; Fortino, K.; Knoll, L. B.; Kortelainen, P. L.; Kutser, T.; Larsen, S.; Laurion, I.; Leech, D. M.; McCallister, S. L.; McKnight, D. M.; Melack, J. M.; Overholt, E.; Porter, J. A.; Prairie, Y.; Renwick, W. H.; Roland, F.; Sherman, B. S.; Schindler, D. W.; Sobek, S.; Tremblay, A.; Vanni, M. J.; Verschoor, A. M.; von Wachenfeldt, E.; Weyhenmeyer, G. A.; Lakes and reservoirs as regulators of carbon cycling and climate. *Limnology and Oceanography* **2009,** *54*, (6), 2298-2314.
1-29. Harrison, J. A.; Maranger, R. J.; Alexander, R. B.; Giblin, A. E.; Jacinthe, P.-A.; Mayorga, E.; Seitzinger, S. P.; Sobota, D. J.; Wollheim, W. M.; The regional and global significance of nitrogen removal in lakes and reservoirs. *Biogeochemistry* **2009,** *93*, (1), 143-157.
1-30. Adrian, R.; O'Reilly Catherine, M.; Zagarese, H.; Baines Stephen, B.; Hessen Dag, O.; Keller, W.; Livingstone David, M.; Sommaruga, R.; Straile, D.; Van Donk, E.; Weyhenmeyer Gesa, A.; Winder, M.; Lakes as sentinels of climate change. *Limnology and Oceanography* **2009,** *54*, (6part2), 2283-2297.

1-31. Carpenter, S. R.; Cottingham, K. L.; Resilience and Restoration of Lakes. *Conservation Ecology* **1997,** *1*, (1), 2.
1-32. Magnuson, J. J.; Robertson, D. M.; Benson, B. J.; Wynne, R. H.; Livingstone, D. M.; Arai, T.; Assel, R. A.; Barry, R. G.; Card, V.; Kuusisto, E.; Granin, N. G.; Prowse, T. D.; Stewart, K. M.; Vuglinski, V. S.; Historical trends in lake and river ice cover in the Northern Hemisphere. *Science* **2000,** *289*, (5485), 1743-1746.
1-33. Latifovic, R.; Pouliot, D.; Analysis of climate change impacts on lake ice phenology in Canada using the historical satellite data record. *Remote Sensing of Environment* **2007,** *106*, (4), 492-507.
1-34. Roberts, K. E.; Lamoureux, S. F.; Kyser, T. K.; Muir, D. C. G.; Lafrenière, M. J.; Iqaluk, D.; Pieńkowski, A. J.; Normandeau, A.; Climate and permafrost effects on the chemistry and ecosystems of High Arctic Lakes. *Scientific Reports* **2017,** *7*, (1), 13292.
1-35. Lehnherr, I.; St. Louis, V. L.; Muir, D. C. G.; Sharp, M. J.; Gardner, A. S.; Lamoureux, S.; Smol, J. P.; St. Pierre, K. A.; Michelutti, N.; Schiff, S. L.; Emmerton, C. A.; Tarnocai, C.; Talbot, C.; The world's largest High Arctic lake responds rapidly to climate warming. *Nature Commun.* **2018,** *9*, 1290.
1-36. Tranter, M.; Wadham, J. L.; 7.5 - Geochemical Weathering in Glacial and Proglacial Environments A2 - Holland, Heinrich D. In *Treatise on Geochemistry (Second Edition)*, Turekian, K. K.; Ed. Elsevier: Oxford, 2014; pp 157-173.
1-37. Hawes, I.; Howard-Williams, C.; Fountain, A. G.; Ice-based freshwater ecosystems. In *Polar Lakes and Rivers: Limnology of Arctic and Antarctic Aquatic Ecosystems*, Vincent, W. F.; Laybourn-Parry, J.; Eds. Oxford University Press: New York, NY, 2008; pp 103-118.
1-38. Milner, A. M.; Khamis, K.; Battin, T. J.; Brittain, J. E.; Barrand, N. E.; Füreder, L.; Cauvy-Fraunié, S.; Gíslason, G. M.; Jacobsen, D.; Hannah, D. M.; Hodson, A. J.; Hood, E.; Lencioni, V.; Ólafsson, J. S.; Robinson, C. T.; Tranter, M.; Brown, L. E.; Glacier shrinkage driving global changes in downstream systems. *Proceedings of the National Academy of Sciences* **2017,** *114*, (37), 9770-9778.
1-39. Hood, E.; Battin, T. J.; Fellman, J.; O'Neel, S.; Spencer, R. G. M.; Storage and release of organic carbon from glaciers and ice sheets. *Nature Geoscience* **2015,** *8*, (2), 91-96.
1-40. Zdanowicz, C.; Krummel, E. M.; Lean, D.; Poulain, A. J.; Yumvihoze, E.; Chen, J. B.; Hintelmann, H.; Accumulation, storage and release of atmospheric mercury in a glaciated Arctic catchment, Baffin Island, Canada. *Geochim. Cosmochim. Acta* **2013,** *107*, 316-335.
1-41. Malard, F.; Uehlinger, U.; Zah, R.; Tockner, K.; Flood-pulse and riverscape dynamics in a braided glacial river. *Ecology* **2006,** *87*, (3), 704-716.
1-42. Telling, J.; Boyd, E. S.; Bone, N.; Jones, E. L.; Tranter, M.; MacFarlane, J. W.; Martin, P. G.; Wadham, J. L.; Lamarche-Gagnon, G.; Skidmore, M. L.; Hamilton, T. L.; Hill, E.; Jackson, M.; Hodgson, D. A.; Rock comminution as a source of hydrogen for subglacial ecosystems. *Nature Geosci.* **2015,** *8*, (11), 851-+.
1-43. Wadham, J. L.; Hawkings, J.; Telling, J.; Chandler, D.; Alcock, J.; O'Donnell, E.; Kaur, P.; Bagshaw, E.; Tranter, M.; Tedstone, A.; Nienow, P.; Sources, cycling and export of nitrogen on the Greenland Ice Sheet. *Biogeosciences* **2016,** *13*, (22), 6339-6352.
1-44. Hawkings, J.; Wadham, J.; Tranter, M.; Telling, J.; Bagshaw, E.; Beaton, A.; Simmons, S. L.; Chandler, D.; Tedstone, A.; Nienow, P.; The Greenland Ice Sheet as a hot spot of phosphorus weathering and export in the Arctic. *Global Biogeochemical Cycles* **2016,** *30*, (2), 191-210.

1-45. Hawkings, J. R.; Wadham, J. L.; Benning, L. G.; Hendry, K. R.; Tranter, M.; Tedstone, A.; Nienow, P.; Raiswell, R.; Ice sheets as a missing source of silica to the polar oceans. *Nature Commun.* **2017,** *8*.
1-46. Hawkings, J. R.; Wadham, J. L.; Tranter, M.; Raiswell, R.; Benning, L. G.; Statham, P. J.; Tedstone, A.; Nienow, P.; Lee, K.; Telling, J.; Ice sheets as a significant source of highly reactive nanoparticulate iron to the oceans. *Nature Communications* **2014,** *5*.
1-47. Lehnherr, I.; Methylmercury biogeochemistry: a review with special reference to Arctic aquatic ecosystems. *Environmental Reviews* **2014,** *22*, (3), 229-243.
1-48. Selin, N. E.; Global Biogeochemical Cycling of Mercury: A Review. *Annual Review of Environment and Resources* **2009,** *34*, (1), 43-63.
1-49. Streets, D. G.; Devane, M. K.; Lu, Z.; Bond, T. C.; Sunderland, E. M.; Jacob, D. J.; All-Time Releases of Mercury to the Atmosphere from Human Activities. *Environmental Science ; Technology* **2011,** *45*, (24), 10485-10491.
1-50. Durnford, D.; Dastoor, A.; Figuera-Nieto, D.; Ryjkov, A.; Long range transport of mercury to the Arctic and across Canada. *Atmos. Chem. Phys.* **2010,** *10*, 6063-6086.
1-51. Lim, C.-J.; Cheng, M.-D.; Schroeder, W. H.; Transport patterns and potential sources of total gaseous mercury measured in Canadian high Arctic in 1995. *Atmospheric Environment* **2001,** *35*, (6), 1141-1154.
1-52. Chan, H. M.; Kim, C.; Khoday, K.; Receveur, O.; Kuhnlein, H. V.; Assessment of dietary exposure to trace-metals in Baffin Inuit food. *Environmental Health Perspectives* **1995,** *103*, (7-8), 740-746.
1-53. Laird, B. D.; Goncharov, A. B.; Egeland, G. M.; Chan, H. M.; Dietary Advice on Inuit Traditional Food Use Needs to Balance Benefits and Risks of Mercury, Selenium, and n3 Fatty Acids. *J. Nutr.* **2013,** *143*, (6), 923-930.
1-54. Schuster, P. F.; Schaefer, K. M.; Aiken, G. R.; Antweiler, R. C.; Dewild, J. F.; Gryziec, J. D.; Gusmeroli, A.; Hugelius, G.; Jafarov, E.; Krabbenhoft, D. P.; Liu, L.; Herman-Mercer, N.; Mu, C.; Roth David, A.; Schaefer, T.; Striegl, R. G.; Wickland, K. P.; Zhang, T.; Permafrost Stores a Globally Significant Amount of Mercury. *Geophysical Research Letters* **2018,** *45*, (3), 1463-1471.
1-55. Schuster, P. F.; Striegl, R. G.; Aiken, G. R.; Krabbenhoft, D. P.; Dewild, J. F.; Butler, K.; Kamark, B.; Dornblaser, M.; Mercury Export from the Yukon River Basin and Potential Response to a Changing Climate. *Environ. Sci. Technol.* **2011,** *45*, (21), 9262-9267.
1-56. Zhang, Y.; Jacob, D. J.; Horowitz, H. M.; Chen, L.; Amos, H. M.; Krabbenhoft, D. P.; Slemr, F.; St. Louis, V. L.; Sunderland, E. M.; Observed decrease in atmospheric mercury explained by global decline in anthropogenic emissions. *PNAS* **2016,** *113*, (3), 526-531.
1-57. Cole, A. S.; Steffen, A.; Eckley, C. S.; Narayan, J.; Pilote, M.; Tordon, R.; Graydon, J. A.; St. Louis, V. L.; Xu, X.; Branfireun, B.; A Survey of Mercury in Air and Precipitation across Canada: Patterns and Trends. *Atmosphere* **2014,** *5*, 635-668.
1-58. Fisher, D.; Zheng, J.; Burgess, D.; Zdanowicz, C.; Kinnard, C.; Sharp, M.; Bourgeois, J.; Recent melt rates of Canadian arctic ice caps are the highest in four millennia. *Global and Planetary Change* **2012,** *84–85*, 3-7.
1-59. Fisher, J. A.; Jacob, D. J.; Soerensen, A. L.; Amos, H. M.; Steffen, A.; Sunderland, E. M.; Riverine source of Arctic Ocean mercury inferred from atmospheric observations. *Nature Geoscience* **2012,** *5*, (7), 499-504.
1-60. Shiklomanov, I. A.; Shiklomanov, A. I.; Lammers, R. B.; Peterson, B. J.; Vorosmarty, C. J.; The Dynamics of River Water Inflow to the Arctic Ocean. In *The Freshwater Budget of*

the Arctic Ocean, Lewis, E. L.; Jones, E. P.; Lemke, P.; Prowse, T. D.; Wadhams, P.; Eds. Springer Netherlands: Dordrecht, 2000; pp 281-296.
1-61. Carmack, E. C.; Yamamoto-Kawai, M.; Haine, T. W. N.; Bacon, S.; Bluhm, B. A.; Lique, C.; Melling, H.; Polyakov, I. V.; Straneo, F.; Timmermans, M. L.; Williams, W. J.; Freshwater and its role in the Arctic Marine System: Sources, disposition, storage, export, and physical and biogeochemical consequences in the Arctic and global oceans. *J. Geophys. Res. Biogeosci.* **2016,** *121*, (3), 675-717.
1-62. Vellinga, M.; Wood, R. A.; Global Climatic Impacts of a Collapse of the Atlantic Thermohaline Circulation. *Climatic Change* **2002,** *54*, (3), 251-267.
1-63. England, J.; Atkinson, N.; Bednarski, J.; Dyke, A. S.; Hodgson, D. A.; Ó Cofaigh, C.; The Innuitian Ice Sheet: configuration, dynamics and chronology. *Quaternary Science Reviews* **2006,** *25*, (7), 689-703.
1-64. Smith, I. R.; Late Quaternary glacial history of Lake Hazen Basin and eastern Hazen Plateau, northern Ellesmere Island, Nunavut, Canada. *Canadian Journal of Earth Sciences* **1999,** *36*, (9), 1547-1565.
1-65. Emmerton, C. A.; St Louis, V. L.; Lehnherr, I.; Graydon, J. A.; Kirk, J. L.; Rondeau, K. J.; The importance of freshwater systems to the net atmospheric exchange of carbon dioxide and methane with a rapidly changing high Arctic watershed. *Biogeosciences* **2016,** *13*, (20), 5849-5863.
1-66. Lehnherr, I.; St Louis, V. L.; Kirk, J. L.; Methylmercury Cycling in High Arctic Wetland Ponds: Controls on Sedimentary Production. *Environ. Sci. Technol.* **2012,** *46*, (19), 10523-10531.
1-67. Lehnherr, I.; St Louis, V. L.; Emmerton, C. A.; Barker, J. D.; Kirk, J. L.; Methylmercury Cycling in High Arctic Wetland Ponds: Sources and Sinks. *Environ. Sci. Technol.* **2012,** *46*, (19), 10514-10522.
1-68. Keatley, B. E.; Douglas, M. S. V.; Smol, J. P.; Prolonged ice cover dampens diatom community responses to recent climatic change in High Arctic lakes. *Arctic Antarctic and Alpine Research* **2008,** *40*, (2), 364-372.
1-69. Emmerton, C. A.; St Louis, V. L.; Humphreys, E. R.; Gamon, J. A.; Barker, J. D.; Pastorello, G. Z.; Net ecosystem exchange of CO2 with rapidly changing high Arctic landscapes. *Global Change Biology* **2016,** *22*, (3), 1185-1200.
1-70. Emmerton, C. A.; St. Louis, V. L.; Lehnherr, I.; Humphreys, E. R.; Rydz, E.; Kosolofski, H. R.; The net exchange of methane with high Arctic landscapes during the summer growing season. *Biogeosciences* **2014,** *11*, (12), 3095-3106.
1-71. Panchen, Z. A.; Arctic plants produce vastly different numbers of flowers in three contrasting years at Lake Hazen, Quttinirpaaq National Park, Ellesmere Island, Nunavut, Canada. *The Canadian Field-Naturalist* **2016,** *130*, (1), 56-63.
1-72. Panchen, Z. A.; Gorelick, R.; Canadian Arctic Archipelago Conspecifics Flower Earlier in the High Arctic than the Mid-Arctic. *International Journal of Plant Sciences* **2016,** *177*, (8), 661-670.
2-1. Radić, V.; Bliss, A.; Beedlow, A. C.; Hock, R.; Miles, E.; Cogley, J. G.; Regional and global projections of twenty-first century glacier mass changes in response to climate scenarios from global climate models. *Climate Dynamics* **2013,** *42*, (1), 37-58.
2-2. Bliss, A.; Hock, R.; Radić, V.; Global response of glacier runoff to twenty-first century climate change. *Journal of Geophysical Research: Earth Surface* **2014,** *119*, (4), 717-730.

2-3. Huss, M.; Hock, R.; Global-scale hydrological response to future glacier mass loss. *Nature Climate Change* **2018**.
2-4. Pfeffer, W. T.; Arendt, A. A.; Bliss, A.; Bolch, T.; Cogley, J. G.; Gardner, A. S.; Hagen, J.-O.; Hock, R.; Kaser, G.; Kienholz, C.; Miles, E. S.; Moholdt, G.; Mölg, N.; Paul, F.; Radi; Valentina; Rastner, P.; Raup, B. H.; Rich, J.; Sharp, M. J.; The Randolph Glacier Inventory: a globally complete inventory of glaciers. *J. Glaciol.* **2014,** *60*, (221), 537-552.
2-5. Stocker, T. F.; Qin, D.; Plattner, G.-K.; Tignor, M.; Allen, S. K.; Boschung, J.; Nauels, A.; Xia, Y.; Bex, V.; Midgley, P. M.; *IPCC 2013: Climate Change 2013: The Physical Science Basis. Contribution of Working Group I to the Fifth Assessment Report of the Intergovernmental Panel on Climate Change*. Cambridge University Press: Cambridge, UK and New York, NY, USA, 2013; p 1535 pp.
2-6. Hood, E.; Battin, T. J.; Fellman, J.; O'Neel, S.; Spencer, R. G. M.; Storage and release of organic carbon from glaciers and ice sheets. *Nature Geoscience* **2015,** *8*, (2), 91-96.
2-7. Zdanowicz, C.; Krummel, E. M.; Lean, D.; Poulain, A. J.; Yumvihoze, E.; Chen, J. B.; Hintelmann, H.; Accumulation, storage and release of atmospheric mercury in a glaciated Arctic catchment, Baffin Island, Canada. *Geochim. Cosmochim. Acta* **2013,** *107*, 316-335.
2-8. Beal, S. A.; Osterberg, E. C.; Zdanowicz, C. M.; Fisher, D. A.; Ice Core Perspective on Mercury Pollution during the Past 600 Years. *Environ. Sci. Technol.* **2015,** *49*, (13), 7641-7647.
2-9. Warner, K. A.; Saros, J. E.; Simon, K. S.; Nitrogen Subsidies in Glacial Meltwater: Implications for High Elevation Aquatic Chains. *Water Resources Research* **2017,** *53*, (11), 9791-9806.
2-10. Schroth, A.; W.; Crusius, J.; Chever, F.; Bostick Benjamin, C.; Rouxel Olivier, J.; Glacial influence on the geochemistry of riverine iron fluxes to the Gulf of Alaska and effects of deglaciation. *Geophysical Research Letters* **2011,** *38*, (16).
2-11. Hodgkins, R.; Cooper, R.; Wadham, J.; Tranter, M.; Suspended sediment fluxes in a high-Arctic glacierised catchment: implications for fluvial sediment storage. *Sedimentary Geology* **2003,** *162*, (1-2), 105-117.
2-12. Hawkings, J. R.; Wadham, J. L.; Tranter, M.; Raiswell, R.; Benning, L. G.; Statham, P. J.; Tedstone, A.; Nienow, P.; Lee, K.; Telling, J.; Ice sheets as a significant source of highly reactive nanoparticulate iron to the oceans. *Nature Communications* **2014,** *5*.
2-13. Wadham, J. L.; Hawkings, J.; Telling, J.; Chandler, D.; Alcock, J.; O'Donnell, E.; Kaur, P.; Bagshaw, E.; Tranter, M.; Tedstone, A.; Nienow, P.; Sources, cycling and export of nitrogen on the Greenland Ice Sheet. *Biogeosciences* **2016,** *13*, (22), 6339-6352.
2-14. Weyhenmeyer, G. A.; Conley, D. J.; Large differences between carbon and nutrient loss rates along the land to ocean aquatic continuum—implications for energy:nutrient ratios at downstream sites. *Limnology and Oceanography* **2017**, n/a-n/a.
2-15. Bouwman, A. F.; Bierkens, M. F. P.; Griffioen, J.; Hefting, M. M.; Middelburg, J. J.; Middelkoop, H.; Slomp, C. P.; Nutrient dynamics, transfer and retention along the aquatic continuum from land to ocean: towards integration of ecological and biogeochemical models. *Biogeosciences* **2013,** *10*, (1), 1-22.
2-16. Frost, P. C.; Kinsman, L. E.; Johnston, C. A.; Larson, J. H.; Watershed discharge modulates relationships between landscape components and nutrient ratios in stream seston. *Ecology* **2009,** *90*, (6), 1631-1640.
2-17. Tranvik, L. J.; Downing, J. A.; Cotner, J. B.; Loiselle, S. A.; Striegl, R. G.; Ballatore, T. J.; Dillon, P.; Finlay, K.; Fortino, K.; Knoll, L. B.; Kortelainen, P. L.; Kutser, T.; Larsen, S.;

Laurion, I.; Leech, D. M.; McCallister, S. L.; McKnight, D. M.; Melack, J. M.; Overholt, E.; Porter, J. A.; Prairie, Y.; Renwick, W. H.; Roland, F.; Sherman, B. S.; Schindler, D. W.; Sobek, S.; Tremblay, A.; Vanni, M. J.; Verschoor, A. M.; von Wachenfeldt, E.; Weyhenmeyer, G. A.; Lakes and reservoirs as regulators of carbon cycling and climate. *Limnology and Oceanography* **2009,** *54*, (6), 2298-2314.

2-18. Weyhenmeyer, G. A.; Kosten, S.; Wallin, M. B.; Tranvik, L. J.; Jeppesen, E.; Roland, F.; Significant fraction of CO2 emissions from boreal lakes derived from hydrologic inorganic carbon inputs. *Nature Geosci* **2015,** *8*, (12), 933-936.

2-19. Song, C.; Sheng, Y.; Ke, L.; Nie, Y.; Wang, J.; Glacial lake evolution in the southeastern Tibetan Plateau and the cause of rapid expansion of proglacial lakes linked to glacial-hydrogeomorphic processes. *Journal of Hydrology* **2016,** *540*, 504-514.

2-20. Stokes, C. R.; Popovnin, V.; Aleynikov, A.; Gurney, S. D.; Shahgedanova, M.; Recent glacier retreat in the Caucasus Mountains, Russia, and associated increase in supraglacial debris cover and supra-/proglacial lake development. *Annals of Glaciology* **2007,** *46*, 195-203.

2-21. Carrivick, J. L.; Tweed, F. S.; Proglacial lakes: character, behaviour and geological importance. *Quaternary Science Reviews* **2013,** *78*, 34-52.

2-22. Köck, G.; Muir, D. C. G.; Yang, F.; Wang, X.; Talbot, C.; Gantner, N.; Moser, D.; Bathymetry and Sediment Geochemistry of Lake Hazen (Quttinirpaaq National Park, Ellesmere Island, Nunavut). *Arctic* **2012,** *65*, (1), 56-66.

2-23. Lehnherr, I.; St. Louis, V. L.; Muir, D. C. G.; Sharp, M. J.; Gardner, A. S.; Lamoureux, S.; Smol, J. P.; St. Pierre, K. A.; Michelutti, N.; Schiff, S. L.; Emmerton, C. A.; Tarnocai, C.; Talbot, C.; The world's largest High Arctic lake responds rapidly to climate warming. *Nature Commun.* **2018,** *9*, 1290.

2-24. Serreze, M. C.; Raup, B.; Braun, C.; Hardy, D. R.; Bradley, R. S.; Rapid wastage of the Hazen Plateau ice caps, northeastern Ellesmere Island, Nunavut, Canada. *The Cryosphere* **2017,** *11*, (1), 169-177.

2-25. Thompson, W.; Climate. In *Resource description and analysis: Ellesmere Island, National Park Reserve.* , National Resource Conservation Selection, Prairie and Northern Region, Parks Canada, Department of Canadian Heritage: Winnipeg, Manitoba, 1994; p 78.

2-26. Emmerton, C. A.; St Louis, V. L.; Lehnherr, I.; Graydon, J. A.; Kirk, J. L.; Rondeau, K. J.; The importance of freshwater systems to the net atmospheric exchange of carbon dioxide and methane with a rapidly changing high Arctic watershed. *Biogeosciences* **2016,** *13*, (20), 5849-5863.

2-27. Gardner, A. S.; Moholdt, G.; Wouters, B.; Wolken, G. J.; Burgess, D. O.; Sharp, M. J.; Cogley, J. G.; Braun, C.; Labine, C.; Sharply increased mass loss from glaciers and ice caps in the Canadian Arctic Archipelago. *Nature* **2011,** *473*, (7347), 357-360.

2-28. Runkel, R. L.; Crawford, C. G.; Cohn, T. A.; Load estimator (LOADEST): a FORTRAN program for estimating constituent loads in streams and rivers. In *USGS Techniques and Methods Book 4*, U.S. Geological Survey: Reston, Virginia, USA, 2004.

2-29. Lorenz, D.; Runkel, R.; De Cicco, L. *rloadest: river load estimation*, U.S. Geological Survey: Mounds View, Minnesota, USA.; 2015.

2-30. Findlay, D. L.; Response of Phytoplankton Communities to Acidification and Recovery in Killarney Park and the Experimental Lakes Area, Ontario. *AMBIO: A Journal of the Human Environment* **2003,** *32*, (3), 190-195.

2-31. Findlay, D. L.; Kling, H. J. *Protocols for measuring biodiversity: Phytoplankton in fresh water lakes*; Department of Fisheries and Oceans Canada: Winnipeg, MB, 1998; p 19 pp.
2-32. Borcard, D.; Gillet, F.; Legendre, P.; *Numerical Ecology with R*. Springer: New York USA, 2011.
2-33. Oksanen, J.; Blanchet, F. G.; Friendly, M.; Kindt, R.; Legendre, P.; McGlinn, D.; Minchin, P. R.; O'Hara, R. B.; Simpson, G. L.; Solymos, P.; Stevens, M. H. H.; Szoecs, E.; Wagner, H. *Package 'vegan'*, 2.4-6; 2018.
2-34. Reist, J. D.; Gyselman, E.; Babaluk, J. A.; Johnson, J. D.; Wissink, H. R.; Evidence for two morphotypes of Arctic char (*Salvelinus alpinus* (L.)) from Lake Hazen, Ellesmere Island, Northwest Territories, Canada. *Nordic J. Freshwater Res.* **1995,** *71*, 396-410.
2-35. Babaluk, J. A.; Halden, N. M.; Reist, J. D.; Kristofferson, A. H.; Campbell, J. L.; Teesdale, W. J.; Evidence for non-anadromous behaviour of arctic charr (Salvelinus alpinus) from Lake Hazen, Ellesmere Island, northwest Territories, Canada, based on scanning proton microprobe analysis of otolith strontium distribution. *Arctic* **1997,** *50*, (3), 224-233.
2-36. Babaluk, J. A.; Wissink, H. R.; Troke, B. G.; Clark, D. A.; Johnson, J. D.; Summer Movements of Radio-Tagged Arctic Charr (Salvelinus Alpinus) in Lake Hazen, Nunavut, Canada. *Arctic* **2001,** *54*, (4), 418-424.
2-37. Guiguer, K. R. R. A.; Reist, J. D.; Power, M.; Babaluk, J. A.; Using stable isotopes to confirm the trophic ecology of Arctic charr morphotypes from Lake Hazen, Nunavut, Canada. *J. Fish Biol.* **2002,** *60*, (2), 348-362.
2-38. Babaluk, J. A.; Sawatzky, C. D.; Wastle, R. J.; Reist, J. D.; Biological data of Arctic char, Salvelinus alpinus, from Lake Hazen, Quttinirpaaq National Park, Nunavut, 1958-2001. In Babaluk, J. A.; Ed. Fisheries and Oceans Canada: [Ottawa] :, 2007.
2-39. Sinnatamby, R. N.; Reist James, D.; Power, M.; Identification of the maternal source of young-of-the-year Arctic charr in Lake Hazen, Canada. *Freshwater Biology* **2013,** *58*, (7), 1425-1435.
2-40. Heiri, O.; Lotter, A. F.; Lemcke, G.; Loss on ignition as a method for estimating organic and carbonate content in sediments: reproducibility and comparability of results. *Journal of Paleolimnology* **2001,** *25*, (1), 101-110.
2-41. Berg, P.; Risgaard-Petersen, N.; Rysgaard, S.; Interpretation of measured concentration profiles in sediment pore water. *Limnology and Oceanography* **1998,** *43*, (7), 1500-1510.
2-42. Zdanowicz, C. M.; Zielinski, G. A.; Wake, C. P.; Characteristics of modern atmospheric dust deposition in snow on the Penny Ice Cap, Baffin Island, Arctic Canada. *Tellus* **1998,** *50B*, 506-520.
2-43. Kępski, D.; Błaś, M.; Sobik, M.; Polkowska, Ż.; Grudzińska, K.; Progressing Pollutant Elution from Snowpack and Evolution of its Physicochemical Properties During Melting Period—a Case Study From the Sudetes, Poland. *Water, Air, and Soil Pollution* **2016,** *227*, 112.
2-44. Boyer, E. W.; Hornberger, G. M.; Bencala, K. E.; McKnight, D. M.; Effects of asynchronous snowmelt on flushing of dissolved organic carbon: a mixing model approach. *Hydrological Processes* **2001,** *14*, (18), 3291-3308.
2-45. Graly, J. A.; Drever, J. I.; Humphrey, N. F.; Calculating the balance between atmospheric CO_2 drawdown and organic carbon oxidation in subglacial hydrochemical systems. *Global Biogeochemical Cycles* **2017,** *31*, (4), 709-727.

2-46. Anderson, S. P.; Drever, J. I.; Frost, C. D.; Holden, P.; Chemical weathering in the foreland of a retreating glacier. *Geochimica Et Cosmochimica Acta* **2000,** *64*, (7), 1173-1189.
2-47. Malard, F.; Uehlinger, U.; Zah, R.; Tockner, K.; Flood-pulse and riverscape dynamics in a braided glacial river. *Ecology* **2006,** *87*, (3), 704-716.
2-48. Hawkings, J.; Wadham, J.; Tranter, M.; Telling, J.; Bagshaw, E.; Beaton, A.; Simmons, S. L.; Chandler, D.; Tedstone, A.; Nienow, P.; The Greenland Ice Sheet as a hot spot of phosphorus weathering and export in the Arctic. *Global Biogeochemical Cycles* **2016,** *30*, (2), 191-210.
2-49. Rose, K. C.; Hamilton, D. P.; Williamson, C. R.; McBride, C. G.; Fischer, J. M.; Olson, M. H.; Saros, J. E.; Allan, M. G.; Cabrol, N.; Light attenuation in glacier-fed lakes. *Journal of Geophysical Research-Biogeosciences* **2014,** *119*, 1446-1457.
2-50. Crookshanks, S.; Gilbert, R.; Continuous, diurnally fluctuating turbidity currents in Kluane Lake, Yukon Territory. *Canadian Journal of Earth Sciences* **2008,** *45*, (10), 1123-1138.
2-51. Weyhenmeyer, G. A.; Synchrony in relationships between the North Atlantic Oscillation and water chemistry among Sweden's largest lakes. *Limnology and Oceanography* **2004,** *49*, (4), 1191-1201.
2-52. Hamilton, P. B.; Gajewski, K.; Atkinson, D. E.; Lean, D. R. S.; Physical and chemical limnology of 204 lakes from the Canadian Arctic Archipelago. *Hydrobiologia* **2001,** *457*, 133-148.
2-53. Saros, J. E.; Rose, K. C.; Clow, D. W.; Stephens, V. C.; Nurse, A. B.; Arnett, H. A.; Stone, J. R.; Williamson, C. E.; Wolfe, A. P.; Melting Alpine Glaciers Enrich High-Elevation Lakes with Reactive Nitrogen. *Environmental Science ; Technology* **2010,** *44*, (13), 4891-4896.
2-54. Pettersson, K.; Mechanisms for internal loading of phosphorus in lakes. *Hydrobiologia* **1998,** *373*, (0), 21-25.
2-55. Boström, B.; Andersen, J. M.; Fleischer, S.; Jansson, M.; Exchange of phosphorus across the sediment-water interface. *Hydrobiologia* **1988,** *170*, 229-244.
2-56. Bergström, A.-K.; The use of TN:TP and DIN:TP ratios as indicators for phytoplankton nutrient limitation in oligotrophic lakes affected by N deposition. *Aquatic Sciences* **2010,** *72*, (3), 277-281.
2-57. Burgin, A.; J.; Hamilton, S.; K.; Have we overemphasized the role of denitrification in aquatic ecosystems? A review of nitrate removal pathways. *Frontiers in Ecology and the Environment* **2007,** *5*, (2), 89-96.
2-58. Wetzel, R. G.; *Limnology*. 3rd ed.; Academic Press: San Diego, California, 2001; p 1006.
2-59. Beutel, M. W.; Inhibition of ammonia release from anoxic profundal sediments in lakes using hypolimnetic oxygenation. *Ecological Engineering* **2006,** *28*, (3), 271-279.
2-60. Cole, J. J.; Caraco, N. F.; Kling, G. W.; Kratz, T. K.; Carbon Dioxide Supersaturation in the Surface Waters of Lakes. *Science* **1994,** *265*, (5178), 1568.
2-61. Christie, R. L. *Bedrock geology*; Defence Research Board Canada: Ottawa, 1958; pp 16-18.
2-62. Tranter, M.; Sharp, M. J.; Lamb, H. R.; Brown, G. H.; Hubbard, B. P.; Willis, I. C.; Geochemical weathering at the bed of Haut Glacier d'Arolla, Switzerland: a new model. *Hydrol. Processes* **2002,** *16*, (5), 959-993.
2-63. Paltan, H.; Dash, J.; Edwards, M.; A refined mapping of Arctic lakes using Landsat imagery. *International Journal of Remote Sensing* **2015,** *36*, (23), 5970-5982.

2-64. Liermann, S.; Beylich, A. A.; van Welden, A.; Contemporary suspended sediment transfer and accumulation processes in the small proglacial Sætrevatnet sub-catchment, Bødalen, western Norway. *Geomorphology* **2012,** *167-168*, 91-101.
2-65. McLaren, I. A. *Aquatic Biology*; Defence Research Board Ottawa, ON, May 1959, 1959; pp 70-72.
2-66. Michelutti, N.; Wolfe Alexander, P.; Vinebrooke Rolf, D.; Rivard, B.; Briner Jason, P.; Recent primary production increases in arctic lakes. *Geophysical Research Letters* **2005,** *32*, (19).
2-67. Christoffersen, K. S.; Amsinck, S. L.; Landkildehus, F.; Lauridsen, T. L.; Jeppesen, E.; Lake Flora and Fauna in Relation to Ice-Melt, Water Temperature and Chemistry at Zackenberg. In *Advances in Ecological Research*, Academic Press: 2008; Vol. 40, pp 371-389.
2-68. Rothhaupt, K. O.; Laboratorary Experiments with a Mixotrophic Chrysophyte and Obligately Phagotrophic and Photographic Competitors. *Ecology* **1996,** *77*, (3), 716-724.
2-69. Vollenweider, R. A.; Munawar, M.; Stadelman, P.; A Comparative Review of Phytoplankton and Primary Production in the Laurentian Great Lakes. *Journal of Fisheries Research Board of Canada* **1974,** *31*, (5), 739-762.
2-70. Vörös, L.; Callieri, C.; V.-Balogh, K.; Bertoni, R. In *Freshwater picocyanobacteria along a trophic gradient and light quality range*, Phytoplankton and Trophic Gradients, Dordrecht, 1998//, 1998; Alvarez-Cobelas, M.; Reynolds, C. S.; Sánchez-Castillo, P.; Kristiansen, J.; Eds. Springer Netherlands: Dordrecht, 1998; pp 117-125.
2-71. Huisman, J.; Weissing, F. J.; Biological conditions for oscillatons and chaos generated by multispecies competition. *Ecology* **2001,** *82*, (10), 2682-2695.
2-72. Laybourn-Parry, J.; Marshall, W. A.; Photosynthesis, mixotrophy and microbial plankton dynamics in two high Arctic lakes during summer. *Polar Biology* **2003,** *26*, (8), 517-524.
2-73. McLaren, I. A.; Zooplankton of Lake Hazen, Ellesmere Island, and a nearby pond, with special reference to the copepod Cyclops Scutifer Sars. *Canadian Journal of Zoology* **1964,** *42*, (4), 613-629.
2-74. Rautio, M.; Bayly, I. A. E.; Gibson, J. A. E.; Nyman, M.; Zooplankton and zoobenthos in high-latitude water bodies. In *Polar Lakes and Rivers: Limnology of Arctic and Antarctic Aquatic Ecosystems*, Vincent, W. F.; Laybourn-Parry, J.; Eds. Oxford University Press: New York, USA, 2008; pp 231-247.
2-75. Heathcote, A. J.; Anderson, N. J.; Prairie, Y. T.; Engstrom, D. R.; del Giorgio, P. A.; Large increases in carbon burial in northern lakes during the Anthropocene. *Nature Communications* **2015,** *6*.
2-76. Sondergaard, M.; Jensen, J. P.; Jeppesen, E.; Role of sediment and internal loading of phosphorus in shallow lakes. *Hydrobiologia* **2003,** *506*, (1-3), 135-145.
2-77. Wik, M.; Varner, R. K.; Anthony, K. W.; MacIntyre, S.; Bastviken, D.; Climate-sensitive northern lakes and ponds are critical components of methane release. *Nature Geoscience* **2016,** *9*, (2), 99-105.
2-78. Maranger, R.; Jones Stuart, E.; Cotner James, B.; Stoichiometry of carbon, nitrogen, and phosphorus through the freshwater pipe. *Limnology and Oceanography Letters* **2018,** *3*, (3), 89-101.
2-79. Prowse, T.; Bring, A.; Mård, J.; Carmack, E. C.; Holland, M.; Instanes, A.; Vihma, T.; Wrona, F. J.; Arctic Freshwater Synthesis: Summary of key emerging issues. *Journal of Geophysical Research Biogeosciences* **2015,** *120*, 1887-1893.

2-80. Holmes, R. M.; McClelland, J. W.; Peterson, B. J.; Shiklomanov, I. A.; Shiklomanov, A. I.; Zhulidov, A. V.; Gordeev, V. V.; Bobrovitskaya, N. N.; A circumpolar perspective on fluvial sediment flux to the Arctic ocean. *Global Biogeochem. Cycles* **2002,** *16*, (4), 45-1-45-14.
2-81. Lammers, R. B.; Shiklomanov, A. I.; Vörösmarty, C. J.; Fekete, B. M.; Peterson, B. J.; Assessment of contemporary Arctic river runoff based on observational discharge records. *J. Geophys. Res. Atmos.* **2001,** *106*, (D4), 3321-3334.
3-1. Cole, J. J. *et al.* Plumbing the global carbon cycle: Integrating inland waters into the terrestrial carbon budget. *Ecosystems* **2007**, *10*, 171-184.
3-2. Duarte, C. M.; Prairie, Y. T. Prevalence of heterotrophy and atmospheric CO_2 emissions from aquatic ecosystems. *Ecosystems* **2005**, *8*, 862-870.
3-3. Raymond, P. A. *et al.* Global carbon dioxide emissions from inland waters. *Nature* **2013**, *503*, 355-359.
3-4. Weyhenmeyer, G. A. *et al.* Significant fraction of CO_2 emissions from boreal lakes derived from hydrologic inorganic carbon inputs. *Nat. Geosci.* **2015,** *8*, 933-936.
3-5. Cory, R. M.; Ward, C. P.; Crump, B. C.; Kling, G. W. Sunlight controls water column processing of carbon in arctic fresh waters. *Science* **2014**, *345*, 925.
3-6. Vachon, D.; Lapierre, J.-F.; del Giorgio, P. A. Seasonality of photochemical dissolved organic carbon mineralization and its relative contribution to pelagic CO_2 production in northern lakes. *J. Geophys. Res. Biogeosci.* **2016***, 121*, 864-878.
3-7. Marcé, R. *et al.* Carbonate weathering as a driver of CO_2 supersaturation in lakes. *Nat. Geosci.* **2015,** *8*, 107-111.
3-8. Stokes, C. R.; Popovnin, V.; Aleynikov, A.; Gurney, S. D. ; Shahgedanova, M. Recent glacier retreat in the Caucasus Mountains, Russia, and associated increase in supraglacial debris cover and supra-/proglacial lake development. *Ann. Glaciol.* **2007***, 46*, 195-203.
3-9. Song, C.; Sheng, Y.; Ke, L.; Nie, Y. ; Wang, J. Glacial lake evolution in the southeastern Tibetan Plateau and the cause of rapid expansion of proglacial lakes linked to glacial-hydrogeomorphic processes. *J. Hydrol***. 2016***, 540*, 504-514.
3-10. Pelto, M. in *Recent Climate Change Impacts on Mountain Glaciers*, 211-214 (John Wiley ; Sons Ltd.; 2017).
3-11. Nie, Y. *et al.* A regional-scale assessment of Himalayan glacial lake changes using satellite observations from 1990 to 2015. *Remote Sens. Environ*. **2017***,* 189, 1-13.
3-12. Crawford, J. T.; Dornblaser, M. M.; Stanley, E. H.; Clow, D. W.; Striegl, R. G. Source limitation of carbon gas emissions in high-elevation mountain streams and lakes. *J. Geophys. Res. Biogeosci.* **2015**, 120, 952-964.
3-13. Tranter, M. ; Wadham, J. L. in *Treatise on Geochemistry (Second Edition)* (ed Karl K. Turekian) 157-173 (Elsevier, 2014).
3-14. Tranter, M. *et al.* Geochemical weathering at the bed of Haut Glacier d'Arolla, Switzerland: a new model. *Hydrol. Processes* **2002**, *16*, 959-993.
3-15. Graly, J. A.; Drever, J. I. ; Humphrey, N. F. Calculating the balance between atmospheric CO_2 drawdown and organic carbon oxidation in subglacial hydrochemical systems. *Global Biogeochem. Cycles* **2017**, *31*, 709-727.
3-16. Raiswell, R. Chemical models of solute acquisition in glacial melt waters. *Journal of Glaciology* **1984**, *30*, 49-57.
3-17. Sharp, M. J.; Tranter, M.; Brown, G. H. ; Skidmore, M. Rates of chemical denudation and CO_2 drawdown in a glacier-covered alpine catchment. *Geology* **1995**, *23*, 61-64.

3-18. Anderson, S. P. Biogeochemistry of Glacial Landscape Systems. *Annu. Rev. Earth Planet. Sci.* **2007**, *35*, 375-399.
3-19. Cooper, R. J.; Wadham, J. L.; Tranter, M.; Hodgkins, R. ; Peters, N. E. Groundwater hydrochemistry in the active layer of the proglacial zone, Finsterwalderbreen, Svalbard. *J. Hydrol.* **2002**, *269*, 208-223.
3-20. Wadham, J. L.; Cooper, R. J.; Tranter, M. ; Hodgkins, R. Enhancement of glacial solute fluxes in the proglacial zone of a polythermal glacier. *J. Glaciol.* **2001**, *47*, 378-386.
3-21. Anderson, S. P.; Drever, J. I.; Frost, C. D. ; Holden, P. Chemical weathering in the foreland of a retreating glacier. *Geochim. Cosmochim. Acta* **2000**, *64*, 1173-1189.
3-22. Hodson, A.; Tranter, M. ; Vatne, G. Contemporary rates of chemical denudation and atmospheric CO_2 sequestration in glacier basins: an Arctic perspective. *Earth Surf. Processes Landforms* **2000**, *25*, 1447-1471.
3-23. Christie, R. L. Bedrock geology. 16-18 (Defence Research Board Canada, Ottawa, 1958).
3-24. Emmerton, C. A. *et al.* The importance of freshwater systems to the net atmospheric exchange of carbon dioxide and methane with a rapidly changing high Arctic watershed. *Biogeosciences* **2016**, *13*, 5849-5863.
3-25. Emmerton, C. A. *et al.* Net ecosystem exchange of CO_2 with rapidly changing high Arctic landscapes. *Global Change Biol.* **2016**, *22*, 1185-1200.
3-26. Fairchild, I. J.; Killawee, J. A.; Hubbard, B. ; Wolfgang, D. Interactions of calcareous suspended sediment with glacial meltwater: a field test of dissolution behaviour. *Chem. Geol.* **1999**, *155*, 243-263.
3-27. Skidmore, M.; Sharp, M. ; Tranter, M. Kinetic isotopic fractionation during carbonate dissolution in laboratory experiments: Implications for detection of microbial CO_2 signatures using δ13C-DIC. *Geochim. Cosmochim. Acta* **2004**, *68*, 4309-4317.
3-28. Hamilton, J. D.; Kelly, C. A.; Rudd, J. W. M.; Hesslein, R. H. ; Roulet, N. T. Flux to the atmosphere of CH_4 and CO_2 from wetland ponds on the Hudson Bay lowlands (HBLs). *J. Geophys. Res.* **1994**, *99*, 1495-1510.
3-29. Waller, R. I. The influence of basal processes on the dynamic behaviour of cold-based glaciers. *Quat. Int.* **2001***, 86*, 117-128.
3-30. Hodgkins, R.; Tranter, M. ; Dowdeswell, J. A. Solute provenance, transport and denudation in a High Arctic glacierized catchment. *Hydrol. Processes* **1997**, *11*, 1813-1832.
3-31. Bluth, G. J. S. ; Kump, L. R. Lithologic and climatologic controls of river chemistry. *Geochim. Cosmochim. Acta* **1994**, *58*, 2341-2359.
3-32. Raymond, P. A. ; Cole, J. J. Gas Exchange in Rivers and Estuaries: Choosing a Gas Trasnfer Velocity. *Estuaries* **2001**, *24*, 312-317.
3-33. Wallin, M. B. *et al.* Spatiotemporal variability of the gas transfer coefficient ($k$$CO_2$) in boreal streams: Implications for large scale estimates of CO_2 evasion. *Global Biogeochemi. Cycles* **2011**, *25*, GB3025.
3-34. Battin, T. J. *et al.* Biophysical controls on organic carbon fluxes in fluvial networks. *Nat. Geosci.* **2008**, *1*, 95.
3-35. Espírito-Santo, F. D. B. *et al.* Size and frequency of natural forest disturbances and the Amazon forest carbon balance. *Nat. Commun.* **2014**, *5*, 3434.
3-36. Brienen, R. J. W. *et al.* Long-term decline of the Amazon carbon sink. *Nature* **2015***, 519*, 344.

3-37. Hamilton, P. B.; Gajewski, K.; Atkinson, D. E. ; Lean, D. R. S. Physical and chemical limnology of 204 lakes from the Canadian Arctic Archipelago. *Hydrobiologia* **2001**, *457*, 133-148.
3-38. Lehnherr, I. *et al.* The world's largest High Arctic lake responds rapidly to climate warming. *Nat. Commun.* **2018**, *9*, 1290.
3-39. Wetzel, R. G. *Limnology*. 3rd edn, 316 (Academic Press, 2001).
3-40. Marzeion, B.; Kaser, G.; Maussion, F. ; Champollion, N. Limited influence of climate change mitigation on short-term glacier mass loss. *Nat. Clim. Change* **2018**, *8*, 305-308.
3-41. Bliss, A.; Hock, R. ; Radić, V. Global response of glacier runoff to twenty-first century climate change. *J. Geophysical Res. Earth Surf.* **2014,** *119*, 717-730.
3-42. Huss, M. ; Hock, R. Global-scale hydrological response to future glacier mass loss. *Nat. Clim. Change* **2018**, *8*, 135-140.
3-43. Sharp, M. J. *et al.* Mountain Glaciers and Ice Caps. 7.33-7.42 (Arctic Monitoring and Assessment Program, Oslo, Norway, 2011).
3-44. Carpenter, S. R. ; Cottingham, K. L. Resilience and Restoration of Lakes. *Conservation Ecology* **1997**, *1*, 2.
3-45. Gíslason, S. R. *et al.* Direct evidence of the feedback between climate and weathering. *Earth Planet. Sci. Lett.* **2009**, *277*, 213-222.
3-46. Carrivick, J. L. ; Tweed, F. S. Proglacial lakes: character, behaviour and geological importance. *Quat. Sci. Rev.* **2013**, *78*, 34-52.
3-47. Köck, G. *et al.* Bathymetry and Sediment Geochemistry of Lake Hazen (Quttinirpaaq National Park, Ellesmere Island, Nunavut). *Arctic* **2012**, *65*, 56-66.
3-48. Wang, J.; Han, H. ; Zhang, S. Carbon dioxide flux in the ablation area of Koxkar glacier, western Tien Shan, China. *Ann. Glaciol.* **2014**, *55*, 231-238.
3-49. Gray, L. Using multiple RADARSAT InSAR pairs to estimate a full three-dimensional solution for glacial ice movement. *Geophys. Res. Lett.* **2011**, *38*, L05502.
3-50. Smith, I. R. Late Quaternary glacial history of Lake Hazen Basin and eastern Hazen Plateau, northern Ellesmere Island, Nunavut, Canada. *Canadian Journal of Earth Sciences* **1999**, *36*, 1547-1565.
3-51. Thompson, W. in *Resource description and analysis: Ellesmere Island, National Park Reserve.* 78 (National Resource Conservation Selection, Prairie and Northern Region, Parks Canada, Department of Canadian Heritage, 1994).
3-52. Johnson, M. S. *et al.* Direct and continuous measurement of dissolved carbon dioxide in freshwater aquatic systems-method and applications. *Ecohydrology* **2010**, *3*, 68-78.
3-53. Gardner, A. S. *et al.* Sharply increased mass loss from glaciers and ice caps in the Canadian Arctic Archipelago. *Nature* **2011**, *473*, 357-360.
3-54. Nowak, A. ; Hodson, A. J. Changes in meltwater chemistry over a 20-year period following a thermal regime switch from polythermal to cold-based glaciation at Austre Broggerbreen, Svalbard. *Polar Res.* **2014***, 33*, 22779.
3-55. Runkel, R. L.; Crawford, C. G. ; Cohn, T. A. in *USGS Techniques and Methods Book 4* (U.S. Geological Survey, 2004).
3-56. rloadest: river load estimation (U.S. Geological Survey, Mounds View, Minnesota, USA.; 2015).
3-57. Holland, H. D. *The Chemistry of the Atmosphere and Oceans*. (John Wiley ; Sons, Inc.; 1978).

3-58. Raymond, P. A. *et al.* Scaling the gas transfer velocity and hydraulic geometry in streams and small rivers. *Limnol. Oceanogr. Fluids Environ.* **2012**, *2*, 41-53.
3-59. Liss, P. S. ; Slater, P. G. Flux of gases across air-sea interface. *Nature* **1974**, *247*, 181-184.
3-60. Wanninkhof, R.; Ledwell, J. R. ; Broecker, W. S. Gas exchange-wind speed relation measured with sulfur hexafluoride on a lake. *Science* **1985**, *227*, 1224-1227.
3-61. Jähne, B.; Heinz, G. ; Dietrich, W. Measurement of the diffusion coefficients of sparingly soluble gases in water. *J. Geophys. Res. Oceans* **1987**, *92*, 10767-10776.
3-62. Wanninkhof, R. ; Knox, M. Chemical enhancement of CO_2 exchange in natural waters. *Limnol. Oceanogr.* **1996**, *41*, 689-697.
3-63. Bade, D. L. ; Cole, J. J. Impact of chemically enhanced diffusion on dissolved inorganic carbon stable isotopes in a fertilized lake. *J. Geophys. Res. Oceans* **2006**, *111*, C01014.
3-64. Pedersen, E. P.; Elberling, B. ; Michelsen, A. Seasonal variations in methane fluxes in response to summer warming and leaf litter addition in a subarctic heath ecosystem. *J. Geophys. Res. Biogeosci.* **2017**, *122*, 2137-2153.
3-65 Assayag, N.; Rive, K.; Ader, M.; Jezequel, D. ; Agrinier, P. Improved method for isotopic and quantitative analysis of dissolved inorganic carbon in natural water samples. *Rapid Commun. Mass Spectrom.* **2006***, 20*, 2243-2251.
3-66 Rice, E. W.; Baird, R. B.; Eaton, A. D. ; Clesceri, L. S. (ed American Water Works Association) *Standard Methods for the Examination of Water and Wasterwater* (2012).
3-67 Hawkings, J. R. *et al.* Ice sheets as a missing source of silica to the polar oceans. *Nat. Commun.* **2017**, 8.
3-68 Millero, F. J. Carbonate constants for estuarine waters. *Mar. Freshwater Res.* **2010**, *61*, 139-142.
4-1. Collins, M. R. K.; J; Arblaster, J.-L.; 2013: Long-term Climate Change: Projections, Commitments and Irreversibility. In Climate Change 2013: The Physical Science Basis. Contribution of Working Group I to the Fifth Assessment Report of the Intergovernmental Panel on Climate Change, T.F. Stocker, D. Q.; G.-K. Plattner, M.; Tignor, S.K. Allen, J. Boschung, A. Nauels, Y. Xia, V. Bex, P.M. Midgley, Ed. Cambridge University Press: Cambridge, U.K. and New York 2013.
4-2. Gardner, A. S.; Moholdt, G.; Wouters, B.; Wolken, G. J.; Burgess, D. O.; Sharp, M. J.; Cogley, J. G.; Braun, C.; Labine, C.; Sharply increased mass loss from glaciers and ice caps in the Canadian Arctic Archipelago. *Nature* **2011,** *473*, (7347), 357-360.
4-3. Lenaerts, J. T. M.; van Angelen, J. H.; van den Broeke, M. R.; Gardner, A. S.; Wouters, B.; van Meijgaard, E.; Irreversible mass loss of Canadian Arctic Archipelago glaciers. *Geophys. Res. Lett.* **2013,** *40*, (5), 870-874.
4-4. Lawrence, D. M.; Slater, A. G.; A projection of severe near-surface permafrost degradation during the 21st century. *Geophys. Res. Lett.* **2005,** *32*, (24), GL025080.
4-5. Macdonald, R. W.; Barrie, L. A.; Bidleman, T. F.; Diamond, M. L.; Gregor, D. J.; Semkin, R. G.; Strachan, W. M. J.; Li, Y. F.; Wania, F.; Alaee, M.; Alexeeva, L. B.; Backus, S. M.; Bailey, R.; Bewers, J. M.; Gobeil, C.; Halsall, C. J.; Harner, T.; Hoff, J. T.; Jantunen, L. M. M.; Lockhart, W. L.; Mackay, D.; Muir, D. C. G.; Pudykiewicz, J.; Reimer, K. J.; Smith, J. N.; Stern, G. A.; Schroeder, W. H.; Wagemann, R.; Yunker, M. B.; Contaminants in the Canadian Arctic: 5 years of progress in understanding sources, occurrence and pathways. *Sci. Total Environ.* **2000,** *254*, (2), 93-234.

4-6. Beal, S. A.; Osterberg, E. C.; Zdanowicz, C. M.; Fisher, D. A.; Ice Core Perspective on Mercury Pollution during the Past 600 Years. *Environ. Sci. Technol.* **2015,** *49*, (13), 7641-7647.
4-7. Rydberg, J.; Klaminder, J.; Rosén, P.; Bindler, R.; Climate driven release of carbon and mercury from permafrost mires increases mercury loading to sub-arctic lakes. *Sci. Total Environ.* **2010,** *408*, (20), 4778-4783.
4-8. Zdanowicz, C.; Krummel, E. M.; Lean, D.; Poulain, A. J.; Yumvihoze, E.; Chen, J. B.; Hintelmann, H.; Accumulation, storage and release of atmospheric mercury in a glaciated Arctic catchment, Baffin Island, Canada. *Geochim. Cosmochim. Acta* **2013,** *107*, 316-335.
4-9. Hawkings, J. R.; Wadham, J. L.; Benning, L. G.; Hendry, K. R.; Tranter, M.; Tedstone, A.; Nienow, P.; Raiswell, R.; Ice sheets as a missing source of silica to the polar oceans. *Nature Commun.* **2017,** *8*.
4-10. Schuster, P. F.; Striegl, R. G.; Aiken, G. R.; Krabbenhoft, D. P.; Dewild, J. F.; Butler, K.; Kamark, B.; Dornblaser, M.; Mercury Export from the Yukon River Basin and Potential Response to a Changing Climate. *Environ. Sci. Technol.* **2011,** *45*, (21), 9262-9267.
4-11. Wrona, F. J.; Johansson, M.; Culp, J. M.; Jenkins, A.; Mård, J.; Myers-Smith, I. H.; Prowse, T. D.; Vincent, W. F.; Wookey, P. A.; Transitions in Arctic ecosystems: Ecological implications of a changing hydrological regime. *J. Geophys. Res. Biogeosci.* **2016,** *121*, (3), 650-674.
4-12. Scheuhammer, A. M.; Meyer, M. W.; Sandheinrich, M. B.; Murray, M. W.; Effects of Environmental Methylmercury on the Health of Wild Birds, Mammals, and Fish. *Ambio* **2007,** *36*, (1), 7.
4-13. Laird, B. D.; Goncharov, A. B.; Egeland, G. M.; Chan, H. M.; Dietary Advice on Inuit Traditional Food Use Needs to Balance Benefits and Risks of Mercury, Selenium, and n3 Fatty Acids. *J. Nutr.* **2013,** *143*, (6), 923-930.
4-14. Chételat, J.; Amyot, M.; Arp, P.; Blais, J. M.; Depew, D.; Emmerton, C. A.; Evans, M.; Gamberg, M.; Gantner, N.; Girard, C.; Graydon, J.; Kirk, J.; Lean, D.; Lehnherr, I.; Muir, D.; Nasr, M.; J. Poulain, A.; Power, M.; Roach, P.; Stern, G.; Swanson, H.; van der Velden, S.; Mercury in freshwater ecosystems of the Canadian Arctic: Recent advances on its cycling and fate. *Sci. Total Environ.* **2015,** *509*, 41-66.
4-15. Carmack, E. C.; Yamamoto-Kawai, M.; Haine, T. W. N.; Bacon, S.; Bluhm, B. A.; Lique, C.; Melling, H.; Polyakov, I. V.; Straneo, F.; Timmermans, M. L.; Williams, W. J.; Freshwater and its role in the Arctic Marine System: Sources, disposition, storage, export, and physical and biogeochemical consequences in the Arctic and global oceans. *J. Geophys. Res. Biogeosci.* **2016,** *121*, (3), 675-717.
4-16. Herdendorf, C. E.; Large Lakes of the World. *J. Great Lakes Res.* **1982,** *8*, (3), 379-412.
4-17. Lehnherr, I.; St. Louis, V. L.; Muir, D. C. G.; Sharp, M. J.; Gardner, A. S.; Lamoureux, S.; Smol, J. P.; St. Pierre, K. A.; Michelutti, N.; Schiff, S. L.; Emmerton, C. A.; Tarnocai, C.; Talbot, C.; The world's largest High Arctic lake responds rapidly to climate warming. *Nature Commun.* **2018,** *9*, 1290.
4-18. France, R. L.; The Lake Hazen trough - a late winter oasis in a polar desert. *Biol. Conserv.* **1993,** *63*, 149-151.
4-19. Cornwall, C.; Horiuchi, A.; Lehman, C. *Sunrise/Sunset Calculator*, US Department of Commerce: 2017.

4-20. Edlund, S. A.; Vegetation. In *Resource Description and Analysis - Ellesmere Island National Park Reserve*, Natural Resource Conservation Section Prairie and Northern Region Parks Canada Department of Canadian Heritage: Winnipeg, Canada, 1994; p 55.
4-21. Thompson, W.; Climate. In *Resource description and analysis: Ellesmere Island, National Park Reserve.* , National Resource Conservation Selection, Prairie and Northern Region, Parks Canada, Department of Canadian Heritage: Winnipeg, Manitoba, 1994; p 78.
4-22. Bintanja, R.; Andry, O.; Towards a rain-dominated Arctic. *Nature Clim. Change* **2017,** *7*, (4), 263-267.
4-23. Guiguer, K. R. R. A.; Reist, J. D.; Power, M.; Babaluk, J. A.; Using stable isotopes to confirm the trophic ecology of Arctic charr morphotypes from Lake Hazen, Nunavut, Canada. *J. Fish Biol.* **2002,** *60*, (2), 348-362.
4-24. Köck, G.; Muir, D. C. G.; Yang, F.; Wang, X.; Talbot, C.; Gantner, N.; Moser, D.; Bathymetry and Sediment Geochemistry of Lake Hazen (Quttinirpaaq National Park, Ellesmere Island, Nunavut). *Arctic* **2012,** *65*, (1), 56-66.
4-25. St. Louis, V. L.; Rudd, J. W. M.; Kelly, C. A.; Bodaly, R. A.; Paterson, M. J.; Beaty, K. G.; Hesslein, R. H.; Heyes, A.; Majewski, A. R.; The Rise and Fall of Mercury Methylation in an Experimental Reservoir†. *Environ. Sci. Technol.* **2004,** *38*, (5), 1348-1358.
4-26. Kirk, J. L.; Louis, V. L. S.; Sharp, M. J.; Rapid reduction and reemission of mercury deposited into snowpacks during atmospheric mercury depletion events at Churchill, Manitoba, Canada. *Environ. Sci. Technol.* **2006,** *40*, (24), 7590-7596.
4-27. Lehnherr, I.; St Louis, V. L.; Emmerton, C. A.; Barker, J. D.; Kirk, J. L.; Methylmercury Cycling in High Arctic Wetland Ponds: Sources and Sinks. *Environ. Sci. Technol.* **2012,** *46*, (19), 10514-10522.
4-28. Berg, T.; Bartnicki, J.; Munthe, J.; Lattila, H.; Hrehoruk, J.; Mazur, A.; Atmospheric mercury species in the European Arctic: measurements and modelling. *Atmos. Environ.* **2001,** *35*, 2569-2582.
4-29. Emmerton, C. A.; St Louis, V. L.; Lehnherr, I.; Graydon, J. A.; Kirk, J. L.; Rondeau, K. J.; The importance of freshwater systems to the net atmospheric exchange of carbon dioxide and methane with a rapidly changing high Arctic watershed. *Biogeosciences* **2016,** *13*, (20), 5849-5863.
4-30. Arendt, A.; Bliss, A.; Bolch, T.; Cogley, J. G.; Gardner, A. S.; Hagen, J. O.; Hock, R.; Huss, M.; Kaser, G.; Kienholz, C.; Pfeffer, W. T.; Moholdt, G.; Paul, F.; Radić, V.; Andreassen, L.; Bajracharya, S.; Barrand, N. E.; Beedle, M.; Berthier, E.; Bhambri, R.; Brown, I.; Burgess, E.; Burgess, D. O.; Cawkwell, F.; Chinn, T.; Copland, L.; Davies, B.; De Angelis, H.; Dolgova, E.; Earl, L.; Filbert, K.; Forester, R.; Fountain, A. G.; Frey, H.; Giffen, B.; Glasser, N.; Guo, W. Q.; Gurney, S.; Hagg, W.; Hall, D. K.; Haritashya, U. K.; Hartmann, G.; Helm, C.; Herreid, S.; Howat, I.; Kapustin, G.; Khromova, T.; König, M.; Kohler, J.; Kriegel, D.; Kutuzov, S.; Lavrentiev, I.; LeBris, R.; Liu, S. Y.; Lund, J.; Manley, W.; Marti, R.; Mayer, C.; Miles, E. S.; Li, X.; Menounos, B.; Mercer, A.; Mölg, N.; Mool, P.; Nosenko, G.; Negrete, A.; Nuimura, T.; Nuth, C.; Pettersson, R.; Racoviteanu, A.; Ranzi, R.; Rastner, P.; Rau, F.; Raup, B.; Rich, J.; Rott, H.; Sakai, A.; Schneider, C.; Seliverstov, Y.; Sharp, M.; Sigurðsson, O.; Stokes, C.; Way, R. G.; Wheate, R.; Winsvold, S.; Wolken, G. J.; Wyatt, F.; Zheltyhina, N.; Randolph Glacier Inventory – A Dataset of Global Glacier Outlines: Version 5.0. In 5.0 ed.; Global Land Ice Measurements from Space: Boulder Colorado USA, 2015.

4-31. Appling, A. P.; Leon, M. C.; McDowell, W. H.; Reducing bias and quantifying uncertainty in watershed flux estimates: the R package loadflex. *Ecosphere* **2015,** *6*, (12), 1-25.
4-32. Runkel, R. L.; Crawford, C. G.; Cohn, T. A.; Load estimator (LOADEST): a FORTRAN program for estimating constituent loads in streams and rivers. In *USGS Techniques and Methods Book 4*, U.S. Geological Survey: Reston, Virginia, USA, 2004.
4-33. Lorenz, D.; Runkel, R.; De Cicco, L. *rloadest: river load estimation*, U.S. Geological Survey: Mounds View, Minnesota, USA.; 2015.
4-34. Hintelmann, H.; Ogrinc, N.; Determination of stable mercury isotopes by ICP/MS and their application in environmental studies. *Biogeochemistry of Environmentally Important Trace Elements* **2003,** *835*, 321-338.
4-35. Dommergue, A.; Ferrari, C. P.; Gauchard, P.-A.; Boutron, C. F.; Poissant, L.; Pilote, M.; Jitaru, P.; Adams, F. C.; The fate of mercury species in a sub-arctic snowpack during snowmelt. *Geophys. Res. Lett.* **2003,** *30*, (12), GL017308.
4-36. Barkay, T.; Kroer, N.; Poulain, A. J.; Some like it cold: microbial transformations of mercury in polar regions. *Polar Res.* **2011,** *30*, 15.
4-37. Willis, C. E.; Kirk, J. L.; St. Louis, V. L.; Lehnherr, I.; Ariya, P. A.; Rangel-Alvarado, R. B.; Sources of Methylmercury to Snowpacks of the Alberta Oil Sands Region: A Study of In Situ Methylation and Particulates. *Environ. Sci. Technol.* **2018,** *52*, (2), 531-540.
4-38. Lahoutifard, N.; Sparling, M.; Lean, D.; Total and methyl mercury patterns in Arctic snow during springtime at Resolute, Nunavut, Canada. *Atmos. Environ.* **2005,** *39*, (39), 7597-7606.
4-39. St. Pierre, K. A.; St. Louis, V. L.; Kirk, J. L.; Lehnherr, I.; Wang, S.; La Farge, C.; Importance of Open Marine Waters to the Enrichment of Total Mercury and Monomethylmercury in Lichens in the Canadian High Arctic. *Environ. Sci. Technol.* **2015,** *49*, (10), 5930-5938.
4-40. Kirk, J. L.; St. Louis, V. L.; Hintelmann, H.; Lehnherr, I.; Else, B.; Poissant, L.; Methylated Mercury Species in Marine Waters of the Canadian High and Sub Arctic. *Environ. Sci. Technol.* **2008,** *42*, (22), 8367-8373.
4-41. St. Louis, V. L.; Sharp, M. J.; Steffen, A.; May, A.; Barker, J.; Kirk, J. L.; Kelly, D. J. A.; Arnott, S. E.; Keatley, B.; Smol, J. P.; Some sources and sinks of monomethyl and inorganic mercury on Ellesmere island in the Canadian high arctic. *Environ. Sci. Technol.* **2005,** *39*, (8), 2686-2701.
4-42. Steffen, A.; Douglas, T.; Amyot, M.; Ariya, P.; Aspmo, K.; Berg, T.; Bottenheim, J.; Brooks, S.; Cobbett, F.; Dastoor, A.; Dommergue, A.; Ebinghaus, R.; Ferrari, C.; Gardfeldt, K.; Goodsite, M. E.; Lean, D.; Poulain, A. J.; Scherz, C.; Skov, H.; Sommar, J.; Temme, C.; A synthesis of atmospheric mercury depletion event chemistry in the atmosphere and snow. *Atmos. Chem. Phys.* **2008,** *8*, (6), 1445-1482.
4-43. Poulain, A. J.; Garcia, E.; Amyot, M.; Campbell, P. G. C.; Ariya, P. A.; Mercury distribution, partitioning and speciation in coastal vs. inland High Arctic snow. *Geochim. Cosmochim. Acta* **2007,** *71*, (14), 3419-3431.
4-44. Obrist, D.; Agnan, Y.; Jiskra, M.; Olson, C. L.; Colegrove, D. P.; Hueber, J.; Moore, C. W.; Sonke, J. E.; Helmig, D.; Tundra uptake of atmospheric elemental mercury drives Arctic mercury pollution. *Nature* **2017,** *547*, 201-204.
4-45. Søndergaard, J.; Riget, F.; Tamstorf, M. P.; Larsen, M. M.; Mercury Transport in a Low-Arctic River in Kobbefjord, West Greenland (64A degrees N). *Water Air Soil Pollut.* **2012,** *223*, (7), 4333-4342.

46. Søndergaard, J.; Tamstorf, M.; Elberling, B.; Larsen, M. M.; Mylius, M. R.; Lund, M.; Abermann, J.; Riget, F.; Mercury exports from a High-Arctic river basin in Northeast Greenland (74 degrees N) largely controlled by glacial lake outburst floods. *Sci. Total Environ.* **2015,** *514*, 83-91.
4-47. Vermilyea, A. W.; Nagorski, S. A.; Lamborg, C. H.; Hood, E. W.; Scott, D.; Swarr, G. J.; Continuous proxy measurements reveal large mercury fluxes from glacial and forested watersheds in Alaska. *Sci. Total Environ.* **2017,** *599-600*, 145-155.
4-48. Tranter, M.; Sharp, M. J.; Lamb, H. R.; Brown, G. H.; Hubbard, B. P.; Willis, I. C.; Geochemical weathering at the bed of Haut Glacier d'Arolla, Switzerland: a new model. *Hydrol. Processes* **2002,** *16*, (5), 959-993.
4-49. Parks, J. M.; Johs, A.; Podar, M.; Bridou, R.; Hurt, R. A.; Smith, S. D.; Tomanicek, S. J.; Qian, Y.; Brown, S. D.; Brandt, C. C.; Palumbo, A. V.; Smith, J. C.; Wall, J. D.; Elias, D. A.; Liang, L. Y.; The Genetic Basis for Bacterial Mercury Methylation. *Science* **2013,** *339*, (6125), 1332-1335.
4-50. Wadham, J. L.; Tranter, M.; Hodson, A. J.; Hodgkins, R.; Bottrell, S.; Cooper, R.; Raiswell, R.; Hydro-biogeochemical coupling beneath a large polythermal Arctic glacier: Implications for subice sheet biogeochemistry. *J. Geophys. Res. Earth Surf.* **2010,** *115*.
4-51. Chandler, D. M.; Wadham, J. L.; Lis, G. P.; Cowton, T.; Sole, A.; Bartholomew, I.; Telling, J.; Nienow, P.; Bagshaw, E. B.; Mair, D.; Vinen, S.; Hubbard, A.; Evolution of the subglacial drainage system beneath the Greenland Ice Sheet revealed by tracers. *Nature Geosci.* **2013,** *6*, (3), 195-198.
4-52. Hattersley-Smith, G.; Studies of englacial profiles in the Lake Hazen area of northern Ellesmere Island. *J. Glaciol.* **1960,** *3*, (27), 610-625.
4-53. Hintelmann, H.; 11 Organomercurials. Their Formation and Pathways in the Environment. In *Organometallics in Environment and Toxicology: Metal Ions in Life Sciences*, The Royal Society of Chemistry: 2010; Vol. 7, pp 365-401.
4-54. Smol, J. P.; Douglas, M. S. V.; Crossing the final ecological threshold in high Arctic ponds. *PNAS* **2007,** *104*, (30), 12395-12397.
4-55. Burn, C. R.; Tundra lakes and permafrost, Richards Island, western Arctic coast, Canada. *Can. J. Earth Sci.* **2002,** *39*, (8), 1281-1298.
4-56. Hinkel, K. M.; Sheng, Y.; Lenters, J. D.; Lyons, E. A.; Beck, R. A.; Eisner, W. R.; Wang, J.; Thermokarst Lakes on the Arctic Coastal Plain of Alaska: Geomorphic Controls on Bathymetry. *Permafrost Periglacial Processes* **2012,** *23*, (3), 218-230.
4-57. Sinnatamby, R. N.; Babaluk, J. A.; Power, G.; Reist, J. D.; Power, M.; Summer habitat use and feeding of juvenile Arctic charr, Salvelinus alpinus, in the Canadian High Arctic. *Ecol. Freshwater Fish* **2012,** *21*, 309-322.
4-58. Lehnherr, I.; St Louis, V. L.; Kirk, J. L.; Methylmercury Cycling in High Arctic Wetland Ponds: Controls on Sedimentary Production. *Environ. Sci. Technol.* **2012,** *46*, (19), 10523-10531.
4-59. Mason, R. P.; Reinfelder, J. R.; Morel, F. M. M.; Bioaccumulation of mercury and methylmercury. *Water, Air, and Soil Pollution* **1995,** *80*, (1), 915-921.
4-60. Gilbert, R.; Lamoureux, S.; Processes affecting deposition of sediment in a small, morphologically complex lake. *J. Paleolimnol.* **2004,** *31*, (1), 37-48.
4-61. Lammers, R. B.; Shiklomanov, A. I.; Vörösmarty, C. J.; Fekete, B. M.; Peterson, B. J.; Assessment of contemporary Arctic river runoff based on observational discharge records. *J. Geophys. Res. Atmos.* **2001,** *106*, (D4), 3321-3334.

4-62. Holmes, R. M.; McClelland, J. W.; Peterson, B. J.; Shiklomanov, I. A.; Shiklomanov, A. I.; Zhulidov, A. V.; Gordeev, V. V.; Bobrovitskaya, N. N.; A circumpolar perspective on fluvial sediment flux to the Arctic ocean. *Global Biogeochem. Cycles* **2002,** *16*, (4), 45-1-45-14.
4-63. Poissant, L.; Amyot, M.; Pilote, M.; Lean, D.; Mercury Water−Air Exchange over the Upper St. Lawrence River and Lake Ontario. *Environ. Sci. Technol.* **2000,** *34*, (15), 3069-3078.
4-64. Paltan, H.; Dash, J.; Edwards, M.; A refined mapping of Arctic lakes using Landsat imagery. *International Journal of Remote Sensing* **2015,** *36*, (23), 5970-5982.
4-65. Zajaczkowski, M.; Sediment supply and fluxes in glacial and outwash fjords, Kongsfjorden and Adventfjorden, Svalbard. *Pol. Polar Res.* **2008,** *29*, (1), 59-72.
4-66. Pfeffer, W. T.; Arendt, A. A.; Bliss, A.; Bolch, T.; Cogley, J. G.; Gardner, A. S.; Hagen, J.-O.; Hock, R.; Kaser, G.; Kienholz, C.; Miles, E. S.; Moholdt, G.; Mölg, N.; Paul, F.; Radi; Valentina; Rastner, P.; Raup, B. H.; Rich, J.; Sharp, M. J.; The Randolph Glacier Inventory: a globally complete inventory of glaciers. *J. Glaciol.* **2014,** *60*, (221), 537-552.
4-67. Lehnherr, I.; St. Louis, V. L.; Hintelmann, H.; Kirk, J. L.; Methylation of inorganic mercury in polar marine waters. *Nature Geosci.* **2011,** *4*, (5), 298-302.
4-68. St. Pierre, K. A.; Chételat, J.; Yumvihoze, E.; Poulain, A. J.; Temperature and the Sulfur Cycle Control Monomethylmercury Cycling in High Arctic Coastal Marine Sediments from Allen Bay, Nunavut, Canada. *Environ. Sci. Technol.* **2014,** *48*, (5), 2680-2687.
4-69. Smith, K. L.; Robison, B. H.; Helly, J. J.; Kaufmann, R. S.; Ruhl, H. A.; Shaw, T. J.; Twining, B. S.; Vernet, M.; Free-Drifting Icebergs: Hot Spots of Chemical and Biological Enrichment in the Weddell Sea. *Science* **2007,** *317*, (5837), 478-482.
4-70. Zhang, Y.; Jacob, D. J.; Horowitz, H. M.; Chen, L.; Amos, H. M.; Krabbenhoft, D. P.; Slemr, F.; St. Louis, V. L.; Sunderland, E. M.; Observed decrease in atmospheric mercury explained by global decline in anthropogenic emissions. *PNAS* **2016,** *113*, (3), 526-531.
4-71. Cole, A. S.; Steffen, A.; Eckley, C. S.; Narayan, J.; Pilote, M.; Tordon, R.; Graydon, J. A.; St. Louis, V. L.; Xu, X.; Branfireun, B.; A Survey of Mercury in Air and Precipitation across Canada: Patterns and Trends. *Atmosphere* **2014,** *5*, 635-668.
5-1. Wetzel, R. G.; *Limnology*. 3rd ed.; Academic Press: San Diego, California, 2001.
5-2. Marzeion, B.; Kaser, G.; Maussion, F.; Champollion, N.; Limited influence of climate change mitigation on short-term glacier mass loss. *Nature Climate Change* **2018,** *8*, 305-308.
5-3. Huss, M.; Hock, R.; Global-scale hydrological response to future glacier mass loss. *Nature Climate Change* **2018**.
5-4. Bliss, A.; Hock, R.; Radić, V.; Global response of glacier runoff to twenty-first century climate change. *Journal of Geophysical Research: Earth Surface* **2014,** *119*, (4), 717-730.
5-5. Radić, V.; Bliss, A.; Beedlow, A. C.; Hock, R.; Miles, E.; Cogley, J. G.; Regional and global projections of twenty-first century glacier mass changes in response to climate scenarios from global climate models. *Climate Dynamics* **2013,** *42*, (1), 37-58.
5-6. Fisher, J. A.; Jacob, D. J.; Soerensen, A. L.; Amos, H. M.; Steffen, A.; Sunderland, E. M.; Riverine source of Arctic Ocean mercury inferred from atmospheric observations. *Nature Geoscience* **2012,** *5*, (7), 499-504.
5-7. Amos, H. M.; Jacob, D. J.; Kocman, D.; Horowitz, H. M.; Zhang, Y.; Dutkiewicz, S.; Horvat, M.; Corbitt, E. S.; Krabbenhoft, D. P.; Sunderland, E. M.; Global Biogeochemical

Implications of Mercury Discharges from Rivers and Sediment Burial. *Environmental Science ; Technology* **2014,** *48*, (16), 9514-9522.

5-8. Lammers, R. B.; Shiklomanov, A. I.; Vörösmarty, C. J.; Fekete, B. M.; Peterson, B. J.; Assessment of contemporary Arctic river runoff based on observational discharge records. *J. Geophys. Res. Atmos.* **2001,** *106*, (D4), 3321-3334.

5-9. Holmes, R. M.; McClelland, J. W.; Peterson, B. J.; Shiklomanov, I. A.; Shiklomanov, A. I.; Zhulidov, A. V.; Gordeev, V. V.; Bobrovitskaya, N. N.; A circumpolar perspective on fluvial sediment flux to the Arctic ocean. *Global Biogeochem. Cycles* **2002,** *16*, (4), 45-1-45-14.

5-10. Lehnherr, I.; St. Louis, V. L.; Muir, D. C. G.; Sharp, M. J.; Gardner, A. S.; Lamoureux, S.; Smol, J. P.; St. Pierre, K. A.; Michelutti, N.; Schiff, S. L.; Emmerton, C. A.; Tarnocai, C.; Talbot, C.; The world's largest High Arctic lake responds rapidly to climate warming. *Nature Commun.* **2018,** *9*, 1290.

5-11. Prowse, T.; Bring, A.; Mård, J.; Carmack, E. C.; Holland, M.; Instanes, A.; Vihma, T.; Wrona, F. J.; Arctic Freshwater Synthesis: Summary of key emerging issues. *J. Geophys. Res. Biogeosci.* **2015,** *120*, 1887-1893.

5-12. Carmack, E. C.; Yamamoto-Kawai, M.; Haine, T. W. N.; Bacon, S.; Bluhm, B. A.; Lique, C.; Melling, H.; Polyakov, I. V.; Straneo, F.; Timmermans, M. L.; Williams, W. J.; Freshwater and its role in the Arctic Marine System: Sources, disposition, storage, export, and physical and biogeochemical consequences in the Arctic and global oceans. *J. Geophys. Res. Biogeosci.* **2016,** *121*, (3), 675-717.

Appendix 1. Supporting information for "Chapter 2. The land-to-ocean aquatic continuum in a glacierized High Arctic watershed: biogeochemical impacts of accelerated glacial melt"

Supporting Figures and Tables

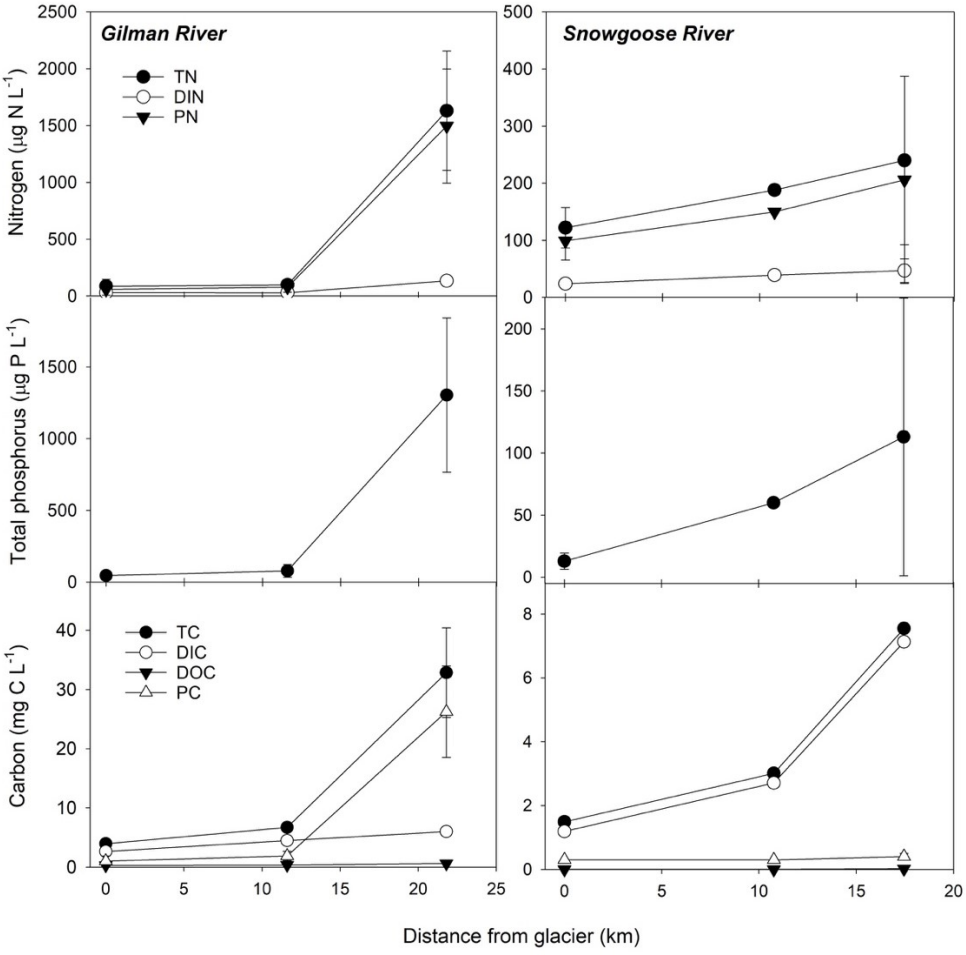

Figure A1-1. Nitrogen, phosphorus and carbon transects along the Gilman (left panels) and Snowgoose (right panels) rivers in summer 2016 (means of 2 transects ± SE). TN, total nitrogen; DIN, dissolved inorganic nitrogen (sum of NH_4^+, NO_2^--NO_3^-); PN, particulate nitrogen; TC, total carbon; DIC, dissolved inorganic carbon; PC, particulate carbon; DOC, dissolved organic carbon. Transects conducted on 11-July and 1-August.

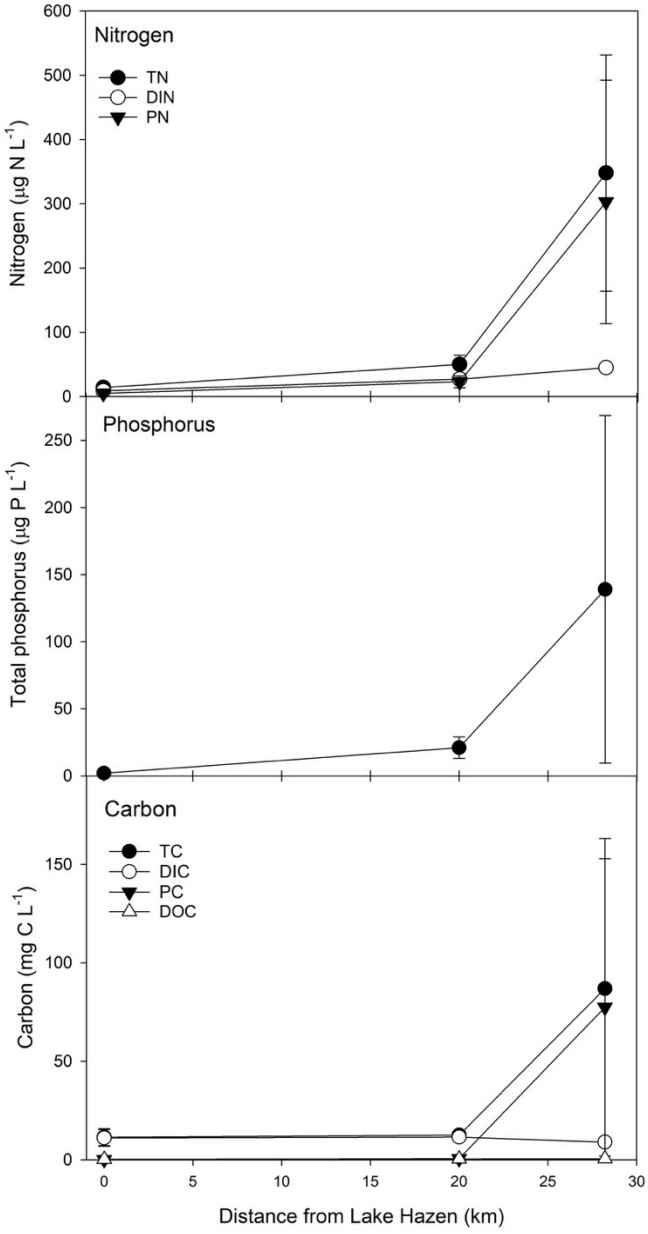

Figure A1-2. Transects of nitrogen, phosphorus and carbon concentrations along the Ruggles River from Lake Hazen to Chandler Fjord in summer 2016 (means of 2 transects ± SE). TN, total nitrogen; DIN, dissolved inorganic nitrogen (sum of NH_4^+, NO_2^--NO_3^-); PN, particulate nitrogen; TC, total carbon; DIC, dissolved inorganic carbon; PC, particulate carbon; DOC, dissolved organic carbon. Transects sampled on 11-July and 2-August.

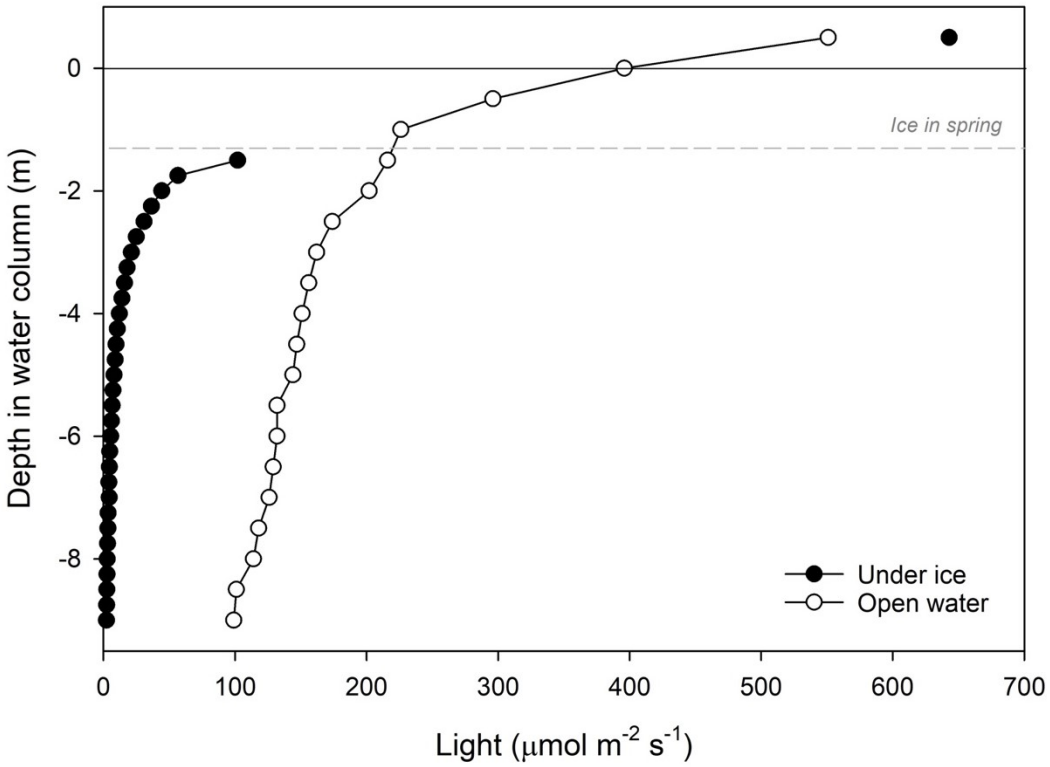

Figure A1-3. Seasonal light profiles of the upper water column of Lake Hazen, measured using a Li-COR 1400 light meter.

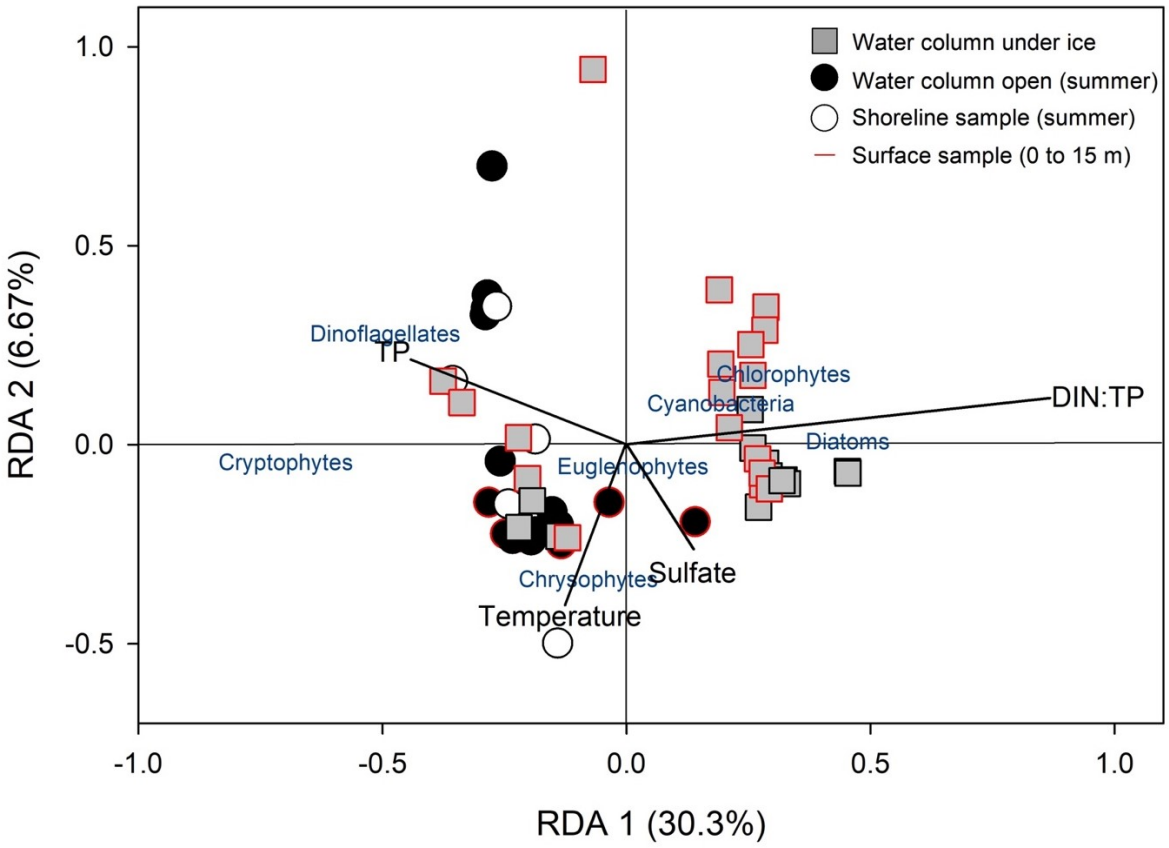

Figure A1-4. Redundancy analysis of phytoplankton community composition by biomass.

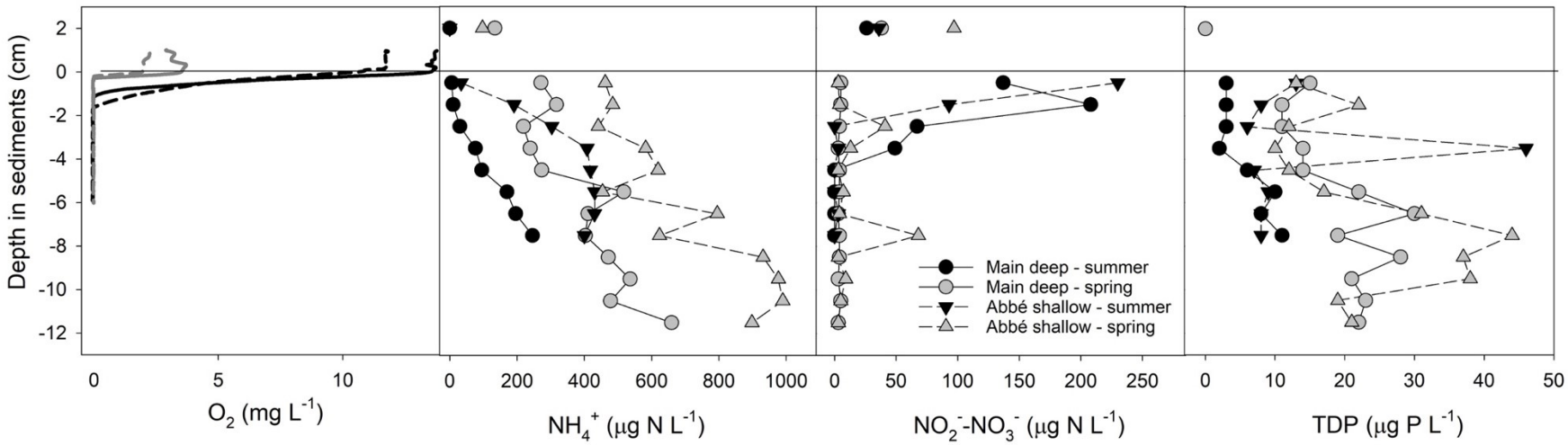

Figure A1-5. Biogeochemical sediment core profiles from the glacially influenced main deep site (S1 in Figure 2-1) and Abbé shallow (S2, ~44 m) in August and the following May. Concentrations in the overlying water were quantified on water samples collected from the top of the core tube before sectioning.

Table A1-1. Sampling and analytical information for the Lake Hazen water column and glacial inflows.

				Snow	Snowmelt	Rivers		Lake Hazen water column			
				Spring	Spring	Summer			Spring		Summer	
Parameter	**Unit**	**Instrument**	**MDL**	**2013,15,17**	**2017**	**2015**	**2016**	**2013**	**2014**	**2017**	**2015**	**2016**
Temperature	°C	YSI EXO2 sonde	n/a		x	x	x	x	x	x	x	x
pH		YSI EXO2 sonde	n/a	x	x	x	x	x	x	x	x	x
Dissolved oxygen	mg L^{-1}	YSI EXO2 sonde	n/a		x	x	x	x	x	x	x	x
Dissolved carbon dioxide	µmol L^{-1}	Varian Chrompack CP-3800	n/a					x	x	x	x	x
Chlorophyll *a* (chl *a*)	mg L^{-1}	Varian Cary 50 Probe UV-Visible Spectrophotometer						x	x	x	x	x
Total suspended solids (TSS)	mg L^{-1}		0.05		x		x			x		x
Total dissolved species (TDS)	mg L^{-1}		0.04	x	x	x	x	x	x	x	x	x
Total nitrogen (TN)	µg L^{-1}	Lachat QuickChem QC8500	7	x	x	x	x	x	x	x	x	x
Particulate nitrogen (PN)	µg L^{-1}		n/a	x	x	x	x	x	x	x	x	x
Ammonium (NH_4^+)	µg L^{-1}	Lachat QuickChem QC8500	3	x	x	x	x	x	x	x	x	x
Nitrite + nitrate (NO_2^- + NO_3^-)	µg L^{-1}	Lachat QuickChem QC8500	2	x	x	x	x	x	x	x	x	x
Total phosphorus (TP)	µg L^{-1}	Lachat QuickChem QC8500	1.4	x	x	x	x	x	x	x	x	x
Total dissolved phosphorus (TDP)	µg L^{-1}	Lachat QuickChem QC8500	1.8	x	x	x	x	x	x	x	x	x
Total carbon (TC)												
Particulate carbon (PC)	mg L^{-1}		n/a	x	x	x	x	x	x	x	x	x
Dissolved organic carbon (DOC)	mg L^{-1}	Shimadzu TOC5000A Total Organic Carbon Analyzer	0.1	x	x	x	x	x	x	x	x	x
Dissolved inorganic carbon (DIC)[1]	mg L^{-1}		n/a	x			x	x	x		x	x
Sulfate (SO_4^{2-})	mg L^{-1}	Dionex DX-600 Ion Chromatograph	0.04	x	x	x	x	x	x	x	x	x
Dissolved silica ($dSiO_2$)	mg L^{-1}	Lachat QuickChem QC8500	0.02		x		x			x		x
Phytoplankton									x	x	x	x
Zooplankton									x		x	

[1] DIC in water samples were analyzed using the Varian Chrompack CP-3800; while DIC in snow samples were analyzed using a Shimadzu TOC-5000A Total Organic Carbon Analyzer.

Table A1-2. LOADEST log-linear models for glacial inflow chemical fluxes, where [C] is in mg L^{-1} and Q is discharge in m^3 s^{-1}. All constituents are dissolved (< 0.45 μm).

Analyte	Model	R^2	p	Bias (%)
NH_4^+	$\ln[NH_4^+] = 0.004\ln Q^2 + 1.17\ln Q - 2.28$	0.937	<0.0001	-13.9
NO_3^--NO_2^-	$\ln[NO_3^-\text{-}NO_2^-] = 0.915\ln Q + 0.239$	0.979	<0.0001	-3.14
$SO_4^{2-}{}_{(aq)}$	$\ln[SO_4^{2-}] = 0.018\ln Q^2 + 0.903\ln Q + 5.92$	0.978	< 0.0001	-15.9
$dSiO_{2(aq)}$	$\ln[SiO_2] = 0.007\ln Q^2 + 0.905\ln Q + 1.06$	0.977	<0.0001	-0.78
DIC	$\ln[DIC] = 0.991\ln Q + 5.07$	0.996	<0.0001	15.5
DOC	$\ln[DOC] = 1.001\ln Q + 2.29$	0.973	<0.001	-1.83

Table A1-3. Sediment core sampling site information.

Site (ID)	Coordinates	Depth (m)	Large glacial influence (Y/N)	Years sampled	
				Summer 2016	Spring 2017
Main deep (S1)	81.825°N, 70.715°W	255-267	Y	x	x
Abbé shallow (S2)	81.842°N, 70.852°W	26-44	Y	x	x
Blister deep (S3)	81.792°N, 71.469°W	251	N	-	x
Blister shallow (S4)	81.805°N, 71.527°W	53	N	-	x
Ruggles River (S5)	81.803°N, 70.504°W	60	N	-	x

Table A1-4. Summary of parameters measured on sediment cores collected from Lake Hazen.

Parameter	Instrument	Resolution (mm)	M.D.L.	Unit	Summer 2016	Spring 2017
Porosity	n/a	10	n/a		x	x
Dissolved oxygen (DO)	Unisense FMM	0.1		mg L^{-1}	x	x
pH	Unisense FMM	0.1			x	x
Redox potential (RD)	Unisense FMM	0.1		mV	x	x
Hydrogen sulfide (H_2S)	Unisense FMM	0.1		µmol L^{-1}	x	
Ammonium (NH_4^+)	Lachat QuickChem QC8500	10	3	µg L^{-1}	x	x
Nitrate + nitrite (NO_3^--NO_2^-)	Lachat QuickChem QC8500	10	2	µg L^{-1}	x	x
Total dissolved phosphorus (TDP)	Lachat QuickChem QC8500	10	1.8	µg L^{-1}	x	x
Sulfate (SO_4^{2-})	Dionex DX-600 Ion Chromatograph	10	0.04	mg L^{-1}	x	x

Table A1-5. Spring physical and chemical limnology of hydrological compartments of the Lake Hazen watershed (mean of *n* ± SE).

	Watershed hydrological compartment				
			L.H. centre surface		
	Snow	**Snowmelt**	**Before snowmelt**	**After snowmelt**	**L.H. bottom**
n samplings [a]	*33*	*3*	*3*	*1*	*4*
Physical					
Temperature (°C)	-	1.09±0.500	0.189±0.050	0.933	3.709±0.085
pH	7.47±0.126	7.13±0.236	7.84±0.050	7.84	7.43±0.117
Gaseous					
O_2 (mg L^{-1})	-	14.3±0.185	15.4±0.152	8.80	10.0±0.580
CO_2 (µmol L^{-1}) [a]	-	-	33.4±1.63	9.59	112±14.7
Bulk/particulate					
TSS (mg L^{-1}) [a]	106±14.9	67.1±23.8	-	-	162±95.2
TN (mg-N L^{-1})	0.128±0.012	0.319±0.155	0.079±0.008	0.066	0.090±0.003
TP (mg-P L^{-1})	0.045±0.004	0.042±0.018	1.47±0.767	0.700	0.002±0.001
TFe (mg L^{-1})	0.222±0.081	4.12±0.011	<D.L.	<D.L.	<D.L.
PN (mg-N L^{-1})	0.059±0.014	0.198±0.013	0.004±0.001	0.016	0.004±0.001
PC (mg-C L^{-1})	2.10±0.194	1.97±0.495	0.060±0.011	0.170	0.048±0.013
Dissolved (<0.45 µm)					
NO_3^- (µg-N L^{-1})	41.6±2.63	84.3±23.8	45.6±0.865	27.7±0.333	72.0±1.68
NH_4^+ (µg-N L^{-1})	8.80±0.746	25.0±5.03	6.38±1.33	4.67±0.33	4.13±1.21
DIN (µg-N L^{-1})	50.4±3.12	109±18.8	51.3±2.67	32.3	75.2±3.17
DIN:TP (mass)	1.39±0.155	3.48±1.01	56.6±20.5	46.2	68.1±23.1
TDP (µg-P L^{-1}) *	2.52±0.308	-	<D.L.	<D.L.	<D.L.
DOC (mg-C L^{-1})	0.254±0.068	1.30±0.240	0.433±0.088	0.400	0.175±0.150
DIC (mg-C L^{-1}) [a]	1.94±0.115	-	10.2±0.723	6.79	11.0±2.04
SO_4^{2-} (mg L^{-1})	1.12±0.100	14.9±2.25	12.0±0.254	5.58	11.3±0.297
$dSiO_2$ (mg L^{-1})	0.085±0.006	0.24±0.020	-	-	-

[a] Snow means of 2013, 2015; before snowmelt mean of 2013, 2014, 2017; after snowmelt – 2014; bottom water mean of 2013, 2 x 2014, 2017.
* Calculated from concentration factor (see methods).

Table A1-6. Summer physical and chemical limnology of hydrological compartments of the Lake Hazen watershed (mean of *n* ± SE) averaged between summers 2015 and 2016.

	Watershed compartment						
	Glacial headwaters	**Glacial deltas**	**L.H. shoreline**	**L.H. centre surface**	**L.H. bottom**	**Ruggles outflow**	**Ruggles at fjord**
n samplings	*6*	*44*	*12*	*2*	*2*	*3*	*2*
Physical							
Temperature (°C)	1.04±0.130	8.01±0.42	5.00±0.537	3.23±0.371	3.46±0.04	3.75±0.286	4.00±0.127
pH	7.33±0.162	7.86±0.08	7.59±0.157	7.81±0.16	7.83±0.08	7.87±0.13	8.06±0.483
Gaseous							
O_2 (mg L^{-1})	14.5±0.399	12.0±0.147	12.4±0.043*	13.6±0.055	13.2±0.160	13.7±0.221	13.9±0.442
CO_2 (µmol L^{-1})	-	-	22.2±0.091*	22.5±2.06	22.1±2.73	-	-
Bulk/particulate							
TSS (mg L^{-1})	158±94.9	562±163	18.1±14.5	1.90	14.7	1.89±0.500	365±227
TN (mg-N L^{-1})	0.108±0.024	0.736±0.172	0.028±0.007	0.060±0.021	0.079±0.001	0.054±0.021	0.044±0.0245
TP (mg-P L^{-1})	0.046±0.020	0.661±0.187	0.003±0.001	0.002±0.001	0.007±0.004	0.002±0.001	0.139±0.130
TFe (mg L^{-1})	4.53±1.44	13.6±2.73	0.328±0.193	0.012±0.009	0.259±0.237	0.172±0.143	8.01±3.36
PN (mg-N L^{-1})	0.075±0.021	0.653±0.147	0.045±0.033	0.008	0.023	0.005±0.001	0.303±0.190
PC (mg-C L^{-1})	1.22±0.327	10.7±3.09	0.696±0.587	0.070±0.021	0.434±0.163	0.122±0.033	77.4±75.5
Dissolved (<0.45 µm)							
NO_3^- (µg-N L^{-1})	19.9±3.70	57.9±5.20	15.9±3.98	27.8±2.60	39.6±3.33	12.7±8.01	31.3±11.8
NH_4^+ (µg-N L^{-1})	5.97±0.958	17.7±6.39	2.99±0.685	1.92±0.274	5.70±1.28	4.83±1.69	13.3±5.8
DIN (µg-N L^{-1})	25.9±3.98	75.6±8.58	18.8±3.94	28.9±3.42	44.5±5.50	17.5±9.46	44.5±6.00
DIN:TP (mass)	1.29±0.601	8.55±4.84	6.43±1.11	22.9±12.1	8.55±4.20	13.2±6.38	2.88±2.73
TDP (µg-P L^{-1})	<D.L.	<D.L.	<D.L. to 3.0	9.5±2.5	11.5±5.5	<D.L.	<D.L.
DOC (mg-C L^{-1})	0.30±0	0.374±0.034	0.225±0.045	0.30±0.14	0.175±0.125	0.30±0.00	0.50±0.00
DIC (mg-C L^{-1})	1.73±0.373	7.00±0.261	5.51±1.41	9.34±2.31	9.77±5.23	10.3±2.61	8.99±0.749
SO_4^{2-} (mg L^{-1})	3.94±0.922	17.6±2.00	6.48±1.57	10.5±0.09	10.3±0.460	7.11±2.85	9.38±2.12
$dSiO_2$ (mg L^{-1})	0.080±0.003	0.290±0.029	0.248±0.074	0.400	0.430	0.260±0.080	0.305±0.085

Table A1-7. Physical and chemical limnology of the glacial river deltas in the Lake Hazen watershed (mean of *n* ± 1 SD) during summers 2015 and 2016.

	Blister	Snowgoose	Abbé	Gilman	H. Nesmith	Turnabout	Very
n samplings	*11*	*11*	*3*	*2*	*3*	*3*	*3*
Physical							
Length (km)	11.2	15.6	20.9	21.2	4.30	55.3	42.5
Watershed area (km^2)	-	222	390	992	1274	678	1035
Glacier area (km^2)	6	87	204	778	1041	259	269
Runoff ($km^3\ yr^{-1}$)		0.016 ± 0.014	0.038 ± 0.033	0.118 ± 0.105	0.183 ± 0.153	0.053 ± 0.041	0.122 ± 0.060
Temperature (°C)	8.90 ± 1.90	7.29 ± 1.53	5.96 ± 1.85	3.43 ± 0.281	6.27 ± 5.06	12.0 ± 0.943	10.3 ± 2.91
pH	7.80 ± 0.446	7.67 ± 0.634	7.94 ± 0.521	8.61 ± 0.157	8.16 ± 0.303	7.85 ± 0.181	8.18 ± 0.063
Gaseous							
O_2 (mg L^{-1})	11.5 ± 0.61	12.0 ± 0.52	13.0 ± 0.19	14.0 ± 0.56	12.8 ± 1.76	11.2 ± 0.44	11.6 ± 1.08
Bulk/particulate							
TSS (mg L^{-1}) [b]	630±292	621±390	225±21.5	1064±154	64.8±10.2	547±367	275±36.9
TN (mg N L^{-1})	0.401 ± 0.677	0.755 ± 1.03	1.55 ± 2.05	1.65 ± 0.716	0.201 ± 0.176	1.94 ± 1.68	0.554 ± 0.200
TP (mg P L^{-1})	0.777 ± 1.64	0.408 ± 0.353	0.927 ± 1.34	1.30 ± 0.760	0.133 ± 0.171	0.408 ± 0.353	0.185 ± 0.169
TFe (mg L^{-1})	8.64 ± 3.27	13.4 ± 4.35	25.8 ± 16.4	47.8 ± 22.1	5.72 ± 2.01	12.8 ± 3.40	5.74 ± 1.25
PN (mg N L^{-1})	0.454 ± 0.677	0.526 ± 0.756	1.48 ± 2.03	1.49 ± 0.710	0.148 ± 0.157	1.73 ± 1.67	0.467 ± 0.186
PC (mg C L^{-1})	4.40 ± 6.73	15.9 ± 26.5	5.66 ± 5.26	26.3 ± 10.9	5.85 ± 6.92	10.8 ± 7.37	10.0 ± 8.39
Dissolved (<0.45 µm)							
NO_3^--NO_2^- (µg N L^{-1})	84.1 ± 31.7	46.6 ± 19.5	22.9 ± 5.89	44.0 ± 14.9	24.5 ± 2.83	71.1 ± 26.8	56.6 ± 19.8
NH_4^+ (µg N L^{-1})	< 3.00	5.61 ± 3.76	6.50 ± 6.61	89.5 ± 17.7	7.25 ± 0.35	84.5 ± 95.6	23.5 ± 22.8
DIN (µg N L^{-1})	85.9 ± 31.5	52.2 ± 17.2	29.4 ± 4.76	133 ± 32.5	31.8 ± 3.19	156 ± 122	80.1 ± 11.3
TDP (µg N L^{-1}) [a]	<D.L. to 6.00	< D.L. to 5.00	<D.L. to 8.00	<D.L.	<D.L.	<D.L. to 11.0	<D.L. to 3.00
DIN:TP (mass)	23.4 ± 46.9	2.28 ± 4.88	0.16 ± 0.16	0.11 ± 0.04	5.16 ± 6.61	1.36 ± 2.01	1.45 ± 1.87
DOC (mg C L^{-1})	0.4 ± 0.1	0.4 ± 0.1	0.4 ± 0.1	0.6 ± 0.1	0.3 ± 0.0	1.1 ± 0.4	0.5 ± 0.1
DIC (mg C L^{-1}) [b]	6.79 ± 0.745	7.31 ± 1.26	5.31±0.577	6.002±0.383	4.96±0.119	8.34±0.129	9.72±0.526
SO_4^{2-} (mg L^{-1})	23.7 ± 8.89	21.2 ± 16.2	11.8 ± 3.62	10.5 ± 0.714	11.2 ± 11.4	12.8 ± 3.89	14.0 ± 5.64
$dSiO_2$ (mg L^{-1}) [b]	0.43 ± 0.15	0.22 ± 0.09	0.14 ± 0.00	0.16 ± 0.02	0.11 ± 0.01	0.44 ± 0.01	0.30 ± 0.01

* TSS, total suspended solids; TN, total nitrogen; TP, total phosphorus; TFe, total iron; PN, particulate nitrogen; PC, particulate carbon. O_2, dissolved oxygen; CO_2, carbon dioxide; CH_4, methane; NO_3^-, nitrate; NH_4^+, ammonium; DIN, dissolved inorganic nitrogen; TDP, total dissolved phosphorus; DOC, dissolved organic carbon; DIC, dissolved inorganic carbon; SO_4^{2-}, sulfate; Cl^-, chloride; Na^+, sodium; K^+, potassium; Ca^{2+}, calcium; Mg^{2+}, magnesium; $dSiO_2$, dissolved silica.

[a] TDP presented as range due to fact that most measurements were below detection (<D.L.), where D.L. = 1.8 µg P L^{-1}.

[b] CO_2, DIC, $dSiO_2$ and TSS concentrations are means from 2016 only.

Table A1-8. Seasonal phytoplankton genus and species diversity in Lake Hazen by taxonomic group.

	Total no.		Total under ice		Total open water		Unique under ice		Unique open water		Shared	
Group	**Genus**	**Species**	**Genus**	**Species**	**Genus**	**Species**	**Genus**	**Species**	**Genus**	**Species**	**Genus**	**Species**
Chlorophyte	10	11	8	9	8	8	2	3	2	2	6	6
Chrysophyte	16	21	12	17	10	11	6	7	4	4	6	10
Cryptophyte	3	7	3	4	3	5	0	2	0	2	3	3
Cyanobacteria	6	6	4	3	2	2	4	4	2	2	0	0
Diatom	17	23	17	20	6	8	11	13	0	2	6	8
Dinoflagellates	3	8	2	5	3	4	0	3	1	3	2	2
Euglenophyte	2	2	2	2	2	1	1	1	0	0	1	1
Total	57	78	48	60	34	39	24	33	9	15	24	30

Table A1-9. Overlying dissolved O_2 concentrations (1 cm overlying core ± SE), and maximum and depth-integrated oxygen consumption rates (in nmol cm^{-2} s^{-1}) for sediment cores collected throughout the Lake Hazen basin. See Table S3 for site information.

Site (ID)	SPRING			SUMMER		
	Overlying O_2 µmol L^{-1}	**Integrated** nmol cm^{-2} s^{-1}	**Maximum** nmol cm^{-2} s^{-1}	**Overlying O_2** µmol L^{-1}	**Integrated** nmol cm^{-2} s^{-1}	**Maximum** nmol cm^{-2} s^{-1}
Main deep (S1)	104 ± 1.69	1.61×10^{-4}	6.18×10^{-3}	426 ± 0.59	1.10×10^{-3}	3.81×10^{-3}
Abbé shallow (S2)	64.2 ± 0.76	3.63×10^{-4}	2.69×10^{-3}	362 ± 2.06	2.56×10^{-3}	2.67×10^{-3}
Blister deep (S3)	270 ± 0.17	1.08×10^{-3}	2.27×10^{-3}		-	-
Blister shallow (S4)	414 ± 0.41	5.19×10^{-4}	5.19×10^{-4}		-	-
Ruggles River (S5)	398 ± 0.55	6.85×10^{-4}	1.16×10^{-3}		-	-

Appendix 2. Supporting information for "Chapter 3. Chemical weathering in glacial meltwaters are creating strong downstream freshwater CO_2 sink"

Supporting Figures and Tables

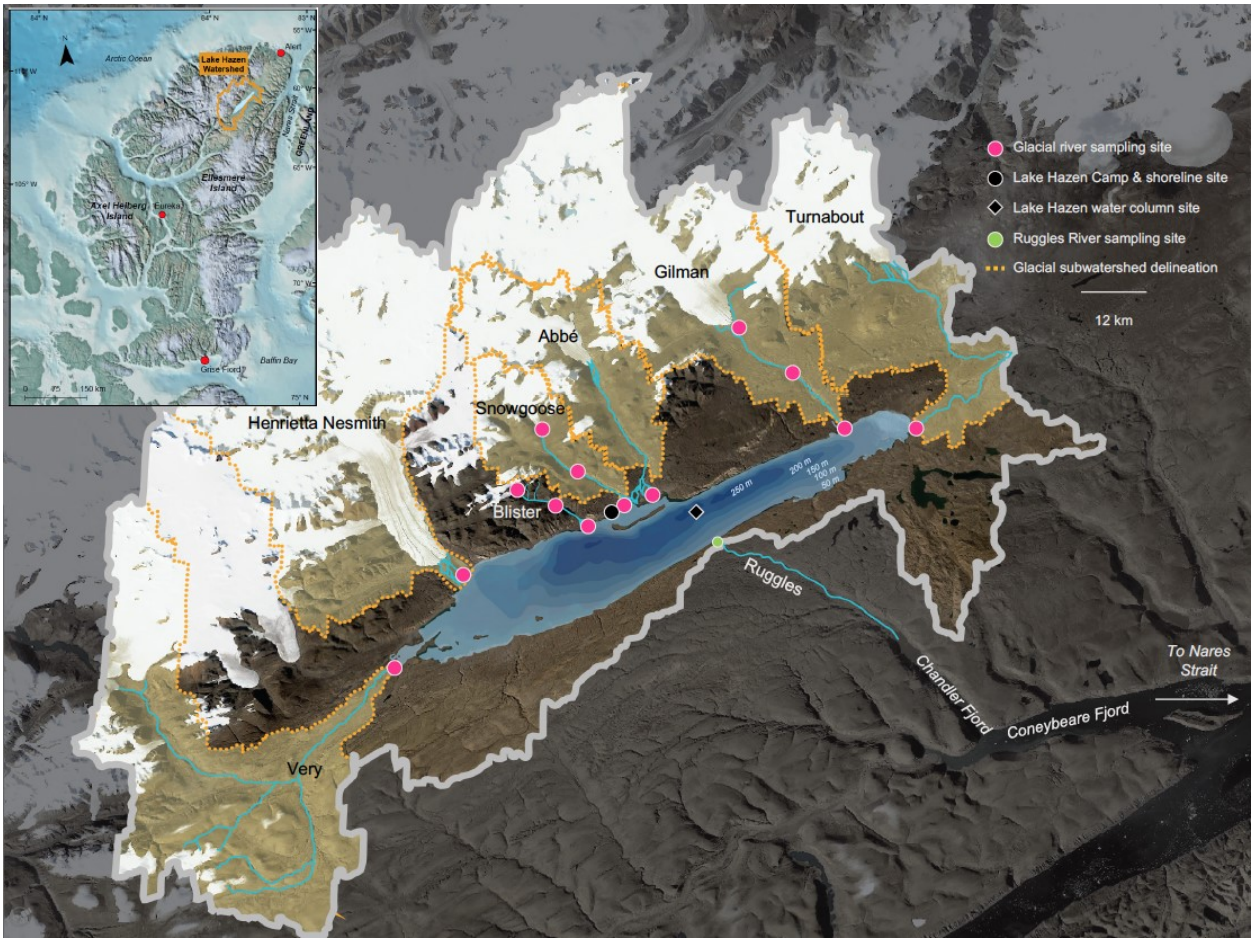

Figure A2-1. Map of Lake Hazen watershed on northern Ellesmere Island, Quttinirpaaq National Park, Nunavut, Canada. Glacial sub-watersheds delineated in yellow, within watershed (grey) boundary. Sampling locations identified in red (glacial rivers) and purple (Lake Hazen), with lake bathymetry from Köck et al. 2012.[1] Watershed characteristics for the sampled glacial rivers and watershed area presented in the inset table, including sub-catchment and glacierized sub-catchment areas, and river length. Background image from Copernicus Sentinel 2.

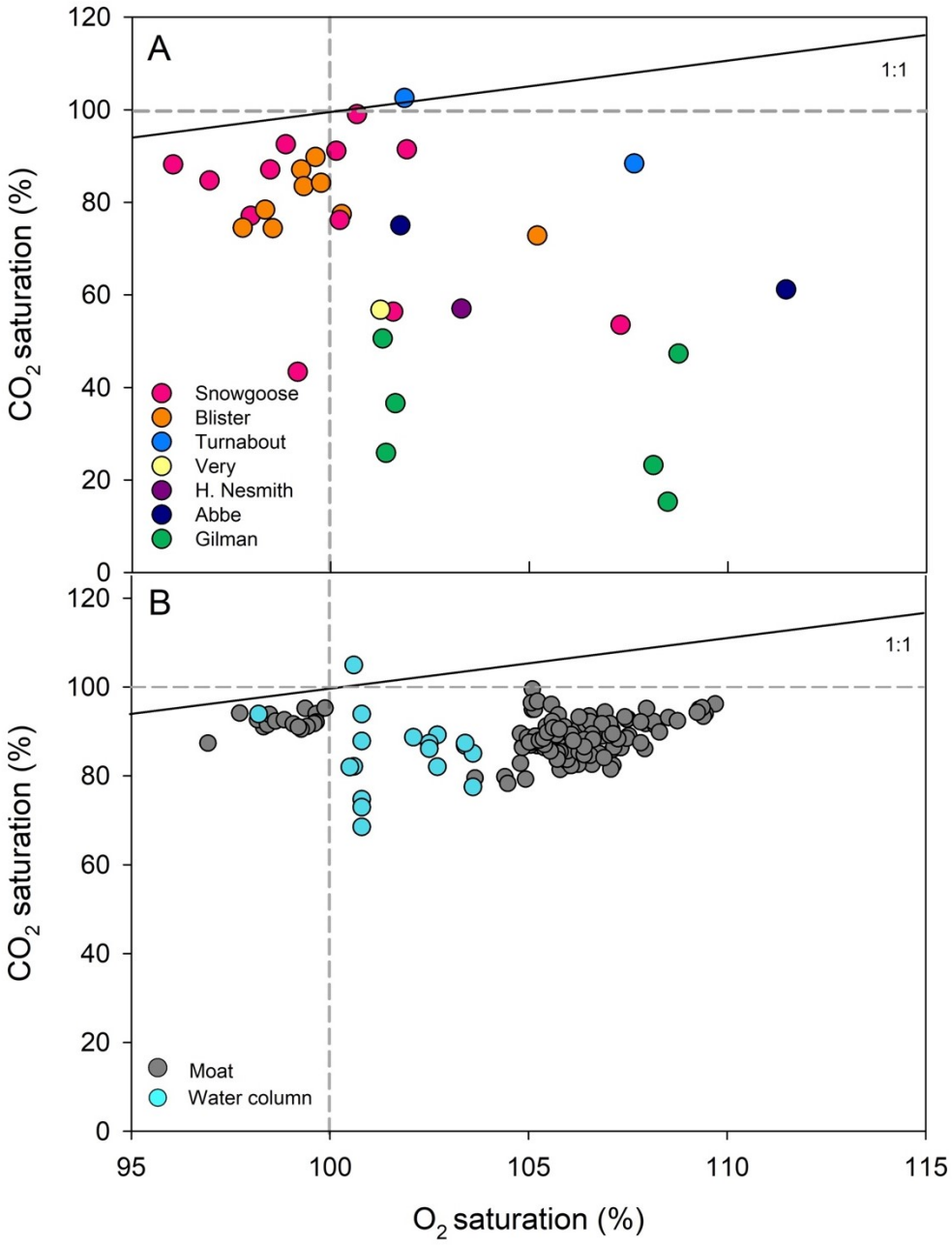

Figure A2-2. Carbon dioxide (CO_2) and oxygen (O_2) saturation in (A) glacial river deltas in 2016 and (B) Lake Hazen in 2015 and 2016. Lake Hazen samples categorized as moat (grey) or water column (light blue); all lake samples measured after ice melt on 26-Jul-2015. Water column CO_2 concentrations calculated at surface pressure.

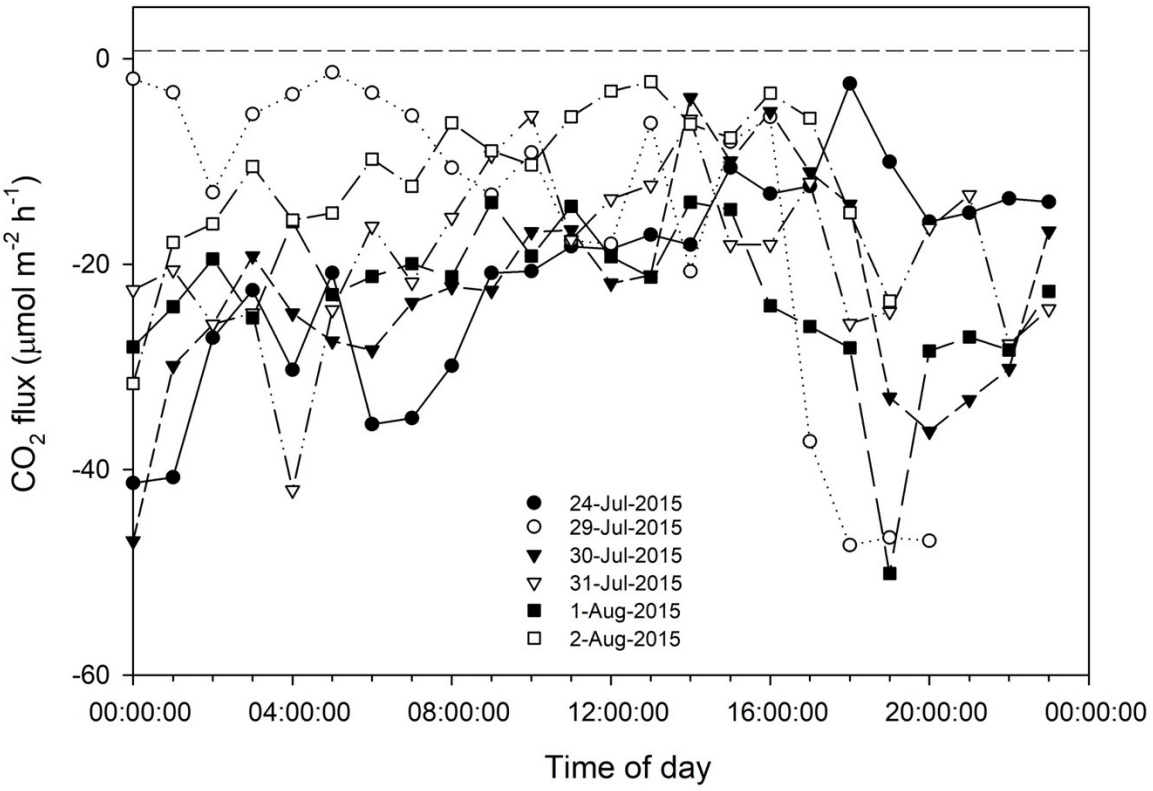

Figure A2-3. Examples of daily instantaneous surface CO_2 fluxes in µmol m^{-2} h^{-1} along the shoreline of Lake Hazen. Hourly fluxes averaged from CO_2 concentrations taken at 15-minute intervals, corrected for chemical enhancement of CO_2 diffusion at high pH, and calculated per hour using *in situ* temperature, barometric pressure and wind speed.

Table A2-1. Temperature, pH and components of the carbon system in the Lake Hazen watershed, glacial river deltas, Lake Hazen moat and water column and Ruggles River outflow. Means (n shown) ± 1 SD shown. Summer water column (0, 250 m) averaged over 2015 and 2016, except for δ^{13}C-DIC (2016 only).*

					Dissolved			Suspended sediments	
	Temp. (°C)	**pH**	**$CO_{2(aq)}$ (µM)**	**Weathering endpoint CO_2 (µM)**	**DIC (µM)**	**δ^{13}C-DIC (‰)**	**DOC (mg L^{-1})**	**% OC**	**δ^{13}C (‰)**
Bi-weekly (n)									
Blister (10)	7.3 ± 1.7	7.6 ± 0.43	17.8 ± 1.9	10.7 ± 8.6	565 ± 62	-2.97 ± 1.86 (*n=6*)	0.4 ± 0.1	1.0	-14.1
Snowgoose (10)	9.5 ± 2.0	7.5 ± 0.6	17.9 ± 4.3	10.3 ± 10.0	609 ± 105	-1.77 ± 1.39	0.4 ± 0.1	1.4	-11.5
Surveys (n)									
Abbé (2)	6.5 ± 2.2	7.6 ± 0.1	16.2 ± 3.4	1.0 ± 0.3	442 ± 48	-1.17 ± 0.01	0.4 ± 0.1		
Gilman (2)	3.4 ± 0.3	8.6 ± 0.2	5.5 ± 2.0	0.9 ± 0.1	500 ± 32	-3.42 ± 0.00	0.6 ± 0.1	1.4	-10.9
H. Nesmith (2)	3.4 ± 1.2	8.1 ± 0.4	15.4	3.6 ± 4.7	413 ± 10	-2.47 ± 2.22	0.3 ± 0.0		
Turnabout (2)	12.0 ± 0.9	7.8 ± 0.1	19.1 ± 2.4	15.7 ± 13.0	695 ± 11	-1.68 ± 1.03	1.1 ± 0.4	3.7	-22.3
Very (2)	8.7 ± 1.0	8.2 ± 0.1	12.7	1.0 ± 0.1	809 ± 44	-2.37 ± 0.67	0.5 ± 0.1	3.7	-9.4
Lake Hazen (n)									
Moat (6)	5.1 ± 2.1	7.6 ± 0.4	23.3 ± 3.8	21.3 ± 6.0	143 ± 140	-	0.3 ± 0.1	-	-
Centre, 0 m (2)		7.8 ± 0.2	22.5 ± 0.5	-	814	0.33 (*n=1*)	0.3 ± 0.1	-	-
Centre, 250 m (2)		7.8 ± 0.1	22.1 ± 3.9	-	897	-0.11(*n=1*)	0.3 ± 0.1	-	-
Ruggles River (n=2) **	3.6 ± 0.6	7.8 ± 0.3	18.2 ± 1.3	14.9 ± 1.1	924 ± 502	0.71 ± 0.01	0.3 ± 0.0	-	-

* $CO_{2(aq)}$, dissolved CO_2; DIC, dissolved inorganic carbon; DOC, dissolved organic carbon; OC, organic carbon.

** The Ruggles River is the outlet of Lake Hazen.

Table A2-2. Weathering indices in glacial rivers of the Lake Hazen watershed in 2015 and 2016. Catchment estimates based on glaciers studied covering 83% of watershed glacierized area. ∑C+, sub-watershed cation equivalent weathering rate. All rates calculated using river valley areas. Weathering yields (∑C+ weathering, $dSiO_2$ yield, solute denudation rates) calculated using watershed areas; CO_2 consumption rates (i.e., surface fluxes) calculated using river valley areas.

INDEX	Unit	Year	Abbé	Blister [a]	Gilman	H. Nesmith	Snowgoose	Turnabout	Very	Watershed[b]
River valley area (RV)	km^2	-	*7.9*	*2.5*	*5.1*	*9.6*	*5.6*	*13.4*	*32.9*	***91.0***
River length	*km*	-	*21*	*11*	*22*	*4.6*	*17*	*42*	*39*	**-**
Proglacial area (PG)	km^2	-	*186*	-	*284*	*233*	*135*	*419*	*766*	***3354***[c]
Glacier area (GL)	km^2	-	*204*	*6*	*708*	*1041*	*87*	*259*	*269*	***3078***
Watershed area (WS)	km^2	-	*390*	-	*992*	*1270*	*222*	*678*	*1035*	***7516***
Modeled run-off	km^3	2015	0.061	0.002	0.20	0.29	0.026	0.082	0.17	**0.82**
		2016	0.015	<0.001	0.043	0.075	0.006	0.043	0.080	**0.29**
∑+ weathering	meq m^{-2} yr^{-1}	2015	176	-	186	213	146	131	168	**170**
		2016	52.4	-	52.4	69.2	55.7	30.8	90.4	**58.5**
$dSiO_2$ yield	mg m^{-2} yr^{-1}	2015	22.8	-	25.2	29.1	18.4	17.2	22.3	**22.5**
		2016	0.362	-	0.368	0.944	0.164	0.281	1.21	**0.553**
Solute denudation	t km^{-2}	2015	8.41	-	8.72	9.92	7.03	6.24	7.98	**8.05**
		2016	2.51	-	2.51	3.31	2.65	2.16	4.34	**2.91**
CO_2 consumption	g C-CO_2 m^{-2} d^{-1}	2015	0.335	0.041	1.45	1.14	0.218	0.259	0.208	**0.519**
		2016	0.087	0.010	0.359	0.326	0.073	0.079	0.101	**0.149**
	Mg C-CO_2 yr^{-1}	2015	106	4.07	297	438	48.8	138	274	**1515**
		2016	29.5	1.10	78.7	135	17.6	45.2	143	**522**

[a] Sub-catchment area for Blister River, not defined in Canadian Digital Elevation Model.
[b] Watershed areal rates are means of the measured sub-catchment rates.
[c] Watershed proglacial area defined as non-glacierized area of watershed, not covered by Lake Hazen (544 km^2).

Table A2-3. Literature documented $CO_{2(aq)}$ undersaturation in glacier-fed freshwater ecosystems*.

Glacier	Randolph Region [a]	Dist. [b] (km)	Glacier area (km^2)	Geology	CO_2 saturation	Unit	CO_2 (M/C)	Ref.
Abbé	Canada Arctic North	21	204	Carbonate	68.1±9.78	% sat.	M	This study
Blister Ice Cap	Canada Arctic North	11	6	Carbonate	81.4±6.91	% sat.	M	This study
Gilman	Canada Arctic North	28	708	Carbonate	20.5±7.46	% sat.	M	This study
Henrietta Nesmith	Canada Arctic North	4.6	1041	Carbonate	57.0	% sat.	M	This study
Snowgoose	Canada Arctic North	17	87	Carbonate	77.6±19.4	% sat.	M	This study
Turnabout	Canada Arctic North	42	259	Carbonate	95.5±10.0	% sat.	M	This study
Very	Canada Arctic North	39	269	Carbonate	56.7	% sat.	M	This study
Saskatchewan	Western Canada	5.5	30	Carbonate	22.1	% sat.	M	This study
Kiattuut Sermiat	Greenland periphery	2.5	36	Granitic	34.8	% sat.	M	This study
Kiattuut Sermiat	Greenland periphery	1	36	Granitic	17.5	% sat.	C	[2]
Austre/Vestre Brøggerbreen	Svalbard	2.5	16	Carbonate	-3.55 to -3.96	Index	C	[3]
Various (Austrian Alps)	Central Europe	0-1.6	0.82-19	Unknown	[c]	Text	M	[4]
Kennicott	Alaska	0.5	420	Mixed	[e]	Visual	C	[5]

[*] Dist., distance of sampling location from glacier; regime, presence (subglacial) or absence (cold) of under ice drainage system; CO_2 (M/C), CO_2 concentrations measured (M) or calculated (C).
[a] Regions defined by Randolph Glacier Inventory (ref [6]). Glacier areas extracted from World Glacier Inventory if not reported.
[b] Minimum distance from glacier = 0.5 km.
[c] pCO_2 data not detailed, but 65% of downstream samplings reported as 'undersaturated'.
[d] Some values fell below atmospheric equilibrium (Figure 6 in ref [5]).

Table A2-4. Best-fit log-linear models of major cation and anion loads in glacial rivers from rLOADEST (Runkel et al. 2015), where Q is discharge in $m^3\ s^{-1}$ and [x] is the analyte load in kg d^{-1}.

Analyte	Model	R^2	p	Bias (%)
$Ca^{2+}_{(aq)}$	$\ln[Ca^{2+}] = 0.940\ln Q + 5.29$	0.989	<0.0001	-5.63
$Mg^{2+}_{(aq)}$	$\ln[Mg^{2+}] = 0.008(\ln Q)^2 + 0.956\ln Q + 2.76$	0.976	<0.0001	-9.00
$Na^{+}_{(aq)}$	$\ln[Na^{+}] = 0.009(\ln Q)^2 + 1.02\ln Q + 2.71$	0.994	<0.0001	4.04
$K^{+}_{(aq)}$	$\ln[K^{+}] = 0.987\ln Q + 1.44$	0.982	<0.0001	9.72
$SO_4^{2-}{}_{(aq)}$	$\ln[SO_4^{2-}] = 0.018(\ln Q)^2 + 0.903\ln Q + 5.92$	0.978	< 0.0001	-15.9
$Cl^{-}_{(aq)}$	$\ln[Cl^{-}] = 0.017(\ln Q)^2 + 1.01\ln Q + 0.969$	0.985	<0.0001	8.64
$HCO_3^{-}{}_{(aq)}$	$\ln[HCO_3^{-}] = 0.992\ln Q + 6.26$	0.992	<0.0001	-8.43
$SiO_{2(aq)}$	$\ln[SiO_2] = 0.007(\ln Q)^2 + 0.905\ln Q + 1.06$	0.977	<0.0001	-0.78
$DIC_{glacier}$	$\ln[DIC_{glacier}] = 1.09\ln Q + 4.90$	0.963	<0.0001	-18.9
DIC_{delta}	$\ln[DIC_{delta}] = 0.991\ln Q + 6.37$	0.996	<0.0001	15.5

References

1 Köck, G. *et al.* Bathymetry and Sediment Geochemistry of Lake Hazen (Quttinirpaaq National Park, Ellesmere Island, Nunavut). *Arctic* **65**, 56-66 (2012).

2 Dubnick, A. *et al.* Hydrological controls on glacially exported microbial assemblages. *J. Geophys. Res. Biogeosci.* **122**, 1049-1061 (2017).

3 Nowak, A. & Hodson, A. J. Changes in meltwater chemistry over a 20-year period following a thermal regime switch from polythermal to cold-based glaciation at Austre Broggerbreen, Svalbard. *Polar Res.* **33**, 22779 (2014).

4 Singer, G. A. *et al.* Biogeochemically diverse organic matter in Alpine glaciers and its downstream fate. *Nat. Geosci.* **5**, 710 (2012).

5 Anderson, S. P., Longacre, S. A. & Kraal, E. R. Patterns of water chemistry and discharge in the glacier-fed Kennicott River, Alaska: evidence for subglacial water storage cycles. *Chem. Geol.* **202**, 297-312 (2003).

6 Pfeffer, W. T. *et al.* The Randolph Glacier Inventory: a globally complete inventory of glaciers. *J. Glaciol.* **60**, 537-552 (2014).

Appendix 3. Supporting information for "Chapter 4. Climate drives catchment-wide changes in mercury cycling in the High Arctic's largest lake by volume (Lake Hazen, Nunavut, Canada)"

METHODS

Inputs to Lake Hazen.

Snowmelt on the lake surface. Integrated snowpack samples were collected at maximum snowpack depth just prior to melt from the surface of Lake Hazen (10 paired sites) in May 2014 and from the lake surface (10 sites) and the adjacent catchment (9 sites) in May 2015 (Table A3-1). At each site, integrated snow core samples were collected from behind the cleaned edge of a snow pit using a dilute HCl-washed stainless steel corer of 4.3 cm inner diameter (ID) and the two person "clean hands, dirty hands" Hg sampling protocol. Snow samples for Hg analyses were placed into double-bagged glass jars with Teflon-lined lids (I-Chem Certified 300 Series 1-L clear jar). Samples for water chemistry analyses were collected in large Ziploc freezer bags pretested for contamination. All snow samples were kept frozen until melting and processing in the Canadian Association of Laboratory Accreditation (CALA)-certified Biogeochemical Analytical Service Laboratory (BASL; University of Alberta, Edmonton AB, Canada).

2014 snowpacks. Low snowpack volume, combined with frequent wind storms, created distinct patches of light and dark snow (see Figure A3-2) on Lake Hazen, depending on how dust drifted and accumulated. There was virtually no snow on the landscape in May 2014; consequently, 10 sites were sampled on the lake ice surface only. At each of the sampling sites, adjacent light and dark patches were sampled separately. At light patches, integrated snowpack samples were collected using a cleaned 4.3 cm diameter stainless-steel corer. At dark patches, where snowpacks were thin due to low albedo caused by high loadings of dark particulate matter, a cleaned stainless-steel spatula was used to scrape integrated snowpack samples from a known surface area of lake ice. Samples were collected and subsequently processed as in 2015 (see main text). For 2014 snowpacks, % coverage of the light and dark snow packs were estimated from 3 aerial photographs of the lake surface using ArcGIS 10.3 (ESRI 2014). Mean 2014 loadings were then weighted according to the mean distribution between light (44.7%) and dark (55.3%) snowpacks.

Snowmelt from the adjacent landscape. Snowmelt runoff samples were collected from three channels (Blister River, Snowgoose River, Skeleton Creek) every 3-5 days between 23 May and 1 June 2014. Snowmelt runoff, and for all water samples described hereafter collected for Hg analyses, were collected by dipping 250 ml amber bottles with Teflon-lined lids (Environmental Sampling Supply, no. 0250-0150-QC) below the water surface using the clean-hands, dirty hands sampling technique. Bottles were triple-rinsed with sample water, and stored double-bagged. Upon return to the clean room of the Lake Hazen Field Laboratory, samples were preserved with concentrated trace-metal grade HCl (0.5% v/v) and kept cool until shipped to the University of Alberta for analyses. Additional bulk water samples were collected for supporting chemistry in acid-washed and triple-rinsed Nalgene bottles and/or polyethylene/polyurethane Platypus™ bags. All samples were processed and preserved either onsite or in the Field Laboratory according to analyte-specific, CALA-approved standard operating procedures and kept cool until shipped for analyses at the BASL.

Glacial melt. Seven glacial rivers (Table A3-6, Figure A3-1) were sampled in summers 2015 (7 – 31 July) and 2016 (2 July – 5 August). The Snowgoose and Blister rivers, both within walking distance of the base camp, were sampled at their deltas every 5-7 days. Five additional glacial rivers (Abbé, Gilman, Henrietta Nesmith, Turnabout, Very; Figure A3-1) were accessed by helicopter once in 2015 (15 July) and twice in 2016 (11, 13 July; 1–2 August). To assess whether Hg concentrations changed over the length of the Blister (2015) and Gilman and Snowgoose (2016) rivers, we also sampled three sites between the glaciers and river deltas (n = 5 transects). Glacial rivers mobilize significant quantities of sediments[1, 2], so at each site, we collected four samples to assess the differences between unfiltered (bulk) and filtered (dissolved) concentrations of MeHg and THg. Samples for dissolved MeHg and THg analyses were filtered through acid-washed 0.45-µm cellulose nitrate filter towers (Nalgene™ Rapid-Flow Filters, Thermo Fisher no. 126-0045) immediately upon return to the Field Laboratory. The filtrate was then dispensed into new bottles and acidified as above. To determine concentrations of MeHg and THg on suspended particles in the glacial river water, we collected bulk water samples from the Blister, Snowgoose, Turnabout, Very, and Gilman rivers into Whirlpak® bags. All samples

were frozen at the Lake Hazen base camp, and subsequently freeze-dried and homogenized prior to analyses.

Sources of particulate Hg. Surface soils can be a potential source of local airborne particulate matter, Hg and nutrients. As such, we collected triplicate 5 cm long soil core samples, 2.54 cm in diameter, at 5 sites along a transect extending from Lake Hazen to the foothills of the Grant Land Mountains in July 2015. To identify other possible sources of particulate Hg in water samples, coal samples and floating foam (Figure A3-6) at the lake edge near Blister Creek and the Gilman River were opportunistically sampled in 2015 and 2016. All samples were kept frozen and freeze-dried just prior to analysis.

MeHg and THg Analysis. For MeHg analysis, 44-46 mL of water samples were distilled at 128°C with 200 µL ammonium pyrrolidine dithiocarbamate (APDC), while 100-200 mg of solid samples were soaked overnight in ~45 mL milli-Q water with 500 µL of 50% H_2SO_4 and 200 µL of 20% KCl and then distilled the following morning at 147°C. All solid samples were freeze-dried and homogenized prior to the preparation of distillation. All samples were spiked with $Me^{201}Hg$. Relative standard deviations (RSD) between duplicate samples on unfiltered (bulk) and filtered (dissolved) water samples were less than 25% and 15%, respectively. Duplicate samples with RSDs greater than 20% were run in triplicate; however, samples with high suspended particulate loads are inherently variable. RSD on duplicate solid samples were between <1 and 14%, except for the coal from the Gilman River (55%). The low precision observed in this sample was likely due to challenges associated with matrix homogenization. Solid sample method accuracy and precision were assessed using reference material SQC1238 (MeHg in sediment with certified value of 10.0 ± 0.291 ng g^{-1}, acceptable range of 5.13 to 14.9 ng g^{-1}; Sigma-Aldrich). Mean SQC1238 concentrations using this method was 11.9 ± 0.833 ng g^{-1}. There was no reference material for MeHg in water. Concentrations of MeHg standards (isotopic $Me^{201}Hg$ and bulk MeHgCl from Brooks Rand) were checked annually by Flett Research Ltd. (Winnipeg, MB, Canada).

For THg analysis on water samples, relative standard deviations on unfiltered (bulk) and filtered (dissolved) duplicate water samples were generally less than 15%. THg concentrations on solid samples (coal, foam, soils, suspended sediment material) were determined using a Direct

Mercury Analyzer (DMA-80). Duplicate recoveries (where sufficient sample available) were between 2 and 36%. Mean recovery of reference material MESS-4 (marine sediment, National Research Council Canada) was 0.075 ± 0.002 mg kg^{-1}, well within the certified range of 0.02-0.14 mg kg^{-1}.

Hg^0 efflux estimation. As we did not directly measure Hg^0 in 2015 or 2016, we used the mean Hg^0 concentrations in Lake Hazen reported in Lehnherr *et al*. (2012)[3] (29.1 ± 10.7 pg L^{-1}), based on 3 discrete samplings in 2005 (6, 12, 19-July-2005). GEM efflux was estimated by multiplying the mean GEM flux rate by the daily ice-free areas for Lake Hazen, obtained using the MODIS snow cover product (MOD10A1), as described in Lehnherr *et al* [4]. Diffusive gaseous elemental Hg^0 fluxes are estimated using equation 1([5]):

$$\text{Flux} = k(C_w - C_{eq}) \quad [1]$$

Where k is the wind-speed derived gas transfer velocity (cm hr^{-1}), C_w is the concentration of Hg^0 in the water (pg L^{-1}) and C_{eq} is the aqueous concentration of Hg^0 if the water were at atmospheric equilibrium with respect to Hg^0, based on an atmospheric concentration of 1.7 pg L^{-1} ([6]). Flux calculations for Hg^0 are described in detail elsewhere[6, 7].

In 2015, we simultaneously logged water temperature with a YSI EXO 2 sonde about 30 cm below the water surface along the shoreline of Lake Hazen and wind speed with a Met One 014A anemometer at 1 m above the ground, interfaced with a Campbell Scientific CR10x datalogger at 15 minute intervals. Wind speeds were corrected to 10 m (U_{10}) following Crusius and Wanninkhof (2003)[8]. In 2016, wind speed was measured continuously, but not water temperature, therefore we only obtained spot estimates (n=18) with sufficient information for calculating fluxes. Mean Hg^0 flux rates were 0.323 ± 0.183 ng m^{-2} hr^{-1} (n=375). We then multiplied the mean flux rate by the daily ice-free areas for 2015 and 2016.

RESULTS AND DISCUSSION

Snow and snowmelt (2014). In 2014, mean MeHg and THg concentrations in snow were 1.97±2.13 ng L^{-1}, 172±313 ng L^{-1}, significantly higher than in 2015 (0.358±0.134 ng L^{-1} and 4.73±1.02 ng L^{-1}). MeHg and THg concentrations in the dark snow were 3.51±2.25 and 339±400 ng L^{-1}, respectively. These concentrations were greater (though not statistically significant,

Tables S3 and S4) than in the light snow, where MeHg and THg concentrations were 0.579±0.200 and 21.4±9.67 ng L^{-1}. In 2014, high particulate loads in the snow (Figure A3-2) decreased the albedo, further concentrating the Hg through multiple spring freeze-thaw cycles[9]. These concentrations are much higher than those previously recorded in arctic snowpacks, even during atmospheric mercury depletion events (AMDEs; e.g., THg concentrations >60 ng L^{-1} [10]) and are likely largely a result of frequent dust storms during winter 2014. Dusts deposited to the Arctic can originate from distant sources[11, 12], but we believe the 2014 dusts to be largely local, pursuant to our observation of a prolonged (2-3 days) dust storm in late May 2014. Concentrations of MeHg and THg in local soils were 0.053-0.292 ng g^{-1} and 7.42-29.9 ng g^{-1}, respectively, and within the range of other sites in the Canadian Arctic Archipelago (0.02-2.11 ng g^{-1}; 1.64-49.0 ng g^{-1})[13]. While low, these concentrations could easily account for the Hg concentrations observed within the 2014 snowpacks. Snowmelt MeHg and THg concentrations decreased throughout the 2014 melt season from 0.292±0.145 to 0.073±0.002 ng L^{-1} and 14.1±8.53 to 2.07±0.347 ng L^{-1}, respectively, consistent with snowpack elution[9, 14].

Unfiltered MeHg loadings were not statistically different between 2014 and 2015 (0.303±0.309 mg ha^{-1} and 0.404±0.348 mg ha^{-1}; $t=-1.33$, $p > 0.05$), but unfiltered THg loadings in 2014 were higher than in 2015 (16.0±20.8 mg ha^{-1} and 5.09±3.31 mg ha^{-1}; $t=2.86$, $p < 0.05$). Although concentrations of both MeHg and THg were higher and more variable in the dark versus light snow in 2014, loadings were approximately equal between the snow types due to differences in snowpack volumes (dark volume << light volume).

Possible sources of dissolved MeHg and THg within Lake Hazen. Although Lake Hazen was an overwhelming sink of both MeHg and THg, exports of dissolved MeHg and THg to the Ruggles River marginally exceeded inputs. There are two possible processes by which partitioning between particulate and dissolved phases of Hg may occur within Lake Hazen: 1) particle scavenging in surface waters, and 2) particle dissolution at the redox boundary[15]. Firstly, foams of biological origin ($\partial^{13}C = -26.7 \pm 1.27$‰; see Figure A3-5) opportunistically sampled along the shores of Lake Hazen had very high concentrations of MeHg (1.28±0.847 ng g^{-1}) and THg (474±61.3 ng g^{-1}). Periodicity in ultra-oligotrophic polar water bodies can lead to the formation of nutrient-rich, metabolically-active foams concentrating algal and cyanobacterial detritus[16]. These foams are hotspots of biological activity and thus may also be important highly

localized zones of Hg cycling; however, this has never been specifically examined to our knowledge. Secondly, the bottom waters of Lake Hazen become anoxic during the winter with active microbial respiration within the sediments (Figure 4-4). Sediment core profiles exhibit distinct peaks in MeHg concentrations and genes of the *mer* operon have been isolated from sediments within Lake Hazen[17] suggesting the potential for biological transformation (oxidation/reduction/methylation) of Hg within the Lake Hazen sediments.

Supporting Figures and Tables

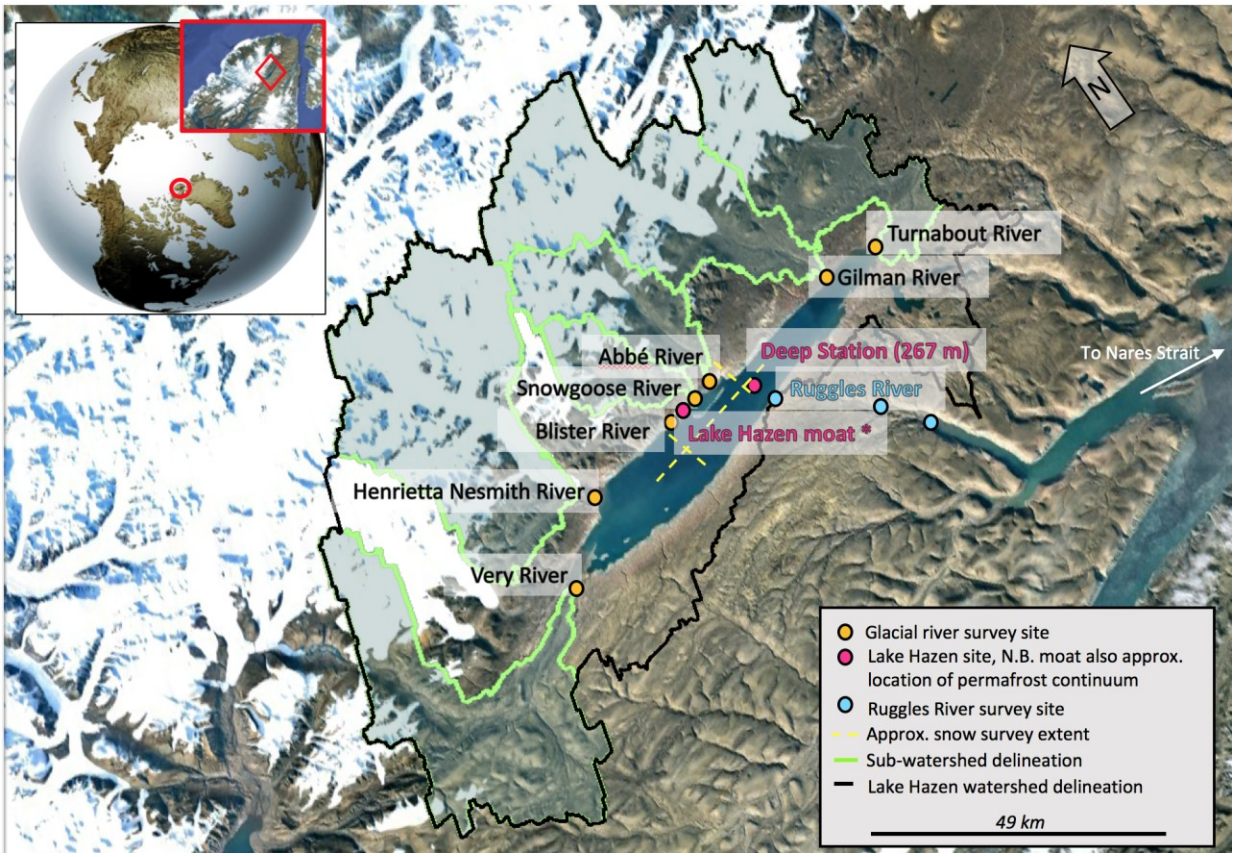

Figure A3-1. Sampling sites within the Lake Hazen watershed, northern Ellesmere Island, Nunavut, Canada. Satellite imagery from Landsat (Google Earth).

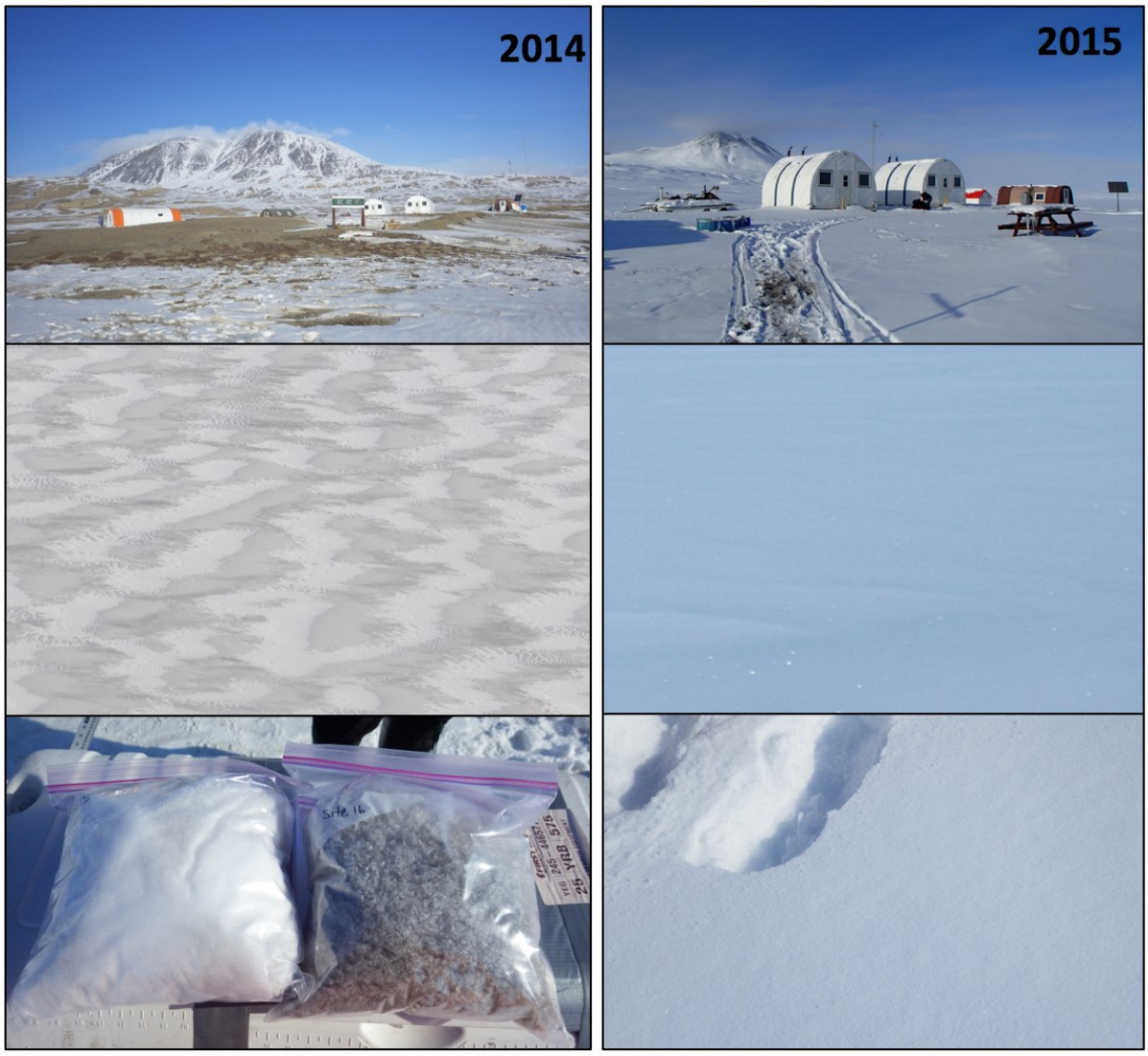

Figure A3-2. Snow conditions on the Lake Hazen watershed in 2014 (left column) and 2015 (right column). Top: Lake Hazen base camp in Quttinirpaaq National Park on May 14th in 2014 and 2015. Middle: aerial view of lake ice surface. Bottom: close-up view of snow samples; 2014 photo shows adjacent light (left) and dark (right) patches of snow.

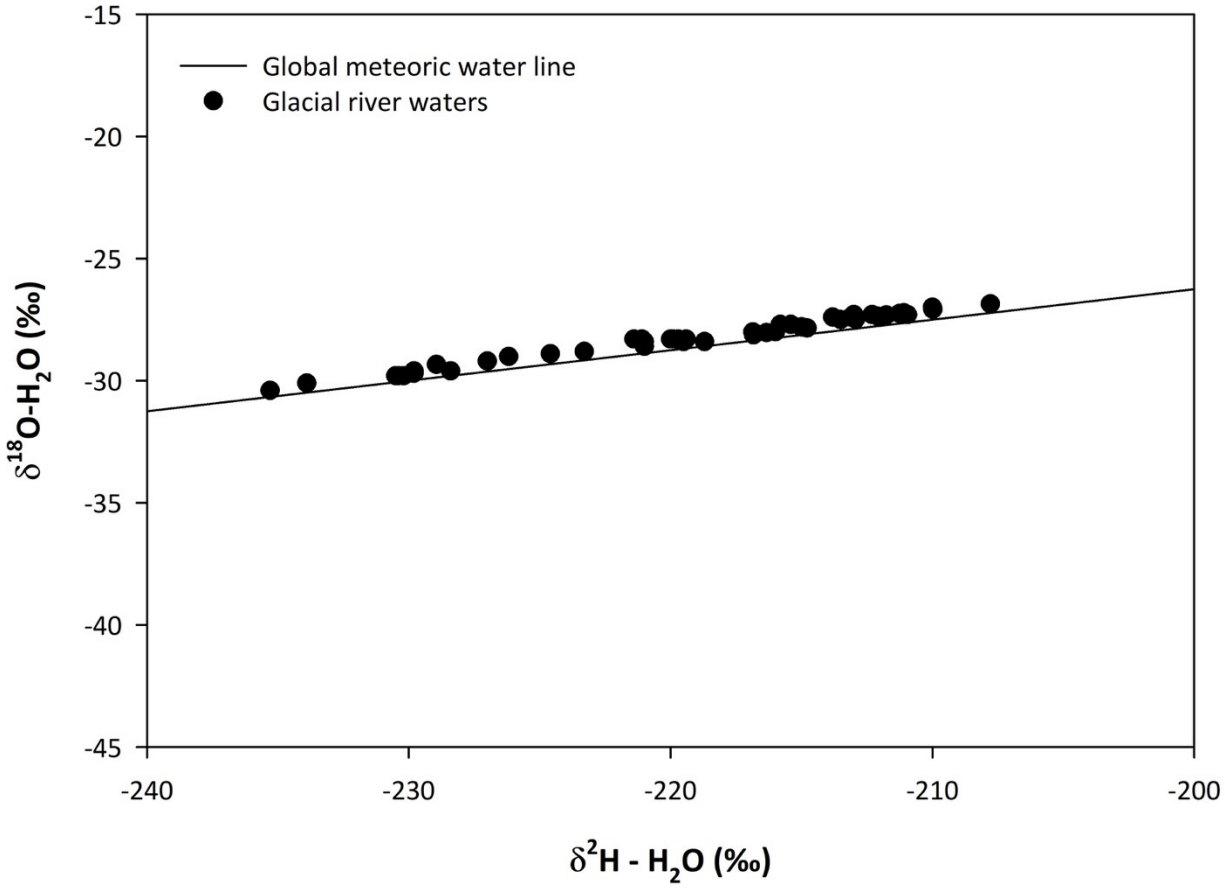

Figure A3-3. Isotopic signatures (δ^{18}O-H_2O and (δ^{2}H-H_2O) of glacial river samples relative to global meteoric water line.

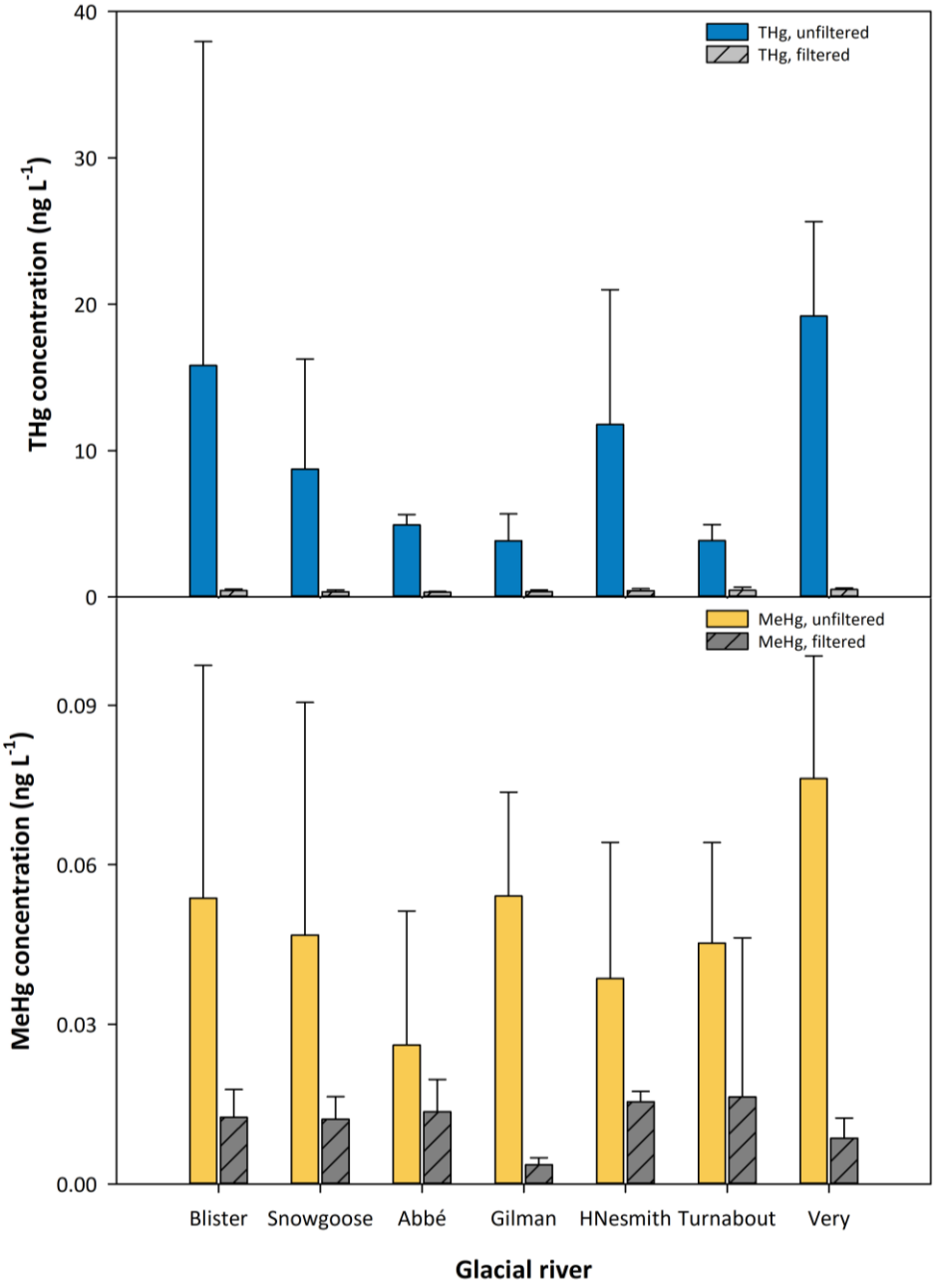

Figure A3-4. THg and MeHg concentrations in glacial rivers. Blister and Snowgoose rivers sampled every 5-7 days (n=11); other rivers sampled 1-2 times per summer (n=3, but n=2 for Gilman). Means (± 1SD) pooled over 2015 and 2016.

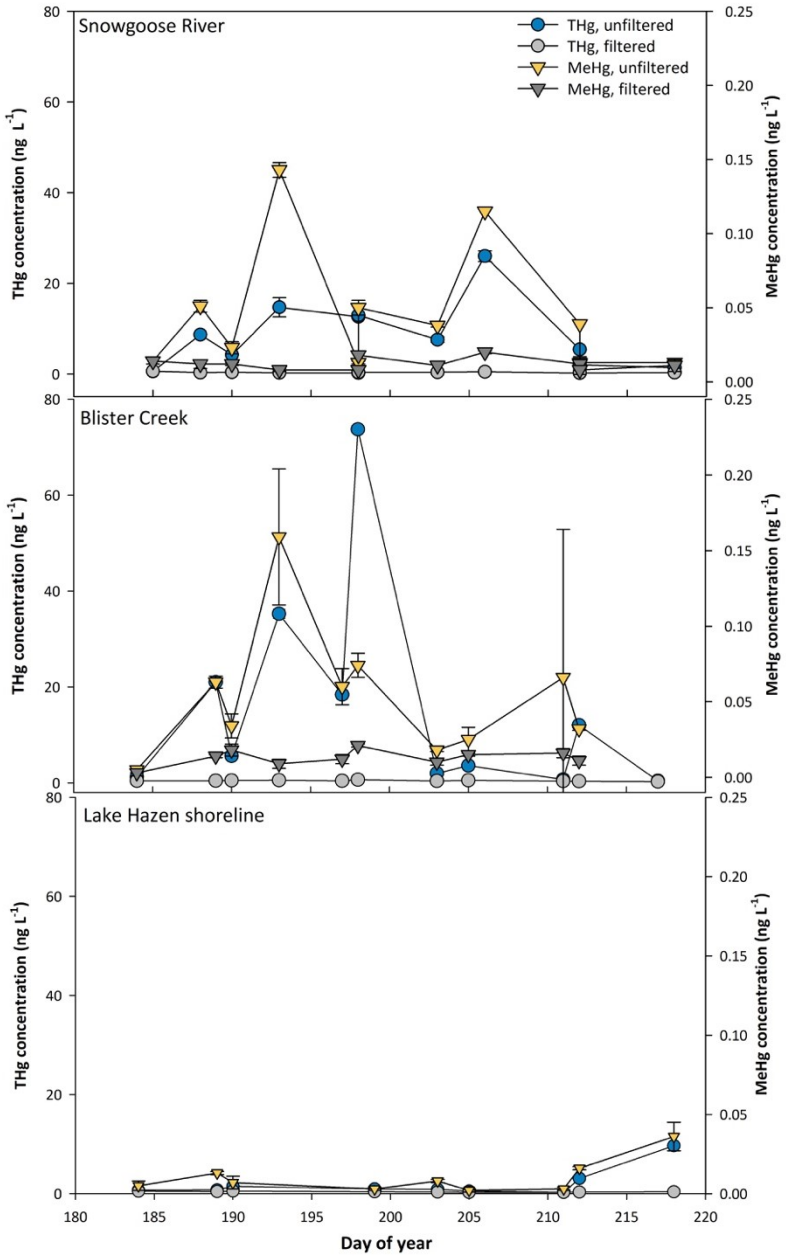

Figure A3-5. Concentrations of unfiltered (bulk) and filtered (dissolved) total mercury (THg) and methylmercury (MeHg) throughout the melt season in the Snowgoose and Blister river deltas and along the Lake Hazen shoreline. Mean (n=2) ± 1 SD shown. Data from 2015 and 2016 pooled.

Figure A3-6. Foam material collected along shoreline of Lake Hazen near the Gilman River.

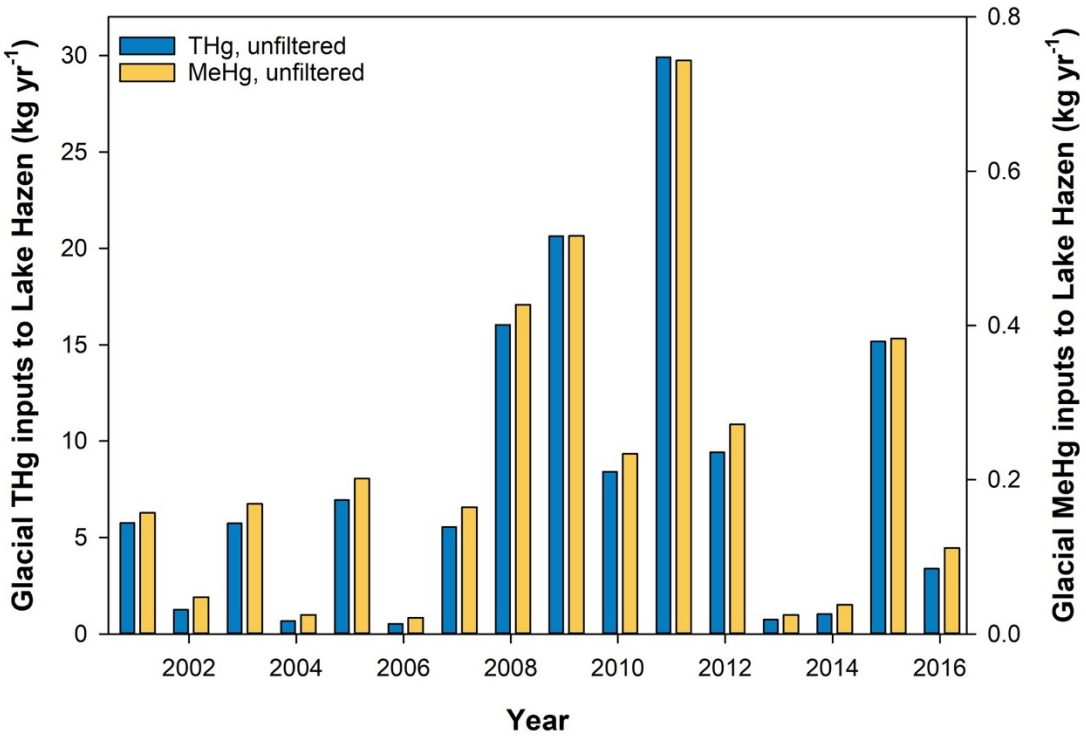

Figure A3-7. Modeled bulk (unfiltered) total mercury (THg) and methylmercury (MeHg) inputs from the glacial rivers to Lake Hazen from 2001 to 2016.

Table A3-1. Sampling sites and parameters samples in the Lake Hazen watershed.

Sample type and site	Year(s) sampled	*n* sites	Times sampled	Parameters sampled
Snow: 9 paired lake	2014	9	1	MeHg $_{\text{unfiltered/filtered}}$, THg $_{\text{unfiltered/filtered}}$
Snow: 10 lake + 10 land	2015	20	1	MeHg $_{\text{unfiltered/filtered}}$, THg $_{\text{unfiltered/filtered}}$
Snowmelt stream	2014	3	10	MeHg $_{\text{unfiltered}}$, THg $_{\text{unfiltered}}$, sonde
GLACIAL RIVERS				
Blister River				
Delta	2015, 2016	1	11	MeHg $_{\text{unfiltered/filtered}}$, THg $_{\text{unfiltered/filtered}}$, PC, TSS*, sonde
Transect	2015	4	1	MeHg $_{\text{unfiltered/filtered}}$, THg $_{\text{unfiltered/filtered}}$, PC, sonde
Snowgoose River				
Delta	2015, 2016	1	11	MeHg $_{\text{unfiltered/filtered}}$, THg $_{\text{unfiltered/filtered}}$, PC, TSS*, sonde
Transect	2016	2	2	MeHg $_{\text{unfiltered/filtered}}$, THg $_{\text{unfiltered/filtered}}$, PC, TSS*, sonde
Abbé River delta	2015, 2016	1	3	MeHg $_{\text{unfiltered/filtered}}$, THg $_{\text{unfiltered/filtered}}$, PC, TSS*, sonde
Gilman River				
Transect	2016	3	2	MeHg $_{\text{unfiltered/filtered}}$, THg $_{\text{unfiltered/filtered}}$, PC, TSS*, sonde
H. Nesmith River delta	2015, 2016	1	3	MeHg $_{\text{unfiltered/filtered}}$, THg $_{\text{unfiltered/filtered}}$, PC, TSS*, sonde
Turnabout River delta	2015, 2016	1	3	MeHg $_{\text{unfiltered/filtered}}$, THg $_{\text{unfiltered/filtered}}$, PC, TSS*, sonde
Very River delta	2015, 2016	1	3	MeHg $_{\text{unfiltered/filtered}}$, THg $_{\text{unfiltered/filtered}}$, PC, TSS*, sonde
Permafrost thaw stream	2015, 2016	1	5	MeHg $_{\text{unfiltered/filtered}}$, THg $_{\text{unfiltered/filtered}}$, PC, TSS*, sonde
Lake Hazen moat	2015, 2016	1	9	MeHg $_{\text{unfiltered/filtered}}$, THg $_{\text{unfiltered/filtered}}$, PC, TSS*, chl *a*, sonde
Lake Hazen water column, spring	2014, 2017	1	45	MeHg $_{\text{unfiltered}}$, THg $_{\text{unfiltered}}$, PC, TSS*, chl *a*, sonde
Lake Hazen water column, summer	2015, 2016	1	18	MeHg $_{\text{unfiltered/filtered}}$, THg $_{\text{unfiltered/filtered}}$, PC, TSS*, chl *a*, sonde
Ruggles River, LH outflow	2015, 2016	1	3	MeHg $_{\text{unfiltered/filtered}}$, THg $_{\text{unfiltered/filtered}}$, PC, TSS*, sonde
Ruggles River, fjord inflow	2016	1	2	MeHg $_{\text{unfiltered/filtered}}$, THg $_{\text{unfiltered/filtered}}$, PC, TSS*, sonde

- MeHg, methylmercury; THg, total mercury; PC, particulate carbon; TSS, total suspended sediments; chl *a*, chlorophyll *a*; sonde, sonde parameters (temperature, pH, turbidity, dissolved oxygen, chl *a*)

*TSS only sampled in 2016.

Table A3-2. Concentrations of total mercury (THg) and methylmercury (MeHg) by hydrologic pool in the Lake Hazen watershed (unfiltered, unless otherwise stated). LH, Lake Hazen; RR, Ruggles River.

	Unfiltered THg (ng L^{-1})		Filtered THg (ng L^{-1}) [c]		Unfiltered MeHg (ng L^{-1})		Filtered MeHg (ng L^{-1}) [c]	
Pool (*n*)	Mean	Range	Mean	Range	Mean	Range [b]	Mean	Range
Snow 2014 (*19*) [a]	172	8.14-1204	2.81	0.695-8.17	2.00	0.310 - 9.10	0.362	0.073-1.23
Snow 2015 (*20*) [a]	4.73	3.03-6.54	0.612	0.245-1.25	0.350	0.138 - 0.664	0.146	0.039-0.252
Snowmelt (*10*)	6.43	1.81-24.0	-	-	0.148	0.068 - 0.458	-	-
Glacial river deltas (*36*)	9.73	0.414-73.7	0.405	0.195-0.685	0.0487	0.007 – 0.159	0.012	<DL-0.051
Non-glacial stream (*5*)	1.05	0.764-1.23	1.00	0.745-1.18	0.0252	0.022 – 0.030	0.027	0.021-0.038
LH moat (*9*)	2.03	0.271-9.68	0.369	0.245-0.522	0.0103	< DL – 0.036	0.007	<DL-0.011
LH water column, spring (*45*)	0.246	0.022-1.92	-	-	0.0118	< DL – 0.065	-	-
LH water column, summer (*18*)	0.359	0.060-1.11	0.181	0.079-0.367	< DL [b]	< DL – 0.012	< DL	<DL-0.008
RR, LH outflow (*3*)	0.598	0.171-1.20	0.292	0.261-0.323	0.007	< DL – 0.013	-	< DL – 0.013
RR, fjord outflow (*2*)	10.1	8.33-12.0	0.452	0.387-0.517	0.0647	0.058 – 0.071	0.011	< DL – 0.016

[a] Snow concentrations separated by sampling year due to differences in snowpack (see Methods and Tables S3, S4).
[b] < DL, below detection limit (< 0.007 ng L^{-1}).
[c] Filtered (< 0.45 μm) concentrations.

Table A3-3. Concentrations and loadings of unfiltered total mercury (THg) in snow from the Lake Hazen watershed in 2014 and 2015.

		Concentration ($ng\ L^{-1}$)	Loading ($mg\ ha^{-1}$)		
Year	Snow type	Mean ± 1 SD	Mean ± 1 SD	F/t *	p-value
2014	Light	21.4 ± 9.67	10.1 ± 5.34	2.61	0.111
	Dark	339 ± 400	22.6 ± 29.2		
2015	Land	4.91 ± 0.938	4.54 ± 3.09	1.08	0.302
	Lake	4.59 ± 1.12	5.53 ± 3.58		
2014 vs. 2015	Light/Lake			3.25	0.00265

* F/t: For intra-annual comparisons, results of ANOVA are presented (F-value). For inter-annual comparison, results of a t-test (t-value) shown.

Table A3-4. Concentrations and loadings of unfiltered methylmercury (MeHg) in snow from the Lake Hazen watershed in 2014 and 2015.

		Concentration ($ng\ L^{-1}$)	Loading ($mg\ ha^{-1}$)		
Year	Snow type	Mean ± 1 SD	Mean ± 1 SD	F/t *	p-value
2014	Light	0.579 ± 0.200	0.268 ± 0.097	0.690	0.409
	Dark	3.51 ± 2.25	0.342 ± 0.449		
2015	Land	0.303 ± 0.074	0.301 ± 0.247	0.016	0.900
	Lake	0.387 ± 0.157	0.486 ± 0.406		
2014 vs. 2015	Light/Lake			-2.40	0.0255

* F/t: For intra-annual comparisons, results of ANOVA shown (F-value). For inter-annual comparison, results of a t-test (t-value) shown.

Table A3-5. Log-linear models from LOADEST for prediction of daily THg/MeHg (UF, unfiltered; F, filtered) fluxes in glacial rivers.

Response	Model	R^2	p	Bias (%)
THg, unfiltered	$\ln(load_{THg, UF}) = -0.001\ln Q^2 + 1.07\ln Q - 11.2$	0.965	<0.001	4.59
THg, filtered	$\ln(load_{THg, F}) = 0.003\ln Q^2 + 1.02\ln Q - 14.1$	0.998	<0.001	4.66
MeHg, unfiltered	$\ln(load_{MeHg, UF}) = -0.004\ln Q^2 + 1.03\ln Q - 16.2$	0.980	<0.001	-5.10
MeHg, filtered	$\ln(load_{MeHg, F}) = -0.006\ln Q^2 + 1.02\ln Q - 17.1$	0.980	<0.001	3.21

Table A3-6. Physical features (mean±1SD) of, and total mercury (THg) and methylmercury (MeHg) exports (± SE) from, the glacier-fed river deltas draining into Lake Hazen*.

'	River length (km)	Area (km^2)	Glacier area (km^2)	T (°C)	pH	Runoff (km^3)		Unfiltered THg (kg yr^{-1})		Unfiltered MeHg (g yr^{-1})	
						2015	2016	2015	2016	2015	2016
Blister (BC)	11.2	-	6	8.90±1.90	7.80±0.45	0.002	<0.001	0.03±0.01	0.01±0.00	0.11±0.00	0.03±0.00
Snowgoose (SG)	15.6	222	87	7.29±1.53	7.67±0.63	0.03	0.01	0.44±0.16	0.14±0.04	1.51±0.36	0.51±0.10
Abbé (AR)	20.9	390	204	5.96±1.85	7.94±0.52	0.06	0.02	1.03±0.44	0.24±0.08	3.38±0.94	0.87±0.19
Gilman (GR)	21.2	992	708	3.43±0.28	8.61±0.16	0.20	0.04	3.27±1.92	0.72±0.28	9.99±3.69	2.45±0.61
Henrietta Nesmith (HN)	4.3	1274	1041	6.27±5.06	8.16±0.30	0.29	0.08	4.95±3.14	1.25±0.50	14.9±5.87	4.23±1.09
Turnabout (TR)	55.3	678	259	12.0±0.94	7.85±0.18	0.08	0.02	1.38±0.64	0.39±0.14	4.48±1.32	1.37±0.31
Very (VR)	42.5	1035	269	10.3±2.91	8.18±0.06	0.17	0.08	3.01±1.15	1.37±0.49	8.97±2.80	4.50±1.16
Watershed	-	7516	3074	-	-	0.95	0.28	16.4±8.65	8.35±1.77	50.3±17.4	16.2±4.01

* Physical parameters (T, pH) averaged (mean±1SD) over weekly samplings (n=16, 7-Jul to 31-Jul-2015 and 2-Jul to 5-Aug-2016) for SG and BC, and over annual samplings (n=3, 15-Jul-2015, 11-Jul-2016, 1-Aug-2016) for AR, TR, VR, HN and GR (n=2, 11-Jul-2016, 1-Aug-2016). Note that non-delta transect data are not included in these estimates.

* River length, approx. distance between glacier and Lake Hazen following river channel; Area, sub-catchment area; Glacier area, sub-catchment area covered by glaciers; T, water temperature.

Table A3-7. Glacial sub-catchment area-normalized annual fluxes (±SE) of runoff, THg and MeHg in the Lake Hazen watershed.

River	Area (km^2)	Runoff ($x10^5$ m^3 km^{-2} yr^{-1}) 2015	Runoff ($x10^5$ m^3 km^{-2} yr^{-1}) 2016	THg flux (g km^{-2} yr^{-1}) 2015	THg flux (g km^{-2} yr^{-1}) 2016	MeHg flux (mg km^{-2} yr^{-1}) 2015	MeHg flux (mg km^{-2} yr^{-1}) 2016
Blister	-	-	-	-	-	-	-
Snowgoose	222	1.18	0.297	1.96±0.73	0.61±0.20	6.78±1.63	2.28±0.47
Abbé	390	1.56	0.381	2.63±1.14	0.61±0.20	8.68±2.40	2.23±0.48
Gilman	992	1.93	0.435	3.30±1.94	0.72±0.28	10.1±3.72	2.47±0.61
Henrietta Nesmith	1274	2.29	0.588	3.88±2.46	0.98±0.39	11.7±4.61	3.32±0.85
Turnabout	678	1.20	0.350	2.04±0.94	0.57±0.20	6.61±1.95	2.02±0.46
Very	1035	1.60	0.769	2.91±1.11	1.32±0.47	8.67±2.70	4.35±1.12

Table A3-8. Concentrations of THg and MeHg (ng g^{-1}) in freeze-dried solid samples collected from throughout the Lake Hazen watershed in 2015, 2016.

Sample type	Site (*n*)[a]	THg (ng g^{-1})	MeHg (ng g^{-1})
Soils	Various (5)	21.2±8.84	0.157±0.098
Foam	Lake Hazen (2)	474±61.3	1.28±0.847
Coal (no amber)	Blister Creek (1)	7.10	0.036±0.004
Coal (no amber)	Gilman River (1)	94.3±34.2	0.016±0.009
Coal (with amber)	Gilman River (1)	14.9±3.20	0.033±0.003
Suspended sediment	Gilman River (2)	35.2±22.4	0.109
Suspended sediment	Snowgoose River (1)	25.6±1.17	0.042±0.006
Suspended sediment	Blister River (2)	14.2±4.42	-
Suspended sediment	Turnabout River (1)	4.65	-
Suspended sediment	Very River (1)	100	-

[a] Mean ± 1 SD shown, where *n* is the number of samplings. Where n=1, SD of duplicate runs is presented if possible. Where no SD shown, insufficient sample available for duplicate analysis.

References

1. Overeem, I.; Hudson, B. D.; Syvitski, J. P. M.; Mikkelsen, A. B.; Hasholt, B.; van den Broeke, M. R.; Noël, B. P. Y.; Morlighem, M., Substantial export of suspended sediment to the global oceans from glacial erosion in Greenland. *Nature Geosci.* **2017**.
2. Ladegaard-Pedersen, P.; Sigsgaard, C.; Kroon, A.; Abermann, J.; Skov, K.; Elberling, B., Suspended sediment in a high-Arctic river: An appraisal of flux estimation methods. *Sci. Total Environ.* **2017,** *580*, 582-592.
3. Lehnherr, I.; St Louis, V. L.; Emmerton, C. A.; Barker, J. D.; Kirk, J. L., Methylmercury Cycling in High Arctic Wetland Ponds: Sources and Sinks. *Environ. Sci. Technol.* **2012,** *46*, (19), 10514-10522.
4. Lehnherr, I.; St. Louis, V. L.; Muir, D. C. G.; Sharp, M. J.; Gardner, A. S.; Lamoureux, S.; Smol, J. P.; St. Pierre, K. A.; Michelutti, N.; Schiff, S. L.; Emmerton, C. A.; Tarnocai, C.; Talbot, C., The world's largest High Arctic lake responds rapidly to climate warming. *Nature Commun.* **2018,** *9*, 1290.
5. Wanninkhof, R.; Ledwell, J. R.; Broecker, W. S., Gas exchange-wind speed relation measured with sulfur hexafluoride on a lake. *Science* **1985,** *227*, 1224-1227.
6. St Louis, V. L.; Hintelmann, H.; Graydon, J. A.; Kirk, J. L.; Barker, J.; Dimock, B.; Sharp, M. J.; Lehnherr, I., Methylated mercury species in Canadian high arctic marine surface waters and snowpacks. *Environ. Sci. Technol.* **2007,** *41*, (18), 6433-6441.
7. Poissant, L.; Amyot, M.; Pilote, M.; Lean, D., Mercury Water−Air Exchange over the Upper St. Lawrence River and Lake Ontario. *Environ. Sci. Technol.* **2000,** *34*, (15), 3069-3078.
8. Crusius, J.; Wanninkhof, R., Gas transfer velocities measured at low wind speed over a lake. *Limnol. Oceanogr.* **2003,** *48*, (3), 1010-1017.
9. Tranter, M.; Brimblecombe, P.; Davies, T. D.; Vincent, C. E.; Abrahams, P. W.; Blackwood, I., The composition of snowfall, snowpack and meltwater in the Scottish highlands-evidence for preferential elution. *Atmos. Environ.* **1986,** *20*, (3), 517-525.
10. Kirk, J. L.; Louis, V. L. S.; Sharp, M. J., Rapid reduction and reemission of mercury deposited into snowpacks during atmospheric mercury depletion events at Churchill, Manitoba, Canada. *Environ. Sci. Technol.* **2006,** *40*, (24), 7590-7596.
11. Zdanowicz, C. M.; Zielinski, G. A.; Wake, C. P., Characteristics of modern atmospheric dust deposition in snow on the Penny Ice Cap, Baffin Island, Arctic Canada. *Tellus* **1998,** *50B*, 506-520.
12. Tanaka, T. Y.; Chiba, M., A numerical study of the contributions of dust source regions to the global dust budget. *Global Planet. Change* **2006,** *52*, (1–4), 88-104.
13. St. Pierre, K. A.; St. Louis, V. L.; Kirk, J. L.; Lehnherr, I.; Wang, S.; La Farge, C., Importance of Open Marine Waters to the Enrichment of Total Mercury and Monomethylmercury in Lichens in the Canadian High Arctic. *Environ. Sci. Technol.* **2015,** *49*, (10), 5930-5938.
14. Dommergue, A.; Larose, C.; Faïn, X.; Clarisse, O.; Foucher, D.; Hintelmann, H.; Schneider, D.; Ferrari, C. P., Deposition of Mercury Species in the Ny-Ålesund Area (79°N) and Their Transfer during Snowmelt. *Environ. Sci. Technol.* **2010,** *44*, (3), 901-907.
15. Hurley, J. P.; Watras, C. J.; Bloom, N. S., Mercury cycling in a northern wisconsin seepage lake: The role of particulate matter in vertical transport. *Water Air Soil Pollut.* **1991,** *56*, (1), 543-551.

16. Hopkins, D. W.; Elberling, B.; Greenfield, L. G.; Gregorich, E. G.; Novis, P.; O'Donnell, A. G.; Sparrow, A. D., Soil-microorganisms in Antarctic dry valleys: resource supply and utilization. In *Micro-organisms and earth systems - advances in geomicrobiology*, Gadd, G. M.; Semple, K. T.; Lappin-Scott, H. M., Eds. Cambridge University Press: New York, NY, 2005; pp 71-84.
17. Ruuskanen, M. O.; St. Pierre, K. A.; St. Louis, V. L.; Aris-Brosou, S.; Poulain, A. J., Physicochemical drivers of microbial community structure in sediments of Lake Hazen, Nunavut, Canada. *Front. Microbiol.* **2018**.